International Max Planck Research School on
EARTH SYSTEM MODELLING

Center for Environmental Systems Research

Modelling of global crop production and resulting N_2O emissions

Elke Stehfest

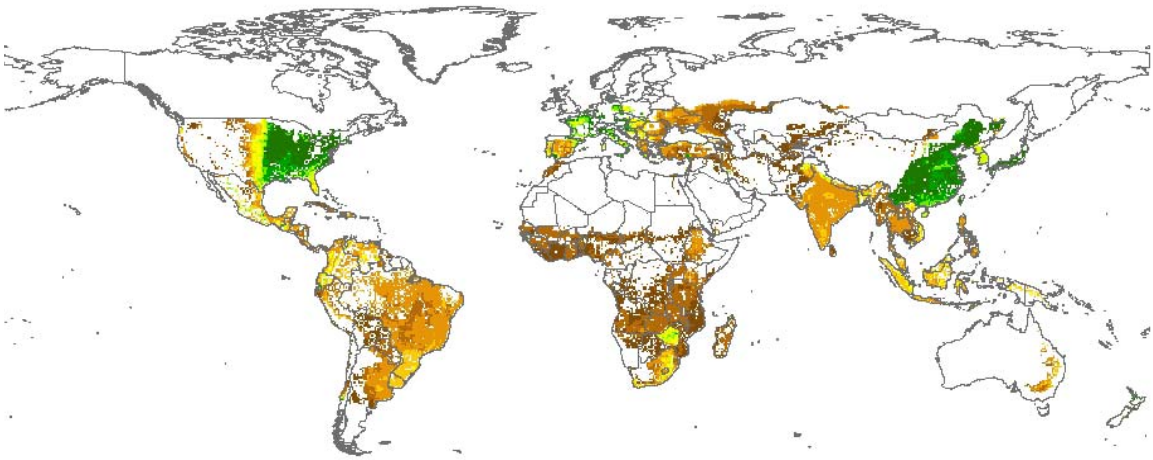

Dissertation

UNIKASSEL
VERSITÄT

Modelling of global crop production and resulting N_2O emissions

Dissertation

Zur Erlangung des akademischen Grades eines

Doktors der Naturwissenschaften (Dr. rer. nat.) im Fachbereich Elektrotechnik / Informatik der Universität Kassel

vorgelegt von

Elke Stehfest

Kassel, 2005

Elke Stehfest
Zentrum für Umweltsystemforschung
Universität Kassel
Kurt-Wolters-Str. 3
34109 Kassel
Germany

Als Dissertation angenommen

vom Fachbereich Elektrotechnik/Informatik der Universität Kassel

auf Grund der Gutachten von

Prof. Dr. Joseph Alcamo

und

Prof. Dr. Bernard Ludwig

Die Disputation fand am 25. November 2005 statt.

Im Rahmen dieser Arbeit sind bislang folgende Veröffentlichungen entstanden:

Stehfest, E. and Müller, C., 2004. Simulation of N_2O emissions from a urine-affected pasture in New Zealand, Journal of Geophysical Research, Vol. 109, D03109, doi:10.1029/2003JD004261

Stehfest, E. and Bouwman, A.F., 2005. N_2O and NO emission from agricultural fields and soils under natural vegetation: summarizing available measurement data and modelling of global annual emissions. Submitted to Nutrient Cycling in Agroecosystems

Stehfest, E. Heistermann, M., Priess, J.A., Ojima, D.S., Alcamo, J. 2005. Simulation of global crop production with the Ecosystem model Daycent. Submitted to Global Biogeochemical Cycles

Danksagung

Bedanken möchte ich mich auf diesem Weg bei all den Menschen, die auf unterschiedliche Weise zum Entstehen dieser Arbeit beigetragen haben: Als erstes bei Prof. Joseph Alcamo für die wissenschaftliche Betreuung und seine Unterstützung bei verschiedenen Forschungskooperationen. Dann bei Jörg Priess für die intensive inhaltliche Begleitung der Arbeit in den letzen drei Jahren und die Durchsicht des Manuskriptes.
Die enge Zusammenarbeit mit Maik Heistermann bei der globalen Ertragsmodellierung war sehr produktiv und hat Spaß gemacht; dafür möchte ich ihm herzlich danken.
Die globalen Simulationen wären außerdem nicht möglich gewesen ohne die große Hilfsbereitschaft und Unterstützung von Achim Manche und seine Vorschläge zur Optimierung der Rechnernutzung.
Der CENTURY Gruppe in Fort Collins/Colorado, insbesondere Bill Parton und Dennis Ojima, gilt mein Dank für die Bereitstellung des Daycent-Modells und die Diskussionen über verschiedene Modellierungsfragen. Außerdem waren die schnellen Antworten von Cindy Keough bei allen Daycent-Problemen immer eine große Hilfe.
Bei Lex Bouwman möchte ich mich herzlich dafür bedanken, dass ich von ihm viel über die Stärken und Schwächen statistischer Datenanalyse lernen konnte. Die Kooperation mit ihm war sehr bereichernd und ermutigend.
Außerdem herzlichen Dank an alle Kollegen und Kolleginnen für die anregende Arbeitsumgebung!

Meinen Eltern

Zusammenfassung

Landwirtschaft spielt eine zentrale Rolle im Erdsystem. Sie trägt durch die Emission von CO_2, CH_4 und N_2O zum Treibhauseffekt bei, kann Bodendegradation und Eutrophierung verursachen, regionale Wasserkreisläufe verändern und wird außerdem stark vom Klimawandel betroffen sein. Da all diese Prozesse durch die zugrunde liegenden Nährstoff- und Wasserflüsse eng miteinander verknüpft sind, sollten sie in einem konsistenten Modellansatz betrachtet werden. Dennoch haben Datenmangel und ungenügendes Prozessverständnis dies bis vor kurzem auf der globalen Skala verhindert.

In dieser Arbeit wird die erste Version eines solchen konsistenten globalen Modellansatzes präsentiert, wobei der Schwerpunkt auf der Simulation landwirtschaftlicher Erträge und den resultierenden N_2O-Emissionen liegt. Der Grund für diese Schwerpunktsetzung liegt darin, dass die korrekte Abbildung des Pflanzenwachstums eine essentielle Voraussetzung für die Simulation aller anderen Prozesse ist. Des weiteren sind aktuelle und potentielle landwirtschaftliche Erträge wichtige treibende Kräfte für Landnutzungsänderungen und werden stark vom Klimawandel betroffen sein. Den zweiten Schwerpunkt bildet die Abschätzung landwirtschaftlicher N_2O-Emissionen, da bislang kein prozessbasiertes N_2O-Modell auf der globalen Skala eingesetzt wurde.

Als Grundlage für die globale Modellierung wurde das bestehende Agrarökosystemmodell Daycent gewählt. Neben der Schaffung einer entsprechenden Simulationsumgebung wurden zunächst die benötigten globalen Datensätze für Bodenparameter, Klima und landwirtschaftliche Bewirtschaftung zusammengestellt. Da für Pflanzzeitpunkte bislang keine globale Datenbasis zur Verfügung steht, und diese sich mit dem Klimawandel ändern werden, wurde eine Routine zur Berechnung von Pflanzzeitpunkten entwickelt. Die Ergebnisse zeigen eine gute Übereinstimmung mit Anbaukalendern der FAO, die für einige Feldfrüchte und Länder verfügbar sind.

Danach wurde das Daycent-Modell für die Ertragsberechnung von Weizen, Reis, Mais, Soja, Hirse, Hülsenfrüchten, Kartoffel, Cassava und Baumwolle parametrisiert und kalibriert. Die Simulationsergebnisse zeigen, dass Daycent die wichtigsten Klima-, Boden- und Bewirtschaftungseffekte auf die Ertragsbildung korrekt abbildet. Berechnete Länderdurchschnitte stimmen gut mit Daten der FAO überein ($R^2 \approx 0.66$ für Weizen, Reis und Mais; $R^2 = 0.32$ für Soja), und räumliche Ertragsmuster entsprechen weitgehend der beobachteten Verteilung von Feldfrüchten und subnationalen Statistiken.

Vor der Modellierung landwirtschaftlicher N_2O-Emissionen mit dem Daycent-Modell stand eine statistische Analyse von N_2O- und NO-Emissionsmessungen aus natürlichen und landwirtschaftlichen Ökosystemen. Die als signifikant identifizierten Parameter für N_2O (Düngemenge, Bodenkohlenstoffgehalt, Boden-pH, Textur, Feldfrucht, Düngersorte) und NO (Düngemenge, Bodenstickstoffgehalt, Klima) entsprechen weitgehend den Ergebnissen einer früheren Analyse. Für Emissionen aus Böden unter natürlicher Vegetation, für die es bislang keine solche statistische Untersuchung gab, haben Bodenkohlenstoffgehalt, Boden-pH, Lagerungsdichte, Drainierung und Vegetationstyp einen signifikanten Einfluss auf die N_2O-Emissionen, während die NO-Emissionen signifikant von Bodenkohlenstoffgehalt und Vegetationstyp abhängen. Basierend auf den daraus entwickelten statistischen Modellen betragen die globalen Emissionen aus Ackerböden 3.3 Tg N a^{-1} für N_2O, und 1.4 Tg N a^{-1} für NO. Solche statistischen Modelle sind nützlich, um Abschätzungen und Unsicherheitsbereiche von N_2O- und NO-Emissionen basierend auf einer Vielzahl von Messungen zu berechnen. Die Dynamik des Bodenstickstoffs, insbesondere beeinflusst durch Pflanzenwachstum, Klimawandel und Landnutzungsänderung, kann allerdings nur durch die Anwendung von prozessorientierten Modellen berücksichtigt werden.

Zur Modellierung von N_2O-Emissionen mit dem Daycent-Modell wurde zunächst dessen Spurengasmodul durch eine detailliertere Berechnung von Nitrifikation und Denitrifikation und die Berücksichtigung von Frost-Auftau-Emissionen weiterentwickelt. Diese überarbeitete Modellversion wurde dann an N_2O-Emissionsmessungen unter verschiedenen Klimaten und Feldfrüchten getestet. Sowohl die Dynamik als auch die Gesamtsummen der N_2O-Emissionen werden befriedigend abgebildet, wobei die Modelleffizienz für monatliche Mittelwerte zwischen 0.1 und 0.66 für die meisten Standorte liegt.

Basierend auf der überarbeiteten Modellversion wurden die N_2O-Emissionen für die zuvor parametrisierten Feldfrüchte berechnet. Emissionsraten und feldfruchtspezifische Unterschiede stimmen weitgehend mit Literaturangaben überein. Düngemittelinduzierte Emissionen, die momentan vom IPCC mit 1.25 +/- 1% der eingesetzten Düngemenge abgeschätzt werden, reichen von 0.77% (Reis) bis 2.76% (Mais). Die Summe der berechneten Emissionen aus landwirtschaftlichen Böden beträgt für die Mitte der 1990er Jahre 2.1 Tg N_2O-N a^{-1}, was mit den Abschätzungen aus anderen Studien übereinstimmt.

Summary

Agricultural systems play a central role in the earth system. They contribute to the anthropogenic greenhouse effect via the emission of CO_2, CH_4 and N_2O, can cause soil degradation and eutrophication of downstream ecosystems, may change regional water cycles and will be strongly affected by climate change. All these processes are strongly interconnected and therefore need to be addressed in a consistent approach. However, knowledge and data gaps have hindered the development of such a modelling framework at the global scale until recently.

In this thesis, a first version of such a consistent global modelling framework is presented, focussing primarily on the simulation of global crop yields and resulting N_2O emissions for the following reasons: First of all, the correct representation of plant growth is a precondition for the simulation of all other processes, and actual and potential crop yields are important driving forces of land-use change and will strongly be affected by climate change. The second focus is on N_2O emissions, as no process-based N_2O model has been applied at the global scale so far.

The existing agroecosystem model Daycent was used as a basis for the consistent modelling of agricultural production and its environmental effects. As a preparatory step, a computational framework for grid-based calculations was developed, and the required global input datasets for soil, climate and agricultural management were compiled. As no global inventory of planting dates existed yet, and as planting dates need to be adjusted under climate change conditions, an algorithm was developed to calculate planting dates of major crops. Results correspond to FAO crop calendars, which are available for a number of countries and crops.

Thereafter, Daycent was parameterised and calibrated to simulate yield levels for wheat, maize, rice, soybeans, tropical cereals, pulses, potato, cassava and cotton. Simulation results show that the Daycent model is capable of reproducing the major effects of climate, soil and management on crop production. Average simulated crop yields per country agree well with FAO data ($R^2 \approx 0.66$ for wheat, rice and maize; $R^2 = 0.32$ for soybean), and spatial patterns of yields mostly correspond to observed crop distributions and subnational census data.

Preceding the modelling of N_2O emissions from agricultural soils with the Daycent model, a statistical analysis of N_2O and NO emission measurements from both natural and agricultural ecosystems was carried out. Similarly to a previous analysis, fertilization rate, soil organic carbon content, soil pH, texture, crop type, and fertilizer type significantly affect N_2O emission from agricultural soils, while NO emissions are significantly determined by fertilization rate, soil nitrogen content, and climate. For emissions from soils under natural vegetation, which had not been subject to such a statistical analysis before, N_2O emissions are significantly affected by soil carbon content, soil pH, bulk density, drainage, and vegetation type, while NO emissions are significantly influenced by carbon content and vegetation type. Based on the resulting statistical models the global annual emissions from fertilized arable land sum up to 3.3 Tg N y^{-1} for N_2O, and to 1.4 N y^{-1} for NO. Statistical models are valuable to calculate best estimates and uncertainty ranges of N_2O and NO emissions based on a plenty of measurement data. However, the dynamics of soil organic nitrogen pools, as especially affected by crop production, climate change and land-use change can only be included by applying process-based agroecosystem models

For the modelling of global N_2O emissions with the Daycent model, its trace gas module was improved by implementing a more detailed representation of nitrification/denitrification processes, and by including freeze-thaw emissions. This revised model version was tested against N_2O emission measurements of agricultural soils under different climate regimes and crop types. Simulation results show that annual emissions are represented well, and that the modelling efficiency on a monthly basis ranges between 0.1 and 0.66 for most sites.

Based on this revised Daycent version, N_2O emission rates are calculated for all crop types for which the Daycent model had been parameterised before. Emission rates and differences between crop types mostly agree with literature. Fertilizer induced emissions, which are currently estimated by the IPCC as 1.25 +/- 1% of the N applied, range between 0.77% (rice) and 2.76% (maize). Simulated N_2O emissions from agricultural soils in the 1990ies add up to 2.1 Tg N_2O-N y^{-1}, which is similar to the estimates from other studies.

Contents

1 GENERAL INTRODUCTION 1

1.1 The role of agriculture in the earth system 1

1.2 Modelling agricultural production 2

1.3 Modelling nitrous oxide emissions 3

1.4 Objectives and Methodology 4

1.5 Thesis outline 6

2 MODELLING OF GLOBAL CROP PRODUCTION 7

2.1 Introduction 7

2.2 Materials and Methods 9

2.2.1 The Daycent model 9

2.2.2 Planting dates 12

2.2.3 Input data and simulation methodology 13

2.3 Results and Discussion 14

2.3.1 Global planting dates 14

2.3.2 Thermal envelopes 18

2.3.3 Global crop yields 19

2.3.4 Uncertainties 23

2.3.5 Selected spatial patterns 25

2.3.6 Simulation of other crops 28

2.3.7 Methodological issues 28

2.4 Conclusions and Outlook 29

2.5 Supplement: Input data used 31

2.5.1 Weather data 31

2.5.2 Soil data 31

2.5.3 Land-use map 31

2.5.4 Crop types and varieties 31

2.5.5 Initial conditions, simulation period 33

2.5.6 Management 33

3 STATISTICAL ANALYSIS OF N_2O AND NO EMISSIONS 35

3.1 Introduction 35

3.2 Data and Methods 39

3.2.1 Data set 39

3.2.2 Data analysis 42

3.2.3 Estimating global annual emissions 44

3.3 Results and Discussion 46

3.3.1 Agricultural fields 46

3.3.2 Soils under natural vegetation 56
3.4 Comparison of N_2O and NO emission estimates with other studies 64
3.4.1 Agricultural fields 64
3.4.2 Soils under natural vegetation 66
3.5 Conclusions 68

4 DAYCENT CASE STUDY IN NEW ZEALAND 71

4.1 Introduction 71
4.2 Materials and Methods 72
4.2.1 Data set 72
4.2.2 The Daycent model 72
4.2.3 Running the model 74
4.2.4 Presentation of results 74
4.3 Results 75
4.3.1 N_2O emissions 75
4.3.2 Precipitation, soil moisture and soil temperature 75
4.3.3 Mineral N 78
4.3.4 Total N gas loss 78
4.4 Discussion 80
4.4.1 N_2O emissions 80
4.4.2 Soil moisture 80
4.4.3 Mineral N 81
4.5 Conclusions 81

5 MODELLING GLOBAL N_2O EMISSIONS FROM AGRICULTURAL SOILS 83

5.1 Introduction 83
5.2 Model development 85
5.2.1 The Daycent model 85
5.2.2 Revision of the trace gas module 86
5.3 Site specific testing 93
5.3.1 Description of test sites 93
5.3.2 Model testing 94
5.3.3 Soil moisture 95
5.3.4 Soil N content 97
5.3.5 N_2O emissions 100
5.3.6 Conclusions from site specific testing 107
5.4 Sensitivity analysis 107
5.5 Global datasets used 110
5.5.1 Land-use map 111
5.5.2 Soil data 111
5.5.3 Weather data 112
5.5.4 Nitrogen deposition 112

5.5.5 Management 112
5.5.6 Initial conditions, simulation period 114
5.5.7 Crop parameters 114
5.6 Estimation of global N_2O emissions from agricultural soils 115
5.6.1 N_2O emission 115
5.6.2 Fertilizer induced emissions 121
5.6.3 Global N_2O emission sum 123
5.7 Conclusions and Outlook 125

6 CONCLUDING REMARKS 127
6.1 Modelling global crop production 127
6.2 Estimating N_2O and NO emissions with statistical models 128
6.3 Process-based modelling of N_2O emissions 129
6.4 Outlook and future research 130

7 BIBLIOGRAPHY 131

APPENDIX A: Additional maps of crop yields **145**

APPENDIX B: Additional maps of N_2O emissions **147**

APPENDIX C: Additional maps for the statistical model **149**

1 General Introduction

1.1 The role of agriculture in the earth system

Humans have transformed about 34% of the earth's land surface to arable land or pasture [*Leff et al.*, 2004], and therefore agricultural systems play a central role in the earth system (Figure 1-1). They contribute to the anthropogenic greenhouse effect via emissions of CO_2 (26%), N_2O (96%), and CH_4 (65%) during land conversion (mainly CO_2) and during permanent management (mainly N_2O and CH_4) [*Duxbury et al.*, 1993]. Additionally, agriculture influences the global and regional climate via changes e.g. in albedo and water fluxes [*Brovkin et al.*, 1998; *Pielke et al.*, 2002]. The human society depends on agricultural production to feed the world's population and will be affected by changes in crop productivity due to climate. In turn, increasing demand for agricultural goods through population growth or changes in diet causes changes in land cover and land use. Beyond, actual and potential yields determine future land use decisions, which again have an impact on soil processes and future yields. Because of this feedback loop it is assumed that accurate simulation of land use can only be achieved by coupled modelling of crop production and land use.

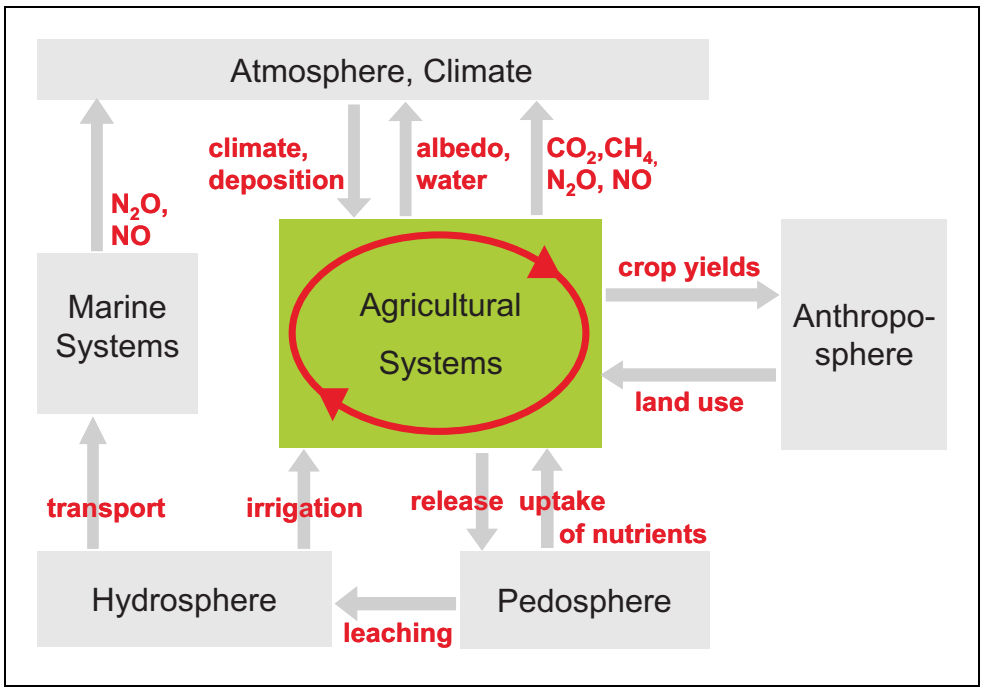

Figure 1-1. Simplified scheme of the earth system and the role of agriculture

These processes of plant growth, trace gas emission and nutrient leaching are strongly interconnected via the underlying nutrient and water fluxes, as illustrated by the following examples: The potential contribution of irrigation and fertilisation to meet increasing food demands can only be assessed adequately by including the processes governing nutrient and water limitation.

Furthermore, greenhouse gas emissions from soils can only be calculated if the carbon dynamics and the nitrogen taken up by the crops are considered. The same applies to problems such as nutrient mining or nutrient leaching, which depend on an accurate calculation of water fluxes, nitrogen uptake by plants and gaseous N emissions.

Computer-assisted mathematical modelling has been proven to be an adequate tool to study such complex systems and to develop scenarios of possible future development. Therefore a consistent modelling framework is needed to study e.g. the effect of climate change on crop yields, to assess future irrigation water requirements, or to calculate trace gas emissions and nutrient leaching caused by agricultural production. At regional scales, detailed process models have already been applied for an integrated consideration of these processes [*Donner and Kucharik*, 2003]. However, limited process understanding and data availability hamper the implementation of such consistent modelling frameworks at the global scale.

1.2 Modelling agricultural production

A central part of such a consistent model of the agricultural system will be the simulation of plant growth, as it largely determines carbon, nutrient and water fluxes within the agricultural system. Realistic calculation of crop growth therefore is a precondition to assess all the environmental effects of agriculture discussed above. Moreover, crop production is the main link to the socio-economic sphere, as land use decisions are determined by actual and potential yields. Finally, climate change is expected to largely affect agricultural production, and such a global crop production model will provide the means to study these effects.

Numerous process-based crop models have been developed during the last decades and are applied – depending on their degree of detail – from plant and plot up to regional scales (e.g. CERES [*Jones and Kiniry*, 1986; *Otter-Nacke et al.*, 1986; *Ritchie et al.*, 1991], WOFOST [*Supit et al.*, 1994] or CROPGRO [*Hoogenboom et al.*, 1992]). However, data and knowledge gaps have hindered a global application of such process models until recently.

Instead, global models have so far relied on rather empirical approaches like the Global Agro-ecological Zoning (GAEZ) model [*Fischer et al.*, 2002], which is based on the agro-ecological zoning approach of the Food and Agricultural Organisation [*FAO*, 1978], or the agricultural part of the terrestrial vegetation model (part of the IMAGE model; [*Alcamo*, 1994]). However, these approaches have several drawbacks: They do not account for nutrient limitation of crop production and they do not include process-based modelling of trace gas emissions, nutrient dynamics in the soil, leaching, erosion and water fluxes that are linked to agricultural production. Therefore many feedback mechanisms and connections to other components of the earth system are neglected or may be inconsistent if represented by other conceptual models.

The availability of improved global datasets, and the continuously increasing computing power make it now possible to adapt detailed process-based crop or agro-ecosystem models to the global scale. One of the afore mentioned models, EPIC, has been applied to the global scale recently [*Tan and Shibasaki*, 2003]. This application of agro-ecosystem models at the global scale will allow to include the complex interaction of processes in the plant-soil system and to address the issues

mentioned above - climate change impact, crop production, soil degradation, greenhouse gas emissions, nutrient leaching, management impact on yields - within a consistent global framework.

1.3 Modelling nitrous oxide emissions

Nitrous oxide (N_2O) emissions from soils are among the major environmental impacts of agricultural production and – different from e.g. CO_2 emissions from agricultural production – no process model for N_2O emissions (neither from agriculture nor from natural systems) has been applied so far to the global scale.

The atmospheric concentration of N_2O has increased from 285 ppbv before the year 1700 [*Stauffer and Neftel*, 1988] to 314 ppbv in the year 1998 [*IPCC*, 2001]. Despite its low concentration it contributes 4-6 % to the anthropogenic greenhouse effect because of its long lifetime of 100 – 150 years and its high absorption capacity (296 x CO_2) [*Rohde*, 1990]. Beyond, nitrous oxide is transformed to other nitrogen oxides in the troposphere that are involved in the destruction of tropospheric ozone [*Crutzen*, 1981].

N_2O emissions mainly originate from nitrification (the oxidation of NH_4^{+-} to NO_3^-) and denitrification (the stepwise reduction of NO_3^- to N_2). Key regulating factors for both processes are e.g. soil water, nitrogen and carbon content and temperature. Beyond, in agricultural soils management events like fertilizer addition, irrigation and tillage largely influence N_2O nitrification and denitrification rates, highlighting the importance of a realistic representation of crop management.

The main natural sources of nitrous oxides are oceans and soils, adding up to a global emission rate of about 10 Tg N_2O -N year $^{-1}$ (Table 1-1). Anthropogenic emissions amount to 4-8 Tg N_2O-N year^{-1}, with agricultural soils and animal manure being the main sources (Table 1-1), and are expected to rise because of increasing fertilizer applications (+ 1% per year) [*FAO*, 2003].

The global source estimates of N_2O emissions as presented in Table 1-1 show wide uncertainty range of up to –85% and +250% (for agricultural emissions). Until now, estimates of global N_2O emissions were based on emission inventories [*Kroeze et al.*, 1999; *Mosier et al.*, 1998; *Olivier et al.*, 1998] or conceptual models [*Bouwman et al.*, 1993; *Bouwman et al.*, 2002b], while only two simple process-based models have been applied to estimate global N_2O emissions [*Nevison et al.*, 1996; *Potter et al.*, 1996]. These two process models do not represent nitrification and denitrification processes, but simulate N_2O emissions as a fraction of gross mineralisation. *Nevison et al.* [1996] derive an empirical function that relates N_2O emissions directly to mineralisation rates in soils under natural vegetation and agriculture, and adds an additional fraction of N_2O lost from excess N in agricultural soils. The model of *Potter et al.* [1996] only covers natural N_2O emissions and uses soil moisture to calculate the relative emissions of NO, N_2O and N_2 from mineralisation, applying the hole-in-the-pipe concept by *Davidson* [1991].

Table 1-1. Source estimates for global N_2O emissions [Tg N_2O-N $year^{-1}$], adopted from IPCC (2001)

Reference	*Mosier et al.* [1998] *Kroeze et al.* [1999]		*Olivier et al.* [1998]	
Base year	1994		1990	
Sources	Tg N $year^{-1}$	range	Tg N $year^{-1}$	range
Ocean	3.0	1 – 5	3.6	2.8 – 5.7
Atmosphere	0.6	0.3 – 1.2	0.6	0.3 – 1.2
Wet forest soils	3.0	2.2 – 3.7		
Dry savannah soils	1.0	0.5 – 2.0		
Temperate forest soils	1.0	0.1 – 2.0		
Temperate grassland soils	1.0	0.5 – 2.0		
All soils			6.6	3.3 – 9.9
Natural sub-total	**9.6**	**4.6 – 15.9**	**10.8**	**6.4 – 16.8**
Agricultural soils [a]	4.2	0.6 – 14.8	1.9	0.7 – 4.3
Biomass burning	0.5	0.2 – 1.0	0.5	0.2 – 0.8
Industrial Sources	1.3	0.7 – 1.8	0.7	0.2 – 1.1
Cattle and feedlots	2.1	0.6 – 3.1	1.0	0.2 – 2.0
Anthropogenic sub-total	**8.1**	**2.1 – 20.7**	**4.1**	**1.3 – 7.7**
Total sources	**17.7**	**6.7 – 36.6**	**14.9**	**7.7 – 24.5**
Imbalance (trend)	3.9	3.1 – 4.1		
Total sinks (stratospheric)	12.3	9 – 16		
Implied total source	**16.2**			

[a] direct and indirect emissions.

More detailed process models that explicitly simulate nitrification and denitrification like DNDC [*Li et al.*, 1992], Daycent [*Parton et al.*, 1996] or modelling package Expert-N [*Engel and Priesack*, 1993] have been developed predominantly for laboratory or plot scale applications. So far, only in a small number of studies, these models have been applied to regional scales by grid-based modelling [e.g. *Butterbach-Bahl et al.*, 2004; *Schulte-Bisping et al.*, 2003] or through extrapolation of field simulations [*Del Grosso et al.*, 2005].

The application of such process-based models at the global scale will help to reduce the uncertainty in emission estimates and will allow studying the combined effects of climate change and agricultural management on N_2O emissions and other environmental impacts.

1.4 Objectives and Methodology

The overall objective of this thesis is to develop a modelling framework for the consistent process-based simulation of

- global agricultural production and
- N_2O emissions from agriculture

and to apply this tool to estimate current agricultural production and resulting N_2O emissions.

This work is the first version of a simulation model for the globally most important agricultural systems and is being embedded in the global land use model LANDSHIFT that is currently developed at the Center for Environmental Systems Research at the University of Kassel [*Heistermann and Priess*, 2005].

The global modelling framework is based on the Daycent model [*Parton et al.*, 1996], the daily time step version of the Century model [*Parton et al.*, 1988], as these models had already been tested for a number of different climatic regions throughout the world [*Kelly et al.*, 1997; *Motavalli et al.*, 1994; *Silver et al.*, 2000]. Furthermore, the most important processes like biomass production, trace gas emissions, carbon and nutrient dynamics, water fluxes and management practices are implemented in great detail. Model inter-comparisons had proven a high performance of the Century model for long term carbon dynamics [*Smith et al.*, 1997] and N_2O emissions [*Frolking et al.*, 1998]. Beyond, the technical reasons of source code availability, acceptable computing, and the availability of input parameters at the global scale also contributed to this decision.

For the intended global scale application of the Daycent model to simulate agricultural crop production and N_2O emissions the following procedure was chosen:

A Preparation of global input datasets and modelling environment

As a preparation for the global simulations, the required input data sets for soils, climate and management parameters were compiled and an adequate computing environment was prepared to enable an application of the point model Daycent in a spatial grid.

B Modelling of global crop production

For the simulation of the global crop production the original Daycent version [*Parton et al.*, 2001] was parameterised for nine major crops which in total cover ~ 67% of the global agricultural area. In an iterative process, the Daycent model was parameterised, calibrated and tested with respect to the following processes and functions:

- Effect of water limitation on crop production
- Nitrogen dynamics
- Crop yield formation
- Agricultural management, especially planting dates and fertilizer applications

For model testing, national averages of simulated crop yields were compared with census data [*FAO*, 2004], and spatial patterns of crop yields were compared with sub-national yield data.

C Statistical analysis of N_2O and NO emission measurements

For the modelling of N_2O a preparatory study had been envisioned: A compilation of available N_2O and NO emissions data from field measurements was used to derive quantitative relations between environmental and management factors and resulting N_2O and NO emissions. These quantitative relations were intended to improve the existing trace gas module in the Daycent model. As this

analysis did not yield new or more accurate correlations than the ones already implemented in the Daycent model, no model improvement could be derived from this step. Instead, the data compilation was used to derive statistical models for N_2O and NO emissions from agricultural soils and soils under natural vegetation. These statistical models can be applied in regions where process modelling is not possible due to data constraints, they can be used as a countercheck for simulation results from process models, and might replace earlier emission-factor approaches as e.g. applied by the *IPCC* [1996].

D Modelling of N_2O emissions from agricultural soil

For process-based modelling of N_2O emissions from agricultural soils with the Daycent model as adopted for global crop modelling, the trace gas sub-model is modified with respect to the limitations identified by literature reviews, discussions with the model developers [*Ojima et al.*, 2004] and own simulation studies.

This revised Daycent version is then tested against measured soil water contents, soil nitrogen contents and N_2O emissions from agricultural soils under different climate and management regimes. A sensitivity analysis is carried out to assess the influence of climate and soil parameters on simulated N_2O emissions.

Based on the compilation of global input data sets for soils, climate and management parameters, the revised Daycent version is used to estimate current N_2O emissions from agricultural soils at the global scale.

1.5 Thesis outline

According to the objectives and the working plan presented in the previous section, the core chapters of the thesis are structured in three parts. Part I of this thesis (Chapter 2) describes the adaptation of the Daycent model to simulate yields of wheat, rice, maize and soybean, including the calculation of global planting dates. Simulation results are tested against national production data obtained from the FAO. Simulation results for additional crop types (potato, cassava, tropical cereals, pulses and cotton) are presented in appendix A.

In part II (Chapter 3) a compilation of published N_2O and NO emission measurements is used to derive qualitative effects of environmental and management factors on N_2O and NO emissions and to develop statistical models for these emissions.

In part III (Chapters 4 and 5) the Daycent model is adapted to simulate N_2O emissions from agricultural production throughout the world. Chapter 4 describes the results of a Daycent simulation study in New Zealand and identifies a number of model limitations that need to be addressed to improve model performance with respect to N_2O emissions. In Chapter 5 a revised version of the Daycent model is introduced and tested against N_2O field measurements from agricultural soils under different crops and in different climate zones. Based on that, a sensitivity analysis is presented, and the revised Daycent version is applied to estimate N_2O emissions from agricultural fields under the management regimes of the 1990ies. Chapter 6 summarizes and discusses the main conclusions resulting from Chapters 1-5.

2 Modelling of global crop production [a]

Summary

Agriculture has become a key element within the earth system as it changes global biogeochemical and water cycles, while global environmental change affects land productivity and thus future land use decisions. To address these issues and their complex interdependency in a consistent modelling approach we adapted the agro-ecosystem model Daycent for the simulation of major crops at the global scale. Based on a global compilation of environmental and management data and an algorithm to calculate global planting dates, Daycent was parameterised and calibrated to simulate global yield levels for wheat, maize, rice and soybeans. Simulation results show that the Daycent model is able to reproduce the major effects of climate, soil and management on crop production. Average simulated crop yield per country agree well with FAOSTAT yield levels ($R^2 \approx 0.66$ for wheat, rice and maize; $R^2 = 0.32$ for soybean) and spatial patterns of yields mostly correspond to observed crop distributions and sub-national census data.

2.1 Introduction

Modelling plant growth has a tradition starting long before today's computer models. Classical works such as by Liebig (1841) or Mitscherlich (1909) are still influential. Their core questions – *what is limiting crop growth and what is the optimal management?* – are still being addressed by modern crop models. However, the scope of crop modelling has expanded. An important new motivation for crop modelling are questions regarding the impact of climate change and an increasing human population on future food security. Crop modelling has thus been applied to assess the availability of additional land for agriculture [*Fischer et al.*, 2002; *Kenny et al.*, 2000], to investigate the impact of climate change on future land use [*Alcamo et al.*, 1998] or on future economic welfare [*Matsuoka et al.*, 2001; *USGCRP*, 2001].

There is also a concern about the adverse environmental effects of agriculture. Water quality is affected by the export of nutrients (mainly nitrogen and phosphorus) and pesticides from agro-ecosystems, leading to eutrophication and declining biodiversity [*Howarth et al.*, 1996; *Stoate et al.*, 2001]. Water withdrawals for irrigation can lead to severe water stress in downstream areas [*Saiko and Zonn*, 2000; *Zaitchik et al.*, 2002]. Beyond, unsustainable and inadequate management might cause severe and sometimes irreversible degradation of soil quality, e.g. in terms of nutrient mining, salinisation or compaction of soil [*Oldeman et al.*, 1990]. Furthermore, agriculture is a major emitter of greenhouse gases and thus contributing to climate change. *Duxbury* [1993] estimates that agriculture accounts for 92% of all anthropogenic emissions of N_2O (26% for CO_2, 65% for CH_4).

[a] This work was done in cooperation with Maik Heistermann, Center for Environmental Systems Research, Kassel

The processes underlying these different aspects of crop production and its modelling are strongly interconnected and should therefore be treated within a consistent framework, as illustrated by the following examples: The potential contribution of irrigation and fertilisation to meet increasing food demands can only be assessed if the model is able to account for the processes governing nutrient and water limitation. Greenhouse gas emissions from soils can only be calculated if the nitrogen and carbon removed by crop growth are adequately considered. The same applies to problems such as nutrient mining or nutrient leaching. On a large scale *Donner and Kucharik.* [2003] have taken a first step towards such an integrated consideration of fertilizer application, crop growth and nitrate leaching in the entire Mississippi basin. Last but not least, models need to incorporate actual management in terms of fertilisation and irrigation in order to be tested against actual crop yields.

However, existing simulation models often focus on special aspects of the agricultural plant-soil system:
A large number of models has been developed in order to optimise agricultural management strategies, but also to investigate the effect of climatic variability and soil hydrology on crop yields. These models employ detailed representations of plant phenology and physiology, resulting in laborious parameterisation and calibration. Examples are the CERES model family [*Jones and Kiniry*, 1986; *Otter-Nacke et al.*, 1986; *Ritchie et al.*, 1991], WOFOST [*Supit et al.*, 1994] or CROPGRO [*Hoogenboom et al.*, 1992]. These models have yet been applied over a wide range of scales, e.g. *Eitzinger et al.* [2004] applied WOFOST for lysimeter studies; regional to sub-continental modelling studies were performed with CERES [*Saarikko*, 2000] and WOFOST [*Boogaard et al.*, 2002]. The EPIC model [*Sharpley and Williams*, 1990; *Williams et al.*, 1984] was originally developed to study the impact of soil erosion on yields, but includes a detailed description of crop growth as well. Another group of models focuses on soil biogeochemistry and nutrient cycling, e.g. RothC [*Coleman et al.*, 1997; *Jenkinson et al.*, 1991] for organic carbon turnover, CENTURY [*Parton et al.*, 1988] for carbon, nitrogen, phosphorus and sulphur cycles, DNDC [*Li et al.*, 1992] and CASA [*Potter et al.*, 1993] for N_2O emissions, and MEM [*Cao et al.*, 1995] for CH_4 emissions. These models pay more attention to soil processes, such as decomposition, nitrification and denitrification. However, there are efforts to improve the representation of crop growth in such models [*Zhang et al.*, 2002]. Reviews about the general features and mechanisms of process-based crop models are e.g. provided by *Tubiello and Ewert* [2002] who focus on the effects of elevated CO_2 concentrations and by *Lipiec et al.* [2003] who deals with crop growth, water movement and solute transport.

As pointed out, the detailed representation of processes makes parameterisation of such models a demanding task. Notorious data and knowledge gaps have yet hindered the application of such detailed simulations on the global scale. Instead, reduced form and rather empirical models have been developed for global scale applications, of which the Global Agro-Ecological-Zones (GAEZ) approach is most advanced [*Fischer et al.*, 2002]. The methodology of GAEZ is based on the AEZ approach [*FAO*, 1978] and combines the concepts of climatic envelopes with phenological modelling and the incorporation of reduction factors for soil, terrain and climate impacts on crop yields.

Only recently, one of the above mentioned process models, EPIC, was tested on the global scale for wheat, maize, rice and soybeans [*Tan and Shibasaki*, 2003]. Considering the increased availability

of global data on agricultural management, soils and climate, it is now possible to apply more sophisticated process models on the global scale. This will allow models to include the complex interaction of processes in the plant-soil system and to address the issues mentioned above - *climate change impact, crop production, soil degradation, greenhouse gas emissions, nutrient leaching, management impact on yields* - within a *consistent* global framework.

The objective of this paper is the adaptation and application of a detailed process model, the Daycent model, to the computation of global crop production, in order to address these diverse aspects of the global agricultural systems, and to present first results of simulated global crop yields. The Daycent model, which operates at a daily time step, and the CENTURY model (monthly time steps) [*Parton et al.*, 1988] were originally developed to investigate carbon and nitrogen dynamics in the US Great Plains, but have since then been successfully tested on several temperate [*Kelly et al.*, 1997] and tropical sites [*Motavalli et al.*, 1994; *Silver et al.*, 2000]. The daily time step of Daycent allows for a more detailed consideration of soil water fluxes, plant phenology and particularly processes determining the emission of N_2O and NO. Beyond, the decision to employ the Daycent model was strongly influenced by the model's detailed representation of soil biogeochemistry, as nutrient pool dynamics strongly determine nutrient availability and thus crop yield, and also influence future land use options.

In the next chapter we provide an overview of the main mechanisms determining plant growth and yield formation in the Daycent model and discuss the various input data used for its application to global crop modelling, including crop parameterisation, climate and soil data as well as management information. In chapter 2.3 we present the results for planting dates and the global yield distribution of wheat, rice, maize, and soybean. The results are compared against average country data as reported by FAO and against spatial patterns derived from selected sub-national census data. In chapter 2.4, we conclude with the identification of major achievements and deficits of our approach and an outlook on improvements planned for future model versions.

2.2 Materials and Methods

2.2.1 The Daycent model

The Daycent model is a terrestrial ecosystem model designed to simulate C, N, P and S dynamics of agricultural and natural systems [*Del Grosso et al.*, 2000; *Parton et al.*, 2001]. It is driven by daily precipitation, maximum and minimum daily temperatures and a daily scheduling of management events. Therefore most soil processes operate on a daily scale, while plant growth is simulated weekly. The soil water sub-model, which is part of the land surface processes representation [*Parton et al.*, 1998] simulates soil water content and water fluxes (i.e., runoff, leaching, evaporation, and plant transpiration) for user-defined soil layers. The soil organic matter (SOM) sub-model calculates decomposition for dead plant material and three SOM pools with different turnover times. Nitrification, denitrification, and N trace gas fluxes are tightly associated with the SOM sub-model. Both sub-models are described in the literature [*Century-Manual*, 2005], therefore we will only present their impacts on plant growth and the plant growth sub-model itself in more detail.

Potential production is calculated as a function of solar insolation, biomass, temperature (using a crop specific optimum temperature growth function) and the energy-biomass conversion factor "prdx". The prdx reflects the genetic potential of crop type and variety, but also management conditions like row distance, and is the main plant growth calibration parameter. The potential production is reduced by water stress as illustrated in Figure 2-1a. If the ratio between available water and potential evapotranspiration (available water / PET) drops below an upper threshold, potential production is linearly reduced down to a lower threshold of available water to PET, below which no production is possible. This water-limited potential production is further limited by the availability of nitrogen for meeting the C/N ratios of new biomass. These C/N ratios depend on N availability, and increase during crop growth, as a function of effective temperature sum as shown in Figure 2-1b. It is assumed that the maximum C/N ratios are reached at the onset of grain-fill. The mineral nitrogen available for growth can be supplied from fertilizer addition of nitrate or ammonium, nitrogen fixation, from mineralisation of the soil organic matter, and from dry or wet deposition. Loss of nitrogen occurs via leaching and gaseous emissions.

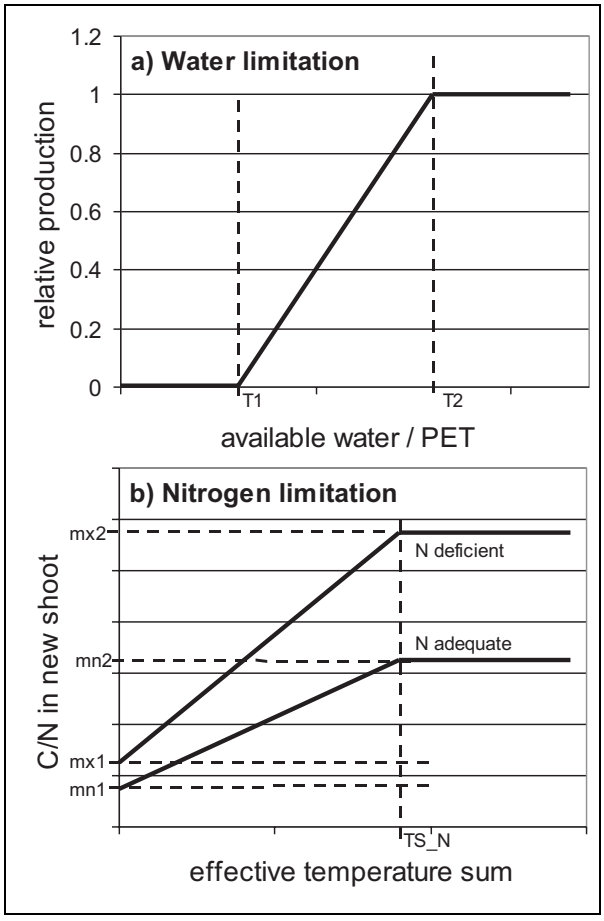

Figure 2-1. Schematic representation of the of water (a) and nitrogen (b) limitation during the growth cycle in the Daycent model [adopted from the *Century-Manual*, 2005]. Abbreviations used: C (carbon); N (nitrogen); PET (potential evapotranspiration. Parameters names used: T1 (ratio of available water to PET, below which no production is possible); T2 (ratio of available water to PET, above which production is not limited by water stress); TS_N (temperature sum at which highest minimum and maximum C/N ratios are reached); mn1 (lower limit of C/N ratio at zero biomass); mx1 (upper limit of C/N ratio at zero biomass); mn2 (upper limit of C/N ratio for effective temperature sum > TS_N); mn2 (upper limit of C/N ratio for effective temperature sum > TS_N).

The resulting biomass production is partitioned between roots and shoots, whereby the initially low shoot allocation increases during plant growth. In principle there are only two biomass compartments in the crop module, and only at harvest a certain fraction of the shoot, determined by the "harvest index", is removed as grain. This harvest index is a crop- and variety-specific parameter that can be reduced by water stress, expressed as the ratio between actual and potential transpiration during the last month before harvest. For the calculation of actual and potential transpiration refer to e.g. *Parton* [1978] and the *Century Manual* [2005]. The harvest date is scheduled when a crop-specific temperature sum is reached, following the growing degree days concept [*Wang*, 1960].

The described mechanisms bring about especially sensitive parameters and important implications for simulated yields, which are described in the following section.

Water limitation

As described above, water limitation in Daycent incrementally reduces potential production (at each time step) and harvest index (before harvesting) by relating PET to available soil water and potential to actual transpiration, respectively. PET and transpiration are crop-independent, and transpiration is not included explicitly in water limitation of weekly production but has a direct impact on the available soil water in the next time step. This approach does not allow for a consideration of crop-specific differences in water-use efficiency (e.g. for C4 plants). Instead, plant-specific behaviour is reflected in different sensitivities to drought conditions (parameters T1 and T2 in Figure 2-1).

Temperature

Temperature influences incremental biomass production at each time-step and, via accumulation of growing degree-days, the total duration of plant growth. This causes a complicated overall effect on final crop yield as higher temperatures often increase daily production, but leave less time for the plant to grow. Therefore the optimum temperature for total yield is lower than the optimum temperature for daily biomass production, assuming constant temperature over the entire growth period. Figure 2-2 illustrates this for maize. Temperatures close to T_{base} would result in theoretically infinite duration of the growth cycle and thus in highest grain production. Within the range of realistic growth periods, the crop yield can show a local maximum (e.g. maize), a plateau (e.g. rice) or a steady decrease (e.g. wheat), depending on the crop specific parameters. It is unclear whether this effect can be found in reality or not, and to what extent local crop varieties might compensate for it by higher temperature sum requirements. Nevertheless, it is commonly accepted that at least the shortening of grain-fill duration by high temperatures has significant impact on grain yield formation [*Acevedo et al.*, 2002; *White and Reynolds*, 2001; *Wilhelm et al.*, 1999].

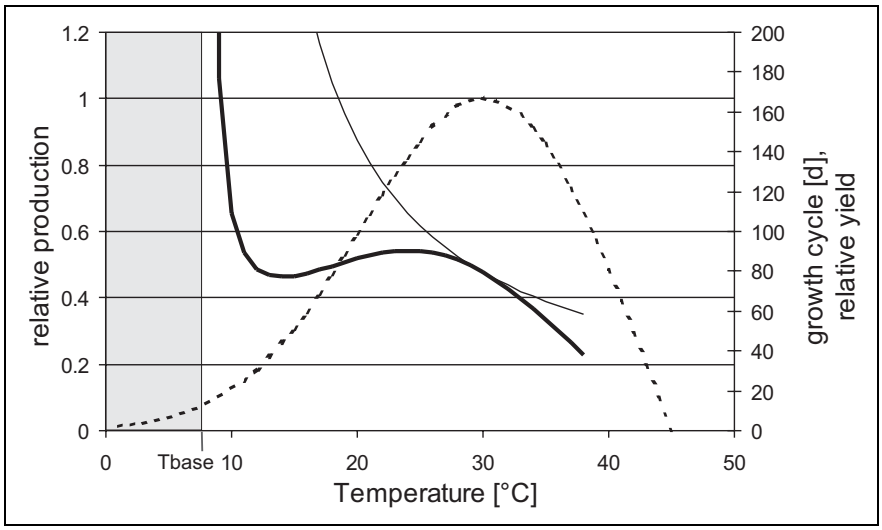

Figure 2-2. Daily production (dashed line), the duration of crop growth until the temperature sum for maturity is reached (thin line) and the resulting relative grain yield (thick line) as functions of temperature [derived from the Daycent parameterisation for maize]. Temperature is assumed to be constant over the entire growth cycle.

Nitrogen

Plant growth essentially needs minimum amounts of nitrogen per unit of assimilated carbon and therefore available nitrogen sets an upper limit to biomass production at each time step. In agricultural systems the fertilizer input largely governs the availability of nitrogen and thus constrains maximum production. At near steady-state conditions, the yield levels and the associated nitrogen removal with grain will not significantly exceed the annual nitrogen added to the soil in terms of mineral fertilizer, manure, plant residues and depositions from the atmosphere (except for legumes). In fact, yields may be lower because of nitrogen losses via leaching and gaseous emissions.

2.2.2 Planting dates

As crop yields are sensitive to planting dates and the length of the growing season planting data for different regions of the world are an important input parameter that determines regional crop response to climate conditions. Although some organizations or projects provide information on crop-specific planting dates [*FAO-Geoweb*, 2004; *USDA*, 2004b] this information is not sufficient for a global yield modelling exercise because of several reasons. First, not all countries and not all crops are covered by these databases. Second, planting dates often differ within one country which is only considered for very large countries in these databases. Third, planting dates change with climate change [*Kucharik*, 2003; *Myneni and Nemani*, 1997], and any project that aims to simulate future crop yields can not rely on static crop calendars.

Therefore we developed a scheme to calculate global planting dates on a global 30 arc minutes grid, based on average monthly climate (Climate Research Unit, monthly average for temperature and precipitation for 1961-1990 [*New et al.*, 2000]). For all grid cells within a crop-specific thermal envelope a more detailed consideration of potential growth and water limitation is implemented. For crops that can either be grown as winter or summer crops (e.g. wheat) we assume that the

(higher yielding) winter variety is grown wherever the temperature is not falling below a critical temperature during winter (-10°C), but drops below the vernalisation temperature (6°C). These values are adjusted to account for the use of monthly mean temperatures. Planting dates for winter crops are then calculated so that a certain effective temperature sum, which is needed for germination and establishment of seedlings, is reached before the coldest month. For all summer crops the planting date algorithm uses a simplified yield modelling routine to calculate crop yields for all 12 potential planting months, and the planting month with the highest crop yield is then selected as the "optimal" planting month.

The "simplified yield modelling routine" includes a monthly production function and a reduction of potential production by water stress expressed as available water to PET, both analogous to the Daycent algorithms. Accordingly, crop growth continues until the temperature sum for harvest is reached. No yield is formed if temperature drops below a critical value during the growth cycle (like in Daycent), and if the duration of crop growth exceeds or under-runs a crop-specific minimum or maximum threshold. Based on the thus calculated yields of all possible planting months the optimum planting date is selected. Sequential cropping is not implemented in this first version though the algorithms are suitable to optimise double or triple cropping as well.

2.2.3 Input data and simulation methodology

All data sets used for the global simulation, its spatial resolution and the reference time period are listed in Table 2-1, while a comprehensive description of these data and the simulation methodology is provided in the Chapter 2.5.

Table 2-1. Data sets used and simulation settings

Data set	Spatial reference	Temporal reference	Source
Weather data	0.5° lat x 0.5° lon	monthly averages 1961-1990	[*New, et al.*, 2000]
Soil data – Bulk density, C, N	5 arc min x 5 arc min		[*Global_Soil_Data_ Task_Group*, 2000]
Soil data – pH, texture	5 arc min x 5 arc min		*[FAO*, 1995]
Land use	Crop fraction on 5 arc min grid	early 1990ies	[*Leff, et al.*, 2004]
Management – fertilizer nitrogen application	Country averages	mid 1990ies	[*IFA*, 2002]
Management – manure nitrogen application	Country averages	mid 1990ies	[*Siebert*, 2005]
Planting dates	0.5° lat x 0.5° lon	Based on climate 1961-1990	This paper
Fertilizer application dates	Depending on planting & harvesting dates; 0.5° lat x 0.5° lon, application in four events	Based on climate 1961-1990	This paper
Manure application dates	Depending on planting &harvesting dates; 0.5° lat x 0.5° lon, application in two events	Based on climate 1961-1990	This paper
Irrigated area	Irrigated fraction on 5 arc min grid	mid 1990ies	[*Döll and Siebert*, 2000]
Global simulation	0.5° lat x 0.5° lon, using dominant soil type of 5 arc min soil map	30 years, last 10 year averages as results	

2.3 Results and Discussion

2.3.1 Global planting dates

The planting dates for wheat, rice, maize and soybean calculated as described in Chapter 2.2.2 are shown in Figure 2-3. The only possible way of validating these results is by comparing them to crop calendars [*FAO-Geoweb*, 2004; *USDA*, 2004b] which are in most cases not spatially explicit, but provided as country-specific values. Therefore simulated planting dates were averaged over the entire crop-specific area within one country [*Leff et al.*, 2004] and then compared to the crop calendar (Figure 2-5). This approach will certainly cause problems in countries where planting dates and crop distributions are not homogenous within the crop area. In addition to the actual planting date the planting routine indicates whether a crop can be grown at all under the temperature regime of a certain location (see Chapter 2.2.2). In Figure 2-3 these temperature envelopes are marked in grey.

Wheat

Planting dates for wheat are primarily determined by criteria allowing winter or only summer wheat cropping. The expansion of winter wheat to high latitudes, which is determined by the minimum winter temperature, is met reasonably well as shown in Figure 2-4 for China and the US. The growing of winter wheat towards lower latitudes is restricted by low temperatures needed for vernalisation. But even in regions where temperature does not fall below the vernalisation threshold the simulated optimal planting date for summer wheat is before the coldest month, i.e. around December for the Northern Hemisphere, e.g. in Spain and the southern USA, (Figure 2-3a), which is also reported by USDA data [*USDA*, 2004b].

In addition to the summer-winter wheat pattern it can be observed that planting of winter wheat is simulated later in the year towards lower latitudes. The crop calendars from USDA for European countries report planting dates from Sep-Oct in Sweden to Nov-Dec in Spain [*USDA*, 2004b], and the simulated planting dates agree very well with this trend (Figure 2-3a). The explanation for this effect is that in the North the development to the phenological state essential before the onset of winter is slower and, additionally, winter begins earlier.

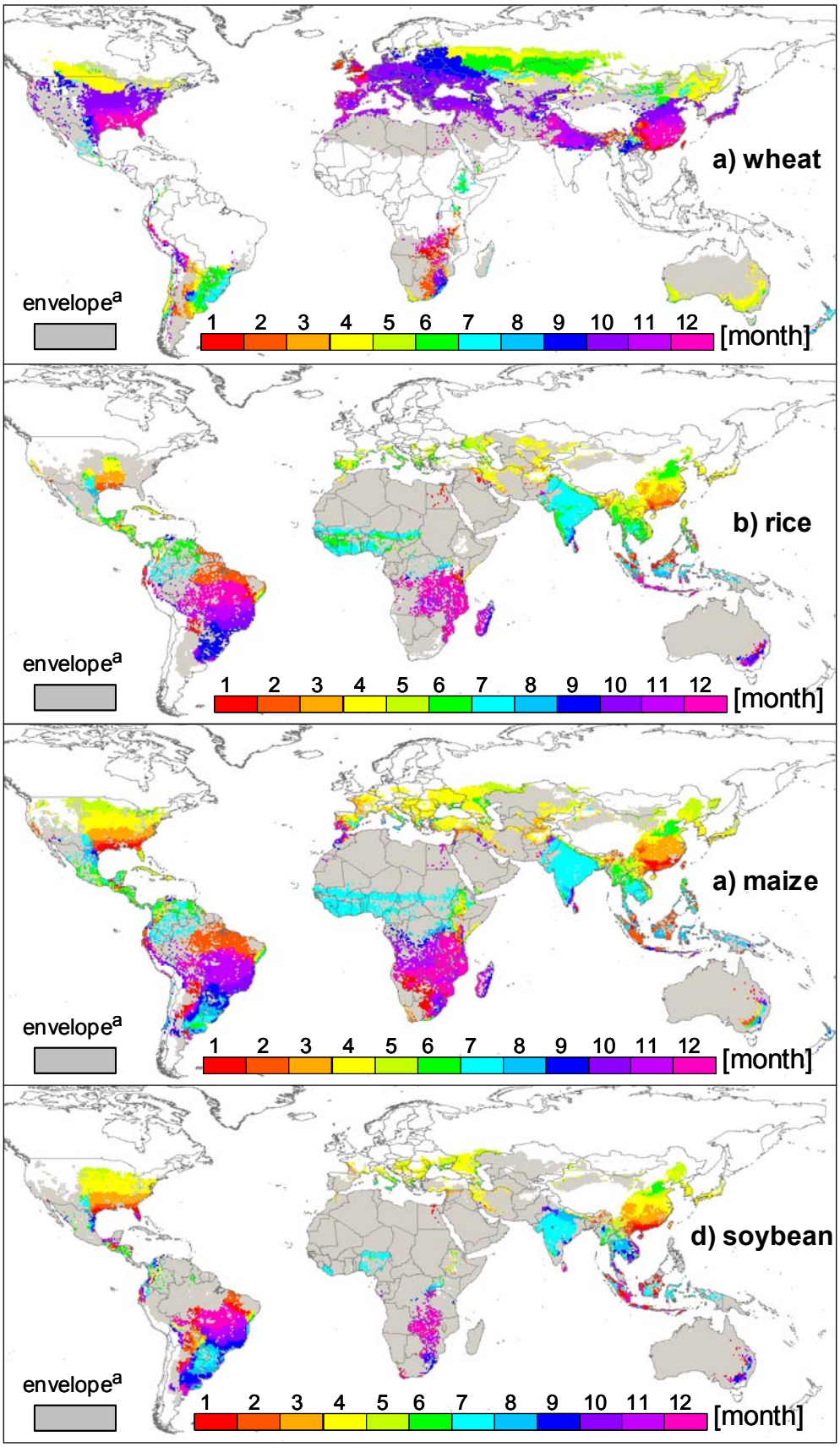

Figure 2-3. Global planting dates for wheat (a), rice (b), maize (c) and soybean (d), masked with the crop area according to *Leff et al.* [2004].

[a] The complete envelope comprises the coloured planting date areas plus the grey area.

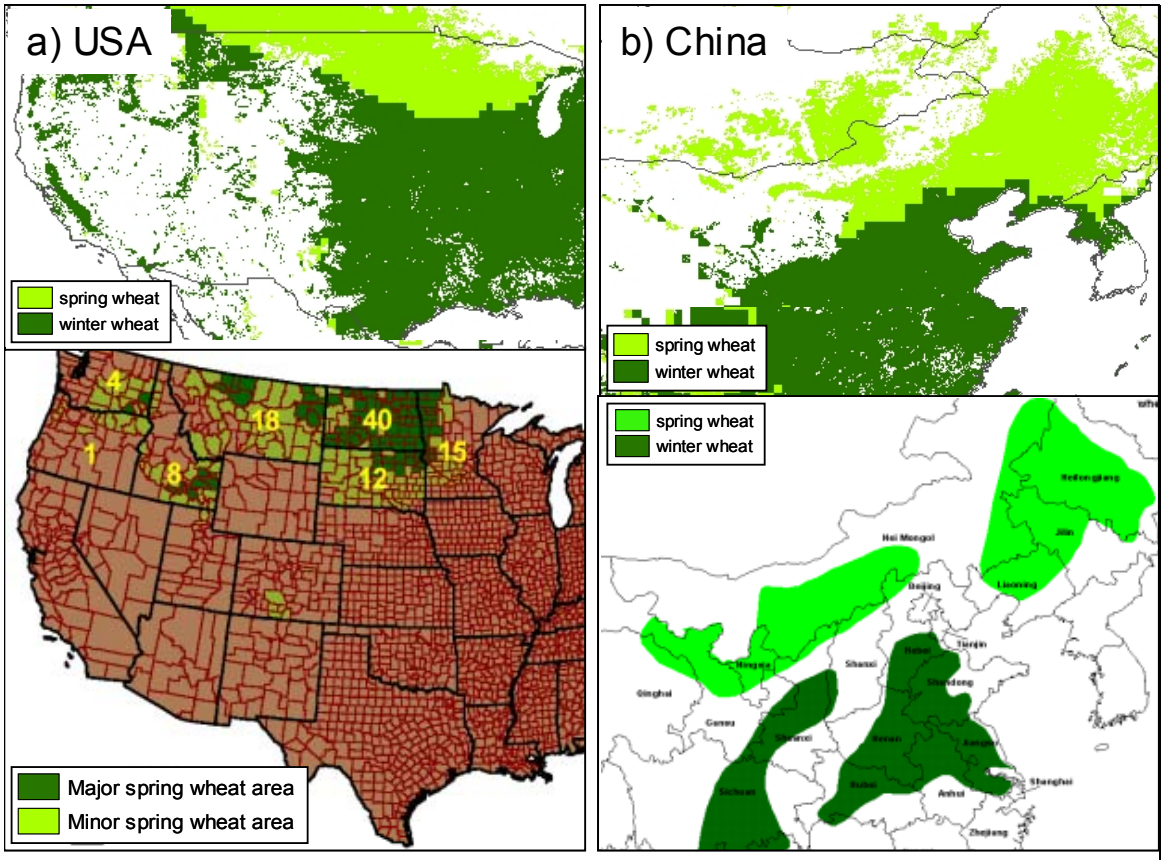

Figure 2-4. Areas of winter and summer wheat cropping in the USA (a) and China (b) as simulated by the planting date algorithm (top) and according to *USDA* [2004b] (bottom).

Figure 2-5a shows the country-level comparison between simulated planting dates and crop calendars. For countries where both winter and summer wheat are grown the two varieties are represented by separate data points (Canada, Russian Federation). A significant clustering of planting dates can be observed around Sept-Dec (northern-hemisphere winter wheat and southern Hemisphere spring wheat) and May-September (northern-hemisphere spring wheat and southern Hemisphere winter wheat) with winter wheat countries accounting for the majority of the data points represented.

Figure 2-5a generally indicates that simulated planting dates for wheat agree reasonably well with crop calendars, only South Africa and Zimbabwe are far off. This is due to the planting routine selecting the optimum planting date under *rain-fed* conditions. In countries where almost 100% of the respective crop is irrigated like in Zimbabwe and South Africa, this may differ from the actual (irrigated) planting date, and when calculating the irrigated planting date it agrees with the crop calendar. This trade-off between temperature and water limitation is also present in the rest of southern Africa, where the planting routine predicts October to December for wheat (therefore summer wheat) to take full advantage of the rainy season, while the crop calendars' planting dates are around June (therefore winter wheat), to benefit from the lower and thus more suitable winter temperature, even though there is no significant irrigation (data not shown). It therefore has to be concluded that the planting date routine overemphasizes the water over the temperature regime, which causes false estimations in some arid countries.

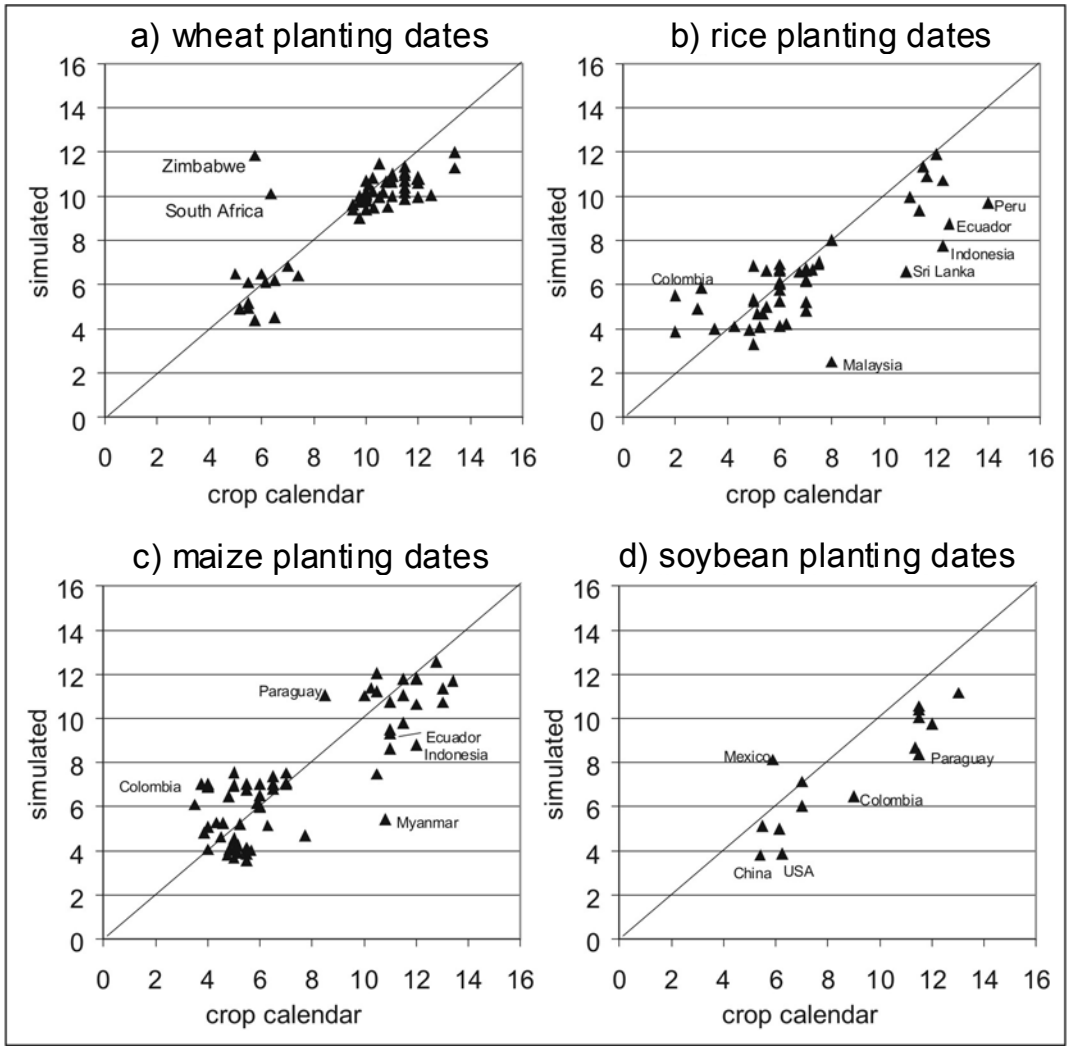

Figure 2-5. Comparison of simulated planting dates and FAO crop calendars [*FAO-Geoweb*, 2004] per country for wheat (a), rice (b), maize (c) and soybean (d).

Another miscalculation of planting dates occurs in the high latitudes, where snowmelt can provide a considerable amount of water in summer-dry areas, and where crops are therefore planted soon after. The planting date routine does not include a snow module so far, and therefore calculates later planting dates. This phenomenon only affects the coldest margins of cropping areas with additional occurrence of pronounced droughts during spring and summer. It is relatively uncommon and not significant for most countries. But for Kazakhstan the systematic underestimation (Figure 2-5a and 2-5c) can partly be explained by the ignorance of melting water.

Rice, maize and soybean

Planting dates for rice, maize and soybean (Figure 2-3b-d) show similar patterns and problems and will therefore be discussed together. Their agreement with crop calendars is reasonably good though some significant discrepancies occur in all plots. These can partly be explained in the following way:

Many islands or insular states exhibit complex precipitation patterns, often completely differing on opposite sites of an island, which make it impossible to estimate a single planting date. Therefore simulated planting dates differ significantly from crop calendars for some Southeast-Asian countries like Indonesia (rice and maize), and Malaysia and Sri Lanka (rice).

A similar problem occurs in countries with strong climatic and elevation gradients like in the north-western Andes states of Latin America, causing almost chaotic planting date patterns in Colombia, Ecuador and Peru. Averaging over these data leads to almost random agreement or disagreement with crop calendars for these three countries.

Another inaccuracy is caused by the discrepancy between real crop area and the area over which the average is calculated. The global map of crop distribution [*Leff et al.*, 2004] only includes sub-national data for Canada, the USA, Mexico, Brazil, Argentina, Turkey, the Russian Federation, China, India and Australia, but for all other countries the crop area is almost identical to the agricultural area and therefore often differs from the "real" crop area as e.g. reported in *FAO-GeoWeb* [2004], which was not available in a geo-referenced electronic format. This leads to inaccuracies in the averages, especially if planting dates show strong gradients within a country. The only way of addressing this problem is by including sub-national data and/or the maps provided by *FAO-GeoWeb* [2004] to improve the crop distribution map.

The fourth problem occurs if there is a wide range of planting dates within a country's crop area. In some cases FAO provides the complete range of planting dates, and therefore FAO average and simulated average may agree, but sometimes only the crop calendar for the main region or even two crop calendars (for several African countries) are given. For the US and China, the *USDA* [2004b] provides information that rather applies to the northern area, while stating that planting dates are 1-2 months ahead in the southern part. As we consequently applied the crop calendar as it is and did not manipulate it based on such statements, simulated average planting dates of rice, maize and soybean are ahead of time for these countries (Figures 2-5b-d). Another example for this phenomenon are some central African countries like Congo, where a steep north-south gradient of planting dates is observed and therefore two crop calendars are provided. The same shift is present in the simulated planting dates, proving that the essential mechanisms are very well captured. In these cases (Congo, Uganda) only one crop calendar and the simulated average over the respective area are compared.

2.3.2 Thermal envelopes

The (thermal) envelope allowing the production of a specific crop calculated by the planting date routine is presented in Figure 2-3, by the coloured presentation of the actual planting date (on the actual crop area) and in grey (outside the actual crop area). A grey envelope area extending to higher latitudes than the crop area indicates a "larger" envelope than actually used for crop growth. No additional grey envelope area towards the poles indicates an agreement between the envelope and the crop distribution or a too restrictive envelope, though this conclusion is only valid if the crop distribution map includes sub-national data that are detailed enough to reflect small scale crop distribution. In the southern hemisphere the envelope of all crops is expanding further south than the crop area, while in the northern Hemisphere northern borders of envelope and crop area almost match. The only exceptions are the Russian Federation, where the area of all crops seems to expand

further north than the respective envelope because of too coarse sub-national data, and China, where the envelope is too restrictive for rice. That also agrees with a comparison to the crop distributions provided by *FAO-GeoWeb* [2004] or *USDA* [2004b], which were both not available electronically.

2.3.3 Global crop yields

Based on the planting dates and the input datasets listed above Daycent simulations were carried out. Yields were averaged over the last ten years of the 30-year simulation period and are presented as maps in Figure 2-6.

Several strategies can be employed to test the performance of a global crop production model. The use of experimental site data is desirable in that such data usually comprise detailed information about weather, soil, management and yields. However, it was beyond the scope of this study to compile site data from all around the world in order to represent the various climate, soil and management conditions. The second way is to compare the simulated yields against census data, which is available on the sub-national to national scale. Since the Daycent model will be integrated into a global land use change model, it is important that it captures the differences in national yield levels. We thus decided to test our simulation results against FAOSTAT data [*FAO*, 2004] which is provided for all countries of the world. Furthermore, we used sub-national county level census for selected countries in order to test whether Daycent is able to capture the spatial variability of yields (Chapter 3.5).

In order to determine national averages of simulated yields we first calculated average rain-fed and average irrigated yield by (1) assigning the simulation result of a 30 min cell to all underlying 5min cells and (2) calculating the weighted average over all crop cells of the 5min land use map. We then weighted rain-fed and irrigated yields according to the fraction of irrigated area per crop which we derived by relating crop-specific irrigated area for the late 1990s as provided from FAO AQUASTAT [*FAO*, 2001b] to total crop-specific area (FAOSTAT, averaged over the years 1998-2000). If no AQUASTAT data were available for a certain crop or country, the national mean fraction of irrigated area was used for non-rice crops, while for rice we then applied the global average fraction of irrigated rice (64%) as derived from AQUASTAT.

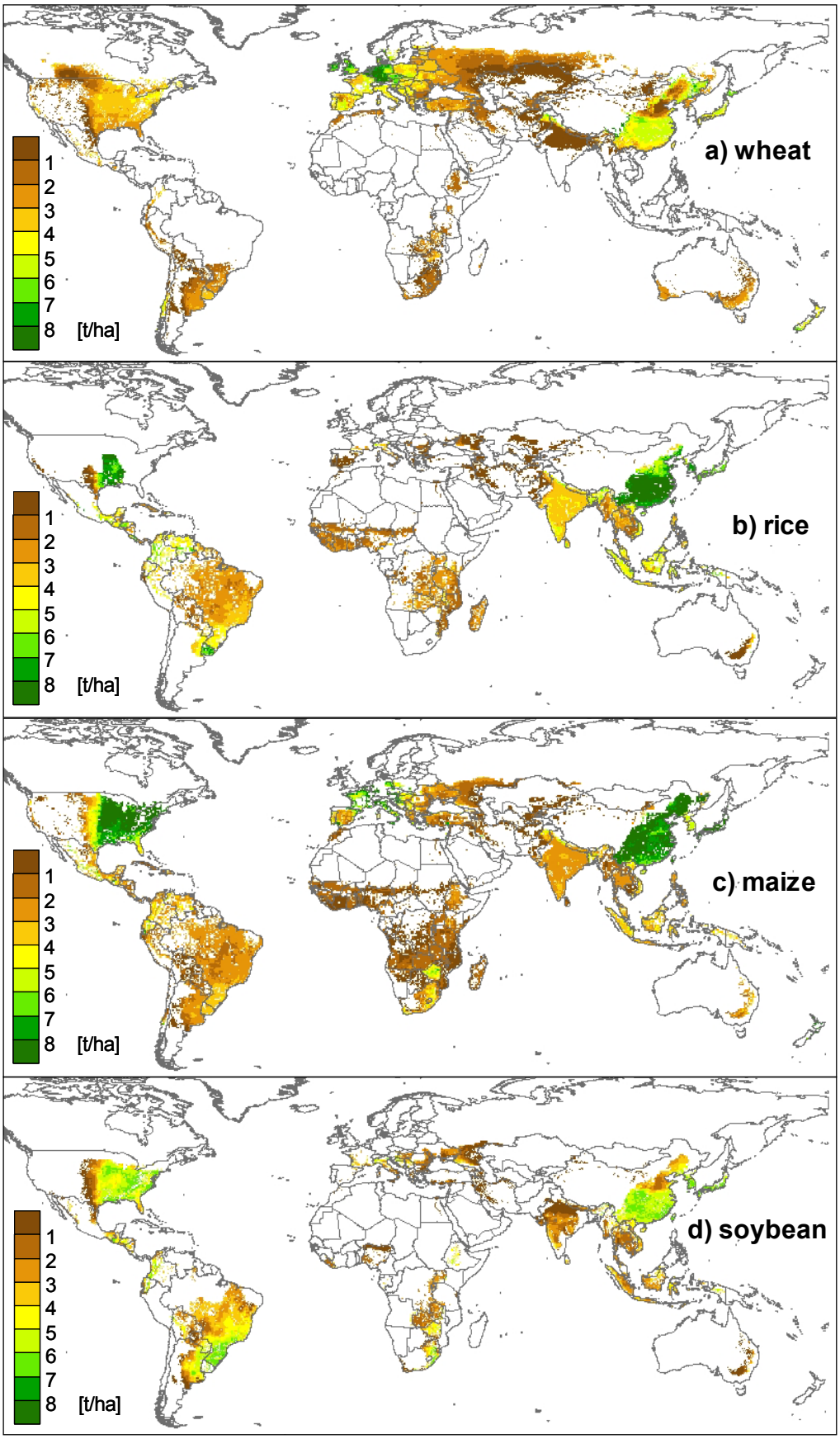

Figure 2-6. Global yield levels for rain-fed wheat (a), rice (b), maize (c) and soybean (d) simulated by Daycent.

The comparison between the simulated national averages and the national reported yield levels (FAO, average over the years 1991-2000) is shown in Figure 2-7. We chose the FAO 1991-2000 average yield levels because the management data with respect to irrigation and particularly fertilisation is representative of the mid 1990s. The analysis was carried out for all countries with an average agricultural area exceeding 1200 ha (in the years 1991-2000). The single scatter plots only show countries that possess both a reported FAO yield and a simulated yield. To highlight the relevance of a country's crop production we created "bubble plots", with the area of each bubble proportional to a crop's harvested area within that country. These plots are shown in Figure 2-8.

Three different measures of agreement are presented in Table 2-2. The R^2, the R^2 weighted for a crop's area and the R^2 weighted for a crop's total production within one country in order to reflect the relative importance for the global crop market.

For wheat all three measures of R^2 are very similar, while for rice large producer countries are better estimated than others, which causes a higher weighted R^2. For maize, weighting by area does not affect the R^2 much, but weighting by production results in a lower R^2, as some countries (especially China) with high yield levels show a considerable deviation from the reported FAO yield. For soybean, the effect of weighting is strongest, as simulation results for the few countries dominating global production are – except for China – much closer to reported yield than on average.

In total, the level of agreement for wheat, rice and maize (unweighted $R^2 \approx 0.66$) seems acceptable considering the uncertainties inherent to data and computation of crop yields. An independent estimation of the simulation success would only be possible by a comparison with other global crop model results. This is not possible at the moment, as only one other global crop model has been applied to represent FAO yield data – the EPIC model –, but no measures of agreement or deviation are reported [*Tan and Shibasaki*, 2003]. Other large-scale crop modelling studies report R^2 values of e.g. 0.46 [*Kucharik*, 2003] and 0.0–0.74 [*Challinor et al.*, 2004]. Beyond, we have shown that - except for China - the model captures the yield levels of the major crop producers correctly. On the other hand, we found that the lack of nitrogen limitation for soybeans has severe implications for the level of agreement between simulated and reported yields, and that the provisional approach to account for phosphate limitation (as described in Chapter 2.5) improves accordance with FAO data, but still leaves much of the variability unexplained.

Table 2-2. Coefficients of determination for country averages of wheat, rice, maize and soybean yields as presented in Figure 8.

	R^2	R^2 weighted for area	R^2 weighted for production
Wheat	0.663	0.659	0.652
Rice	0.657	0.785	0.795
Maize	0.672	0.659	0.522
Soybean	0.321	0.558	0.418

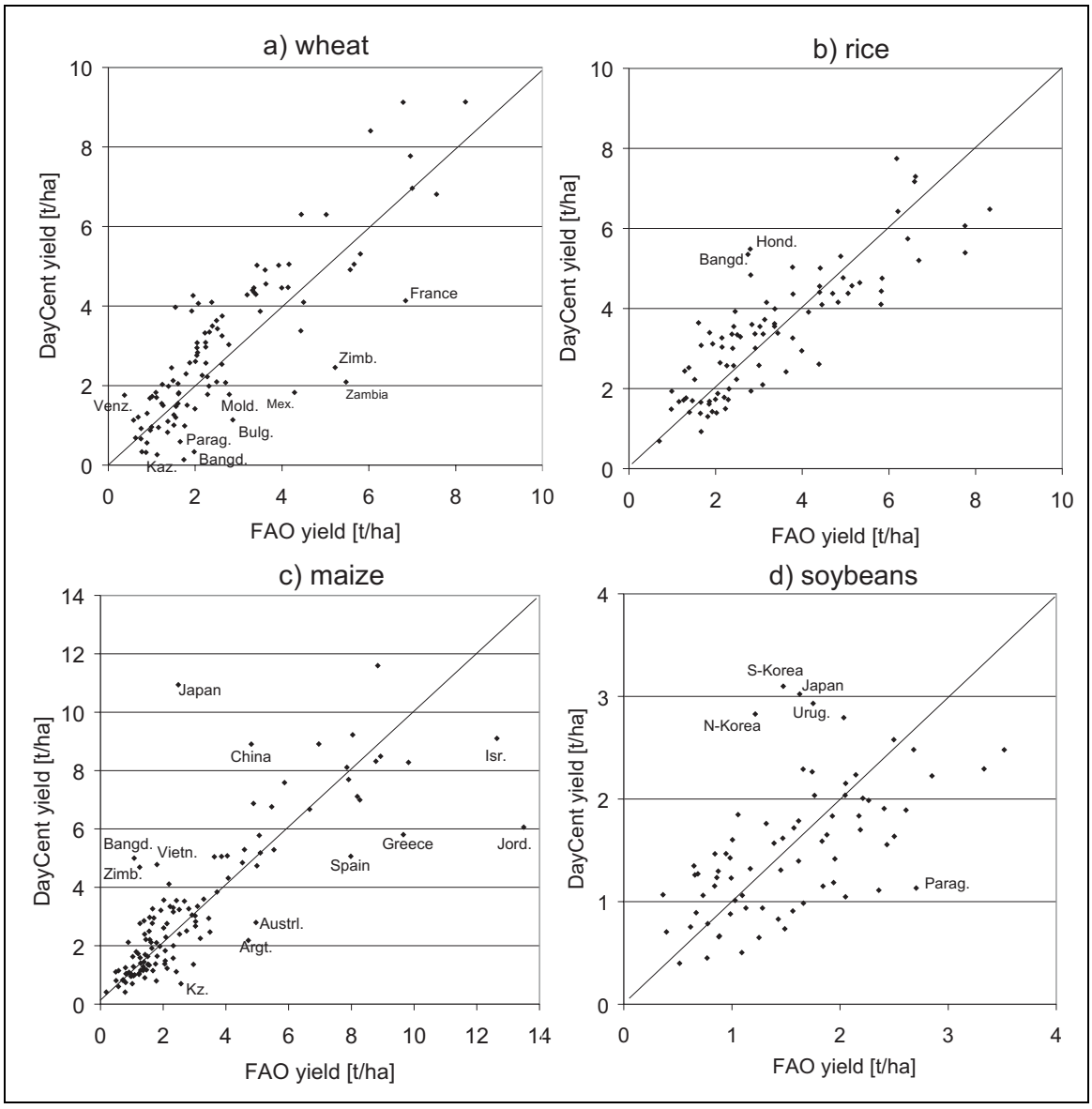

Figure 2-7. Comparison of simulated yields and FAOSTAT data per country for wheat (a), rice (b), maize (c) and soybean (d).

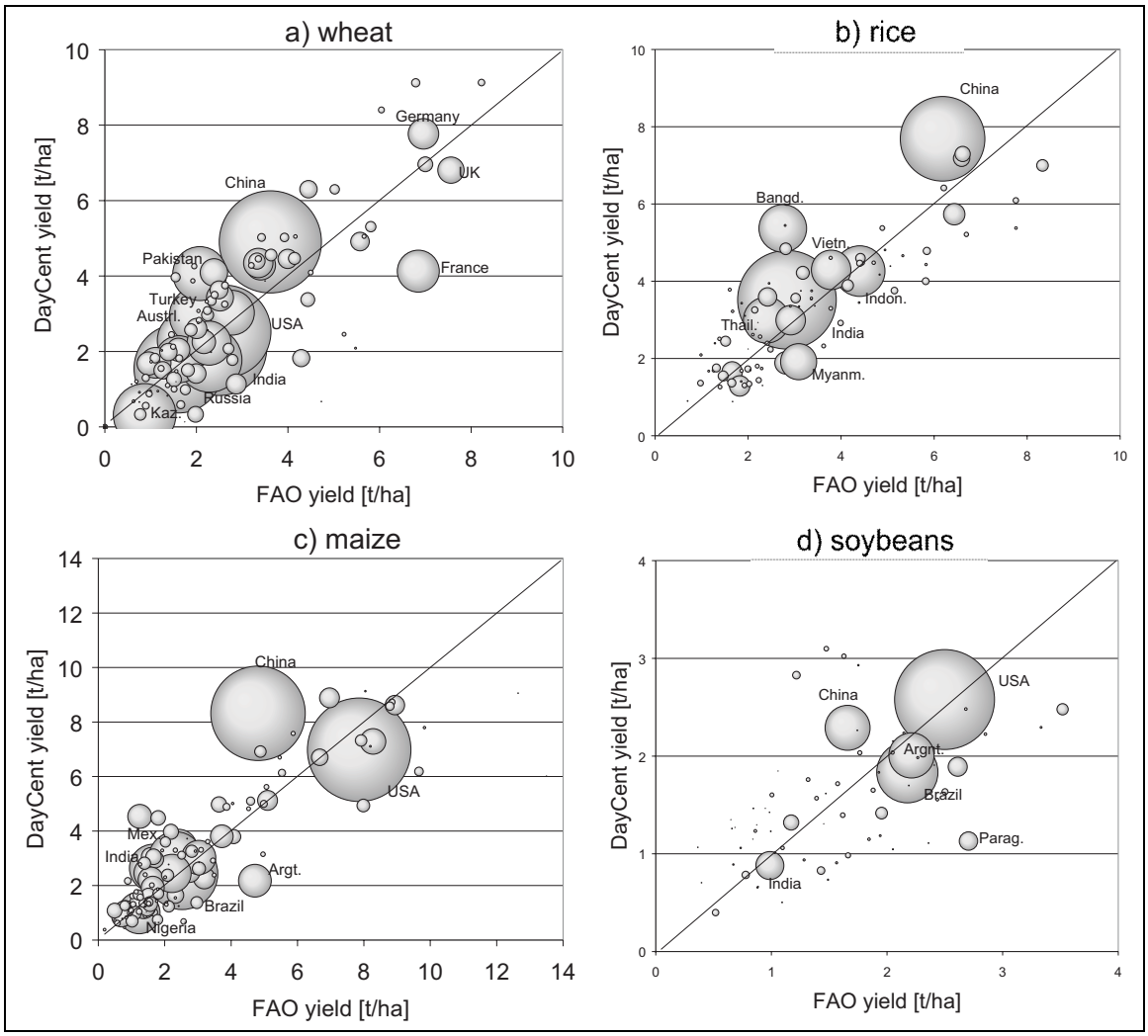

Figure 2-8. Comparison of simulated yields and FAOSTAT data per country for wheat (a), rice (b), maize(c), soybean (d). Areas of circles represent crop area.

2.3.4 Uncertainties

During model testing, the uncertainty in a number of input data sets was identified to strongly affect simulation results. The most important parameters and effects are therefore discussed in the following.

Fertilizer application rates

One of the most sensitive parameters for Daycent crop growth is the availability of nitrogen, mainly determined by inputs of mineral fertilizer or manure. In the long run, FAO yield levels can only be reached if the total nitrogen input approximately equals the nitrogen removal associated with this yield level, whereby nutrient mining can compensate for insufficient nitrogen supply to some extent. Large discrepancies between nitrogen application rates as reported by the International Fertilizer Association (IFA) and the amount of nitrogen that would be removed with the FAO yields cause a significant underestimation of crop yields for several countries: France,

Bulgaria, Moldova Republic, Lithuania, Bolivia (wheat) and Argentina, Bolivia and Moldova Republic (maize).

On the other hand there are several countries where the input of mineral fertilizer reported by IFA largely exceeds the nitrogen that would be removed with FAO yield levels. In some of these cases, if a country's climate is favourable for the respective crop or if the fraction of irrigated area is high, the high nitrogen input causes an overestimation of crop yields. This can be seen for Honduras, Pakistan and Venezuela (wheat), for Bangladesh and Honduras (rice), and for Bangladesh, Guatemala, Japan, Viet Nam and Zimbabwe (maize). As an example we show for maize the total annual nitrogen input through manure and mineral fertilizer versus the annual nitrogen removal that would be associated with FAO yield levels (Figure 2-9).

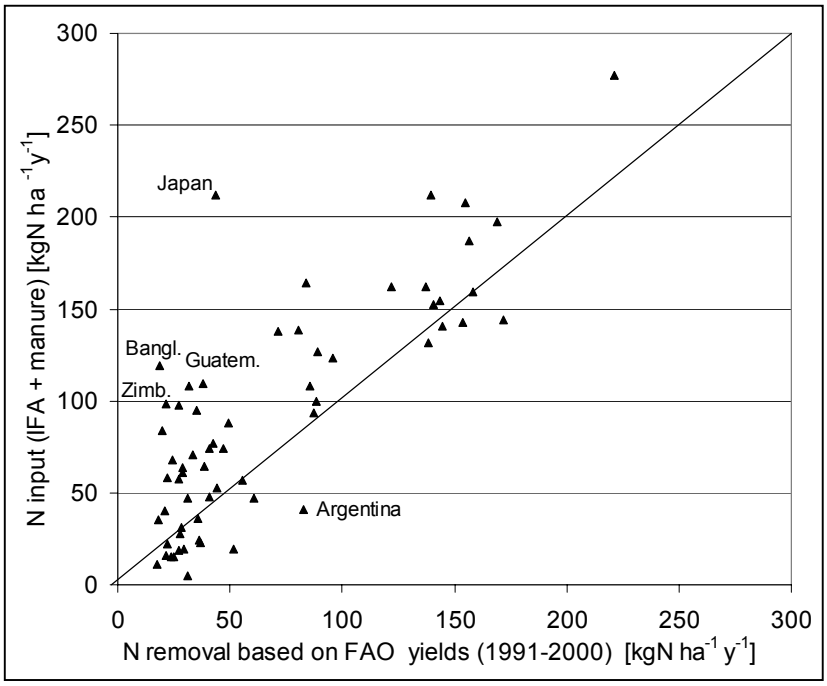

Figure 2-9. Comparison of total N input (mineral fertilizer + manure) and N removal through harvest according to FAO (yield * N content) for maize.

Irrigated area

In large areas of the world irrigation significantly increases agricultural production, and many countries have significant fractions of irrigated cropland. Therefore data on the actual fraction of irrigated area *by crop* is crucial to correctly estimate a country's average crop yield. Crops like maize and soybean have particularly high water demands [*Allen et al.*, 1998] and are thus known to be irrigated above-average [*Iglesias and Minguez*, 1997; *Kapetanaki and Rosenzweig*, 1997]. If no crop specific irrigation data are available, the yields of these crops are therefore likely to be underestimated. This can be seen for maize yields in Spain, Greece, Australia, Israel and Jordan, and for soybean yields in Syria, Spain, Greece and Australia. Accordingly, crops which are commonly irrigated below average tend to be overestimated as can be seen e.g. for wheat in Spain, Greece and Israel.

Crop specific area

As described above, national yield levels were derived by averaging the simulated yields over the entire crop area of the land use map, weighted by crop fraction. This will lead to false estimates in countries where the real crop area differs from the land use map similarly as it has already been discussed for the averaging of planting dates (Chapter 3.1). *Leff et al.* [2004]consider sub-national data for Argentina, Australia, Brazil, Canada, China, India, Kazakhstan, Mexico, the Russian Federation, Turkey and the US. In all other countries, they distributed the specific crop area homogeneously over the entire agricultural area. Furthermore, for some countries the spatial resolution of the sub-national census is very coarse and covers very different climatic conditions (e.g. Australia and the Russian Federation). The problem of heterogeneous crop distribution can only be solved by including more detailed sub-national statistics which was done in our study only for soybeans in Australia and Italy [*ABS*, 2000; *Eurostat*, 2004]. For most other countries, additional sub-national data was either not directly available (not as geo-referenced digital data, e.g. USDA and FAO-GeoWeb) or its consideration would have been beyond the scope of this study. Thus, strong deviations remain. For example in Paraguay, simulated yields and crop area according to USDA are concentrated in the southeast, while the crop areas according to *Leff et al.* [2004], which were used for averaging, are distributed almost over the entire county. This 'mislocation' leads to an underestimation of all crops yields (Figure 2-7) except for rice, which is irrigated by 100% and therefore not affected by this problem.

Planting dates

The planting date is another crucial parameter for simulated crop yields, as it influences the temperature and precipitation regime under which the crop will grow. In general, the planting date routine produces reliable estimates (Chapter 2.3.1). However, the underestimation of crop yields in some arid countries can be attributed to incorrect planting dates. For non-rice crops we use the "rain-fed" planting date, as in most regions rain-fed agriculture is dominating, and in many cases the availability of water for irrigation is assumed to follow the seasonal fluctuation of precipitation. But for arid areas, where rain-fed cropping is virtually impossible and the entire crop area is irrigated, planting dates may be rather adjusted to the temperature regime. But as there is no straightforward concept to decide whether to use irrigated or rain-fed planting dates we decided to keep the rain-fed planting dates and only explain when this leads to potentially incorrect results. Wheat in Zimbabwe, Zambia and Bangladesh is irrigated by almost 100%, and only our irrigated planting dates agree with those provided by the FAO-GeoWeb (Chapter 2.3.1). Using the rain-fed planting dates leads to a strong underestimation of yields for these countries (Figure 2-7a), while with irrigated planting dates simulated yields almost double.

2.3.5 Selected spatial patterns

National averages of crop yields as presented in the previous section are strongly determined by national fertilizer application rates, therefore a model's accurate sensitivity to spatial parameters like climate and soil can be more rigorously assessed by comparing spatial patterns of crop yields.

In the following, we compare the simulated spatial patterns of wheat yield to sub-national census data from the US [*USDA*, 2004a], averaged over the years 1992-95, and from Australia, averaged

over the years 1993-95. We chose these examples, as both countries have significant climatic gradients and because yield data were available at the county level.

Wheat cropping in the US

In Figure 2-10 we present the spatial pattern of wheat yield in the USA. The census also provides the fraction of irrigated wheat for many countries, particularly west of 95°E, where most irrigated wheat areas can be found. This information was used to calculate weighted simulated rain-fed and irrigated yield averages on the county level. Finally, we masked the county areas using *Leff et al.* [2004].

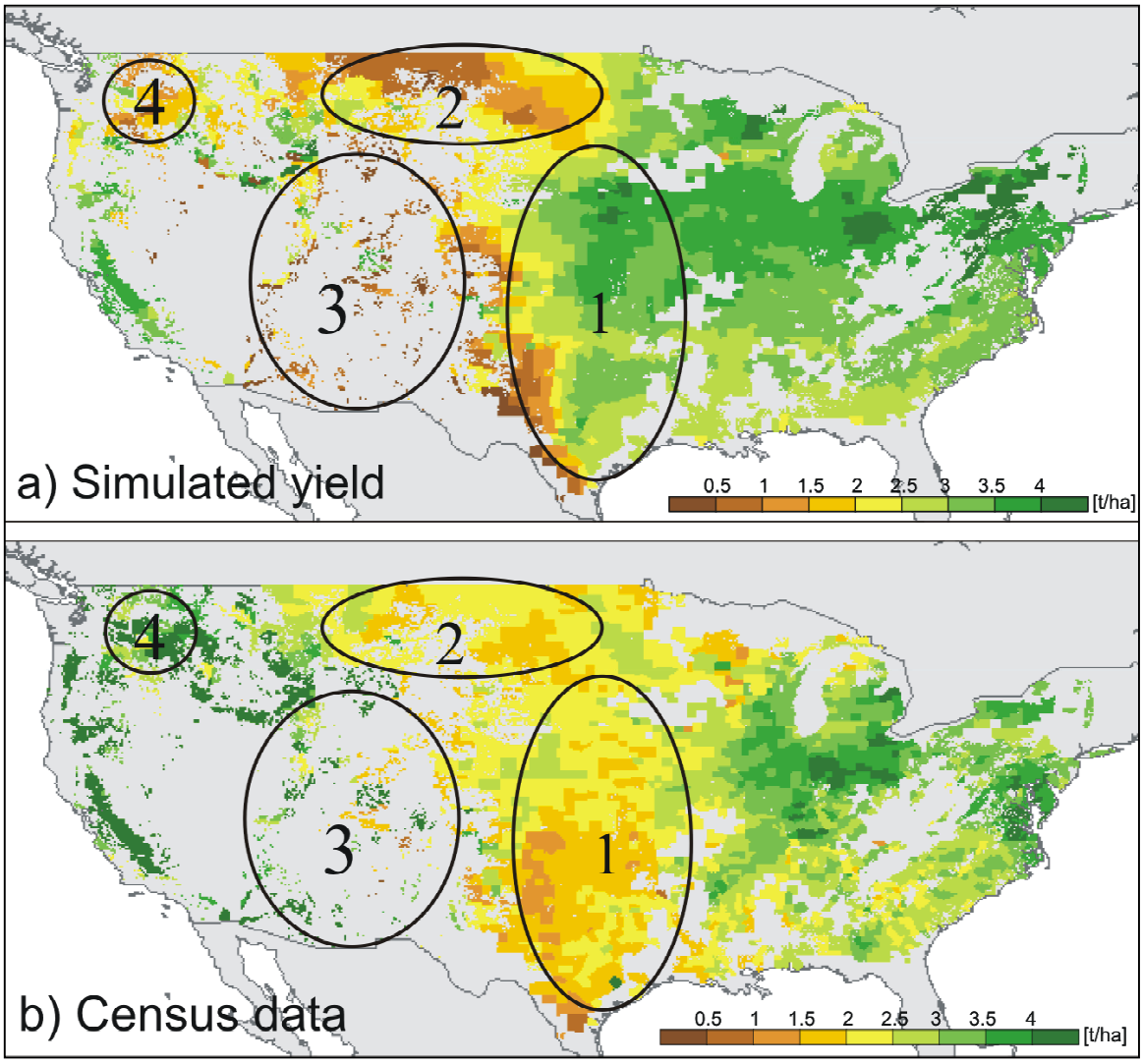

Figure 2-10. County averages of simulated wheat yields (a) and USDA census data (b) for wheat yields in the US. Circles indicate regions that are explicitly discussed in the text.

Yield levels are estimated accurately in the eastern part of the country, ranging from about 4 t ha^{-1} in the northeast to about 3 t ha^{-1} in the south-eastern part. This north-south gradient can be attributed to higher temperatures causing a shorter growing period and partly also lower weekly production. The east-west transition to lower yielding areas in the Great Plains is located too far westwards in the Daycent results compared to the county data (Figure 2-10, circle 1). Beyond, the

simulated east-west yield gradient is much too sharp. The second significant discrepancy between simulation results and county data occurs in the Northern Great Plains of the US (Figure 2-10, circle 2). The low simulated yields in circle 3 and circle 4 show only rain-fed yields, as no irrigation data were available for these counties. However, *Döll and Siebert* [*Döll and Siebert*, 2000] show irrigated areas in these counties which explains the high census yield.

The discrepancies in circles 1 and 2 might be explained by the following:

(i) Imperfect representation of water stress in the Daycent model, (Chapter 2.2.1) may lead to the observed underestimation of the drought effect in the eastern part of the Great Plains, while we overestimate the impact of drought in the western part of the mid-west. Accordingly, we seem to overestimate the impact of water stress in the Northern Great Plains of the US, were water is limiting crop production.

(ii) Spatial variability of fertilizer input might be important, too. For our simulation, we apply only one fertilisation rate for the entire US (80 kg ha^{-1}), although fertilizer application varies spatially [*Donner and Kucharik*, 2003].

(iii) Impacts of interannual climate variability might cause a discrepancy because of different reference time periods. For our global simulation, we used climate normal data for 1961-90, while the census data is representing average yield only for the years 1992-95.

Wheat cropping in Australia

For Australia the fraction of wheat area according to *Leff et al.* [2004], the simulated wheat yield and county data of wheat levels are presented in Figure 2-11. Wheat specific irrigation data were not available, and as the average irrigated fraction of agricultural area only amounts to 5%, simulated county averages were calculated only based on the rain-fed yield. To ease and accentuate the interpretation, a black line was drawn along the northern edge of wheat cropping [*Leff et al.*, 2004] and superimposed to all maps.

Except for the eastern and north-eastern regions the transition from high wheat fractions (around 80%) to virtually no wheat cropping is very sharp, indicating that wheat is dominating agricultural area up to its northern margin imposed by a strong climatic gradient. This rather sharp transition from suitable to non-suitable conditions is present both in the simulation results and the county data. South of this line simulated yields and county data show similar gradients with highest yielding areas in the south-west, the south-east and Tasmania. Beyond these common features difference in yield levels can be attributed to the similar mechanisms already described above:

(i) Irrigation of wheat leads to high average yield levels under the arid conditions of some central counties, though the absolute wheat area in these counties is very small (Figure 2-11a).

(ii) An inconsistency of reference periods causes an apparently slight overestimation of wheat yield. While we used 30-year averages of climate, county-specific yield data were only available for the years 1992-1994, which were significantly lower than longer-term averages (in 1994 Australian yields only reached half of the normal level [*FAO*, 2004]).

(iii) Steep slopes in the south-eastern part of Australia are restricting wheat yields and wheat area (Figure 2-11a), which is not included in the model and therefore leads to the observed overestimation (see Chapter 2.3.7).

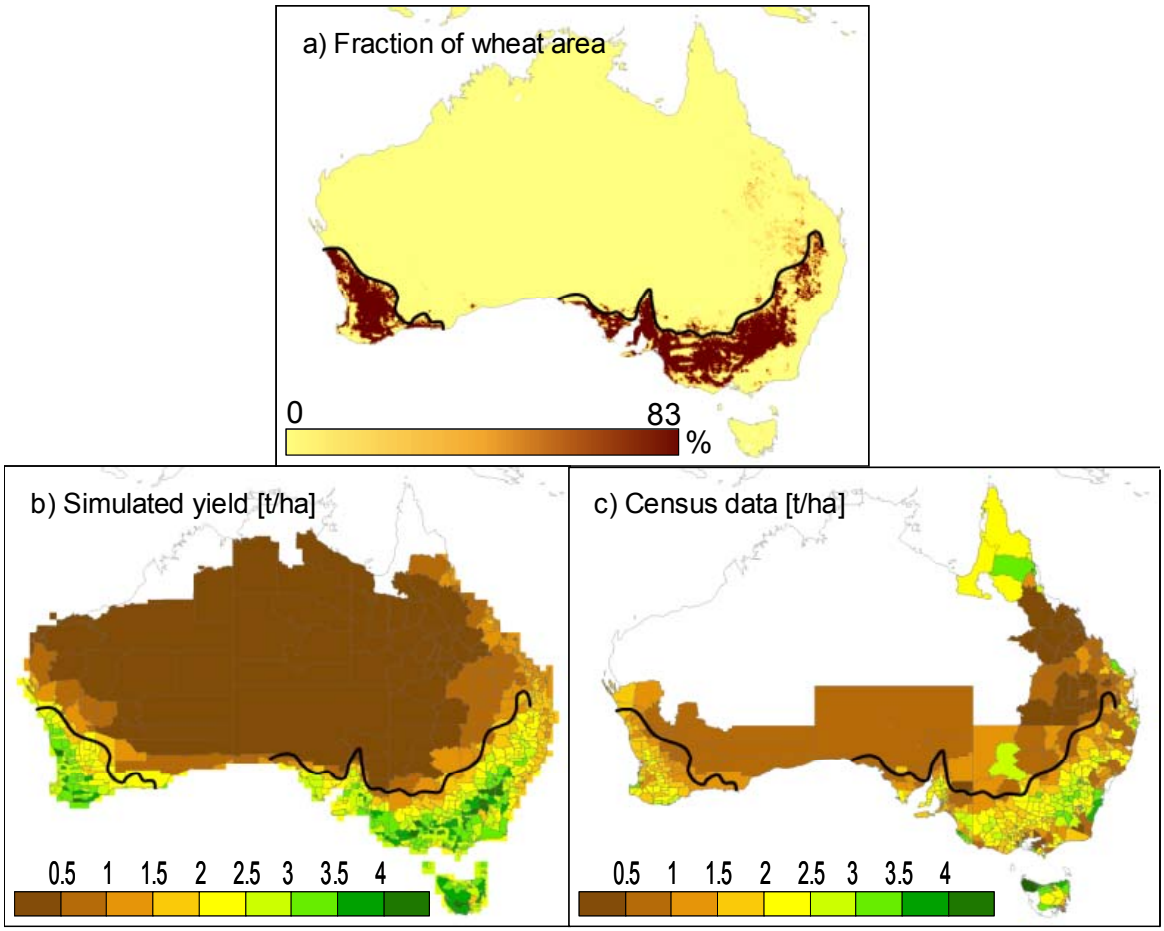

Figure 2-11. Fraction of wheat area (a) and county averages of simulated wheat yields (b) and census data (c) for wheat cropping in Australia.

2.3.6 Simulation of other crops

The four crops presented in this paper cover about 40% of the global agricultural area. In addition, we also calibrated Daycent for the simulation of sorghum, temperate and tropical pulses, potato, sweet potato, cassava and cotton. A presentation of these additional results is not possible within a single paper, and would not have provided additional insight, as most of the effects discussed here are also relevant for the other crops. Therefore it was decided to provide global yield maps for these crops in the appendix (Appendix A). It is important to note that these results have been checked internally, but were not submitted for external review.

2.3.7 Methodological issues

In a strict sense, the comparison of average national simulated crop yields and FAO data is no validation of the Daycent model. After parameterising the model based on literature reviews (e.g. effective temperature sum, base temperature, C/N ratios, harvest index, drought and frost tolerance)

average national crop yields were simulated and then – if necessary – calibrated to FAO yield data by modifying the crop-specific energy-biomass conversion factor "prdx". The final results were again compared to these FAO yield data and to selected spatial patterns of yield as derived from sub-national census. Though that is not a validation of the model, it still serves as an evaluation of model performance, as only one parameter was calibrated for datasets containing 74-127 records.

Another critical methodological aspect is the climate data set. Because of mainly technical reasons we used 30-year averages of monthly precipitation and temperature from the years 1961-1990, although management and FAOSTAT data refer to the mid-1990s, and although this approach does not account for inter-annual and daily climate variability. The sensitivity of the model to monthly instead of daily values and to the reference time period was tested by additional simulations with (1) daily climate data on a 2.5° grid [*ECMWF*, 2004], and (2) with monthly average for the years 1991-2000 [*Mitchell and Jones*, 2005]. The results of the first analysis were dominated rather by the effect of the coarser spatial resolution than the finer temporal resolution. For countries with relatively small-scale gradients of elevation, climate and – as a result – land use like Switzerland the yields were significantly lower (up to 20%) compared to the standard simulation because temperatures on a 2.5° grid cell tend to be lower than the actual temperatures over the agricultural area within this grid cell, which often is located only at the lower elevations (data not shown). As for the second analysis, using average climate from 1991-2000 [*Mitchell and Jones*, 2005], the global results indicate a low sensitivity to the different reference time periods (good agreement between simulation results for 61-90 and 91-00; bias = 1.02, $R^2 = 0.96$).

The Daycent model does not account for the impact of slope on crop yields. However, slope impact on crop yield is undisputed, is substantiated by statistical analysis [*Jiang and Thelen*, 2004; *Ping et al.*, 2004], and can be attributed e.g. to water stress through increased surface runoff, and to erosion reducing soil fertility and decreasing the rootable depth [*Strauss and Klaghofer*, 2001]. Furthermore sloping land restricts accessibility and the use of machinery, and has strong gradients in micrometeorological parameters. Most national averages are calculated accurately without slope effects because for most countries the agricultural areas are restricted to rather plain lowlands. Nevertheless there are some countries where significant fractions of cultivated land are sloping. This might cause the systematic over-estimation of simulated yields for non-rice crops in e.g. North- and South Korea and Japan.

A consistent implementation of slope effects in Daycent can not rely on simple yield reduction factors like the GAEZ model [*Fischer et al.*, 2002], but would require a process-based approach like in the EPIC model [*Williams et al.*, 1984].

2.4 Conclusions and Outlook

As we have seen, large scale crop modelling is subject to a wide range of uncertainties, with respect to both input data (particularly management), and the representation of processes influencing crop growth (e.g. formulation of water stress, phenological stages, impact of slope, etc.). Despite these uncertainties there is an urgent need for global crop models to assess future large-scale changes in land use, to study the impacts of climatic change on crop yields in different world regions, to examine the environmental consequences of agricultural practises, and to analyse

potential feedbacks between the terrestrial and the climate system. Therefore an integrated approach is needed to model plant production, the water cycle and carbon and nitrogen fluxes.

The adaptation and application of the Daycent model presented here provides an appropriate tool to address these issues, as it includes a detailed representation of soil biogeochemistry and is able to reproduce the major effects of climate, soil and management on crop production. We have shown that average simulated crop yields per country agree well with FAOSTAT yield levels ($R^2 \approx 0.66$ for wheat, rice and maize; $R^2 = 0.32$ for soybean) and that spatial patterns of yields mostly correspond to observed crop distributions and sub-national census data.

Beyond, our study demonstrated that further improvement of the Daycent model will be achieved by implementing water stress as the relationship between crop-specific actual and potential transpiration, by including phosphorous limitation for legumes and by accounting for the effect of slope on surface runoff, water and nutrient availability.

To account for the diversity of agricultural management at the global scale it is crucial to include regional differences in crop varieties and sub-national variability of management practices, e.g. based on the Farming Systems Map [*Dixon et al.*, 2001], and to implement sequential cropping and crop rotations, which are relevant for soil nutrient dynamics and realistic planting dates.

Among the different possible validation strategies for global crop models the approach followed here will be substantially improved if more accurate maps of global crop distribution are available to calculate national averages of planting dates and crop yields. Furthermore, remote sensing data (particularly leaf area index estimates) bear potentials e.g. for the identification of planting dates and phenological development, and the effect of water and nutrients on crop yields should be evaluated in more detail, possibly by using site data of crop growth. A first initiative on such a database that should cover the variety of environmental and management conditions around the world was taken recently during a crop-modelling workshop at Rothamsted, UK [*Scholze et al.*, 2005].

With a tool at hand that integrates plant growth, water, carbon and nutrient cycles at the global scale it is now possible to study the effects of climate change and inter-annual climate variability on crop yields in different world regions, to assess the impact of agricultural management on soil nitrogen dynamics and trace gas fluxes, and to calculate agricultural water demand and the impact of irrigation on crop yields.

Acknowledgements

We like to thank the Century developing team, especially Bill Parton and Cindy Keough, at Fort Collins/Colorado for providing and assisting us with the Daycent model. We thank Chris Kucharik (SAGE, University of Madison-Wisconsin) for helpful comments and critical review, and we are grateful for the support provided by the International Max Planck Research School on Earth System Modelling (Hamburg, Germany) and the STORMA project, funded by the German Research Foundation

2.5 Supplement: Input data used

2.5.1 Weather data

The Daycent model uses daily data on precipitation and maximum and minimum temperature, but on the global scale the choice of climate datasets is very limited. There are daily weather data on a 2.5° x 2.5° grid, provided by several research centres like ECMWF or NOAA, either as model results or as reanalysis data [*ECMWF*, 2004; *NOAA-CIRES*, 2004]. A finer 0.5° x 0.5° spatial resolution of weather data can be obtained from the Climate Research Unit, East Anglia, but only as monthly averages. For our core modelling we used the monthly averages of temperature and precipitation for the period of 1961-1990 [*New et al.*, 2000]. In order to test the effect of the temporal resolution and the reference period we carried out sensitivity simulations with the daily ECMWF reanalysis data [*ECMWF*, 2004] and the monthly averages for the period 1991-2000 [*Mitchell and Jones*, 2005]. The results of this analysis are discussed in Chapter 2.3.7.

2.5.2 Soil data

A global map of soil properties at five arc minutes resolution can be obtained from the Data and Information System (DIS) framework activity of the International Geosphere–Biosphere Programme (IGBP) [*Global_Soil_Data_Task_Group*, 2000]. This map contains bulk density, organic carbon and nitrogen content. For texture and pH we used the FAO TERRASTAT database [*FAO*, 2002], also providing a five arc minutes resolution. Input data like field capacity, wilting point, and hydraulic conductivity were calculated from these basic data by applying the formulas suggested by *Saxton et al.* [1986]. To save computing time we did not work on the smallest spatial resolution of input datasets (5 arc minutes soil map) but on a 0.5 degree grid, using the dominant soil type from the finer 5 arc minutes grid.

2.5.3 Land-use map

In order to compare national census data to the simulated yields a land-use map was needed to average the yields over agricultural area or, ideally over the area planted with a specific crop. We used the global map on the distribution of major crops by *Leff et al.* [2004], which provides the fraction of crop-specific area within each five arc minute grid cell.

2.5.4 Crop types and varieties

For the four crops presented here (wheat, rice, maize and soybean), at least two different parameterisations were used to cover the full climatic range under which these crops can be grown. These parameterisations differ in the effective temperature sum needed to reach maturity (ETS_{harv}). Wheat is represented as spring wheat and winter wheat; for rice, maize and soybean we started with a single variety and then added a parameterisation to also include cooler regions where these crops are cultivated.

Additionally we assumed a low-yielding variety for soybean. As a legume, soybean is not significantly limited by nitrogen, but mainly by other elements like phosphorus, which is not

included in our simulations so far. The results of a standard simulation revealed that most countries whose soybean yields were overestimated by more than 50% are also characterized by extraordinary low phosphate application rates below 10 kg ha^{-1} (Figure 2-12). We therefore concluded that for these countries overestimation was due to a lack of phosphorus limitation in the model. We thus decided to emulate this limitation by attributing less productive soybean varieties to countries that are overestimated by more than 50% *and* have phosphate application below 10 kg ha^{-1}. This was implemented by reducing the productive potential of soybean in these countries by 50% (relating to the value of prdx). Note that there are also countries with phosphate application rates below 10 kg ha^{-1} that are *not* overestimated (Figure 2-12). For these countries the climatically constrained yield is so low that it can also be achieved with low phosphate application.

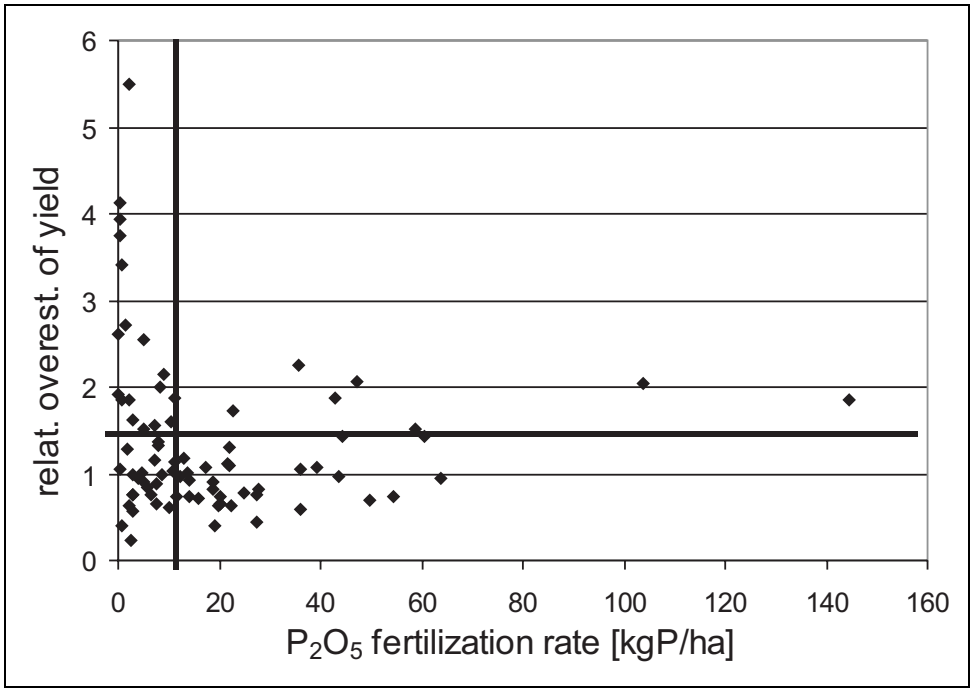

Figure 2-12. Relative overestimation of average soybean yields versus application of Phosphate fertilizer per country according to *IFA* [2002]. Overestimation = (simulated yield – FAOSTAT data) / FAOSTAT data. Bars indicate overestimation of 50% and a Phosphate application rate of 10 kg/ha^{-1}. For countries with an overestimation > 50% and a P application rate < 10 kg N ha^{-1} it is assumed that soybean yield is limited by availability of Phosphate (for details see Chapter 2.5.5).

The planting date routine (Chapter 2.2.2) was used to calculate the potential distribution of crop varieties based on the temperature sum required for maturity. If both varieties of a crop could be grown, it was assumed that winter wheat or the tropical varieties of rice, maize or soybean are preferred.

All crop parameters both for the planting date routine and for the actual Daycent simulations can be obtained from the authors.

2.5.5 Initial conditions, simulation period

Matter fluxes between the organic soil pools and the mineralisation of organic matter release mineral nitrogen, which directly affects plant growth. The rate at which mineral nitrogen is released by these processes depends on the pool sizes and the related transition rates, following first order dynamics. Thus, the initial conditions for the organic matter pools can be crucial with respect to the simulation of yields. Although the carbon and nitrogen content of the soil is provided by IGBP-DIS, these values may not be in equilibrium under the conditions simulated by Daycent (with respect to climate, land cover and land use). Ideally one would first calculate equilibrium levels of soil organic matter under natural conditions and then retrace a site's development from that state, but as a complete spatially explicit history of global land use could not be constructed in this project, we applied a simpler approach. To avoid the initial effects of changing pool sizes we used a spin-up time of 20 years. Though soil organic matter pools were not always in perfect equilibrium after this rather short period, yields did not change by more than 20% thereafter.

2.5.6 Management

The term "management" comprises all activities that are undertaken on a field during the year, like planting, fertilizer application, ploughing, irrigation, and their timing. Though these parameters have an essential influence on crop production, they are often not directly available on the global scale. Therefore the next paragraph describes all management activities and underlying assumptions that were included in the Daycent simulations except for planting dates, which have been described in Chapter 2.2.2.

Management – Fertilizer application

Only nitrogen was considered as a nutrient in Daycent and therefore fertilizer application only includes mineral nitrogen. We are aware that this is a simplification as according to the Law of the Minimum, any nutrient might cause growth limitation. However, nitrogen is the most important nutrient, and we assume that if farmers apply nitrogen fertilizer at a certain rate, they will apply other nutrients accordingly. This assumption is confirmed by the FAO statistics of fertilizer consumption on country level, where e.g. nitrogen and phosphate consumption show a strong correlation (correlation coefficient of 0.987 for the year 1995). However, as already discussed above and will be discussed later, this approach does not hold for legumes since nitrogen is sufficiently provided by fixation.

The amount of nitrogen fertilizer applied per country and crop was derived from the international fertilizer industry association [*IFA*, 2002], which provides this information for important crop-producing countries and their main crops. The database contains the crop-specific fertilizer application rate and the fraction of area fertilized, which were multiplied to get average application rates. For country-crop combinations with no IFA data available (approximately 17% in cropland area) we calculated the amount of nitrogen that would be removed with yield levels according to FAO statistics as a proxy for nitrogen input and therefore assumed that the difference between the removed nitrogen and the reported manure application rate is applied as mineral fertilizer. To account for nitrogen losses we increased these values uniformly by 10%. However, fertilizer efficiency is often as low as 50% [*Cassman et al.*, 2002; *Frink et al.*, 1999] because of leaching and

gaseous emissions. As a consequence, the simulations might show nutrient mining or underestimated yield levels for these countries. In addition to the total amount of applied fertilizer, the model is sensitive to the type of mineral nitrogen (nitrate or ammonia). This is due to the processes of denitrification, nitrification and the fact that mainly nitrate is susceptible to leaching losses. We quantified the typical ratio between ammonia and nitrate as a global variable, derived from *USGS* [2003], resulting into 85% ammonia and 15% nitrate.

Management – Organic manure application

Nitrogen application from manure was derived from *Siebert* [2005]. Based on global livestock densities [*Gerber*, 2004] for 12 animal types and their specific nitrogen excretion, they calculated total nitrogen excretion per grid cell, applying a grid resolution of 5 arc minutes. However, we decided to aggregate the nitrogen application via manure to the country level. This was done (i) to avoid artificial spatial yield patterns caused by nitrogen availability from manure and (ii) to be consistent with the application of mineral fertilizer, which is also available on country level. For aggregation, we averaged manure application rates over the entire agricultural area of a country and reduced the overall value by 20% in order to account for application losses [*Bouwman et al.*, 1997; *ECETOC*, 2004; *FAO*, 2001a].

Management – Fertilizer and Manure application Dates

Application dates of mineral fertilizer and manure are difficult to estimate at the global scale. As they are mainly linked to planting dates and crop growth, we applied the following rules to define the application events: Manure is always applied in two identical applications 10 and 30 days after planting. Mineral fertilizer is equally distributed over four application events, taking place 45, 76, 107 and 138 days before the assumed harvest date. If the effective crop growth period is shorter than 140 days the fertilizer is applied in four equal intervals over this period, starting with the planting date. We are aware that fertilizer application in four events does not reflect agricultural practice, but this approach was necessary to achieve realistic fertilizer efficiencies. E.g., in reality farmers adjust fertilizer application to rainfall events in order to minimize losses, which is not implemented in the simulation model.

Management – Irrigation

The global irrigation map by *Döll and Siebert* [2000] contains information on the fraction of irrigated area within one five minute grid cell. For all 30 minutes grid cells that contain at least one 5 minutes cell irrigated by more than 1% we simulated irrigated yield. Irrigation was assumed to completely prevent water limitation on growth, therefore enough water was added at each time step to keep the soil water content at 100% field capacity.

Other management data

For other management events we made very simple global assumptions. It is assumed that 75% of the shoot is removed at harvest as straw, and that cultivation events are restricted to one single ploughing just before planting. Ploughing events in Daycent affect decomposition rates of organic matter and further homogenise the ploughing layer with respect to soil texture.

3 Statistical analysis of N_2O and NO emissions

Summarizing available measurement data from agricultural fields and soils under natural vegetation, and modelling of global annual emissions [a]

Summary

The number of published N_2O and NO emissions measurements is increasing steadily, providing additional information about driving factors of these emissions and allowing an improvement of statistical N-emission models. We summarized information from 1008 N_2O and 189 NO emission measurements for agricultural fields, and 207 N_2O and 210 NO emission measurements for soils under natural vegetation to assess the effect of various climate, soil, management and measurement-related factors. We developed statistical models of significant factors to calculate global annual N_2O and NO emissions from fertilized fields and soils under natural vegetation. The factors found to have a significant effect on agricultural N_2O emissions were fertilization rate, soil organic carbon content, soil pH, texture, crop type, and fertilizer type, while NO emission is significantly determined by fertilization rate, soil nitrogen content, and climate. The 20% increase in the number of N_2O measurements for agriculture does not provide a considerable improvement or reduction of uncertainty compared to an earlier analysis because the representation of variability within agro-ecosystems did not improve. The additional NO measurements in agricultural systems yielded a considerable improvement compared to earlier analyses. Natural N_2O emissions are significantly affected by soil carbon content, soil pH, bulk density, drainage, and vegetation type. For NO emissions from natural ecosystems soil carbon content and vegetation type were identified to have a significant influence. Estimated global annual emissions from fertilized arable land and grassland amount to 3.3 and 0.8 Tg for N_2O-N, respectively, and for NO-N to 1.4 and 0.4 Tg, respectively. For emissions from soils under natural vegetation no global emission estimates are calculated with the global statistical emission models as they do not cover the entire range of natural systems or are too uncertain (for NO emissions).

3.1 Introduction

Human activities like fertilizer production and fossil fuel combustion have caused a major increase in both nitrous oxide (N_2O) and nitric oxide (NO) emissions. Atmospheric N_2O rises by 0.7 ppbv per year, causes 6% of the anthropogenic greenhouse effect and also contributes to the stratospheric ozone depletion [*IPCC*, 2001]. NO is involved in the regional balance of oxidants of the atmosphere and its re-deposition causes eutrophication and acidification of ecosystems. Natural sources of N_2O are soils and oceans, and the anthropogenic increase is mainly caused by accelerated soil emissions through the application of fertilizer and animal manure. NO emissions

[a] This work was done in cooperation with A.F. Bouwman, RIVM, the Netherlands

mainly stem from fossil fuel combustion, while soil emissions (both natural and accelerated by fertilizer addition) are dominant in remote areas. Despite more than three decades of research yielding numerous publications on N_2O and NO flux measurements, there is still a large uncertainty about the contribution of individual sources [*IPCC*, 2001].

A comprehensive review on the factors identified to influence N_2O and NO emission rates can be obtained elsewhere [*Firestone and Davidson*, 1989]. Here we will briefly summarize only the major controls of N_2O and NO emissions corresponding to the factors included in the data set of measurements compiled for this study.

In soils N_2O and NO are intermediate products of nitrification and denitrification, while denitrification is also a sink for N_2O [*Tiedje*, 1988]. The availability of ammonium (NH_4^+) and oxygen are the most important factors regulating nitrification [*Firestone and Davidson*, 1989], while (anaerobic) denitrification is mainly controlled by oxygen supply, and the availability of organic carbon (C), and nitrate (NO_3^-) or other nitrogen (N) oxides [*Tiedje*, 1988]. The mechanism of N_2O and NO emissions from soils can be described using the conceptual hole-in-the-pipe model [*Firestone and Davidson*, 1989], whereby rates of nitrification and denitrification are represented by the N flow through leaky pipes. The size of the holes represents the relative amounts of leaking N_2O and NO and is controlled by factors like soil water and oxygen, gas diffusion and soil reaction (pH).

The availability ammonium and nitrate, the main controls on nitrification and denitrification, respectively, is fundamentally liked to the amount of nitrogen cycled between vegetation and soil. Annual N cycling largely differs between natural ecosystems and is strongly related to the net primary production and soil organic matter decomposition, which are both mainly controlled by soil moisture and temperature. Therefore, tropical forests generally cycle 2-4 times more N between soil and vegetation than do most temperate ecosystems [*Jordan*, 1985; *Vitousek*, 1984]. Beyond these climatic differences phosphorous instead of nitrogen may be limiting growth in many tropical ecosystems with strongly leached soils [*Vitousek*, 1984] and biological N fixation may supply the N needed for growth and for replenishing denitrification and leaching losses. In contrast, N-limited temperate forests generally have high C/N ratios in litter and slower decomposition and N mineralisation rates [*Robertson and Tiedje*, 1984; *Vitousek and Sanford*, 1986]. An important anthropogenic input to "natural" ecosystems is atmospheric N deposition, with annual rates often exceeding 10 kg ha^{-1} [*Van Drecht et al.*, 2005], which is a threshold above which changes to sensitive natural ecosystems may occur [*Bobbink et al.*, 1998].

Apart from the availability of N, climate also governs the amount of N_2O and NO that is formed during nitrification and denitrification. During denitrification the ratio of N_2O/N_2 generally increases with decreasing temperature [*Firestone and Davidson*, 1989; *Keeney et al.*, 1979], and temporary accumulation of soil N due to wet-dry or freeze-thaw cycles, can cause high N_2O emissions despite the low temperatures. Therefore, in continental temperate climates N_2O emissions during early spring, winter and autumn may account for an important part of the annual N_2O emission (e.g. [*Kaiser and Ruser*, 2000]. Many studies indicate that NO emissions are positively correlated with temperature [*Saad and Conrad*, 1993; *Williams and Fehsenfeld*, 1991]. However, the relationship between temperature and NO fluxes is subject to considerable uncertainty [*Meixner*, 1994] and numerous exceptions have been observed in temperate and tropical [*Skiba et al.*, 1997].

As all microbial activity depends on water as a solvent, aerobic microbial activity primarily increases with soil water content until it becomes limiting for oxygen diffusion, resulting in maximum activity at about 50% water-filled pore space (WFPS) [*Firestone and Davidson*, 1989]. Likewise emissions of NO from nitrification show a maximum at about 50% WFPS, while N_2O emissions peak at about 55% WFPS. Rising soil water content steadily increases denitrification by providing both the fluid environment and a barrier to the diffusion of inhibitory oxygen. At the same time the fraction of denitrified N lost as NO or N_2O decreases with soil water content, because under low gas diffusivity N_2O and NO are more likely to be re-consumed by denitrifiers before being emitted from the soil [*Davidson*, 1991]. Under wet conditions uptake of N_2O from the atmosphere may even occur [*Ryden*, 1981].

Limited gas diffusion and oxygen supply which increase denitrification rates are not only caused by high soil water content, but are also favoured by impeded drainage, shallow groundwater, soil structure, soil compaction or high bulk density, fine soil texture or soil surface sealing. E.g. fine-textured soils have more capillary pores within aggregates than do sandy soils, thereby holding soil water more tightly. As a result, anaerobic conditions favouring N_2O emissions may be more easily reached after rainfall or irrigation events and maintained for longer periods within aggregates in fine-textured soils than in coarse-textured soils. In contrast, aeration is generally better in well-drained, coarse textured soils, thus favouring NO emissions. Besides these soil factors, the soil water and oxygen status mainly depend on rainfall and irrigation events and therefore are highly dynamic.

Many studies observed low denitrification rates under low pH, which might either be attributed to a direct effect on denitrifying enzyme activity or to less C being available under low pH conditions [*Simek and Cooper*, 2002]. But as the N_2O reductase is sensitive to proton activity, the N_2O fraction may be larger at low soil pH [*Alexander*, 1977]. However, it is not certain if this may compensate the inhibiting effect of low pH on denitrification [*Ellis et al.*, 1998]. For nitrification acidic conditions also favour the production of N_2O by both autotrophic and heterotrophic nitrifiers [*Martikainen and Boer*, 1993]. Additionally, there are indications that NO production in alkaline soils is dominated by nitrification, but dominated by denitrification in acidic soils [*Remde and Conrad*, 1991].

It should be noted that not all NO emitted by soils ends in the troposphere. Depending on the characteristics of the vegetation type, part of the NO emitted from soils is re-absorbed by the canopy [*Ganzeveld et al.*, 2002].

All the above mechanisms apply to both natural and agricultural systems. Agricultural soils form a special case because the amount of available N is strongly determined by management. Denitrification [*Simek et al.*, 2000], and associated N oxide fluxes are strongly stimulated by fertilizer N inputs in agricultural soils [*Bouwman*, 1996; *Veldkamp and Keller*, 1997], animal manure [*Aulakh et al.*, 2000], crop residues [*Vos et al.*, 1994; *Wagner-Riddle et al.*, 1997], atmospheric N deposition [*Skiba et al.*, 1998], or biological N fixation by leguminous crops (such as alfalfa, soybeans, pulses, and clovers which can fix atmospheric N_2 and generally receive no or small amounts of N fertilizer) [*Shelton et al.*, 2000].

Apart from management practices influencing the N flow, there may be other factors related to agricultural management that affect the conditions for denitrification and nitrification. For example,

in wetland rice the anaerobic conditions during the rice growing season result in low N_2O emissions. However, in management strategies with intermittent drainage, and after post-harvest drainage the N_2O emissions may be considerable [*Xu et al.*, 1997]. Further management practices influencing denitrification, nitrification and the relative amounts of N_2O and NO can be fertilizer type (N form, use of slow-release fertilizers), mode of application (broadcasting, incorporation, injection, application as a solution, etc.), timing of application (basal, split applications), soil management (e.g. conventional tillage, reduced or zero-tillage systems), and water management (irrigation).

Apart from the above mechanisms affecting N_2O and NO emissions rates the actual measured quantities and the calculated annual emissions are also influenced by the experimental settings like frequency and length of the measurement. As studies on agricultural soils often cover only the high emission period after N application the emissions from these short measurement periods tend to be disproportionately high, and even more generally measurement periods shorter than one year prone to false estimations of annual emissions through the omission of seasonal emission dynamics, e.g. freeze-thaw emissions during the winter.

The concern about increased emissions of N_2O and NO has stimulated intense research activities on the controls of nitrification and denitrification. It is a challenge to extract general patterns and chains of cause and effect from the overwhelming number of emission measurements often investigating very specific site characteristics, vegetation or management conditions. One way to learn about the soil N emission processes is by investigating individual parts of the system and building models that combine these parts. From this work several ecosystem models such as Daycent [*Parton et al.*, 1996] and DNDC [*Li et al.*, 1992] have been developed during the last decades.

Parallel to these process-based models, we think it is necessary to also apply statistical methods to the emission measurement data in order to identify correlations between controlling factors and emissions. Such approaches can be used to develop emission factors such as those used by IPCC [*Bouwman*, 1996; *Mosier et al.*, 1998] or simple statistical models that describe the variation of N_2O and NO fluxes at larger scales and can be used to assess management or mitigation options [*Bouwman et al.*, 2002b; *Freibauer and Kaltschmitt*, 2003]. In addition, such approaches are useful to point to problems of biases and under-representation in the data for specific climate or land use conditions. This may be helpful for developing future research directions.

For N_2O and NO emissions from agricultural soils a recent analysis has presented controlling factors and statistical models [*Bouwman et al.*, 2002a, 2002b], while for N_2O and NO emissions from soils under natural vegetation no regional or global statistical emission model is known to the authors. Based on [*Bouwman et al.*, 2002a, 2002b] we summarize in this paper measurements of N_2O and NO emissions reported in the literature together with the factors related to environmental and management conditions and the measurement technique. Compared to the earlier analysis, which solely referred to agricultural systems, we here add new data for agricultural systems, particularly for NO, and also cover N_2O and NO emissions from natural ecosystems.

The aim of this study is to identify the factors with significant influence on N_2O and NO emissions from agricultural fields and soils under natural vegetation, and to develop a statistical model that can be used to estimate global annual emissions from these systems. For natural systems that will

be the first comprehensive statistical analysis of available measurement data, while for agricultural systems the results, particularly for NO emissions, will be improved compared to the previous study.

The data set compiled from the literature is described in Chapter 3.2.1, and the statistical methods used to summarize the data are presented in Chapter 3.2.2. Results and discussion of the data summary for emissions of N_2O and NO and the estimation of global emissions using the models developed are presented separately in Chapter 3.3 for agricultural fields Chapter 3.3.1) and soils under natural vegetation (Chapter 3.3.2), and are followed by a comparison to other studies (Chapter 3.4) and the conclusions (Chapter 3.5).

3.2 Data and Methods

3.2.1 Data set

We used an extended version of the N_2O and NO emission data set presented in *Bouwman et al.* [2002b]. It contains results from field studies that were published in the peer-reviewed literature. Like the first version it includes literature reference, location and various parameters related to climate, soil, management and measurement technique (Table 3-1). The emissions are given as the sum of emissions over the reported measurement period, and for measurements covering more than one year the values are converted to refer to a one-year measurement period. Therefore in the following "emission" always means "emission measured during the length of the experiment" if not noted differently.

While the first study only covered agricultural emissions, the data set now also includes N_2O and NO emissions from soils under natural vegetation and has a larger number of measurements in agricultural fields.

As most studies do not report all parameters of interest, the data set has many missing values. Missing annual precipitation and temperature data for the geographical position of the measurement site is obtained from *New et al.* [1999] on a 0.5 degree grid as described in *Hofstra and Bouwman* [2005]. The data set is unbalanced, as the combinations of classes are not represented by equal numbers. And the data set is biased, as some categories are not represented at all (for example, the data set has no N_2O measurement data in arid ecosystems).

Like in the previous analysis, classes were formed for all factors (Table 3-1). For most soil properties classes were designed with both similar ranges and balanced numbers of measurements. Drainage is reported as either well or poorly drained (including all imperfectly to poorly drained soils). Although some references provide clay, sand and silt content, the clay content is in many cases the only variable reported. Therefore, classes for soil texture (coarse, medium and fine) are based on clay content (Table 3-1).

For agricultural fields the factor climate was classified according to *De Pauw et al.* [1996] for each measurement and grouped into temperate continental, temperate oceanic, subtropical and tropical. The data for soils under natural vegetation had a very unbalanced representation of these four

climate classes, and the factor climate was therefore further aggregated to temperate and tropical (Table 3-1). Climate types 8, 9 and 10 (arid, polar and boreal climates) were not part of the final data set due to lack or complete absence of measurement data. Annual precipitation from the literature reference itself was included as a factor as well as the annual precipitation obtained from the 0.5° x 0.5 climate data set, both having the same classification (Table 3-1). The same applies to annual temperature. Again, classes were created with both equal ranges and similar numbers of measurements in each class.

The classification of factors describing the experimental setting (frequency, method, length) is also shown in Table 3-1. Although there are less measurements for agricultural NO and natural emissions, only in two cases it was necessary to use different classifications than for agricultural N_2O measurements (Table 3-1). We present the number of measurements only for those factors with a significant influence on N_2O or NO emissions (Chapter 3.3). The full data set can be obtained from the authors.

3.2.1.1 Data for agricultural fields

Crops were grouped to the classes bare fields (none), cereals, legumes, wetland-rice, other crops, and grass. Some fertilization experiments in natural forests and savannas were included in the data set but were not considered here. Fertilizer type, application method, timing of application and fertilization rate were grouped according to Table 3-1.

The data set contains a set of 1125 measurements for N_2O and 199 for NO, which is a considerable improvement compared to the 846 (N_2O) and 99 (NO) measurements used previously [*Bouwman et al.*, 2002b]. Some variables and classes were excluded from the analysis before summarizing and analysing the data: (i) Organic soils were excluded as they are known to have very high N-emission and because they strongly influenced the predicted emissions for mineral soils. (ii) Experiments with chemicals or additives like nitrification inhibitors were excluded, because their use is still very limited on the global scale [*Trenkel*, 1997]. (iii) As the annual N input to grazing systems is often not provided we did not include these measurements. The reduced data set then contained 1008 measurements for agricultural N_2O from 204 references and 189 measurements for agricultural NO from 58 references.

3.2.1.2 Data for soils under natural vegetation

Vegetation was classified to coniferous forest, deciduous forest, grassland, rainforest, savannah and tropical dry forest (Table 3-1). In total, the data set contains a set of 247 measurements for N_2O and 231 for NO emissions. From that, some variables and classes were excluded before summarizing and analysing the data: (i) Organic soils because of their extraordinary high emissions and their strong influence on predicted emissions for mineral soils. (ii) The classes deciduous-legume (Alder) forest, marsh, mixed forest and other as they only contain two or three measurements and therefore are not suitable for our analysis. (iii) Two measurements with N_2O uptake greater than 0.4 kg ha^{-1} of N as they caused the predicted emissions to be mostly negative. The reduced data set for soils under natural vegetation then contained 207 measurements for N_2O from 72 references and 210 measurements for NO from 52 references.

Though N deposition has changed the N cycle in large parts of the world it is not considered as a specific parameter in this data set because of limited information provided in the references. However, most N_2O and NO emission measurements from soils under deciduous and coniferous forests stem from highly N affected regions (N deposition > 10 kg N $ha^{-1}y^{-1}$, which is a threshold above which changes to sensitive ecosystems may occur [*Bobbink et al.*, 1998]). Therefore all results derived from these data only apply to N affected coniferous and deciduous forests. The measurements from all other vegetation classes are not or only slightly affected by N deposition and are therefore assumed to apply to the natural state of those systems.

Table 3-1. first part. Factors included in the data set, class codes and description of classes.

Factor	Classes / Code	Description
N_2O / NO emission (kg N ha^{-1})	Continuous variable	Emission measured during the length of the experiment
Soil organic C content (%)	<1, 1-3, >3	
Soil N content (%)	<0.5, 0.5-2, >2	
Soil pH	<5.5, 5.5 – 7.3, >7.3	
Soil CEC	0 - 8, 8-16, 16-14, 24-32, >32	
Soil Bulk density (g cm^{-3})	0-0.5, 0.5-1, 1-1.25, 1.25-1.5, >1.5	
Soil drainage	W	Well drained
	P	Poorly drained
Soil texture	Coarse	Sand, loamy sand, sandy loam, loam, silt loam, silt
	Medium	Sandy clay loam, clay loam, silty clay loam
	Fine	Sandy clay, silty clay, clay
Climate type (agricultural fields)	Temp_C	Temperate continental
	Temp_O	Temperate oceanic
	S-Trop.	Subtropical (summer or winter rains)
	Trop.	Tropical (warm humid, warm seas. dry, cool)
Climate type (natural vegetation)	Temp.	Temperate (continental and oceanic)
	Trop.	Tropical and Subtropical
Annual precipitation. (mm)	0-250, 250-500, 500-750, 750-1000, 1000-1500, 1500-2000, >2000	
Annual temperature (°C)	0-5, 5-10, 10-15, 15-20, 20-25, >25	
Crop type	Cereals	Cereals (excl. maize and wetland rice)
	Grass	Grass
	Leg.	Legumes
	Other	Rotation, Row crops like maize and potato, Irrigated crops and Other crops
	W-Rice	Wetland rice
	None	None
Vegetation type	Conif.	Coniferous Forest [a]
	Decid.	Deciduous Forest [a]
	Grass	Grassland
	Rainf.	Rainforest
	Sav.	Savannah
	Trodryf.	Tropical dry forest

[a] Covering N affected forest only.

Table 3-1. continued. Factors included in the data set, class codes and description of classes

Factor	Classes / Code	Description
Fertilizer type	AA	Anhydrous ammonia
	OAF	Ammonium sulphate, ammonium bicarbonate
	AN	Ammonium nitrate, ammonium sulphate-nitrate
	CAN	Calcium ammonium nitrate
	KN	Potassium nitrate/sodium nitrate /calcium nitrate
	Mix	Combination of various synthetic fertilizers
	OS	Combination of organic and synthetic fertilizers
	Organic	Organic fertilizers
	U	Urea, urine
	UAN	Urea-ammonium nitrate
	ANP	Ammonium phosphate, other NP fertilizers
N application rate (kg ha^{-1})	0-1, 1-50, 50-100, 100-150, 150-200, 200-250, >250 (N_2O)	
	0-1, 1-100, 100-200, >200 (NO)	
Application Method	b	Broadcast
	i	Incorporated
	ib	Incorporated and broadcast
	is	Incorporated and solution
	s	Solution
Timing of Application	1	Single
	2	Single, but part of split
	3	Split
Method of measurements	c	Closed chamber
	co	Soil core method
	g	Soil gradient
	m	Micrometeorological
	o	Open chamber
Frequency of measurement	>1 per day, daily, every 2-3 days, every 4-7 days, less than 1 per week	Where the measurement frequency decreased during an experiment, then the highest frequency was used
Length of experiment (days)	0-50, 50-100, 100-200, 200-300, >300	

[a] Covering N affected forest only

3.2.2 Data analysis

Based on the classification of the factors described above a statistical analysis of the data set was carried out in order to identify factors with a significant influence on N_2O and NO emissions and to develop models to estimate global N_2O and NO emissions. We used the REML directive of Genstat [*Payne et al.*, 2000] as it is better suited for analysing unbalanced data sets with missing values than regression analysis. Emissions are balanced by assuming all factor classes to have an equal number of observations.

The emissions were first log transformed as this resulted in a distribution that is closer to a normal one than the untransformed data. Log transformation requires a preparatory manipulation of negative and zero fluxes. We calculated the minimum detectable fluxes for a one-week

measurement period. This was done on the basis of the minimum detectable fluxes of 1.67 ng $m^{-2}s^{-1}$ for N_2O-N measurements [*Verchot et al.*, 1999] and 0.44 ng $m^{-2}s^{-1}$ for NO-N [*Meixner et al.*, 1997] for closed chamber measurements (N_2O) and open chambers with forced flow-through (NO) (the most common types for these gases in our data set). For all measured fluxes smaller than this detectable weekly flux of 0.01 kg N_2O-N ha^{-1} and 0.003 kg NO-N ha^{-1}, we set the emissions to these values.

Initially, all factors (Table 3-1) were considered in the REML analysis. They were treated as fixed terms, i.e. the REML directive assigns a value to each class of each factor, so that the resulting model with the best possible fit is:

$$\log(N_{\text{emission}}) = A + \sum_{i=1}^{n} E_{\text{i}} \qquad (1)$$

where N_{emission} is the emission of N_2O or NO expressed in kg ha^{-1} of N, A is a constant and E is the effect value for factor i. REML can also handle random effects. Random effects are used when the data set can be divided into subgroups which might have a specific effect on the results, but where group membership can not be surveyed (i.e. new measurements can not be assigned to existing groups). Including random effects may increase the uncertainty of a prediction but decrease the deviance of the model. In this study "reference" is handled as a random effect.

We analysed the significance of factors in two ways. Firstly, significant variables were identified by creating a model that contained all factors. Secondly – in order to exclude interaction effects – factors were added one by one to a core model, only keeping the significant ones in the model before adding the next one. The reason for this stepwise procedure is that in the model with all factors some may not be significant if there are too many other non-significant factors included. The REML directive tests the significance by (i) adding the factors one after the other to the model, whereby the results depend on the order of the factors, and by (ii) dropping one variable at a time from the full model. The Wald statistics tool is used to calculate the change in deviance for a full model and a reduced model that is missing one factor. The significance is then tested by comparing the change in deviance with the chi-Square probability [see e.g. *Snedecor and Cochran*, 1980], indicating the chance that the full model is significantly different from the reduced one ($P \leq 0.05$). Thus a model only containing the significant parameters was obtained.

A data summary for these significant variables was compiled by calculating means (MEA) and medians (MED) in order to investigate the skewness of the data set. Additionally, balanced medians (BMED) and balanced means (BMEA) were calculated for all classes from the statistical (balanced) REML model with the significant factors. As log transformation does only conserve the median, the model described above could only be used to calculate the balanced median (BMED), which is obtained by back-transformation of the REML results. For balanced means (BMEA) a model with the same fixed terms, but without prior log transformation of emissions was fitted. A comparison between these balanced values and the mean and median values can be used to analyse the unbalancedness of the data set. The values in the summary tables are mean and median emissions calculated by averaging reported emission values each having a specific length of experiment. Therefore mean and median emissions represent an average measurement period for the factor class considered.

For the factors found to be significant we assessed whether the differences between classes were significant. Predicted means (not back-transformed) and standard errors of differences were calculated with Genstat for all factor classes, assuming average values for all other classes. The difference between two factor classes is significant, if the standard error of the difference times the excentricity (μ) is smaller than the actual difference. For classes that are expected to have different emissions than another factor class, a one-tailed test with μ = 1.64 is used. If there is no expectation, the test is two-tailed with μ = 1.96.

The uncertainty of the model was investigated by calculating predictions and standard errors for all possible combinations of classes in Genstat, then adding (respectively subtracting) 1.96 times the standard error from the prediction to obtain the upper and lower bound of the 95% confidence interval. Back-transformation of the prediction and its upper and lower bound yield the emission and confidence interval. Since the confidence interval is different for each combination of factor classes, we present the average for all factor class combinations that are covered in the data set.

Once the significant factors are identified, equation 1 (after back-transformation) can be used to calculate emissions as a function of any set of factor-classes:

$$N_{\text{emission}} = e^{A+\sum_{i=1}^{n} E_{\text{i}}} \quad (2)$$

3.2.3 Estimating global annual emissions

We used global maps with 0.5 by 0.5 degree resolution for soil properties [*Batjes*, 2002], climate [*de Pauw et al.*, 1996], fertilizer and manure application [*Bouwman et al.*, 2005], land use and land cover for 1995 [*IMAGE-team*, 2001]. We re-classified the crop categories of the global land use (Table 3-2) and vegetation map (Table 3-3) to make them consistent with the classes used in the statistical model (Table 3-2). We used country data on harvested areas and fertilizer use for 1998 (1997-1999 average) obtained from *Bruinsma* [2003] and *FAO* [2004] to correct the land use maps, and allocated fertilizer use by crop on the basis of *IFA/IFDC/FAO* [2003]. By using harvested areas the cropping intensity may exceed 100% in countries with multiple cropping, such as China and India.

More spatial detail was considered not realistic since data on agricultural management are available at the scale of countries at best. For example, no statistical information is available for fertilizer application mode, while fertilizer application rates are based on expert knowledge for about 90 countries and animal manure application rates are based on information for world regions.

Fertilizer induced emission rates were calculated for each grid cell as the emission rate with N application minus the emissions for the same area under zero N application, all other factors being equal. Subsequently the fertilizer induced emission can be expressed as a percentage of the N applied as fertilizer or animal manure (FIE). The FIE is then the equivalent of the emission factor expressing the anthropogenic N_2O emission for fertilizers, animal manure and other N inputs as used by *IPCC* [1997]. The exponential nature of the model (equation 2) causes fertilizer induced emission rates to be positively correlated to background emissions.

As the results for N_2O and NO emissions from soils under coniferous and deciduous forest only apply to N affected forests the estimation of global emissions excludes temperate forests which receive less than 10 kg N ha^{-1} y^{-1} according to a global N deposition map. This map includes long-range N transport and deposition from the STOCHEM global chemistry-transport model [*Collins et al.*, 1997] with 5 by 5 degree resolution, converted to 1 degree and smoothed, and short-range dry deposition [*Bouwman et al.*, 2002c].

Table 3-2. Assignment of crop categories from the land use data set [*IMAGE-team*, 2001] to the crop types used in the statistical analysis.

Crop category [a] in land use data	Crop type in this study
Temperate cereals	Cereals (excl. maize and wetland rice)
Tropical cereals	Cereals (excl. maize and wetland rice)
Maize	Other
Soybean	Legumes
Pulses	Legumes
Roots and Tubers	Other
Oil crops	Other
Rice, rain fed	Cereals (excl. maize and wetland rice)
Rice, irrigated	Wetland rice
All other crops	Other
Grassland (where manure or synthetic fertilizer is applied)	Grass

[a] Includes rain fed and irrigated crops except for rice.

Table 3-3. Assignment of vegetation categories from the land cover data set [*IMAGE-team*, 2001] to the vegetation types used in the statistical analysis.

Vegetation category in land cover data	Vegetation type in this study
Regrowth forest	– [a]
Extensive grassland	Grass
Ice	– [a]
Tundra	Grass
Wooded tundra	Grass
Boreal forest	Coniferous forest
Cool coniferous forest	Coniferous forest
Temperate mixed forest	Deciduous forest
Temperate deciduous forest	Deciduous forest
Warm mixed forest	Tropical dry forest
Grassland/steppe	Grass
Hot desert	– [a]
Scrubland	Savannah
Savannah	Savannah
Tropical woodland	Tropical dry forest
Tropical forest	Rainforest

[a] Not included.

3.3 Results and Discussion

3.3.1 Agricultural fields

3.3.1.1 Controlling factors for N_2O

From the factors related to soil conditions, soil organic C content, soil pH, and soil texture were found to have a significant influence on N_2O emissions (Table 3-4). For soil organic C content MEA, MED and BMED show continuously increasing emissions with increasing C content (Table 3-4), and only BMEA does not show such a relationship. The class with C content >3% is significantly different from both other classes (Table 3-5), reflecting the positive correlation between soil organic C content and rates of nitrification and denitrification [*Tiedje*, 1988].

For soil pH the MEA, MED, BMEA and BMED all clearly show the lowest emissions for the class with pH >7.3 (Table 3-3). The two classes with lower pH show similar values within unbalanced and balanced means and medians, whereby the medians are lower than the means. The pH class >7.3 is also significantly different from the two classes with lower pH (Table 3-5), suggesting that emissions from acid and acid to neutral soils exceed those under alkaline conditions. This is consistent with increased N_2O production by nitrification under acidic conditions [*Martikainen and Boer*, 1993]. With respect to denitrification an increased fraction of N_2O counteracts a decreased nitrification rate as discussed in the introduction. As it is not possible to distinguish between nitrification and denitrification, the data solely indicate that cumulative N_2O emissions are favoured in acidic to neutral soils.

The data for soil texture seem to be unbalanced as MEA and MED values are lowest for fine textured soils, BMEA values are similar in all classes, and, in contrast, the balancing of logarithmic emissions leads to highest BMED values for fine textured soils (Table 3-4). The BMED values for fine soil texture are significantly higher than those for coarse and medium textures (Table 3-5) and reflect physical conditions typical for fine textured but well-drained soils that are prone to high N_2O emissions.

Climate type is significant, though the differences between most classes are not very pronounced. MEA, BMEA and BMED values for N_2O emissions from agricultural fields are highest for subtropical climates, while the differences between the other classes are small (Table 3-4). Only the BMED for subtropical climates is significantly different from the other climate types (Table 3-5). Surprisingly the results indicate that BMED values for N_2O for tropical climates are similar to those in temperate and lower than in subtropical climates. Although not significantly different, the BMED for continental temperate climates is higher than for oceanic temperate climates, reflecting the higher winter emissions in continental climates.

The management-related factors crop type, fertilizer type and N application rate are significant for N_2O emissions. Both for crop type and for fertilizer type there were no expectations about differences between classes, therefore a two-tailed test was used to assess the significance of differences (Table 3-5). For crop type, some differences between classes in MEA values can be explained by outliers and the unbalancedness of the data set, as MED and BMED values are still very similar (for example legumes compared to none, and grassland compared to cereals, Table 3-4). A consistent picture for MED and BMED is found for wetland rice with lowest, and

cereals and grass with somewhat lower values compared to the other crop types. The differences between factor classes (Table 3-5) show similar results, with wetland rice, cereals and grass being significantly different from all other crop types and among each other; only the difference between cereals and grass is not significant.

N application rate is the factor that explains most of the deviation for observed for N_2O emissions according to the REML analysis. MEA and MED values increase along with N application rates, except for the classes with N input below 100 kg ha^{-1} (Table 3-4) This is caused by the unbalanced design, as values for BMEA and BMED increase almost linearly along with N application rate. Differences between most classes are significant (Table 3-5).

For fertilizer type, only ANP (lowest BMED value) and CAN (highest BMED) are significantly different from most other fertilizer types (Table 3-5). Except for CAN and ANP the pronounced differences for MEA and MED between fertilizer types almost disappear after balancing.

The only measurement-related factor with a significant influence on N_2O emissions is the length of the experiment (Table 3-4). As N_2O is reported as emission over the measurement period, the values increase as expected with the length of this period. Only for BMED the observed increase is continuous, and almost linear. Emissions from short measurement periods tend to be disproportionately high as studies often cover rather the high emission period directly after N application than any other period during the crop-growing season. Differences between classes are significant in all cases but one (Table 3-5).

Table 3-4. Number of observations (N), minimum (Min), maximum (Max), mean (MEA), median (MED), balanced mean (BMEA) and balanced median (BMED, back-transformed after log transformation) emissions [a] for those factors with a significant influence on N_2O emissions from agricultural fields.

Factor/factor Class	N	Min	Max	MEA	MED	BMEA	BMED
N Application rate (kg ha^{-1})							
0-1	255	-0.60	9.00	1.09	0.56	-0.47	0.29
1-50	30	0.01	3.10	1.03	0.94	1.31	0.61
50-100	160	-0.75	12.93	1.62	0.80	1.61	0.71
100-150	183	-0.01	16.31	1.58	0.87	2.13	0.89
150-200	113	0.00	16.78	2.52	1.14	2.52	1.11
200-250	79	0.01	15.60	2.64	1.42	2.83	1.41
>250	188	0.00	56.00	7.50	3.88	5.59	2.26
Soil organic C content (%)							
<1	82	0.01	5.20	1.07	0.59	2.22	0.71
1-3	447	-0.75	31.73	2.11	0.95	1.69	0.71
>3	180	-0.60	30.40	2.93	1.51	2.74	1.34
Soil pH							
<5.5	95	0.00	24.20	2.78	0.91	2.63	1.08
5.5-7.3	465	-0.75	41.80	2.49	1.10	2.74	1.02
>7.3	144	0.00	26.90	1.87	0.65	1.28	0.61
Texture							
Coarse	509	-0.60	46.44	3.21	1.20	2.48	0.80
Medium	219	0.00	56.00	2.56	1.25	2.04	0.68
Fine	158	-0.75	19.00	1.77	0.94	2.14	1.24
Climate							
Temp_C	464	-0.07	56.00	2.17	1.11	1.86	0.77
Temp_O	268	-0.60	31.73	2.80	1.15	1.20	0.71
S-Trop.	144	0.00	41.80	4.27	1.16	3.72	1.72
Trop.	132	-0.75	46.44	2.93	0.98	2.09	0.63
Crop type							
Cereals	184	0.00	56.00	2.09	0.92	2.09	0.77
Grass	282	-0.60	46.44	3.49	1.11	2.57	0.63
Legume	36	0.00	4.20	1.53	1.31	2.70	1.58
Other	289	0.00	41.80	3.39	1.60	2.62	1.16
W-Rice	79	-0.75	4.72	0.79	0.53	0.58	0.31
None	107	0.01	19.60	2.29	1.16	2.74	1.64
Fertilizer type							
AA	38	0.05	19.60	4.07	2.59	3.42	1.04
OAF	74	0.01	36.54	0.97	0.35	1.75	0.82
AN	131	0.00	30.40	3.20	1.41	2.73	1.12
CAN	73	0.05	11.20	2.58	1.80	2.37	1.56
KN	58	0.00	41.80	5.62	1.09	3.41	0.79
Mix	45	0.00	16.78	4.05	3.06	2.09	1.13
OS	48	0.00	31.73	5.64	3.35	2.70	0.81
Organic	88	0.03	56.00	4.49	1.00	2.97	1.15
U	131	-0.01	46.44	2.22	0.69	2.30	0.96
UAN	40	0.03	16.03	3.15	2.70	2.40	0.78
ANP	6	0.06	7.00	1.48	0.36	-1.73	0.26
Length of experiment (days)							
0-50	175	-0.01	16.31	1.19	0.16	1.20	0.28
50-100	111	0.00	15.00	1.15	0.36	1.09	0.61
100-200	311	-0.06	19.60	1.86	0.91	1.76	0.92
200-300	77	-0.10	41.80	5.85	2.10	3.73	1.61
>300	334	-0.75	56.00	4.18	2.10	3.31	2.08

[a] Emission in kg N_2O-N ha^{-1} during the experimental period.

Table 3-5. Significance of differences between classes for BMED for N_2O emissions from agricultural fields for those factors with a significant influence.

Factor/factor Class	N	Factor class									
N Application (kg ha^{-1})		0-1	1-50	50-100	100-150	150-200	200-250				
0-1	255										
1-50	30	●									
50-100	160	●	○								
100-150	183	●	●	●							
150-200	113	●	●	●	○						
200-250	79	●	●	●	●	○					
>250	188	●	●	●	●	●	●				
Soil org. C content (%)		<1	1-3								
<1	82										
1-3	447	○									
>3	180	●	●								
Soil pH		<5.5	5.5-7.3								
<5.5	95										
5.5-7.3	465	□									
>7.3	144	■	■								
Texture		Coarse	Medium								
Coarse	509										
Medium	219	□									
Fine	158	■	■								
Climate		Temp_C	Temp_O	S-Trop.							
Temp_C	464										
Temp_O	268	□									
S-Trop.	144	■	■								
Trop.	132	□	□	■							
Crop type		Cereals	Grass	Leg.	Other	W-Rice					
Cereals	184										
Grass	282	□									
Legumes	36	■	■								
Other	289	■	■	□							
W-Rice	79	■	■	■	■						
None	107	■	■	□	□	■					
Fertilizer type		AA	OAF	AN	CAN	KN	Mix	OS	Org.	U	UAN
AA	38										
OAF	74	□									
AN	131	□	□								
CAN	73	□	■	□							
KN	58	□	□	□	■						
Mix	45	□	□	□	□	□					
OS	48	□	□	□	■	□	□				
Organic	88	□	□	□	□	■	□	□			
U	131	□	□	□	■	□	□	□	□		
UAN	40	□	□	□	■	□	□	□	□	□	
ANP	6	■	■	■	■	■	■	□	■	■	□
Length of experiment (days)		0-50	50-100	100-200	200-300						
0-50	175										
50-100	111	●									
100-200	311	●	●								
200-300	77	●	●	●							
>300	334	●	●	●	○						

Solid = significant; empty = not significant; circle = one-tailed test with excentricity = 1.64; cube = two-tailed test with excentricity = 1.96. See Table 3-1 for class codes.

3.3.1.2 Controlling factors for NO

For NO emissions from agricultural fields four factors with a significant influence were identified, including N application rate, soil N content, climate and length of the experiment (Table 3-6). The values of MEA, MED, BMEA and BMED generally increase along with the amount of N fertilizer applied, though only MEA and MED values for N application rates >200 kg ha^{-1} are markedly higher than the other classes. However, after balancing only the lowest N application rate is significantly different from the others (Table 3-7). This may indicate that the number of measurements is too small to describe the high variability of NO emissions in the data set.

Table 3-6. Number of observations (N), maximum (Max), minimum (Min), mean (MEA), median (MED), balanced mean (BMEA) and balanced median (BMED, back-transformed after log transformation) emissions a for those factors with a significant influence on NO emissions from agricultural fields.

Factor/factor Class	N	Min	Max	MEA	MED	BMEA	BMED
N Application rate (kg ha^{-1})							
0-1	56	-0.18	2.62	0.35	0.09	1.61	0.10
1-100	46	0.00	4.48	0.61	0.15	2.20	0.41
100-200	56	0.00	3.00	0.38	0.14	2.15	0.53
>200	31	0.00	32.00	3.43	0.97	3.37	0.74
Soil N content (%)							
<0.05	12	0.01	1.05	0.24	0.15	1.65	0.37
0.05-0.2	18	0.00	0.47	0.08	0.03	1.93	0.14
>0.2	11	0.00	32.00	4.07	1.21	3.41	0.85
Climate							
Temp_C	71	-0.18	4.48	0.37	0.11	1.57	0.17
Temp_O	22	0.00	32.00	1.69	0.19	4.21	0.30
S-Trop.	53	0.00	8.00	0.70	0.31	1.56	0.40
Trop.	43	0.00	10.70	1.74	0.54	2.00	0.78
Length of experiment (days)							
0-50	107	-0.03	2.62	0.22	0.05	2.04	0.08
50-100	19	0.03	2.54	0.73	0.34	1.71	0.53
100-200	33	-0.18	6.29	1.00	0.42	1.75	0.30
200-300	7	0.28	1.13	0.55	0.39	2.00	0.36
>300	22	0.24	32.00	4.13	1.90	4.17	1.21

For soils with N content >0.2% the values of MEA, MED, BMEA and BMED are higher than for the two classes with lower soil N content, though the class with N content below 0.05% has higher MEA, MED and BMED values than the intermediate class. Emissions from soils with N content >0.2% are only significantly different from the class with 0.05-0.2% N, and even the difference between the two lower classes is significant (Table 3-7). This may be attributed to the small number of measurements, which are less than 20 for all classes.

Climate has a significant influence on NO emissions from agricultural soils. Because of the unbalancedness of the data set, patterns for MEA, MED, BMEA and BMED vary (Table 3-6).

However, highest emissions are calculated for MEA, MED and BMED from tropical systems, and temperate oceanic and subtropical climate types show intermediate values of BMED. The two tropical climate types are significantly different from the temperate continental climate type, while the other differences are not significant (Table 3-7). This finding of highest emissions from tropical systems is consistent with literature [*Davidson and Kingerlee*, 1997; *Yienger and Levy*, 1995].

The factor length of experiment shows an increase in MEA, MED and BMED, though this trend is not continuous because of the small number of measurements in most classes. The shortest measurement period, which contains most measurements, is significantly different from the other classes, while the differences between these other classes are only significant in one case (Table-3-7).

Table 3-7. Significance of differences between classes for BMED of NO emissions from agricultural fields for factors with a significant influence.

Factor/factor class	N	Factor class			
N Application rate (kg ha^{-1})		0-1	1-100	100-200	
0-1	56				
1-100	46	●			
100-200	56	●	○		
>200	31	●	○	○	
Soil N content (%)		<0.05	0.05-0.2		
<0.05	12				
0.05-0.2	18	●			
>0.2	11	○	●		
Climate		Temp_C	Temp_O	S-Trop.	
Temp_C	71				
Temp_O	22	□			
S-Trop.	53	■	□		
Trop.	43	■	□	□	
Length of experiment (days)		0-50	50-100	100-200	200-300
0-50	107				
50-100		●			
100-200		●	○		
200-300	30	●	○	○	
>300	51	●	○	●	○

Solid = significant; empty = not significant; circle = one-tailed test with excentricity = 1.64; cube = two-tailed test with excentricity = 1.96. See Table 3-1 for class codes.

3.3.1.3 Estimation of global annual N_2O emissions

The data analysis identified soil C content, soil pH, texture, climate, crop type, N application rate, fertilizer type and length of experiment as the major controls of N_2O emissions. In contrast to the data summary, the factor fertilizer type is not included in the summary model because there is no statistical information about crop-specific use of fertilizer types on the global scale, and because

differences between most fertilizer types are not significant. Furthermore, the summary model handles N application rate as a continuous variable, while this factor was classified in the data summary for presentation purposes. The effect values for the parameters of the summary model (see equation 1) are listed in Table 3-8. For length of experiment we use the class >300 days to calculate annual emissions.

Table 3-8. Effect values and constant for the N_2O and NO summary model used for global emissions from agricultural fields.

Factor/Factor Class	N_2O model		NO model	
Constant	-1.5160			-2.9950
N Application rate				
per kg N ha^{-1}	0.0038			0.0061
Soil organic C content (for N_2O) / soil N content (for NO) (%)				
	<1	0	<0.05	0
	1-3	0.0526	0.05-0.2	-1.0211
	>3	0.6334	>0.2	0.7892
Soil pH				
<5.5		0		
5.5-7.3		-0.0693		
>7.3		-0.4836		
Texture				
Coarse		0		
Medium		-0.1528		
Fine		0.4312		
Climate				
Temp_C		0		0
Temp_O		0.0226		0.3511
S-Trop.		0.6117		0.5189
Trop.		-0.3022		1.1167
Crop type				
Cereals		0		
Grass		-0.3502		
Legume		0.3783		
Other		0.4420		
W-Rice		-0.8850		
None		0.5870		
Length of experiment				
Per year (>300 days)		1.9910		2.5440

The N_2O emissions calculated with the summary model for agriculture and grassland show that the broad patterns are mainly governed by N application rate, while at smaller scales spatial variability is determined by differences in soil parameters (Figure 3-1). Differences between crop types mainly follow the effect values (Table 3-8), though lower crop-specific effects for grassland are compensated for by higher fertilizer application rates in some regions, and higher crop-specific

effects for legumes are compensated for by lower fertilizer application rates (data not shown). Highest emission rates are calculated for row crops, cereals and legumes in Europe and China.

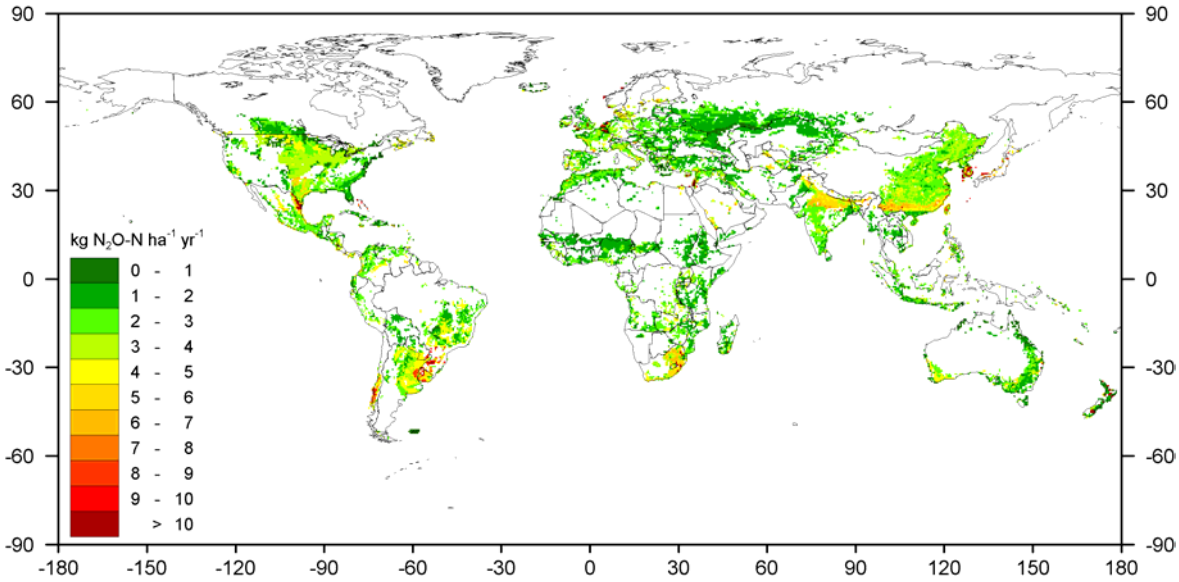

Figure 3-1. Simulated annual N_2O emission rates for agriculture and grassland. Values are weighted averages over the crop and grassland areas within one grid cell and refer to land use in 1998.

The global annual N_2O-N emission from fertilized fields is 3.3 Tg with 0.1 Tg from rice crops, 0.4 Tg from legumes, 1 Tg from cereals and 1.9 Tg from others crops (Table 3-9). Global annual emissions from grassland amount to 0.8 Tg N_2O-N. The mean global FIE (the emission rate with N application minus the emissions for the same area under zero N application, all other factors being equal, expressed as a percentage of the N applied as fertilizer or animal manure) is 0.91% of the N applied in all agricultural crops and grass excluding legumes.

Highest input of synthetic fertilizer to crops occurs in East Asia, South Asia, North America and Europe, which is reflected in the emission estimates, although high fractions of rice cropping result in emissions that are low compared to N input in East Asia (Table 3-9). Even though more than one crop is grown each year in large parts of China and India, the aggregated emission rates are suppressed by wide-spread rice cultivation. For grassland the highest input of synthetic fertilizer occurs in Europe, and application of animal manure is highest in Europe and in North America, thereby producing highest emission sums from these regions. Moreover, the regions with low N application rates but large grassland areas exhibit still high N_2O emission sums because of background emissions.

The average 95% confidence interval (see Chapter 3.2.2) for calculated N_2O emissions is –51% to +107% for N_2O emissions. The upper and lower ranges differ because of the back-transformation. This uncertainty is comparable to that obtained by *Bouwman et al.* [2002b] and that used as an uncertainty range by the *IPCC* [1997].

Table 3-9. Total fertilized area, N fertilizer and animal manure application, N_2O and NO emissions for arable land and grassland [b] for nine world regions [a].

	Cropland					Grassland [b]				
Region	Area	N fertilizer	N manure	N_2O-N emission	NO-N emission	Area	N fertilizer	N manure	N_2O -N emission	NO-N emission
	Mha	Gg y^{-1}	Gg y^{-1}	Gg y^{-1}	Gg y^{-1}	Mha	Gg y^{-1}	Gg y^{-1}	Gg y^{-1}	Gg y^{-1}
North America	134	13545	2532	459	116	173	0	1577	240	86
Latin America	116	5699	3373	363	177	73	55	145	79	58
North Africa and Middle East	61	4163	1271	150	50	30	23	50	32	12
West, East and Southern Africa	164	1202	1523	294	179	61	31	51	56	58
Europe	98	9231	3581	330	144	71	2418	1935	99	57
Former USSR	104	2132	2355	177	64	75	393	493	69	41
South Asia	219	15686	6715	617	265	20	0	229	22	14
East Asia	216	25323	6986	677	173	75	0	193	79	22
Southeast Asia, Oceania and Japan	118	7082	2631	278	220	97	138	144	134	70
World	1229	84063	30968	3345	1388	677	3058	4816	809	417

[a] Totals for the world may differ from the sum of regional values due to rounding.
[b] This includes grassland where manure or fertilizer is applied; grazing land only receiving N input from animal excretion during grazing is excluded.

3.3.1.4 Estimation of global annual NO emissions

The factors found to have an important effect on NO emissions from fertilized fields are N application rate, soil N content, climate, and length of the experiment (Table 3-6). In the summary model the factor N application rate was – as for N_2O – handled as a continuous variable, and for length of experiment we used the class >300 days to calculate annual emissions. As no global map of soil N content was available we used the soil C content map assuming a C/N ratio of 10 globally based on *Brady* [1990] as a proxy for soil N content.

Modelling of global NO emission was carried out analogous to the procedure for N_2O emission, based on significant factors and their effect values (Table 3-8), and using the same assignment between land use types (Table 3-2). Similar to N_2O, broad patterns are mainly governed by N application rate, while at smaller scales spatial variability is mainly determined by differences in N content (Figure 3-2). As differences between crop types are not significant and therefore not included in the model, differences between crops are due to different crop-specific fertilizer application rates (data not shown). Highest emission rates are calculated for all non-rice crops in Europe, and intermediate values are observed in Northern America and China (Figure 3-2). In spite of the low fertilizer input, the NO emissions in many tropical countries are rather high due to the high effect value for tropical climate (Figure 3-2 and Table 3-8). High emissions from South Korea, that could already be observed for N_2O emissions, are caused by exceptionally high fertilizer input rates reported for this country [*IFA/IFDC/FAO*, 2003].

The global annual NO-N emission from fertilized fields is 1.4 Tg (Table 3-9), with 0.1 Tg from rice crops, 0.1 Tg from legumes, 0.4 Tg from cereals and 0.7 Tg from others crops, and total emissions from grassland amount to 0.4 Tg NO-N (Table 3-9). Our estimated global annual emission from agricultural systems therefore is 1.8 Tg NO-N. The calculated FIE for NO from agriculture and grassland excluding legumes is 0.55%.

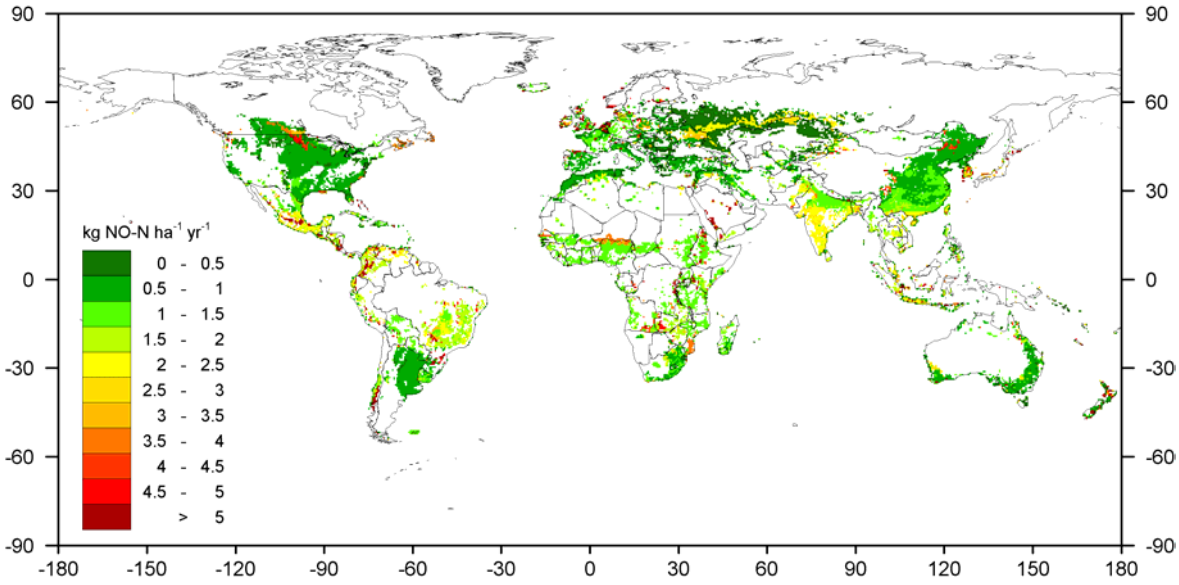

Figure 3-2. Simulated annual NO emission rates for agriculture and grassland. Values are weighted averages over the crop and grassland areas within one grid cell and refer to land use in 1998.

Tropical and subtropical climate promote high NO emissions. However, fertilizer application rates are generally low in these regions. Therefore the correlation between N fertilizer applied and the emission sum is not as strong as observed for N_2O (Table 3-9). Among the highest emissions come from South and East Asia, where fertilizer application rates are comparable to those in industrialized countries, but equally high emissions are calculated for Latin America, Africa, and Oceania, where fertilizer input is rather low. For grasslands, which generally have lower fertilizer and manure application rates, the same can be observed, with high emission sums from Latin America, Africa and Oceania, despite of low N input.

The relative 95%-confidence interval is –80% and +406% for NO emissions from agricultural fields. NO emission estimates are more uncertain than those for N_2O because of the smaller number of available measurements in our data set. There is no uncertainty estimate from the literature to compare with. Bouwman et al. [2002b] did not assess the uncertainty due to the limited number of available measurements, while *Veldkamp and Keller* [1997] used linear regression and obtained an R^2 value, which is not a true estimate of the uncertainty.

3.3.2 Soils under natural vegetation

3.3.2.1 Controlling factors for N_2O

Soil organic C content, soil pH, bulk density and drainage, vegetation type, length of the measurement period and frequency of the measurements have a significant influence on N_2O emissions from soils under natural vegetation (Table 3-10). For soil organic C content MEA, MED, BMEA and BMED show continuously increasing emissions with increasing C content. The classes with C content >1% are significantly different from the class <1% C (Table 3-11).

For soil pH the values for MEA, BMEA and BMED indicate decreasing N_2O emissions with increasing pH (Table 3-10). This is consistent with the findings from agricultural emissions, which had also lowest emissions for the class pH >7.3. The class pH >7.3 is significantly different from both other classes (Table 3-11). As already discussed for agricultural emissions this agrees with literature reporting that N_2O production by autotrophic and heterotrophic nitrifiers is favoured under acidic conditions [*Martikainen and Boer*, 1993]. In contrast, denitrification rates are reported to decrease under acidic conditions which can not be completely compensated by increased N_2O fraction [*Ellis et al.*, 1998]. Our data set suggests that N_2O emissions from soils under natural vegetation are favoured in acidic to neutral compared to alkaline soils, and this is consistent with the results for agricultural fields.

N_2O emissions decrease along with increasing soil bulk density as is apparent for MEA, MED, BMEA and BMED. Higher bulk density may give lower gas diffusivity as discussed in the introduction. Both classes with bulk density >1 g m^{-3} are significantly different from the class with bulk density <1 g m^{-3}, but do not differ significantly between each other (Table 3-11).

MEA and MED values for the factor soil drainage class show lower emissions for poorly drained soils. However, BMEA and BMED are higher for poorly drained than for well-drained soils, as expected because of effects on gas diffusion, and this is a significant difference (Table 3-11).

Reduced gas diffusivity occurring in compacted and poorly drained soils causes both high denitrification rates and associated N_2O emissions, and only at very low gas diffusivity the N_2O / N_2 ratio will decrease [*Davidson*, 1991]. Hence, unless gas diffusion is completely impeded, compacted and imperfectly or poorly drained soils as classified here will normally show elevated N_2O emissions compared to well-aerated soils.

Vegetation type is also a significant factor influencing N_2O emissions from soils under natural vegetation. MEA, BMEA, and BMED values are highest for tropical rainforest, but beyond that the patterns of MEA, MED, BMEA and MED are not consistent as the data are highly unbalanced (Table 3-10). For BMED the hierarchy of emissions is rainforest > coniferous / deciduous forest (N affected) > savannah / tropical dry forest. Differences between classes with a two-tailed test are significant only in a few cases (Table 3-11). Emissions of N_2O from rainforest are significantly higher than from grassland, savannah and tropical dry forest, and emissions from grassland are significantly lower than those from deciduous forest and rainforest. This finding is consistent with the increased cycling of N between soil and vegetation in the tropics compared to most temperate ecosystems [*Jordan*, 1985; *Vitousek*, 1984], as pointed out in the introduction.

Table 3-10. Number of observations (N), minimum (Min), maximum (Max), mean (MEA), median (MED), balanced mean (BMEA) and balanced median (BMED, back-transformed after log transformation) emissions for those factors with a significant influence on N_2O emissions [a] from soils under natural vegetation.

Factor class	N	Min	Max	MEA	MED	BMEA	BMED
Soil organic C content (%)							
<1	5	0.02	0.16	0.06	0.03	0.64	0.06
1-3	38	0.00	2.43	0.36	0.06	0.89	0.12
>3	44	0.00	7.45	1.07	0.31	1.04	0.19
Soil pH							
<5.5	109	-0.03	7.45	0.52	0.04	1.32	0.27
5.5-7.3	29	0.00	1.28	0.24	0.11	0.94	0.21
>7.3	4	0.02	0.04	0.03	0.04	0.32	0.02
Bulk density (g cm^{-3})							
0.5-1	26	0.02	6.89	1.18	0.55	1.19	0.33
1-1.25	58	0.00	7.45	0.43	0.05	0.79	0.08
>1.25	8	0.00	0.31	0.05	0.01	0.59	0.05
Drainage							
P	14	0.00	1.08	0.25	0.08	1.13	0.19
W	121	-0.03	7.45	0.55	0.08	0.58	0.07
Vegetation type							
Conif.	51	-0.03	2.10	0.13	0.01	0.92	0.14
Decid.	18	0.00	1.15	0.48	0.46	0.42	0.15
Grass	31	0.00	1.08	0.11	0.06	0.63	0.07
Rainf.	77	0.00	7.45	0.85	0.21	1.37	0.24
Sav.	17	0.00	0.09	0.02	0.02	0.93	0.07
Trodryf.	13	0.01	0.70	0.11	0.04	0.87	0.08
Length of experiment (days)							
0-50	122	0.00	1.08	0.06	0.02	-1.04	0.01
50-100	10	0.13	3.19	0.90	0.35	-1.60	0.09
100-200	21	-0.03	1.90	0.29	0.10	1.95	0.15
200-300	11	0.00	2.72	0.81	0.35	2.36	0.27
>300	43	0.01	7.45	1.29	0.67	2.62	0.41
Frequency of measurements							
>1 per day	75	0.00	7.45	0.40	0.03	1.92	0.17
Daily	54	0.00	1.08	0.09	0.02	1.69	0.18
Every 2-3 days	6	0.03	0.31	0.14	0.09	2.40	0.24
Every 4-7 days	14	0.08	2.20	0.74	0.30	-0.78	0.08
<1 per week	58	-0.03	5.86	0.69	0.26	-0.94	0.03

[a] Emissions in kg N_2O-N ha^{-1} during the experimental period.

Table 3-11. Significance of differences between classes for BMED of N_2O emissions from soils under natural vegetation for factors with a significant influence.

Factor/Factor Class	N	Factor Class				
Soil organic C-cont. (%)		<1	1-3			
<1	5					
1-3	38	●				
>3	44	●	○			
Soil pH		<5.5	5.5-7.3			
<5.5	109					
5.5-7.3	29	□				
>7.3	4	■	■			
Bulk density (g cm^{-3})		0.5-1	1-1.25			
0.5-1	26					
1-1.25	58	■				
>1.25	8	■	□			
Drainage		P				
P	14					
W	121	■				
Vegetation type		Conif.	Decid.	Grass	Rainf.	Sav.
Conif.	51					
Decid.	18	□				
Grass	31	□	■			
Rainf.	77	□	□	■		
Sav.	17	□	□	□	■	
Trodryf.	13	□	□	□	■	□
Length of experiment (days)		0-50	50-100	100-200	200-300	
0-50	122					
50-100	10	●				
100-200	21	●	○			
200-300	11	●	●	○		
>300	43	●	●	●	○	
Frequency of measurements		1	2	3	4	
>1 per day	75					
Daily	54	□				
Every 2-3 days	6	□	□			
Every 4-7 days	14	□	□	□		
<1 per week	58	■	■	■	■	

Solid = significant; open = not significant; circle = one-tailed test with excentricity = 1.64; cube = two-tailed test with excentricity = 1.96. See Table 3-1 for class codes.

As expected N_2O emissions increase with the length of the experiment, confirming our results for agricultural fields. There is a continuous trend for BMED, while for MEA, MED, and BMEA the class 50-100 days breaks the otherwise continuous increase. The differences between classes are significant in most cases (Table 3-11).

The factor frequency of the measurements also has a significant influence on N_2O emissions (Table 3-10), although only the class with less than one measurement per week is significantly lower than the other classes (Table 3-11).

3.3.2.2 Controlling factors for NO

Soil C content, vegetation type and length of the experiment have a significant influence on NO emissions from soils under natural vegetation. For soil organic C content the values for MEA, MED, BMEA, and BMED all show continuously increasing NO emission (Table 3-12), whereby the class >3% C is significantly different from both other classes (Table 3-13). This finding is consistent with the results for N_2O emissions from agricultural fields and soils under natural vegetation, and with the literature reported in the introduction.

For the factor vegetation type MEA is highest for NO emissions from coniferous, deciduous and tropical dry forest, while these classes exhibit rather small MED values, indicating skewness of the data (Table 3-12). BMEA and BMED for tropical systems differ from MEA and MED, which indicates the unbalancedness of the data set. Most tropical emission measurements stem from soils with a C content > 3%. As emissions are positively correlated to soil organic C content this causes the observed reduction of balanced values. BMED values are highest for coniferous forest, intermediate for savannah, grassland and deciduous forest, and lowest for tropical rainforest. Most classes are significantly different from two or three other classes (Table 3-13). The finding that NO emissions from tropical systems are lower than from temperate systems seems to contradict literature reporting a positive correlation between temperature and NO emissions [*Yienger and Levy*, 1995] or relatively high, though not temperature-dependent, emissions from rainforests [*Kaplan et al.*, 1988]. However, nearly all the temperate forests included in our data set are highly N affected and show NO emissions that exceed those from tropical forests and are not significantly different from those for tropical savannah, which is consistent with the mean biome emission data presented in *Davidson and Kingerlee* [1997].

Finally, our results indicate that the length of the experiment is a significant factor, similar to our results for N_2O and NO from agricultural fields and N_2O emissions from soils under natural vegetation. For NO the experiments generally cover shorter periods than N_2O measurements (see Table 3-12; the class 0-50 days has by far the largest number). BMEA and BMED increase along with the length of experiment, and for MEA and MED the continuous increase is only disturbed by the class 100-200 days.

Table 3-12. Number of observations (N), minimum (Min), maximum (Max), mean (MEA), median (MED), balanced mean (BMEA), balanced median (BMED, back-transformed after log transformation) for those factors with a significant influence on NO emissions [a] from soils under natural vegetation.

Factor class	N	Min	Max	MEA	MED	BMEA	BMED
Soil organic C content (%)							
<1	31	0.00	0.20	0.01	0.00	1.01	0.13
1-3	52	0.00	3.38	0.19	0.01	1.02	0.14
>3	25	0.00	10.85	1.09	0.10	1.31	0.48
Vegetation type							
Conif.	53	0.00	8.04	0.47	0.01	2.01	0.45
Decid.	10	0.00	2.49	0.40	0.01	0.88	0.17
Grass	43	0.00	0.69	0.08	0.00	1.02	0.29
Rainf.	33	0.00	2.38	0.39	0.04	0.39	0.11
Sav.	60	0.00	3.38	0.11	0.00	1.11	0.29
Trodryf.	11	0.00	10.85	1.30	0.02	1.26	0.10
Length of experiment (days)							
0-50	168	0.00	0.47	0.02	0.00	0.09	0.01
50-100	8	0.08	2.82	0.69	0.45	0.59	0.26
100-200	5	0.16	1.31	0.62	0.43	1.32	0.33
200-300	6	0.18	1.09	0.66	0.58	1.38	0.47
>300	23	0.00	10.85	2.15	0.82	2.19	0.60

[a] Emissions in kg NO-N ha^{-1} during the experimental period.

Table 3-13. Significance of differences between classes for BMED of NO emissions from soils under natural vegetation for factors with a significant influence.

Factor/Factor Class	N	Factor Class				
Soil organic C content (%)		< 1	1-3			
<1	31					
1-3	52	○				
>3	25	●	●			
Vegetation type		Conif.	Decid.	Grass	Rainf.	Sav.
Conif.	36					
Decid.	0	■				
Grass	21	□	□			
Rainf.	59	■	□	■		
Sav.	31	□	□	□	■	
Trodryf.	10	■	□	■	□	■
Length of experiment (days)		0-50	50-100	100-200	200-300	
0-50	168					
50-100	8	●				
100-200	5	●	○			
200-300	6	●	○	○		
>300	23	●	○	○	○	

Solid = significant; open = not significant; circle = one-tailed test with excentricity = 1.64; cube = two-tailed test with excentricity = 1.96. See Table 3-1 for class codes.

3.3.2.3 Estimation of global annual N_2O and NO emissions

The data analysis identified soil organic C content, soil pH, bulk density, drainage, vegetation type and length and frequency of experiment as the major controls of N_2O emissions from soils under natural vegetation. The effect values for these parameters in the summary model (see equation 1) are listed in Table 3-14. For the factor length of experiment we used the class >300 days to calculate annual emissions, and as frequency of experiment we applied the class with >1 measurement per day.

Given the high uncertainty of the summary model and the limited representation of different ecosystems and climatic zones in the data set we regard the global emissions maps as an illustration of the interacting effect of significant factors on the global scale and not as reliable estimates of natural N_2O emission rates.

Table 3-14. Effect values for the N_2O and the NO model for soils under natural vegetation.

	N_2O model	NO model
Constant	-2.8900	-3.952
Soil organic C content (%)		
<1	0	0
1 - 3	0.6683	0.0569
>3	1.0918	1.3265
Soil pH		
<5.5	0	
5.5-7.3	-0.2750	
>7.3	-2.4179	
Bulk density (g cm^{-3})		
0-1	0.9941	
1-1.25	-0.3786	
>1.25	-0.8597	
Drainage		
P	0	
W	-1.0462	
Vegetation type		
Conif.	0	0
Decid.	0.0115	-0.9540
Grass	-0.7941	-0.4335
Rainf.	0.4995	-1.4246
Sav.	-0.6881	-0.4238
Trodryf.	-0.5811	-1.5296
Length of experiment		
Per year (>300 days)	3.6120	3.771
Frequency of experiment		
>daily	0	

Increased deposition of reactive N has changed the N cycle in natural ecosystems, most significantly in industrialized regions, whereby substantial changes in sensitive ecosystems may be caused by N inputs exceeding 10 kg $ha^{-1}y^{-1}$ [*Bobbink et al.*, 1998]. As most measurements for coniferous and deciduous forests stem from areas where the annual N deposition is larger than 10 kg ha^{-1} y^{-1}, the results presented for these two systems only apply to areas under elevated N input. The estimation of global annual N_2O and NO emissions from soils under natural ecosystems therefore excludes all temperate forests where N deposition is smaller than 10 kg N ha^{-1} y^{-1}.

The high effect value for rainforest (Table 3-14) leads to rather high N_2O emissions from tropical regions (Figure 3-3). Although most northern regions are excluded (as they are non-N-affected temperate forests) the N_2O emission rates calculated for northern tundra are similarly high as those from tropical systems due to the combined effect of poorly drained soils and low soil bulk density. Low pH values, which are mainly found in tropical regions and high latitudes, further support the occurrence of high emission rates in these two regions (Figure 3-3). The effect of the soil organic C content on simulated global emission patterns is not as strong as could be expected from the summary model, as only few regions have extensive areas with soils C content exceeding 3%.

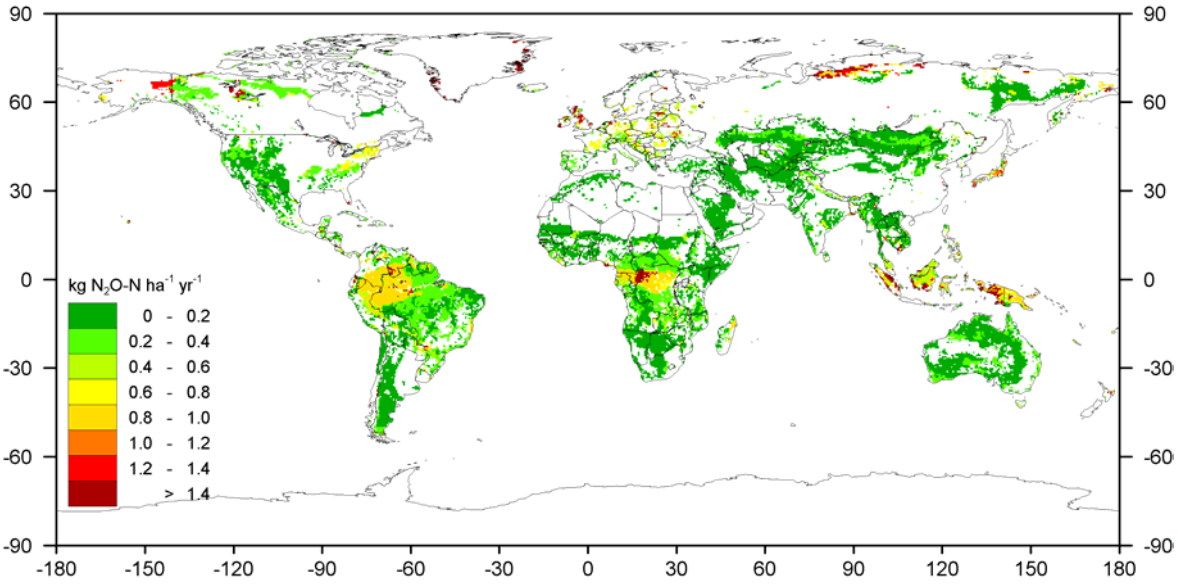

Figure 3-3. Simulated annual N_2O emission rates for natural ecosystems for 1998 land cover. Agricultural area, regrowth forest, arid climate and polar climate are excluded.

The average 95%-confidence interval calculated for all combinations of classes (Chapter 3.2.3) is -84% and +621% for N_2O from soils under natural vegetation. Upper and lower range are different because of the logarithmic back-transformation.

The factors found to have a significant effect on NO emissions from soils under natural vegetation are soil organic C content, vegetation type and length of the experiment (Table 3-12). Like for N_2O, temperate forests with N deposition <10 kg N ha^{-1} y^{-1} were not included in the calculation of global annual emissions. As only a C content >3% affects NO emission markedly (Table 3-14) and as this only occurs in few areas, the differences in emission estimates can directly be attributed to the distribution of vegetation types and their effect values (Table 3-14 and Figure 3-4). Lowest emissions are calculated for rainforest and tropical dry forest. Higher NO-N emissions of about

0.6 kg $ha^{-1}y^{-1}$ are estimated for temperate grasslands and savannah, which together cover the largest area included in the estimation. The area of N affected coniferous and deciduous forest is relatively small, as most of the N affected regions are dominated by agricultural land use. The C content in the data set often exceeds 3%, while in the global soil map it is lower than 3% in most areas. Therefore the statistical model produces lower estimates of NO (and also N_2O) emissions from soils under natural vegetation than one would conclude from the measurement data per se.

The relative 95%-confidence interval for NO emissions from soils under natural vegetation is -73% and +274%. This high uncertainty reflects the fact that only few significant factors could be identified and that the effects of vegetation types are significant only for few classes. In general it has to be noted that results of the statistical analysis for natural NO emissions depending strongly on initial settings like the handling before log transformation and the classification. Though the results for soil organic C content and climate seem to be stable and agree for soil C content with our expectations based on the literature, more measurements are needed to identify more parameters influencing NO emissions on such an aggregated level and with more confidence.

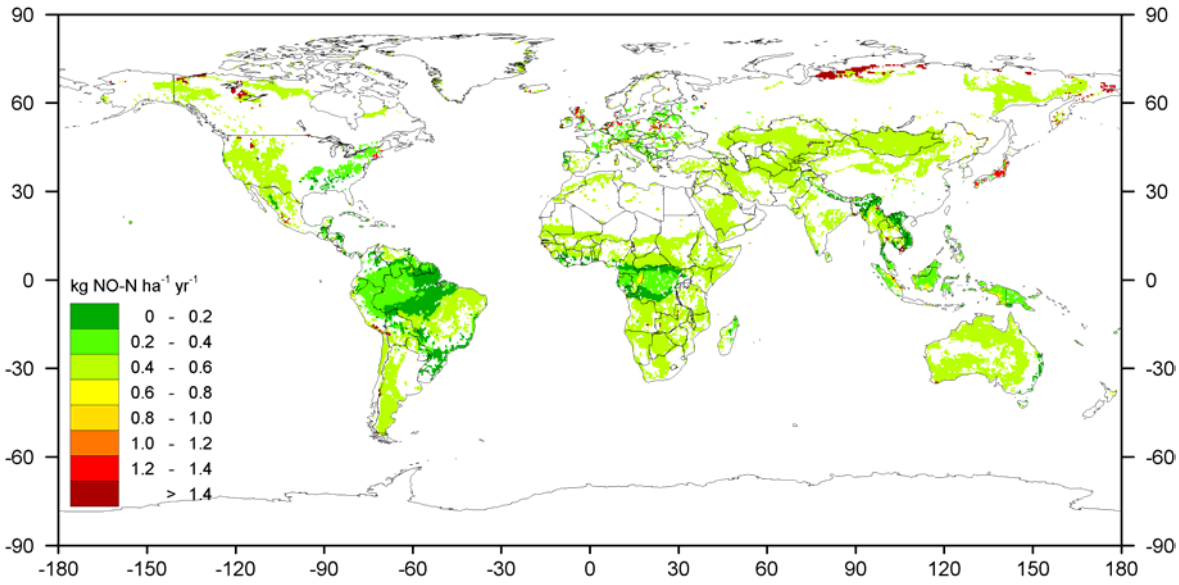

Figure 3-4. Simulated annual NO emission rates for natural ecosystems for 1998 land cover. Agricultural area, regrowth forest, arid climate and polar climate are excluded.

3.4 Comparison of N_2O and NO emission estimates with other studies

3.4.1 Agricultural fields

The results presented in this paper are based on an extended data set that was analysed by *Bouwman et al.* [2002b] (which we will refer to as subset). Regarding the number of N_2O measurements for agricultural fields we see that the data set was extended with 162 measurements, while the increase for NO was 90 (Table 3-15). It is therefore not surprising that our results for N_2O are similar to those found with the data subset. Apparently the 20% increase in the number and the distribution over the various classes, and re-classification of climate types, causes climate to become a significant factor, while soil drainage is not significant as it was for the subset of data (Table 3-16).

For N_2O there is only little reduction of the uncertainty due to the addition of new data, possibly because the subset had already a large number of measurements in primarily temperate climates, and additional measurements in the same climate types do not add much information. Unfortunately, the representation of tropical climates did not increase substantially (relative contribution of subtropical and tropical systems is 13 and 11% in the subset, and is now 14 and 13% respectively), so the representation of global environmental conditions in agricultural systems has not really improved.

Table 3-15. Comparison of number of measurements of N_2O and NO for agricultural fields in this study and *Bouwman et al.* [2002b].

Crop type	Number of N_2O measurements		Number of NO measurements	
	2002	This study	2002	This study
Grass	193	282	23	55
Legumes	36	36	16	14
Wetland rice	61	79	2	2
All other (incl. “not known”)	556	611	58	118
Total	846	1008	99	189

The global estimate for annual N_2O-N emissions from arable land (3.3 Tg) we obtain here exceeds that based on the smaller subset. This difference has several reasons related to the summary model and the handling of the data. Although the models are quite similar, we now include the factor climate, which results in more variation and higher emissions in sub-tropical and tropical climates. In addition, in this study we have a more detailed classification of crop types, which may lead to higher emission estimates in some regions.

Our estimate for annual global N_2O emissions from fertilized grassland differs from the results based on the data subset. In this study the grassland area of about 700 Mha includes primarily managed grassland in mixed agricultural systems and excludes pastoral grazing land [*Bouwman et al.*, 2005]. In contrast, [*Bouwman et al.*, 2002b] considered only those grassland areas receiving fertilizer N inputs and therefore obtained lower N_2O (and NO) emissions.

Table 3-16. Comparison of factors found to be significant for N_2O and NO emissions from agricultural fields in this study and *Bouwman et al.* [2002b].

Factor	Factors for N_2O		Factors for NO	
	Bouwman et al. [2002b]	This study	*Bouwman et al.* [2002b]	This study
	Factors related to environmental conditions			
Soil organic C content	X	X	X	
Soil organic N content				X
Soil texture	X	X		
Soil drainage	X		X	
Soil pH	X	X		
Climate		X		X
	Factors related to management			
N application rate	X	X	X	X
Fertilizer application method				
Fertilizer type	X	X		
Crop type	X	X		
	Factors related to measurements			
Length of experiment	X	X	X	X
Frequency of measurements	X		X	

Freibauer and Kaltschmitt [2003] used stepwise multivariate linear regression to analyse N_2O emissions from Europe. Results were based on 61 measurements for arable sites in temperate oceanic, 46 for arable temperate continental sites, and 72 for grassland sites. In our study we used available data from all over the world, with 464 measurements for temperate oceanic and 268 measurements for temperate continental climates. It is therefore difficult to compare our results in terms of uncertainty with those of *Freibauer and Kaltschmitt* [2003].

Unfortunately, *Freibauer and Kaltschmitt* [2003] did not present an extrapolation for total European emissions. We can therefore only compare the FIE values. Our estimate for FIE for N_2O is 0.91%. Based on their regression, *Freibauer and Kaltschmitt* [2003] calculate FIE values for N_2O for arable soils in temperate oceanic climates of 0.2%, 0.8% in temperate continental climates, and 0.3% for grassland. This contradicts their mean FIE obtained directly from the literature (1.3%, 2.2% and 1.2% for arable soils in temperate oceanic and temperate continental climates, and grassland, respectively). Our FIE and their direct mean values are consistent with the 1.25% currently used as default FIE by the IPCC methodology for national greenhouse gas inventories [*Bouwman*, 1996; *IPCC*, 1997], and with the 0.9% obtained by *Bouwman et al.* [2002b] based on the subset.

For NO the differences are more evident. The 91% increase of the number of measurements for agricultural fields resulted in soil drainage as a significant control of NO emissions, while for the subset this was soil organic C content (Table 3-16). Furthermore, climate is a significant factor additional to the N application rate (significant for both the subset and extended data set). The frequency of measurements was no longer significant, while it was a major factor for the subset.

For NO we believe that results are less uncertain than those based on the subset. This does not mean that the data now represent the full variability of world agricultural systems. However, temperate continental (36%), subtropical (28%) and tropical (23%) are better represented and our analysis is more complete than the subset, allowing to better capture the variability global agricultural conditions.

Our estimated global annual NO emission from agricultural systems (1.8 Tg) is much lower than the 5 Tg estimate in the inventory of *Davidson and Kingerlee* [1997], also lower than the 2.6 Tg reported in a recent summary on the global N cycle [*Galloway et al.*, 2004] and similar to the 1.6 Tg reported by *Bouwman et al.* [2002b]. However, a proper comparison is difficult because of differences in the types and areas of grassland in the various studies.

The calculated FIE for NO from agriculture and grassland excluding legumes of 0.55% agrees with the estimate of 0.5% by [*Veldkamp and Keller*, 1997] and is somewhat lower than the 0.7% of [*Bouwman et al.*, 2002b] based on a smaller data set.

3.4.2 Soils under natural vegetation

For global N_2O and NO emissions from soils under natural vegetation no purely statistical emission model has been developed so far, but empirical approaches have been developed both for global emissions of N_2O [*Bouwman et al.*, 1993; *Kreileman and Bouwman*, 1994] and NO [*Yienger and Levy*, 1995]. Additionally, process-based models have been applied to estimate N_2O emissions [*Nevison et al.*, 1996; *Potter et al.*, 1996]. For N_2O emissions from soils under natural vegetation our study identified vegetation type, soil organic C content, soil pH, bulk density, drainage, length of the measurement period and frequency of the measurements as factors significantly affecting emissions. As described in chapter 3.3, higher emissions from tropical systems compared to temperate systems, as suggested by literature, were identified for tropical rainforest, but not for savannah and tropical dry forests. The effects of all other factors agree well with the mechanisms reported in the literature.

However, the global N_2O emission rates calculated with our statistical model differ from the pattern suggested by the above cited references. The main reason for this discrepancy is that both the empirical model [*Bouwman et al.*, 1993] and the process models [*Nevison et al.*, 1996; *Potter et al.*, 1996] strongly link N_2O emission rates to one or more of the parameters NDVI, NPP, decomposition rate and temperature, which all peak in tropical systems. In addition, the impact of drainage class and bulk density, though partly represented, is weaker in these approaches compared to our statistical model, where these two parameters cause higher emissions from high latitudes than from tropical systems. Therefore the emission sums and average emission rates for broad vegetation classes differ between *Bouwman et al.* [1993] and this study (Table 3-17). While *Bouwman et al.* [1993] covers the entire area of temperate forests and assumes no N deposition, here only N affected temperate forest is included, leading to a smaller area and larger emission rates for this vegetation class. For the three other vegetation classes the areas are not directly comparable because of different classifications (Table 3-17). The emission estimate for closed tropical rainforest is similar, while the emissions calculated open tropical forest and grassland/steppe calculated in this study are lower compared to [*Bouwman et al.*, 1993].

Table 3-17. Comparison of N_2O and NO emission estimates from soils under natural vegetation.

Vegetation classes	Area	Emission (N_2O-N or NO-N)		Area	Emission (N_2O-N or NO-N)	
	Mha	Gg y^{-1}	kg ha^{-1} y^{-1}	Mha	Gg y^{-1}	kg ha^{-1} y^{-1}
A. N_2O emission estimates						
		This study			*Bouwman et al.* [1993]	
Temperate forest [a]	230	147	0.64	2246	500	0.22
Open tropical forest [b]	1598	333	0.21	1028	1000	0.97
Closed tropical forest [c]	854	1170	1.37	1682	2300	1.37
Grassland/steppe	2765	403	0.15	3147	1500	0.48
B. NO emission estimates						
		This study			*Davidson and Kingerlee* [1997]	
Temperate forest [a]	230	105	0.46	100	300	3.00
Open tropical forest [b]	1598	670	0.42	2400	7400	3.08
Closed tropical forest [c]	854	186	0.22	1600	1320	0.83
Grassland/steppe	2765	1559	0.56	900	1100	1.22

[a] N affected temperate forest, except for the estimate of *Bouwman et al.* [1993] which covers the entire temperate forest area.

[b] Including shrubland, savannah and tropical woodland.

[c] Including warm humid, deciduous and montane tropical forest and warm mixed forest.

For global NO emission, the situation is similar. In this study soil organic C content, and length of the experiment were found to exert the effects expected from literature, while the impact of vegetation class partly contradicts expectations. The patterns of global NO emissions from soil under natural vegetation calculated with the statistical model therefore differ from both the empirical model [*Yienger and Levy*, 1995] and the process-based approach [*Potter et al.*, 1996]. Analogous to N_2O, the NO emissions according to *Potter et al.* [1996] are strongly linked to NPP, decomposition rates and temperature, thus predicting highest emissions in tropical systems. In contrast *Yienger and Levy* [1995] basically derived a biome-specific NO emission potential from a compilation of measurement data (which is highest for tropical systems), and superimposed a temperature response function. Though they additionally account for other effects like pulsing, this basic mechanism also causes their emission estimates to roughly increase with decreasing latitude.

A more recent biome stratification of NO emissions based on mean values and expert judgment covers a larger variety of systems though not deriving an empirical model [*Davidson and Kingerlee*, 1997]. The NO emissions calculated in this study are systematically lower than those of *Davidson and Kingerlee* [1997] (Table 3-17), which can be attributed to the effect of C content (Chapter 3.3.2.3.) and to the reduced effect of extreme values through log transformation in our approach. However, the relative emission rates for vegetation classes are similar in both cases, with lowest emissions calculated for tropical rainforest. Given the high uncertainty range of the statistical model and the problematic interaction of the two parameters C content and vegetation class, we recognize that the estimation of global NO emissions from soils under natural vegetation presented is highly uncertain. This is because the available number of measurements does not allow deriving better statistically verified estimates for NO emission from soils under natural vegetation. Therefore global emissions estimates should rather be based on emission averages of vegetation

classes (Table 3-18), though they may not be statistically different, than using a highly uncertain statistical model.

Table 3-18. Mean annual NO emission rates from soils under natural vegetation calculated for this data set

Vegetation type	*Number of measurements*	NO emission [kg N ha^{-1} y^{-1}]
Conif. forest [a]	53	2.1
Decid. forest [a]	10	1.8
Grass	43	2.1
Rainforest	33	1.1
Savannah	60	2.5
Trop. dry forest	11	1.9

[a] Covering N affected forest only.

3.5 Conclusions

Steadily increasing numbers of measurements of N_2O and NO emissions from agricultural fields and natural ecosystems allow us to constantly improve statistical emission models that account for the effects of environmental and management factors.

Based on an extended version of the data set presented in *Bouwman et al.* [2002b] soil factors (soil organic C content, texture, pH), climate, crop type, fertilizer application rate, fertilizer type and length of the experiment were identified to have a significant influence on N_2O emission from agricultural fields. This is consistent with the previous results and does not provide a considerable improvement or reduction of uncertainty. This is because, in spite of the larger number of measurements, the representation of variability within agro-ecosystems did not improve.

Fertilizer application rate, soil N content, climate and length of the experiment have a significant influence on agricultural NO emission rate. This is based on a much larger number of measurements (200%) compared to the previous analysis, now covering a higher diversity of environmental conditions. The uncertainty of NO emission estimates was considerably reduced compared to previous work.

The global emissions calculated for agricultural N_2O of about 4 Tg N_2O-N y^{-1} are in good agreement with other estimates [*Galloway et al.*, 2004], while the global emission sum for NO of about 1.8 Tg N_2O-N y^{-1} is lower than recent estimates.

The uncertainty range calculated for the N_2O model is similar to that of the default IPCC emission factor and to that based on the reduced data set. However, the uncertainty of the IPCC emission factor was based on a data set of about 30 measurements. In addition, the IPCC uncertainty was based on expert judgment [*Bouwman*, 1996] and may be much lower than the statistically-based uncertainty.

N_2O emissions from natural ecosystems are significantly affected by soil organic C content, soil pH, bulk density, drainage, vegetation, length of experiment and frequency of measurements, while natural NO emissions are affected by soil C content, vegetation type and length of the experiment. These results are based on about 200 measurements. Given the incomplete coverage of global vegetation zones and the high uncertainty of the developed statistical model, global annual emission sums cannot be calculated reliably with this approach unless more measurements will be available.

From this analysis we learn that for agricultural N_2O a better understanding of important processes and better emission estimates can be expected by improving the representation of tropical and subtropical agricultural systems. In contrast, agricultural NO measurements in the database already cover temperate and tropical systems likewise, but the number of measurements is substantially lower than for N_2O, which is reflected in a lower number of significant factors and a much higher uncertainty range.

For natural N_2O and NO emissions the number of measurements in the data set is equally low (~200), and the uncertainty ranges for agricultural NO and natural N_2O and NO are similarly high. From this study we therefore learn that in these three cases far more measurement data, preferably covering prolonged periods, are needed to understand the complexity of interactions. This especially applies to NO emissions, for which a similar number of measurements allowed the identification of less significant parameters compared to N_2O emissions.

Although the uncertainty and the incomplete coverage of the statistical models for natural systems so far impairs their application to estimate global emission, this first large scale statistical analysis is an important step towards statistical N_2O and NO emissions estimates for soils under natural vegetation. These statistical models will be needed to estimate global N_2O and NO emissions until comprehensive process-based models with less uncertainty will be available, and even beyond they can serve as a benchmark to these highly dynamic process models.

Acknowledgments

Financial support was granted by the International Max Planck School for Earth Systems Modelling (Hamburg, Germany). The work of AFB is part of the project Integrated Terrestrial Modeling (S/550005/01/DD) of the Netherlands Environmental Assessment Agency, National Institute for Public Health and the Environment. We are grateful for the advice of Leo Boumans on the statistical analysis.

4 Daycent Case Study in New Zealand

Simulation of N_2O emissions from a pasture receiving high urea inputs [a]

Summary

We used the trace gas model Daycent to simulate emissions of nitrous oxide (N_2O) from a urine-affected pasture in New Zealand. The data set for this site contained year-round daily emissions of nitrification-N_2O (N_2O_{nit}) and denitrification-N_2O (N_2O_{den}), meteorological data, soil moisture and at least weekly data on soil ammonium (NH_4^+) and nitrate (NO_3^-) content. Evapotranspiration, soil temperature and most of the soil moisture data were reasonably well represented. Observed and simulated soil NH_4^+ concentrations agreed well, but Daycent underestimated the NO_3^- concentrations possibly due to an insufficient nitrification rate. Modelled N_2O emissions (18.4 kg N_2O-N$ha^{-1}y^{-1}$) showed a similar pattern but exceeded observed emissions (4.4 kg N_2O-N $ha^{-1}y^{-1}$) by more than three times. Modelled and observed N_2O emissions were dominated by peaks following N-application and heavy rainfall events and were favoured under high soil temperatures. The contribution of N_2O_{den} was simulated well except for a 4-week period when WFPS was overestimated and caused high N_2O emissions, which accounted for 1/3 of the simulated annual N_2O emissions. N_2O_{nit} fluxes were overestimated with Daycent because they are calculated as a fixed proportion of NH_4^+ converted to NO_3^- while the data suggest that significant rates of nitrification can occur without inducing significant N_2O emissions. The comprehensive dataset made it possible to explain discrepancies between modelled and observed values. In-depth model validations with detailed datasets are essential to better understand the internal model behaviour and to derive possible model improvements.

4.1 Introduction

The trace gas nitrous oxide (N_2O) contributes to the greenhouse effect, is involved in stratospheric ozone depletion [*Crutzen*, 1981] and is currently increasing at a rate of 0.2-0.3% per year [*Granli and Bøckman*, 1994]. Most N_2O is produced by the soil microbial processes nitrification and denitrification [*Wrage et al.*, 2001]. Research activities during the last decades have identified soil nitrate (NO_3^-) and ammonium (NH_4^+) content, soil moisture, resp. water filled pore space (WFPS), soil temperature, easily metabolisable carbon, soil pH and their interactions as the main controllers for N_2O production and release from soils. This has led to the development of simulation models such as Century/Daycent [*Parton et al.*, 1988] or DNDC [*Li et al.*, 1992]. The models describe the processes related to N_2O production generally in more detail than what is usually available from data sets. To validate such ecosystem models not only the total N_2O emissions (N_2O_{tot}) but also the process driven N_2O emissions from nitrification (N_2O_{nit}) and denitrification (N_2O_{den}) together with

[a] This work was done in cooperation with Christoph Müller, Department. of Plant Ecology, University of Giessen, Germany

the main driving variables are needed. While N_2O_{tot} emissions, soil moisture and soil temperature may be quantified with high resolution automatic techniques [*Stange et al.*, 2000] it is the dearth of N_2O_{nit} and N_2O_{den} and the soil mineral N data which often preclude a more rigorous model testing. Here we present such an in-depth evaluation of the Daycent model [*Parton et al.*, 2001] using a one-year data set obtained from an urine-affected pasture in New Zealand which contains daily data on N_2O_{tot}, N_2O_{nit}, N_2O_{den} emissions and all main driving variables.

4.2 Materials and Methods

4.2.1 Data set

The data used in this paper were obtained from two field experiments located near Lincoln University on the South Island, New Zealand (43°6' S) receiving an annual precipitation of 657 mm. The soil at the experimental site is a Templeton silt loam (Udic Ustochrept; USDA Soil Taxonomy) and had been under a ryegrass (*Lolium perenne*) – white clover (*Trifolium repens*) pasture for 4 years. The effect of sheep urination events was simulated by applying synthetic urine at four times during one year on separate plots each at rates of 500 kg N ha^{-1}. The full data set is published elsewhere [*Müller et al.*, 1997; *Müller and Sherlock*, 2004].

During the one-year study N_2O_{tot} emissions were determined on 235 days and soil variables including soil NO_3^- and soil NH_4^+ were measured on 51 days. All other variables such as soil moisture, soil temperature and rainfall were determined on a daily basis with an automatic weather station. In a separate field experiment the relative importance of nitrification and denitrification to N_2O_{tot} emissions was quantified. The soil and urine application rates were identical to the ones used in the first experiment. The N_2O_{den} fraction was determined by incubating the soil at 0 and 5 Pa acetylene (C_2H_2) [*Müller et al.*, 1998]. Assuming that other N_2O production processes were negligible N_2O_{nit} was calculated by difference (i.e. $N_2O_{nit} = N_2O_{tot} - N_2O_{den}$). Relationships between N_2O_{den}/N_2O_{tot} and mineral N, soil moisture and soil temperature were developed and used to partition the N_2O_{tot} emissions of the full dataset into N_2O_{nit} and N_2O_{den} emissions [*Müller et al.*, 1998; *Müller and Sherlock*, 2004].

4.2.2 The Daycent model

The Daycent model, the daily version of the Century model [*Parton et al.*, 1988], is a terrestrial ecosystem model that can be used to simulate C, N, P and S dynamics of agricultural and natural systems [*Del Grosso et al.*, 2000; *Parton et al.*, 1996; *Parton et al.*, 2001]. The main changes compared to Century are the finer time scale, a higher spatial resolution of the soil processes and the new N trace gas model; daily precipitation, maximum and minimum temperature and optionally wind speed, radiation and humidity drive the model. The land surface submodel [*Parton et al.*, 1998] simulates water content and temperature for various soil layers and evapotranspiration. Plant production is modelled with a maximal production function limited by temperature, available water and nutrients. The assimilated carbon is allocated to five biomass pools which are characterized by nominal C/N ratios and death rates that can further be affected by water and temperature stress. Dead plant material, which is entering the soil organic matter (SOM) submodel, is divided into

structural and metabolic pools (depending on their N and lignin content) and decomposes to three SOM pools with different turnover times. Soil organic matter decomposition is restricted to the top 20 cm of the soil.

The N trace gas model contains a denitrification and nitrification submodel. The **denitrification** submodel relates soil NO_3^- and CO_2 concentrations to maximal total N_2O_{den} and N_2 emissions (D_t) and the effect of WFPS on soil gas diffusivity is included by a dimensionless multiplier [*Del Grosso et al.*, 2000].

$$D_t = \min [F_d(NO_3^-), F_d(CO_2)] * F_d(WFPS) \quad (1)$$

$$Fd(NO_3^-): y = 1.15x^{0.57} \quad (2)$$

$$Fd(CO_2): y = 0.1x^{1.3} \quad (3)$$

$$Fd(WFPS): y = 0.45 + \text{atan}(0.6\,\pi(0.1x - a))/\pi; \qquad a = F(Dfc, CO_2) \quad (4)$$

After calculating $N_2 + N_2O$ emissions from denitrification, the ratio of N_2 to N_2O ($R_{N2/N2O}$) emissions is calculated as a function of WFPS, NO_3^-/CO_2 ratio and gas diffusivity at field capacity (D_{fc}) [*Del Grosso et al.*, 2000; *Wrage et al.*, 2001].

$$R_{N2/N2O} = F_r(NO_3^-/CO_2) * F_r(WFPS) \quad (5)$$

$$F_r(WFPS): y = \max [0.1; 1.5x - 0.32] \quad (6)$$

$$Fr(NO_3^-/CO_2): y = \max [0.16; e^{-0.8(NO_3^-/CO_2)}] * \max [1.7; 38.4 - 350\,Dfc] \quad (7)$$

$$N2Oden = Dt / (1 + RN2/N2O) \quad (8)$$

In the **nitrification** submodel a fixed proportion (2%) of the nitrification rate (F_{NO3}) is assumed to be lost as N_2O_{nit}. Nitrification rate itself is influenced by soil NH_4^+ concentrations, soil temperature (t), pH and WFPS [*Parton et al.*, 1996; *Parton et al.*, 2001].

$$FNO_3 = baseflow + 0.1 * NH_4^+ * F(t) * F(pH) * F(wfps) \quad (9)$$

$$N_2Onit = FNO_3 * 0.02 \quad (10)$$

NO_x emissions are calculated as a soil gas diffusivity (D/D_0) depending fraction of N_2O_{tot} and an additional factor P to account for pulses in NO_x emissions initiated by precipitation on dry soils [*Parton et al.*, 2001].

$$NO_x = R_{NOx} * N_2O_{den} + R_{NOx} * N_2O_{nit} * P \quad (11)$$

$$R_{NOx} = 15.2 + (35.5\,\text{atan}(0.68\pi(10\,D/D_0 - 1.86)))/\pi \quad (12)$$

4.2.3 Running the model

Daycent requires initial variables and parameters for site and soil properties, organic soil and biomass pools, mineral pools, water content and N deposition (Table 4-1). Additionally, daily climate (min. and max. temperature and precipitation) and information on land use is needed. Land management was simulated as a grass-clover vegetation, with monthly mowing removing 75% of the aboveground biomass. Ammonia volatilisation after synthetic urine application is not considered in the model but was assumed to amount to 30% of applied N. One important constraint of the version of Daycent used in these simulations is that management events can only be scheduled on a monthly basis. To match the actual with the modelled fertilizer events the climate data were shifted by 8 days, which resulted in the smallest possible shift with negligible errors in incoming solar radiation. No further correction or "model fitting" was needed. We decided not to do an equilibrium run but calculated 1.5 years before the actual simulation period to account for pool changes that occurred in the first year.

Table 4-1. Initial driving variables for the Daycent model run.

Parameter	(initial) values
Bulk density [g/m^3]	1.2
Clay [%]	20
Silt [%]	60
Sand [%]	20
pH	6
Organic N [%]	0.7
Organic C [%]	7
Wilting point [vol. fraction]	0.15
Field capacity [vol. fraction]	0.45
Sat. hydr. conduct. [cm/s]	0.00403
Land-use	Grass-clover pasture, harvested monthly except for the winter months June and July

4.2.4 Presentation of results

Some of the processes in Daycent are calculated and updated only weekly; therefore some model outputs show seven-day steps (e.g. N plant growth). The output of Daycent (lines) is presented in the graphs versus the observed mean value of the data (dots or dotted lines).

4.3 Results

4.3.1 N_2O emissions

The general pattern of simulated N_2O emissions agreed reasonably well with the observed dynamics (Figure 4-1). During the experimental period the total measured N_2O_{tot} emissions amounted to 4.4 kg N_2O-N ha^{-1}, while total simulated emissions were 18.4 N_2O-N ha^{-1}. Highest N_2O emissions were observed shortly after urine applications and after the heavy rainfall event at day 154 (Figure 4-2). After this rainfall event and after the first urine application the model strongly overestimated the N_2O emissions, while for the other periods simulated and observed values agreed reasonably well (Figure 4-1). The modelled and observed N_2O_{nit} were on average 48 and 32% and the N_2O_{den} 52 and 68% of total N_2O_{tot} emissions. Hence, the model overestimated the contribution of nitrification related N_2O emissions to the overall flux (Figure 4-1).

4.3.2 Precipitation, soil moisture and soil temperature

Rain events >45 mm day^{-1} caused large observed N_2O_{tot} emission peaks at days 154 and 285 (Figure 4-2). The second peak, which coincided with the fertilizer induced peak after the fourth urine application, was modelled reasonably well, while the first peak which occurred 59 days after N application was largely overestimated in the simulation. The rain at day 59 fell on relatively dry soil and caused the model to predict a short-term emission peak that was not measured. However, as measurements were not carried out daily during this period, this short-term emission peak may have been missed.

Soil temperatures in the top 1 cm of the soil profile were simulated well with Daycent, due to its close connection to observed air temperatures (Figure 4-2). Daycent seems to overestimate soil temperature in summer, while underestimating it in winter. After the third N application no large N_2O_{tot} increase occurred despite high mineral N values, probably because soil temperatures were <5°C. Simulated emissions during this period were higher than observed ones, but stayed on a relatively low level due to the temperature effect.

Modelled and observed WFPS values show in general a similar pattern (Figure 4-2). However, while the wetting-up periods agreed well with the observations there were discrepancies during times of soil drying. The largest discrepancy occurred after the third urine application when the soil temperatures were low (Figure 4-2).

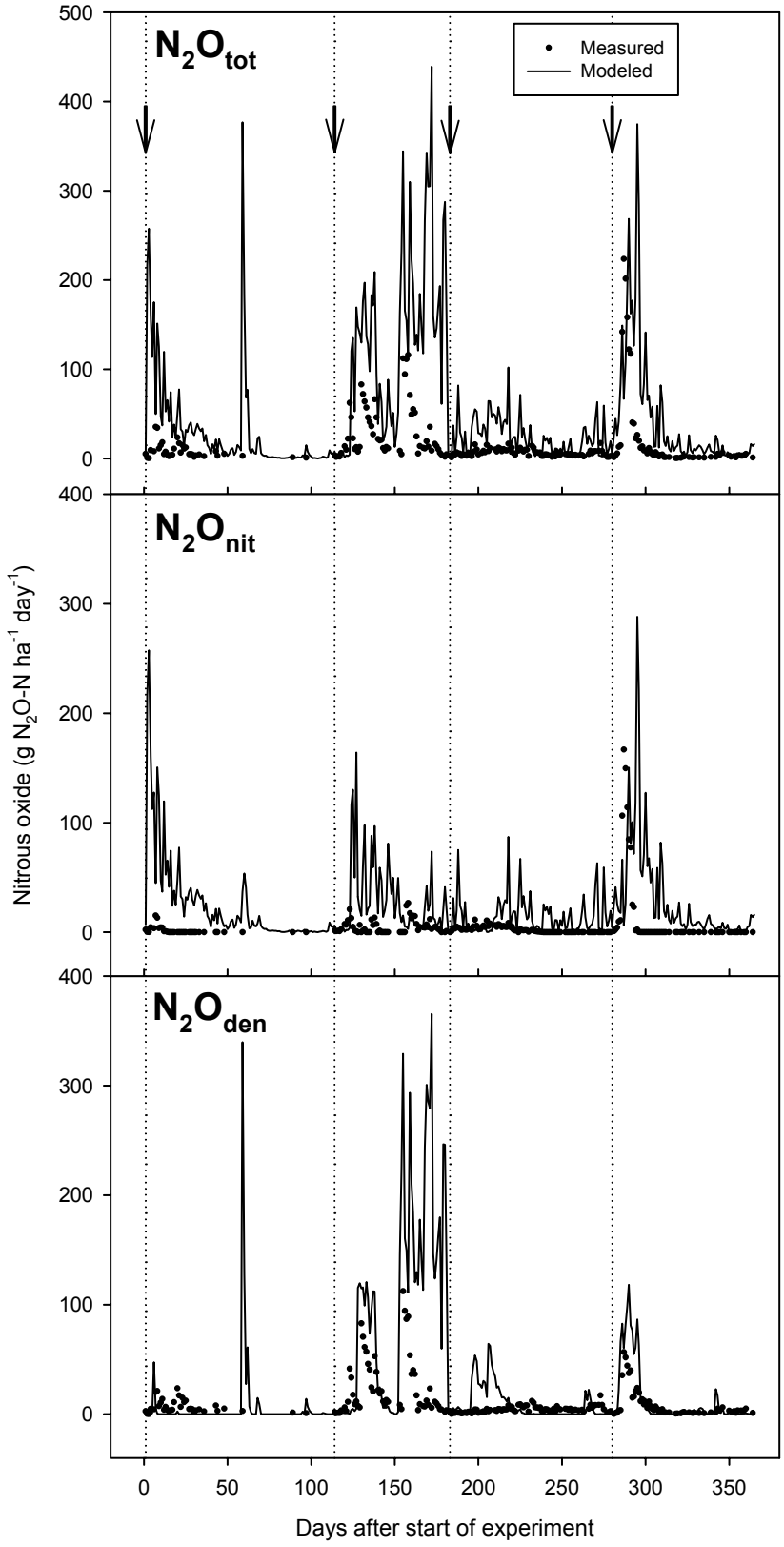

Figure 4-1. Simulated and measured N_2O_{tot}, N_2O_{nit} and N_2O_{den} emissions for the experimental period (arrows indicate the times of synthetic urine applications on separate plots, i.e. between the dotted vertical lines; "measured" N_2O_{nit} and N_2O_{den} were calculated according to [*Müller et al.,* 1998].

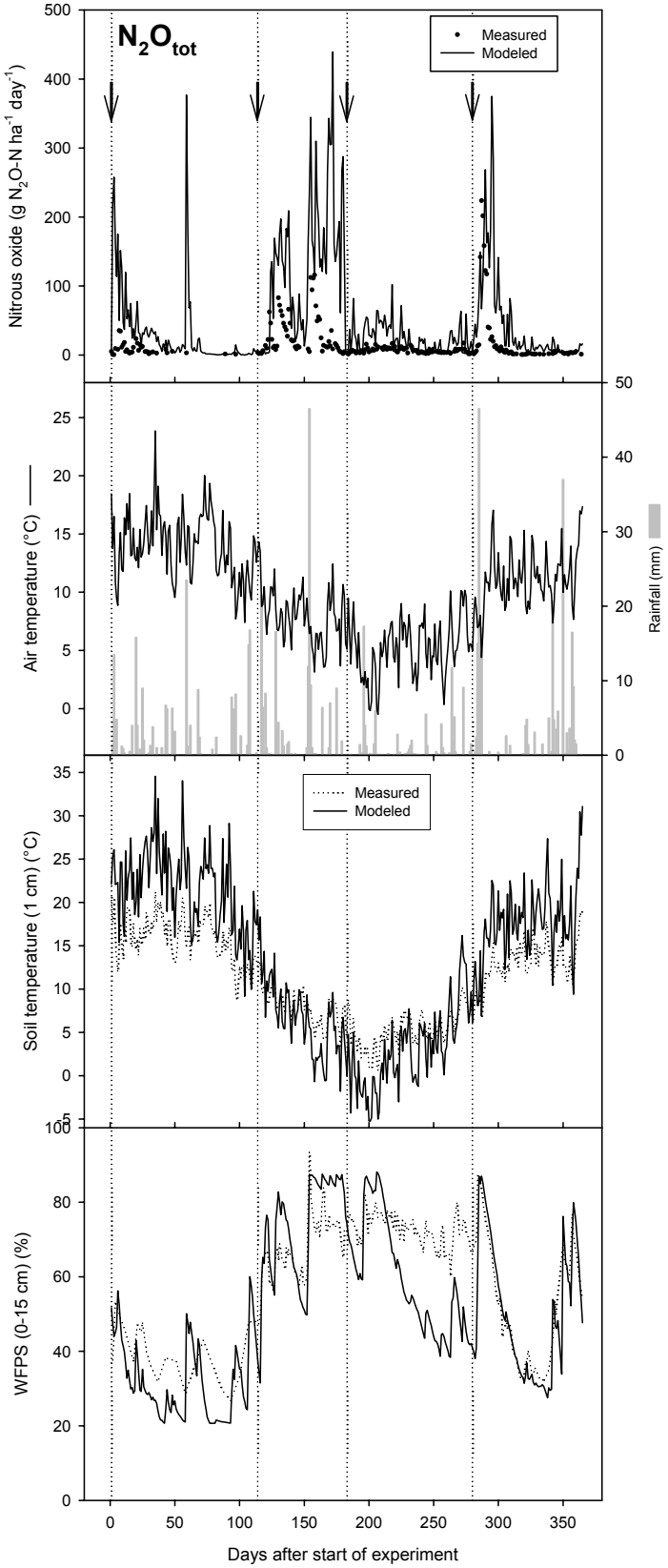

Figure 4-2. Simulated and measured N_2O_{tot}, soil and air temperature, precipitation and WFPS for the experimental period (arrows indicate the times of synthetic urine applications on separate plots, i.e. between the dotted vertical lines).

4.3.3 Mineral N

N fertilization events in Daycent can only occur as NH_4^+ and NO_3^- but not as urea-N, therefore the applied urine N was considered to be NH_4^+. Both observed and modelled results show a sharp increase of NH_4^+ after N application, followed by a gradual decrease (Figure 4-3). While the course of the NH_4^+ content agreed reasonably well after the first and the fourth urea application, simulated NH_4^+ concentrations decreased much slower after the second and the third application (Figure 4-3). This discrepancy can only partly be caused by different plant N uptake, which was 80 kg N ha^{-1} observed and 45 kg N ha^{-1} modelled during this three-month period. Over the entire year, modelled (573 kg N ha^{-1}) and observed plant N uptake (572 kg N ha^{-1}) were the very similar. Soil NO_3^- concentrations were systematically underestimated by Daycent. After the first and the fourth urine application, when NH_4^+ content was simulated well, the NO_3^- concentrations were underestimated by a factor of two, while after the second and the third application, when NH_4^+ content decreased much slower, it was underestimated by a factor of approximately four (Figure 4-3).

The four urine applications were carried out on separate plots; therefore it was assumed that the N-content was zero before the next fertilizer application. Hence, annual sums will not be true annual sums of emissions, because of the exclusion of the long-term effect of the fertilization.

4.3.4 Total N gas loss

The combined N gas (N_2O_{tot} + NO + N_2) loss estimated via Daycent over the entire observation period was 116 kg N ha^{-1} yr^{-1} (18.4 kg N_2O-N; 64.7 kg NO-N; 33.3 kg N_2-N) or 5.8% of the applied N. The simulated NO and N_2 emission were 3.5 and 1.8 times higher than simulated N_2O_{tot} emissions. No validation data existed for NO emissions. Dinitrogen emissions were determined with the acetylene technique (10kPa), which may produce erroneous results when applied to aerobic soils [*Bollmann and Conrad*, 1998]. Therefore, we decided not to validate the simulated N_2 data.

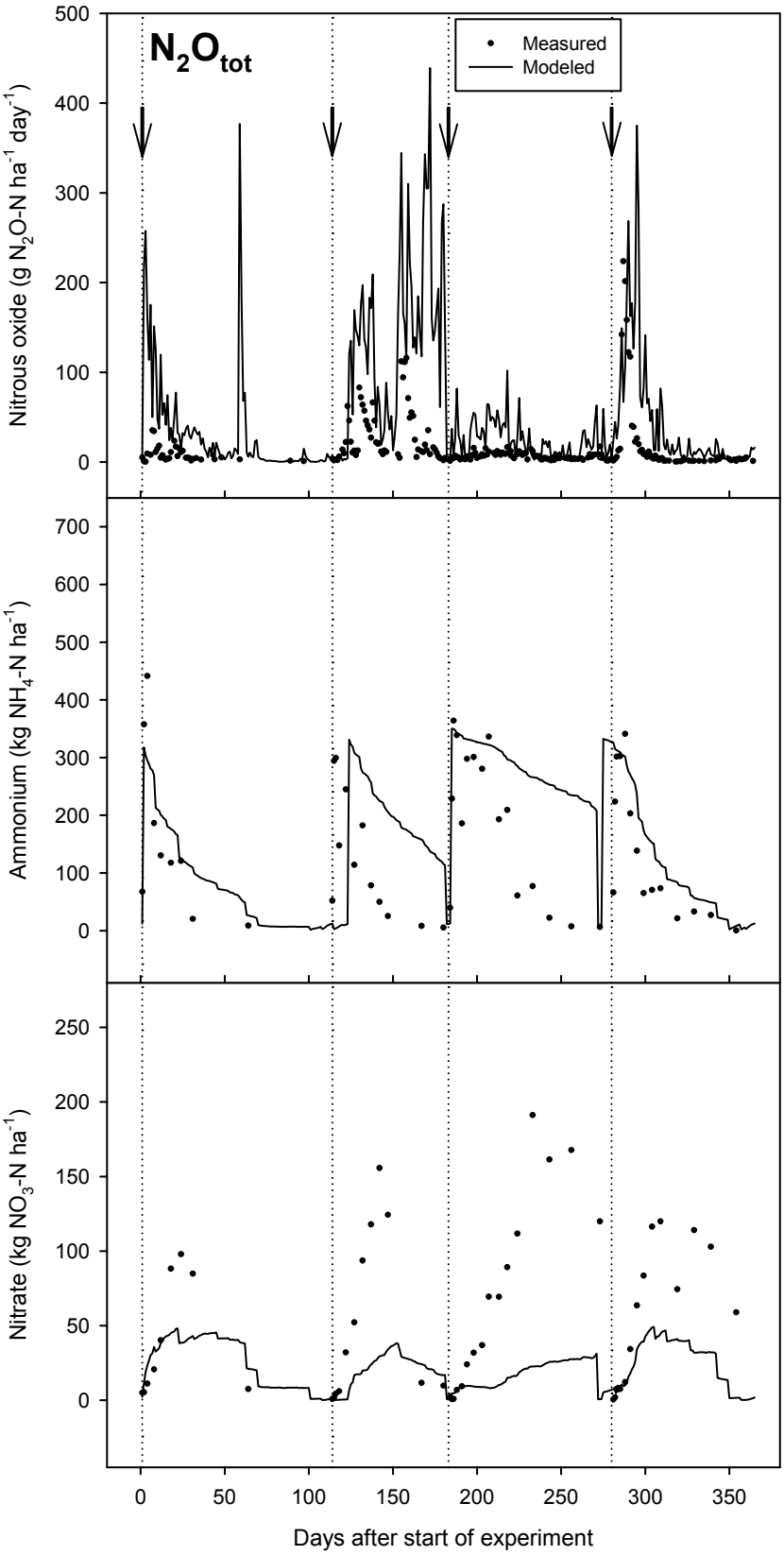

Figure 4-3. Simulated and measured N_2O_{tot}, NH_4^+ and NO_3^- concentrations of the upper 15 cm of the soil (arrows indicate the times of synthetic urine applications on separate plots, i.e. between the dotted vertical lines).

4.4 Discussion

4.4.1 N_2O emissions

For the one-year observations period Daycent overestimated observed N_2O_{tot} by 318%. One reason for this relatively large discrepancy is the period after the strong rainfall event at day 154, where one third of the total simulated annual N_2O flux was emitted within only four weeks (Figure 4-2). During this time, the simulated WFPS was almost 90%, while the observed WFPS was about 70%. Due to the functional relationship between N_2O_{den} and WFPS the N_2O emissions were overestimated. This highlights that periods after extreme events where many of the driving variables for N_2O emissions may be in optimum have to be simulated well because of their importance for the annual balance of N_2O emissions [*Priemé and Christensen*, 2001].

Nitrification contributed significantly to the observed emissions only after the fourth urine application while Daycent also simulated relevant N_2O_{nit} after the first and the second application. Furthermore, between day 180 and 280 no emissions were observed but simulated N_2O_{nit} were still relatively high. In Daycent N_2O_{nit} emissions are functionally related to the nitrification rate and the soil NH_4^+ concentrations (eqts. 9 and 10; Figures 4-1 and 4-3). Instead of relating the N_2O_{nit} to the simulated nitrification rate by a fixed factor it may be more accurate to relate it to the build up of nitrification related nitrite (NO_2^-) which does not occur under conditions which favour quick NO_2^- oxidation [*Venterea and Rolston*, 2000; *Wrage et al.*, 2001].

Simulated N_2O_{den} showed better agreement with observations, apart for the peaks around day 59 and 154 that were discussed above. However, as N_2O_{den} depends on soil NO_3^- concentrations, which are underestimated systematically by a factor of 2-4 during the simulation period, it can be concluded that the simulation procedure is overestimating N_2O_{den}.

Though N_2O_{nit} and N_2O_{den} are considered separately in Daycent, their comparison with observed N_2O_{nit} and N_2O_{den} is not as predicative as for N_2O_{tot} because the acetylene technique used and the application of a relationships observed during a separate field experiment to the entire data set may have produced inaccuracies [*Müller et al.*, 1998]. However, subsequent measurements of the N_2O_{nit} and N_2O_{den} fractions during another field experiment on temperate grassland soil, using *in-situ* ^{15}N-labeling techniques, showed that the N_2O_{nit} fractions were most likely even lower compared to the one presented here [*Müller and Sherlock*, 2004].

4.4.2 Soil moisture

The overestimation of WFPS between day 154 and 220 that has been discussed above may be explained by an overestimated WFPS at field capacity, as the maximal observed WFPS after rainfall events apparently was short-lived and probably related to a water content exceeding field capacity. Reducing the input value for field capacity led to a better simulation of WFPS and significantly reduced the overestimation of N_2O_{den} but was regarded as an illegitimate model tuning (data not shown).

One reason for the discrepancies in WFPS during soil drying especially during times when the soil temperature was low may be the formation of dew, which is not accounted for in the precipitation

data. When calculating daily soil water content from precipitation, evapotranspiration and soil water content of the previous day, a curve very similar to the one modelled in Daycent emerged. This strongly indicates that measured soil water content is higher than could be expected from rain and ET, and dew is very likely to be the reason for this. On the other hand, ET might be overestimated, but the Linacre method used in Daycent and the Penman-Monteith method applied to the data gave almost the same results. Another reason for differing WFPS might be the way in which internal drainage and hysteresis effects are modelled in Daycent. The pedotransfer functions which are used to characterize hydraulic conductivity and drainage may have overestimated internal water flow and redistribution in this soil, but irrespective of the internal flows Daycent simulated no water flowing out of the soil profile during the simulation period (data not shown).

4.4.3 Mineral N

Soil NH_4^+ concentrations are modelled reasonably well after the first and fourth N application. However, after the second and the third application the concentrations were too high which coincided with times of low soil temperature. In the Daycent simulation the main sink for NH_4^+ is immobilization into microbial biomass, followed by plant N uptake, nitrification and gaseous N losses. The Daycent version used for this validation study did not allow application of N in form of urea. Urea hydrolyses quickly to NH_4^+ and in the process increases the soil pH. This can cause high ammonia (NH_3) emissions from soil and can inhibit the activity of microbial transformations [*Brady and Weil*, 2002]. Simulated N leaching was insignificant though data suggest that it also contributed to N removal from the soil. The underestimation of leaching is known to the Century group and has been fixed in the latest version of the model (Bill Parton, pers. comm.). Since modelled and observed plant N uptake agreed well the main reason for the discrepancy in NH_4^+ and NO_3^- concentrations and N_2O emissions is related to the magnitude and interactions of nitrification, leaching and immobilization. In grassland soils, in addition to autotrophic nitrification, also heterotrophic nitrification which is carried out by fungi, may contribute considerably to the NO_3^- built up [*McGill et al.*, 1981]. The speed and interactions of the gross N transformation rates will finally determine the magnitude of N_2O production and emissions from soils [*Müller and Sherlock*, 2004].

4.5 Conclusions

The pattern of modelled and observed N_2O emissions agreed reasonably well, but Daycent overestimated annual emissions by 318%. Analysis of driving variables showed that this was mainly caused by two reasons: a) an overestimation of N_2O_{nit} while NH_4^+ content was modelled accurately and nitrification was underestimated and b) an overestimation of soil WFPS during a period of only four weeks which caused higher than observed N_2O_{den} emissions (30% of total annual emissions) though NO_3^- concentrations were underestimated during this period. Our analysis highlighted the following areas where further model development is needed in Daycent:

1) The inaccuracies in the simulation of NH_4^+ and NO_3^- appear to be related to problems associated with the nitrification submodel and interactions with other processes such as immobilization and leaching.

2) The fixed correlation of the nitrification rate and the N_2O_{nit} emissions to NH_4^+ concentrations may lead to erroneous results because the data suggest that significant rates of nitrification can occur without inducing significant N_2O emissions.

3) Accurate simulation of WFPS is required because of its direct functional relationship to N_2O_{den} and N_2O_{nit} emissions.

4) The addition of different fertilizer types and a finer scheduling of management events are essential for more accurate testing with detailed data sets.

As far as we know there are only a few published N_2O model validations that distinguish N_2O_{nit} from N_2O_{den}. Moreover, Daycent tests of N_2O emissions have rarely included comparisons with observations of the primary drivers of N_2O emissions [e.g. *Frolking et al.*, 1998]. Therefore, validation studies such as the one presented here are valuable and should be carried out with other detailed data sets from other ecosystems because they highlight the directions in which ecosystem models such as Daycent should be developed.

Acknowledgments

We like to thank the Century developing team at Fort Collins/Colorado for providing and assisting us with the Daycent model.

5 Modelling global N_2O emissions from agricultural soils

Summary

Current estimations of global N_2O emissions from agricultural soils amount to 2-3 Tg N_2O-N y^{-1} based on different statistic approaches, with an uncertainty range of 0.6 - 14.6 Tg N_2O-N y^{-1}. A reduction of this uncertainty may be achieved by adapting and applying process-based N_2O emission models based on global datasets of soil properties, climate and agricultural management. Additional model equations were implemented in the trace gas sub-model of the agro-ecosystem model Daycent, refining the calculation of nitrification and denitrification, explicitly addressing soil gas pools, and adding a scheme to account for freeze-thaw emissions in temperate regions. This revised model version is tested against N_2O emission measurements from tropical and temperate agricultural soils under different crop types. Simulation results show that total annual emissions sums are represented well, and that the modelling efficiency on a monthly basis for most sites ranges between 0.1 and 0.66. Sensitivity analysis shows that simulated N_2O emissions are sensitive to changes in agricultural management and climate parameters, and that values of field capacity and hydraulic, which can only be derived from pedotransfer functions at the global scale, may be a considerable source of uncertainty. Based on the revised Daycent version and a global compilation of environmental and agricultural management data, simulated global agricultural emissions amount to 2.1 Tg N_2O-N y^{-1} in the 1990ies, which is similar to other estimates of total N_2O emissions. Simulated fertilizer induced N_2O emissions were in the range between 0.77% (for rice) and 2.76% (for maize) of the nitrogen input via mineral fertilizer or manure.

5.1 Introduction

The atmospheric concentration of N_2O has increased from 285 ppbv before the year 1700 [*Stauffer and Neftel*, 1988] to 314 ppbv in the year 1997 [*IPCC*, 2001]. Despite its low concentration it contributes 4-6% to the anthropogenic greenhouse effect because of its long lifetime of 100 – 150 years and its high absorption capacity (global warming potential is 296 x CO_2) [*Rohde*, 1990]. Beyond, nitrous oxide is transformed to other nitrogen oxides in the troposphere that are involved in the destruction of tropospheric ozone [*Crutzen*, 1981].

This increase in atmospheric N_2O concentration results from direct and indirect emissions due to fertilizer applications (4.2 Tg N_2O-N y^{-1}), from cattle and feedlot (2.1 Tg N_2O-N y^{-1}), industrial sources (1.3 Tg N_2O-N y^{-1}) and biomass burning (0.5 Tg N_2O-N y^{-1}) (Table 5-1). Natural emissions amount to 3 Tg N_2O-N y^{-1} from oceans, to 3 Tg N_2O-N y^{-1} from wet tropical soils, to 3 Tg N_2O-N y^{-1} from other soils and to 0.6 Tg N_2O-N y^{-1} from NH_3 oxidation (Table 5-1).

These estimates are based on several factorial approaches or statistical models and are in agreement with the global imbalance of 3.9 Tg N_2O-N y^{-1} inferred from the observed concentration increase and the stratospheric sinks (Table 5-1). However, the uncertainty range of these estimates is large,

especially for emissions from agricultural soils (-85% to +250%). More recent statistical approaches to estimate N_2O emissions from natural and agricultural soils [*Bouwman et al.*, 2002b], and the one presented in Chapter 3, still show a wide uncertainty range. Statistical models have been useful for these first estimates of N_2O emissions and are and will be valuable for applications like the Kyoto reporting [*IPCC*, 2001] or life cycle assessments, where limited availability of time and data only allows the application of simple statistical or sectoral approaches. However, the application of statistical models is restricted to the boundary conditions under which they were developed, and therefore process models are needed to address the question how the interacting changes in meteorology, anthropogenic emissions, CO_2 concentrations, land-cover and land-use will affect N_2O emissions from soils. Beyond, the uncertainty of N_2O emission estimates may be reduced by applying process-based models, which account for the spatial and temporal variability of environmental and management parameters and their effects on emission processes.

Table 5-1. Source estimates for global N_2O emissions [Tg N_2O-N $year^{-1}$], adopted from *IPCC* [2001].

Reference	*Mosier et al.* [1998] *Kroeze et al.* [1999]		*Olivier et al.* [1998]	
Base year	1994		1990	
Sources	Tg N $year^{-1}$	Range	Tg N $year^{-1}$	Range
Ocean	3.0	1 – 5	3.6	2.8 – 5.7
Atmosphere	0.6	0.3 – 1.2	0.6	0.3 – 1.2
Wet forest soils	3.0	2.2 – 3.7		
Dry savannah soils	1.0	0.5 – 2.0		
Temperate forest soils	1.0	0.1 – 2.0		
Temperate grassland soils	1.0	0.5 – 2.0		
All soils			6.6	3.3 – 9.9
Natural sub-total	**9.6**	**4.6 – 15.9**	**10.8**	**6.4 – 16.8**
Agricultural soils	4.2 [a]	0.6 – 14.8	1.9	0.7 – 4.3
Biomass burning	0.5	0.2 – 1.0	0.5	0.2 – 0.8
Industrial Sources	1.3	0.7 – 1.8	0.7	0.2 – 1.1
Cattle and feedlots	2.1	0.6 – 3.1	1.0	0.2 – 2.0
Anthropogenic sub-total	**8.1**	**2.1 – 20.7**	**4.1**	**1.3 – 7.7**
Total sources	**17.7**	**6.7 – 36.6**	**14.9**	**7.7 – 24.5**
Imbalance (trend)	3.9	3.1 – 4.1		
Total sinks (stratospheric)	12.3	9 – 16		
Implied total source	**16.2**			

[a] direct and indirect emissions.

On the global scale only two process-based models have been used to estimate N_2O in a rather conceptual way: Instead of calculating nitrification and denitrification – the main sources of N_2O – explicitly, emissions are calculated as fractions of gross mineralisation rates. The HRBM model applies an empirical factor to relate N_2O emissions to mineralisation rate [*Nevison et al.*, 1996], while the CASA model calculates N_2O emissions as a function of soil water content and mineralisation rate [*Potter et al.*, 1996].

On the other hand more process-based N_2O emission models such as the Daycent model [*Parton et al.*, 1996], DNDC [*Li et al.*, 1992] or the Expert-N framework [*Engel and Priesack*, 1993] have been developed during the last decades, but have so far only been applied at country and regional scales by grid-based modelling [*Butterbach-Bahl et al.*, 2004; *Schulte-Bisping et al.*, 2003] or through extrapolation of exemplary field simulations [*Del Grosso et al.*, 2002; *Del Grosso et al.*, 2005].

Here, the adaptation and application of the Daycent model [*Parton et al.*, 1996] to simulate N_2O emissions from agricultural soils at the global scale is presented. The Daycent model was selected as it had already been applied to a number of case studies from different climate regions [*Kelly et al.*, 1997; *Motavalli et al.*, 1994; *Silver et al.*, 2000] and as it simulates plant-soil processes and agricultural management in great detail. Beyond, model inter-comparisons have proven that the monthly model version, the Century model [*Parton et al.*, 1988], has a high performance for long term carbon dynamics [*Smith et al.*, 1997] and N_2O emissions [*Frolking et al.*, 1998].

In order to account for model limitations identified by literature reviews, discussions with the model developers [*Ojima et al.*, 2004] and own simulation studies, additional equations were implemented in the Daycent model, including more detailed calculation of nitrification and denitrification, and an approach to calculate freeze-thaw emissions (Chapter 5.2). This revised model version was then tested against measured data of soil water contents, soil ammonia and soil nitrate concentrations and N_2O emissions from different climate regions and crop types (Chapter 5.3). A sensitivity analysis was used to identify the effect of changes in input parameters on simulated emission rates (Chapter 5.4). Based on a compilation of global input datasets required for a global model application (Chapter 5.5), the revised Daycent version is applied to estimate current N_2O emissions from agricultural soils at the global scale (Chapter 5.6).

5.2 Model development

5.2.1 The Daycent model

The Daycent model [*Parton et al.*, 1996] is the daily time step version of the Century model [*Parton et al.*, 1988]. Both models can be characterized as general agro-ecosystem models and are used to simulate carbon, nitrogen, phosphorous and sulphur dynamics of agricultural and natural systems [*Del Grosso et al.*, 2000; *Parton et al.*, 1996; *Parton et al.*, 2001]. While the Century model focuses on long-term soil dynamics (decades to centuries), the Daycent model with its higher temporal resolution can be used to calculate plant production, soil processes and emissions of NO, N_2O, N_2 and CH_4 at shorter time scales. Both models share the same modelling concept which can be divided in (i) the land surface sub-model [*Parton et al.*, 1998] simulating water content and temperature for various soil layers and evapotranspiration, (ii) the plant production sub-model using a maximal production function limited by temperature, availability of water and nutrients, and (iii) the soil organic matter (SOM) sub-model, calculating turnover processes between litter pools and three SOM pools with different turnover times. All sub-models are described in detail in the Century manual [*Century-Manual*, 2005]. A simplified scheme of the SOM dynamics in Century and Daycent is presented in Figure 5-1.

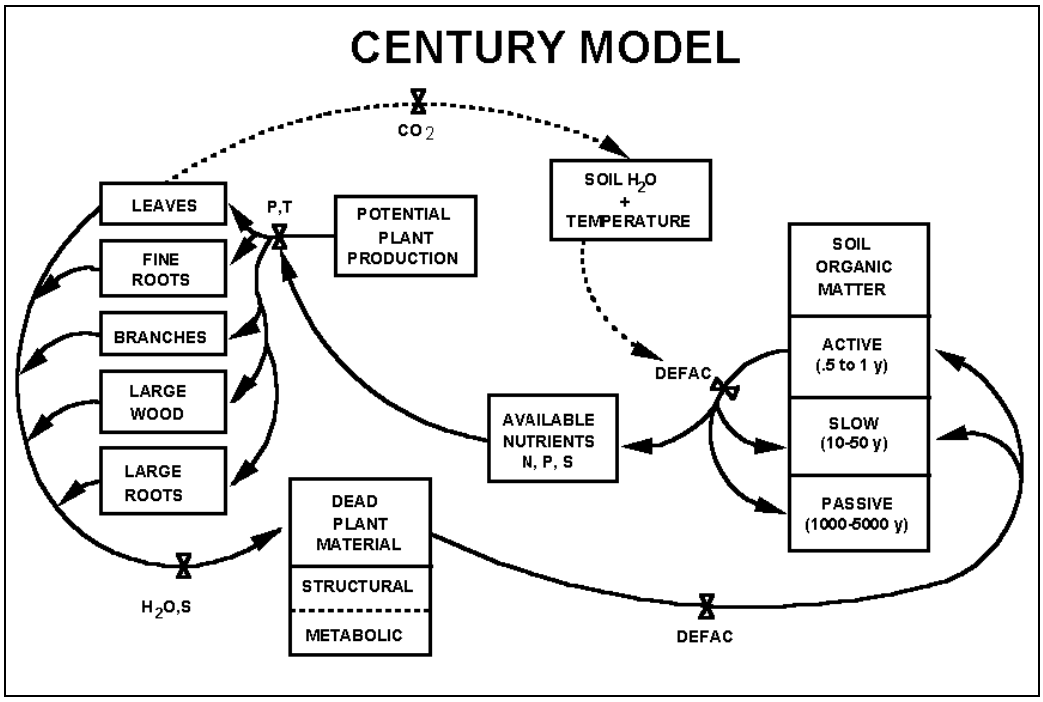

Figure 5-1. Schematic overview of the Century model. Source: *Century Manual* [2005].

5.2.2 Revision of the trace gas module

The Daycent trace gas module [*Del Grosso et al.*, 2000; *Parton et al.*, 1996; *Parton et al.*, 2001] calculates NO, N_2O and N_2 emissions from nitrification and denitrification, the major sources of these gases in soils. In the original version, these processes are simulated in the following way: N_2O emission from nitrification is calculated as a fixed fraction (2%) of the nitrification rate. For denitrification, it is at first assumed that nitrate is entirely transformed to N_2O and N_2, whereby the ratio of N_2O/ N_2 is calculated as a function of water filled pore space (wfps) and NO_3^-/CO_2 ratio. Afterwards, NO emissions are calculated as a function of total N_2O emissions and soil gas diffusivity plus an additional pulse of NO from nitrification after wetting of dry soils.

In the following paragraph an alternative way to calculate gaseous N emissions from nitrification and denitrification is suggested, including an explicit consideration of soil gas pools, and adding a mechanism to account for freezing-thawing emissions, which can contribute substantially to annual N_2O emissions from temperate soils [*Kaiser and Ruser*, 2000]. An overview of the involved processes and their implementation in the revised trace gas module is presented in Figure 5-2 and Tables 5-2 to 5-4.

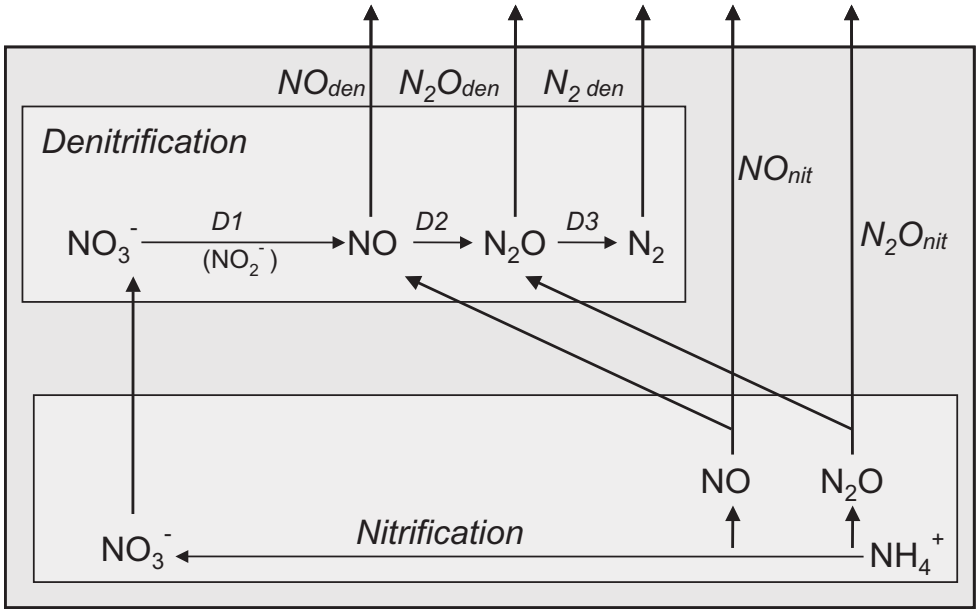

Figure 5-2. Schematic overview of the revised Daycent trace gas module. D1, reduction of nitrate to NO; D2, reduction of NO to N_2O; D3, reduction of N_2O to N_2; N_2den, production of N_2 from denitrification; N_2Oden, production of N_2O from denitrification; N_2Onit, production of N_2O from nitrification; NOden, production of NO from denitrification; NOnit, production of NO from nitrification.

5.2.2.1 Nitrification

Nitrification is an important source of NO and N_2O emissions from soils [*Ambus and Robertson*, 1998; *Kester et al.*, 1997; *Papen and Butterbach-Bahl*, 1999; *Skiba et al.*, 1997], but the mechanisms that lead to the formation of N_2O and NO during nitrification are still unclear. It has been suggested that the NO_2^- produced by nitrifiers is transformed to NO and N_2O by chemodenitrification or by nitrifier denitrification under oxygen stress [*Firestone and Davidson*, 1989; *Poth and Focht*, 1985]. Additionally, oxidative production of N_2O and NO during ammonia oxidation might also occur [*Hooper and Terry*, 1979; *Ritchie and Nicholas*, 1972]. However, a number of major controls of nitrification have been identified. These controls and their implementation in the Daycent trace gas module (Figure 5-2, and Equation 1 to 7.2) are discussed in the following.

In general, the calculation of the nitrification rate (Equation 1 to 4) is the same as in the original Daycent model, only the maximum fraction of ammonium that can be nitrified each day has been increased from 2% to 70%, and the upper limit of nitrification rate (0.4 g N m^{-2} day^{-1}) has been removed (see below).

The nitrification rate in soils strongly depends on the availability of **ammonium** (NH_4^+) as a substrate. However, measured ammonium concentrations may be low compared to nitrification rates, as in most soils nitrification is faster than the production of ammonium through decomposition (ammonification). Only at soil temperatures above 30°C and at low temperatures – combined with poor aeration – ammonification is faster than nitrification [*Scheffer*, 2002]. Beyond,

in fertilized soils the amount of ammonium added to a soil may result in elevated ammonium concentrations during some days or weeks. In spite of the fast nitrification in most soils, the original Daycent version restricted maximum nitrification to 2% of available ammonium and to 0.4 g $Nm^{-2}day^{-1}$. In the revised version, no upper limit is set to the nitrification rate, and the fraction of ammonium that can be nitrified each day is increased to 70%, thereby allowing for the high nitrification rates > 10 g $Nm^{-2}day^{-1}$ observed after fertilization events [*Matson et al.*, 1998].

The oxidation of ammonium to nitrate requires molecular **oxygen,** and therefore the partial pressure of O_2 [pO_2] might be a control of nitrification. However, pO_2 is only limiting at concentrations < 0.5% [*Anderson and Levine*, 1986; *Bollmann and Conrad*, 1998], and therefore it can be assumed that O_2 is non-limiting at aerobic microsites. Soil aerobicity is strongly related to water filled pore space (wfps), and it has been observed that nitrification decreases at wfps above 50% because of increasingly anaerobic conditions in the soil [*Firestone and Davidson*, 1989]. Both in the original and in the revised Daycent versions a linear decrease of the nitrification rate is assumed for wfps exceeding the wfps at field capacity (Equation 1 in Table 5-2).

Like most biological processes, nitrification is positively affected by **temperature** up to an optimum value beyond which further increase in temperature suppresses the process. An exponential increase in nitrification at various temperature ranges below 35°C was observed by *Saad and Conrad* [1993]. There are indications that the optimum temperature for nitrification is a function of the average maximum monthly air temperature for the warmest month of the year [*Malhi and McGill*, 1982; *Stark and Firestone*, 1996], and therefore a respective function had been implemented in the Daycent model [*Parton et al.*, 1996]. For the revised version, this function has been slightly changed to allow low nitrification rates at low temperatures (Equation 3 in Table 5-2).

Table 5-2. Equations for nitrification rate.

Variable	Equation	Eq. No.
Nitrification rate [$gNm^{-2}day^{-1}$]	$R\_Nitr = 0.7 * NH_4 * F\_temp * F\_pH * F\_wfps$	1
Moisture effect [0-1]	if wfps < wfps_fc: $F\_wfps = 1.0/(1.0 + 30.0 * EXP(-9.0 * wfps))$ if wfps > wfps_fc: $F\_wfps = (0.0 - 1.0) / (1.0 - fc) * (wfps - 1.0)$	2
Temperature effect [0-1]	$F\_temp = EXP(3.7*(1-(-5.0- Tsoil)/(-5.0-Tmax)^{7.0})/7.0) * ((-5.0 - Tsoil)/(-5.0-Tmax))^{1.8}$	3
pH effect [0-1]	$F\_pH = 0.56+(1/pH)*atan(Pi*0.45*(pH-5.0))$	4

F_pH, pH effect; F_temp, temperature factor, normalized to maximum temperature of the warmest month; F_wfps, soil moisture effect; NH_4, ammonium content of the soil [gNm^{-1}]; pH, soil pH; R_Nitr, Nitrification rate; Tmax, optimum temperature for nitrification (35°C); Tsoil, soil temperature; wfps, water filled pore space; wfps_fc, wfps at field capacity.

As all microbial activity depends on **soil water** as a solvent, the nitrification rate primarily increases with wfps until soil water becomes limiting for oxygen diffusion as described above. Though this positive correlation between wfps and nitrification rate has been observed in many studies [*Firestone and Davidson*, 1989] the intensity of this effect is still debated, as some observations only show a weak correlation between nitrification induced NO emissions and wfps

[*Martin et al.*, 1998]. For the effect of soil moisture on nitrification, a function based on *Doran* [*Doran et al.*, 1988] had been implemented in Daycent (Equation 2 in Table 5-2) [*Parton et al.*, 2001].

There are only a few studies on the effect of **pH** on nitrification rates. Some studies report pH optimums in the range of 7.5 – 8.0 [*Ward et al.*, 1978], while others state that the pH optimum of a nitrifier community matches the soil pH of the ecosystem they were collected from [*Bramley and White*, 1990]. Following the first approach, the Daycent model applies a logistic function for the effect of pH on nitrification rates (Equation 4 in Table 5-2) [*Parton et al.*, 2001].

As pointed out above, there is still a knowledge gap about the mechanisms of N_2O and NO production from nitrification, and only few studies have investigated the effect of soil parameters on the relative losses of N_2O and NO from nitrification. In general, the loss of NO from gross nitrification varies between 0.1 and 4% [*Baumgärtner and Conrad*, 1992], while the reported N_2O loss can range from 0.008 to 0.2% [*Goodroad and Keeney*, 1984]. Based on these literature results, the simulated potential loss of N_2O was changed from 2% to 0.5% respectively, and the maximum loss of NO was set to 2% (Equation 5.1 and 5.2 in Table 5-3). Given the wide ranges in the observations cited above these settings are inevitably somewhat arbitrary. As the temperature effects on NO and N_2O emissions from nitrification are stronger than the temperature effect on nitrification alone, an additional temperature effect for the fraction of NO and N_2O lost was implemented in the revised Daycent version (Equation 6.1 and 6.2 in Table 5-3).

Table 5-3. Equations for NO and N_2O emissions from nitrification.

Variable	Equation	Eq. No.
NO production [$gNha^{-1}day^{-1}$]	$NOnit = R\_Nitr * 0.02 * F\_temp\_NOnit$	5.1
N_2O production [$gNha^{-1}d^{-1}$]	$N_2O_{nit} = R\_Nitr * 0.005 * F\_temp\_N_2Onit$	5.2
Temperature effect NO [0-1]	$F\_temp\_NOnit = EXP(5.0*(1-((-15.0-Tsoil)/(-15.0-Tmax))^{6.0})/6.0) * ((-15.0-Tsoil)/(-15.0-Tmax))^5$	6.1
Temperature effect N_2O [0-1]	$F\_temp\_N2Onit = EXP(5.0*(1-(-20.0- Tsoil)/(-20.0-Tmax)^{2.0})/2.0) * ((-20.0-Tsoil)/(-20.0-Tmax))^5$	6.2
NO loss from nitrification NO [0-1]	$NO\_loss\_nit = NO_{nit} * max(D / D_{fc} ; 1)$	7.1
N_2O loss from nitrification N_2O [0-1]	$N_2O\_loss\_nit = N_2O_{nit} * max(D / D_{fc} ; 1)$	7.2

D, gas diffusivity of the soil; Dfc gas diffusivity of the soil at field capacity; F_temp_NOnit, temperature factor for NO production from nitrification; F_temp_N2Onit, temperature factor for N_2O production from nitrification; NO_loss_nit, NO loss from NO gas pool produced by nitrification; NOnit, production of NO from nitrification; N_2O_loss_nit, loss of N_2O from N_2O gas pool produced by nitrification; N2Onit, production of N_2O from nitrification; Tmax, optimum temperature for NO and N_2O production from nitrification (35°C); Tsoil, soil temperature; wfps, water filled pore space.

The N_2O and NO produced from nitrification can either diffuse out of the soil or be consumed as a substrate in the denitrification process (see below), depending on the gas diffusivity of the soil. In contrast to the original model formulation, it is assumed that diffusion of N_2O and NO from nitrification is impeded at soil water content exceeding field capacity, whereby the fraction lost is a function of gas diffusivity (Equation 71 and 7.2 in Table 5-3). At lower soil water contents, all N_2O and NO from nitrification is assumed to be directly emitted from the soil.

5.2.2.2 Denitrification

In contrast to nitrification, denitrification is an anaerobic process during which Nitrate is stepwise reduced to Nitrite, NO), N_2O and N_2 as terminal electron acceptor during fermentation, with NO and N_2O as obligatory free intermediates [*Ye et al.*, 1994; *Zumft*, 1993]. Depending on the gas diffusivity of the soil, NO and N_2O either leave the soil or are subject to further reaction.

In the revised Daycent model, the reduction of Nitrate to NO, from NO to N_2O and from N_2O to N_2 is explicitly calculated (Figure 5-2). Thereby it is possible to include the controls of the single reaction steps separately (Equation 8 to 13.3 in Table 5-4), and to account for the losses of NO and N_2O via diffusion (Equation 14.1 to 14.3 in Table 5-4). The major controls of denitrification and their implementation in the Daycent model are presented below. As literature often does not address the single steps of denitrification explicitly, the following discussion mainly refers to total denitrification rate, only adding information for single steps if available.

As **soil water** provides both the fluid environment for bacteria and a barrier to the inhibitory oxygen, denitrification rates increase with increasing soil water content [*Davidson*, 1991]. Below a threshold of water filled pore space, which is close to the wfps at field capacity (~55% wfps) no denitrification is possible [*de Klein and van Logtestijn*, 1996]. Therefore the original Daycent calculates an increase in denitrification rate as a function of wfps and the gas diffusivity at field capacity. This same function is applied for the reduction of Nitrate to NO in the revised version (Equation 11 in Table 5-4), as there is no indication in literature that the subsequent reduction of NO and N_2O steps are affected differently by soil water content. Additionally to its effect on denitrification rates, increasing soil water content also decreases the fraction of NO and N_2O lost from denitrification, as these gases are more likely to be reconsumed under impeded gas diffusion. That is accounted for explicitly in the revised Daycent version by calculating the loss of N-gases from the pools as a function of the pool size and the relative gas diffusivity (see below, Equation 14.1 to 14.3 in Table 5-4).

Denitrification rates increase with increasing **temperature** [*Avalakki et al.*, 1995; *Dawson and Murphy*, 1972]. A temperature increase of 10 °C leads to an increase of the denitrification rate by a factor of 2 (Q_{10} = 2) for soil temperatures between ~ 10 and 35°C as reported in several studies [*Bailey and Beauchamp*, 1973; *Dawson and Murphy*, 1972; *Stanford et al.*, 1975]. Below 10°C, denitrification rates further decline, though denitrification can still be observed in unfrozen soils at temperatures as low as –2°C [*Dorland and Beauchamp*, 1991]. Different effects of temperature on the single steps of denitrification can be indirectly deduced from the observation that the ratio of N_2O/N_2 from denitrification increases with decreasing temperatures [*Firestone and Davidson*, 1989; *Keeney et al.*, 1979], indicating a higher temperature sensitivity of the reduction of N_2O to N_2 than of the reduction of NO to N_2O (Equation 12.1 to 12.3 in Table 5-4).

Denitrification rates strongly increase with increasing **pH**, with optimum conditions in neutral to slightly alkaline soils [*Bremner and Shaw*, 1958; *Federer and Klemedtsson*, 1988; *Wijler and Delwiche*, 1954]. As the N_2O reductase is very sensitive to protone activity, the fraction of N_2O lost from denitrification is larger at low pH [*Alexander*, 1977; *Simek et al.*, 2000; *Wijler and Delwiche*, 1954]. At pH values below 4.6, similar amounts of NO and N_2O are produced [*Wijler and Delwiche*, 1954], while N_2O emissions exceed NO emissions at higher pH values. To account for these different pH dependencies the three steps of denitrification in the revised Daycent version are parameterised with different pH dependencies (Equation 13.1 to 13.3 in Table 5-4).

Table 5-4. Equations for denitrification.

Variable	Equation	Eq. No.
Reduction of nitrate to NO [$gNm^{-2}d^{-1}$]	$D1 = 0.2 * NO_3^- * F\_temp_{D1} * F\_pH_{D1} * F\_wfps$	8
Reduction of NO to N_2O [$gNm^{-2}d^{-1}$]	$D2 = NO\_pool * F\_temp_{D2} * F\_pH_{D2}$	9
Reduction of N_2O to N_2 [$gNm^{-2}d^{-1}$]	$D3 = N2O\_pool * F\_temp_{D3} * F\_pH_{D3}$	10
Soil moisture effect [0-1]	$F\_wfps = [\ 0.45 + \arctan(6.0\ Pi * (wfps - (wfps\_fc + 0.9)/(2))) / Pi\ ] / F\_wfps\ (1.0)$	11
Temperature effect D1 [0-1]	$F\_temp_{D1} = EXP(5.0*(1.0-((-20.0-Tsoil)/(-20.0-Tmax))^{5.0})/5.0)*((-20.0-Tsoil)/(-20.0-Tmax))^{5.0}$	12.1
Temperature effect D1 [0-1]	$F\_temp_{D2} = 1.05^{((Tsoil-22.5)/10)} / 1.05^{((Tmax-22.5)/10)}$	12.2
Temperature effect D3 [0-1]	$F\_temp_{D3} = 1.05^{((Tsoil-22.5)/10)} / 1.05^{((Tmax-22.5)/10)}$	12.3
pH effect D1 [0-1]	$F\_pH_{D1} = 1-1/(1+EXP(pH-2))$	13.1
pH effect D2 [0-1]	$F\_pH_{D2} = (1.0 - 0.8) / (7.0 - 0.0) * (pH - 7.0) + 1.0$	13.2
pH effect D3 [0-1]	$F\_pH_{D3} = (1.0 - 0.8 / (7.0 - 0.0) * (pH - 7.0) + 1.0$	13.3
NO loss [$gNm^{-2}d^{-1}$]	$NO\_loss\_den = NO\_pool * Diff$	14.1
N_2O loss [$gNm^{-2}d^{-1}$]	$N_2O\_loss\_den = N_2O\_pool * Diff$	14.2
N_2 loss [$gNm^{-2}d^{-1}$]	$N_2\_loss\_den = N_2\_pool * Diff$	14.3

Diff, gas diffusivity of the soil; D1, reduction of nitrate to NO; D2, reduction of NO to N_2O; D3, reduction of N_2O to N_2; F_pH_{D1}, pH effect on D1; F_pH_{D2}, pH effect on D2; F_pH_{D3}, pH effect on D3; F_temp_{D1}, temperature effect on D1; F_temp_{D2}, temperature effect on D2; F_temp_{D3}, temperature effect on D3; F_wfps, soil moisture effect on D1; NO_3^-, nitrate content of the soil [gNm^{-2}]; NO_loss_den, NO loss from NO gas pool after reduction of nitrate to NO; N_2O _loss_den, N_2O loss from N_2O gas pool after reduction of NO to N_2O; N2_loss_den, N_2 loss from N_2 gas pool after reduction of N_2O to N_2; NO_pool , NO gas pool of the soil [gNm^{-2}]; N_2O _pool , N_2O gas pool of the soil [gNm^{-2}]; N_2_pool , N_2 gas pool of the soil [gNm^{-2}]; pH, soil pH; Tmax, optimum temperature for denitrification (35°C); Tsoil, soil temperature; wfps, water filled pore space; wfps_fc, wfps at field capacity.

There is a conceptual problem to transfer Q_{10} values or other laboratory data to the equations of the trace gas module. As all fluxes are calculated based on substrate availability, maximum turnover fractions and reduction factors rather maximum fluxes, the experimentally derived parameters can only applied to the first step of a reaction chain, while for all further steps only the additional effect

can be taken into account. Therefore the temperature and pH effect on the reduction of nitrate is calculated based on experimental data, based on the wfps function applied in the original Daycent version, and the temperature function applied in the DNDC model [*Li et al.*, 2000]. For the temperature and pH effects on the reduction of NO and N_2O are implemented as linear reduction factors, as a first approximation of their additional impact.

Gas diffusion from the NO and the N_2O gas pool is calculated after the respective production step has been calculated, thereby leaving only part of the pool for the next step in the chain of reactions (Figure 5-2). The fraction that is emitted from the soil is calculated as a function of soil gas diffusivity, which is a function of soil water content and soil texture (Equation 14.1 to 14.3). Furthermore, after each simulated daily time step, the remaining gas pools are emitted from the soil, as significant accumulation of NO and N_2O does not occur in the topsoil.

5.2.2.3 Freeze-thaw emissions

Freezing and thawing periods strongly affect N_2O and NO emission rates and can substantially contribute to annual emissions [*Edwards and Killham*, 1986; *Goodroad and Keeney*, 1984; *Kaiser and Ruser*, 2000]. A combination of several mechanisms is assumed to cause the observed effects: First, limited gas diffusion in the frozen soil leads to anaerobic conditions favouring denitrification. Second, freezing causes an increase in easily degradable carbon and nitrogen by flushes of mineralisation and by dying microorganisms [*DeLuca et al.*, 1992; *Herrmann and Witter*, 2002; *Schimel and Clein*, 1996]. Third, thawing water may create favourable conditions for denitrification. Beyond, the observed strong and short peaks of N_2O emissions at thawing may partly be attributed to the physical release of gases that had been enclosed in the frozen soil.

Despite their substantial contribution to annual emissions, freeze-thaw emissions are not accounted for in the original Daycent version. In order to represent the effect of freezing on the increase in available soil carbon and nitrogen content, the revised Daycent calculates an increase in decomposition rate during freezing periods. From [*Herrmann and Witter*, 2002] it is derived that about 0.2% of the microbial biomass is decomposed per day and degree below –1 °C, which is in Daycent applied to the "metabolic soil carbon pool", representing microbial biomass. The additional decomposition rate is calculated as

$$\text{Freezing effect} = \min((-0.002 * \text{Temp}), 0.008) \quad \text{at Temp} < -1°C$$

whereby "Temp" is the average daily air temperature. Additionally it is assumed that in frozen soils the reduction of denitrification rates by wfps does not fall below 0.65 to account for limited gas diffusivity in frozen soils. The physical release of accumulated N gases was not implemented explicitly in Daycent as this effect is still debated and may be relevant only in soils where a frozen leaf litter can seal the soil like e.g. in deciduous forests, whereby not being relevant in coniferous forests or on agricultural fields.

5.3 Site specific testing

5.3.1 Description of test sites

In order to test the Daycent model and the revised trace gas module for its applicability to agricultural systems throughout the world, simulations were carried out for field measurements selected from the peer-reviewed literature. The criteria for the selection process were (i) frequency of measurements, (ii) length of experimental period, (iii) availability of data needed for the simulation, (iv) availability of variables like soil water content and soil nitrogen concentration, (v) representation of different crop types and (vi) representation of different climate zones. For this analysis seven agricultural sites covering the crops wheat, barley, maize and grassland under temperate, subtropical and tropical climate were selected. The temperate test sites are located in Germany (wheat, maize, potato), the United States (barley, maize) and Canada (maize), the subtropical site is located in New Zealand (fertilized grassland) and the data representing tropical agriculture stem from Mexico (wheat) and Costa Rica (maize) (Table 5-5).

Table 5-5. Site characteristics and literature reference for agricultural sites used for the Daycent tests.

Site name	Location	Crops	N input [kg N $ha^{-1}y^{-1}$]	Ann. prec. [mm]	Avg. temp [°C]	pH	Texture [%]			Reference
							Clay	Silt	Sand	
Temperate sites										
Flessa C	Scheyern, Germany	barley; mustard; wheat	50; 30; 160	833	7.4	5.9	22	61	16	*Flessa et al.,* 1995
Flessa D	Scheyern, Germany	barley; mustard; wheat	50; 30; 160	833	7.4	6.3	19	60	21	*Flessa et al.,* 1995
Ruser A	Scheyern, Germany	maize	130	833	7.4	6.3	24	55	21	*Ruser et al.,* 2001
Ruser B	Scheyern, Germany	potato	150	833	7.4	6.3	24	55	21	*Ruser et al.,* 2001
Ruser C	Scheyern, Germany	potato; wheat	150; 180	833	7.4	6.3	24	55	21	*Ruser et al.,* 2001
Ruser D	Scheyern, Germany	wheat; maize	180; 130	833	7.4	6.3	24	55	21	*Ruser et al.,* 2001
Ottawa	Ottawa, Canada	maize	155	867	5.7	6.3	10	50	40	*Grant and Patty* , 2003
Colorado	Colorado, USA	maize; barley	200; 200	326	4.9	6.2	36	34	32	*Mosier et al.,* 1986
New Zealand	Christchurch, New Zealand	grassland	4 x 500	657	10.5	6.0	20	60	20	*Müller et al.,* 1998
Tropical sites										
Mexico	Yaqui valley, Mexico	irrigated wheat	250	irrig.	17.6	8.3	44	22	34	*Matson et al.,* 1998
Finca fert	La Selva, Costa Rica	maize	122	3962	25.8	6.9	25	45	30	*Weitz et al.,* 2001
Finca unfert	La Selva, Costa Rica	maize	0	3962	25.8	6.9	25	45	30	*Weitz et al.,* 2001

Land management and soil data required for model input were taken from the references in Table 5-5, while daily climate data needed to drive the model and the measurement data were obtained from the authors or from the Tragnet database [*Ojima et al.*, 2000], where a number of datasets on trace gas emissions are stored. Information exceeding the soil and management information listed in Table 5-5 can be obtained from the literature.

For all simulations the model parameters controlling crop growth and soil processes like decomposition and trace gas production are identical. The only variables changed were site-specific climate, soil properties, and land management. The only exception to that is the maximum nitrate-leaching rate, which was set to a lower value for the grassland site as grasslands are known to loose less nitrogen and as soil nitrate data also suggested lower leaching rates.

The initial conditions at the beginning of the measurements are never available as detailed as needed for the Daycent simulations; especially the distribution of soil organic carbon and nitrogen in the different SOM pools is uncertain, but formulas for approximations do exist [*Century-Parameterisation-Workbook*, 2005]. Therefore the history of land use was simulated whenever such information was available; otherwise assumptions on land use history were made, in order to simulate at least one year ahead to the measurement period of interest.

5.3.2 Model testing

For a comparison between measured and simulated emissions and to assess the model performance, the modelling efficiency (ME) was used [*Janssen and Heuberger*, 1995]:

$$ME = \left(\sum_{i=1}^{N} (P_i - O_i)^2 - \sum_{i=1}^{N} (\overline{O} - O_i)^2 \right) \Big/ \sum_{i=1}^{N} (\overline{O} - O_i)^2$$

where P_i and O_i are the predicted and the observed values, and $\bar{O}$ is the mean observed value. As measurement frequencies range from daily to monthly values, it was decided to test the model performance for all sites based on monthly averages of N_2O emissions. For the intended application of Daycent as a global scale model the main focus is on representing seasonal dynamics and annual emission sums rather than daily N_2O emission rates. Beyond, the high temporal variability of N_2O emission often hinders an accurate day-by-day prediction of emission rates.

Additionally to the modelling efficiency, time series of measurement data and model results are presented, and total emissions over the measurement period are compared. If no daily measurement data were available the emission sum was assumed to be constant until the next measurement date.

Accurate simulation of N_2O emissions largely depends on accurate simulation of control variables like soil moisture, soil temperature, soil ammonium and soil nitrate concentrations. Therefore model performance for these variables was assessed if data were available. Simulated soil water content, which not only influences N emissions but all decomposition processes and plant growth, is compared to observed values at four sites, and model performance is tested by the modelling efficiency on a daily basis (Chapter 5.3.3). A comparison between measured and simulated soil nitrate and ammonium content of the soil and the modelling efficiency on a daily basis is presented for three sites, for which these data were available. For soil ammonium and nitrate content a conceptual problem arises from the daily model time step: In Daycent, these values rather represent

the available N *after* decomposition and plant uptake and *before* nitrification and denitrification of that day and are used as primary drivers for nitrification and denitrification. In reality, measured ammonium and nitrate concentrations are often poor predictors for these processes, as turnover rates can be large compared to concentrations, especially for ammonium and nitrification rates [*Kiese and Butterbach-Bahl*, 2002; *Kiese et al.*, 2002]. In contrast to natural vegetation, high nitrogen concentrations in agricultural systems justify a comparison between simulated and measured ammonium and nitrate content.

5.3.3 Soil moisture

To test the soil hydrology model in Daycent, measured and simulated values of volumetric soil water content (vswc) or water filled pore space (wfps) were compared for both German sites, for the Mexican site and the New Zealand site. Although there are also wfps data for the Costa Rican site, they often exceed 100% and were therefore regarded as unreliable.

Simulated and measured soil water contents agree well for all of these sites (Figure 5-3, 5-4, 5-10, 5-11), the ME ranging from 0.15 to 0.76 (Table 5-6). That indicates that the water fluxes including transpiration and drainage are represented correctly for the different sites and crops, which is a necessary precondition for correct trace gas simulation. Likewise, correct simulation of intermediate model parameters is necessary to assure that an agreement between measured and modelled N_2O emissions is really due to a correct representation of processes and parameters.

One reason for the discrepancies in volumetric soil water content (vswc) at the New Zealand site (Figure 5-10) may be the formation of dew, which was not accounted for in the precipitation data. When calculating daily soil water content from precipitation, evapotranspiration and soil water content of the previous day, a curve very similar to the one modelled in Daycent emerged. This strongly indicates that measured soil water content is higher than could be expected from rain and evapotranspiration, and dew is very likely to be the reason for this (Chapter 4). The vswc at the Mexican site is largely dominated by irrigation and few rainfall events, with a good agreement between model and data (ME = 0.78; Table 5-6). For the Ruser sites the ME for the water filled pore space ranges from 0.15 – 0.61 (Table 5-6), exemplarily the plot “Ruser C” is shown (Figure 5-4). For the “Flessa D” site (Figure 5-3) the ME for wfps is 0.52, and 0.27 for the “Flessa C” site. The main deviation between simulated and observed water content for these two German sites occurs during winter periods, when Daycent underestimated the observed wfps. Despite low precipitation the water content exceeds field capacity (Figure 5-3, Febr./March 1993, and Figure 5-4, Jan/Feb 1997) probably because of frozen soil layers, impeding drainage. Although Daycent in principle does account for this effect, the current simulation of soil temperatures and hydraulic conductivities miscalculates the water content under these conditions. Especially with respect to winter emissions, future work should therefore improve the representation of these mechanisms.

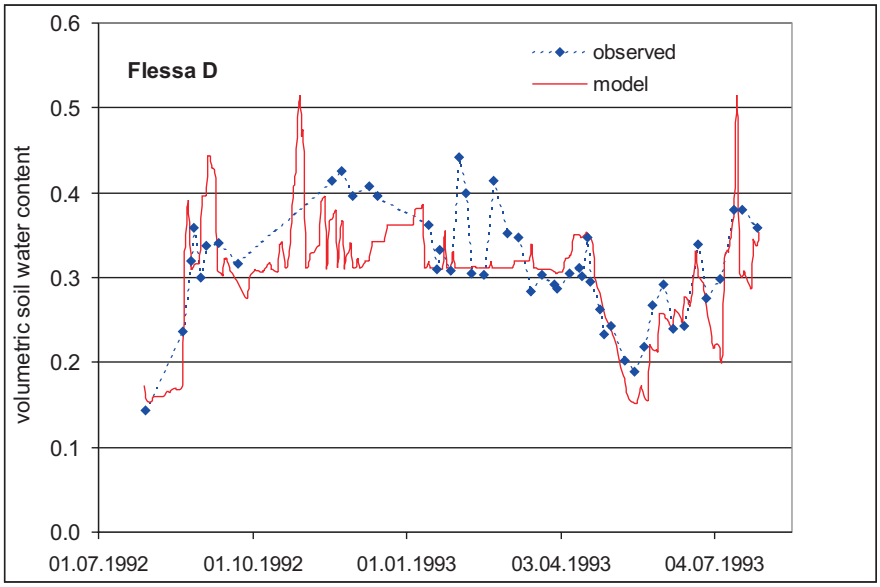

Figure 5-3. Observed and simulated volumetric soil water content (0-25cm) for wheat cropping on a fine-loamy soil near Munich, Germany ("Flessa D"). Field data from *Flessa et al.* [1995].

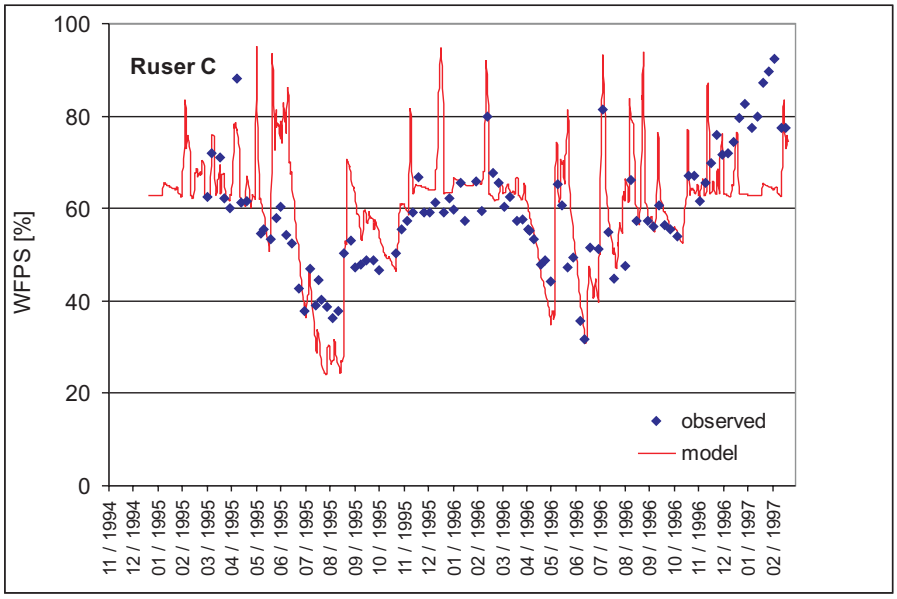

Figure 5-4. Observed and simulated water filled pore space (0-30cm) under a potato - wheat cropping near Munich, Germany ("Ruser C"). Field data from *Ruser et al.* [2001].

Table 5-6. Results from the Daycent tests for different agricultural sites: Modelling efficiency (ME) of soil water, soil ammonium ($NH4^+$), soil nitrate (NO_3^-) and N_2O emissions as simulated by the revised Daycent version, and observed and simulated N_2O emission sums over the experimental period compared to N_2O modelling efficiency and emission sums as simulated by the original Daycent version.

Site name	Soil water	$NH4^+$	NO_3^-	N_2O				N_2O original Daycent [a]	
	ME daily	ME daily	ME daily	ME monthly	Sum Data [$kgNha^{-1}$]	Sum model [$kgNha^{-1}$]	model / data	ME monthly	model / data
Temperate sites									
Flessa C	0.27	0.39	0.33	0.21	9449	6610	70%	-0.27	121%
Flessa D	0.52	0.47	0.64	-0.40	26587	7775	29%	-0.26	57%
Ruser A	0.61		0.46	0.70	2993	2021	68%	-35.62	436%
Ruser B	0.38		-0.14	-0.19	10287	4350	42%	-3.24	198%
Ruser C	0.33		-0.42	0.20	9681	4890	51%	-78.75	440%
Ruser D	0.15		0.02	0.13	4747	3284	69%	-15.09	397%
Ottawa				0.80	2174	1989	91%	0.95	101%
Colorado				0.29	3449	3815	111%	-1.26	111%
New Zealand	0.62	0.42	0.26	0.10	4116	3370	82%	0.38	112%
Tropical sites									
Mexico	0.76			0.17	3075	2555	83%	-22.31	1787%
Fincy fert.				0.66	2683	2555	95%	-230.00	660%
Finca unfert.				-2.34	1199	1301	109%	-13.10	253%

[a] Original Daycent version [*Parton and Ojima*, 2003] as adapted for the simulation of global crop production.

5.3.4 Soil N content

Data on soil nitrate and ammonium content were available for the New Zealand and the Flessa sites, and nitrate content was available for the Ruser sites. The modelling efficiencies are good for New Zealand, the Flessa sites and one Ruser site, while they are low or even negative for the other Ruser data (Table 5-6).

The New Zealand site is dominated by high urea input. Maximum soil ammonium content directly relates to nitrogen input and is therefore predicted very well. The decrease of ammonium content after fertilizer application is fast in summer, autumn and spring, and somewhat lower during winter. Model results agree very well with this pattern (Figure 5-5), which was not the case with the old model version (Chapter 4), in which nitrification rates were underestimated because of the temperature dependency and the limitation of nitrification rate. Soil nitrate content in general is also simulated satisfactorily but is underestimated during winter and tends to decrease too fast, which is probably due to an overestimation of plant N uptake.

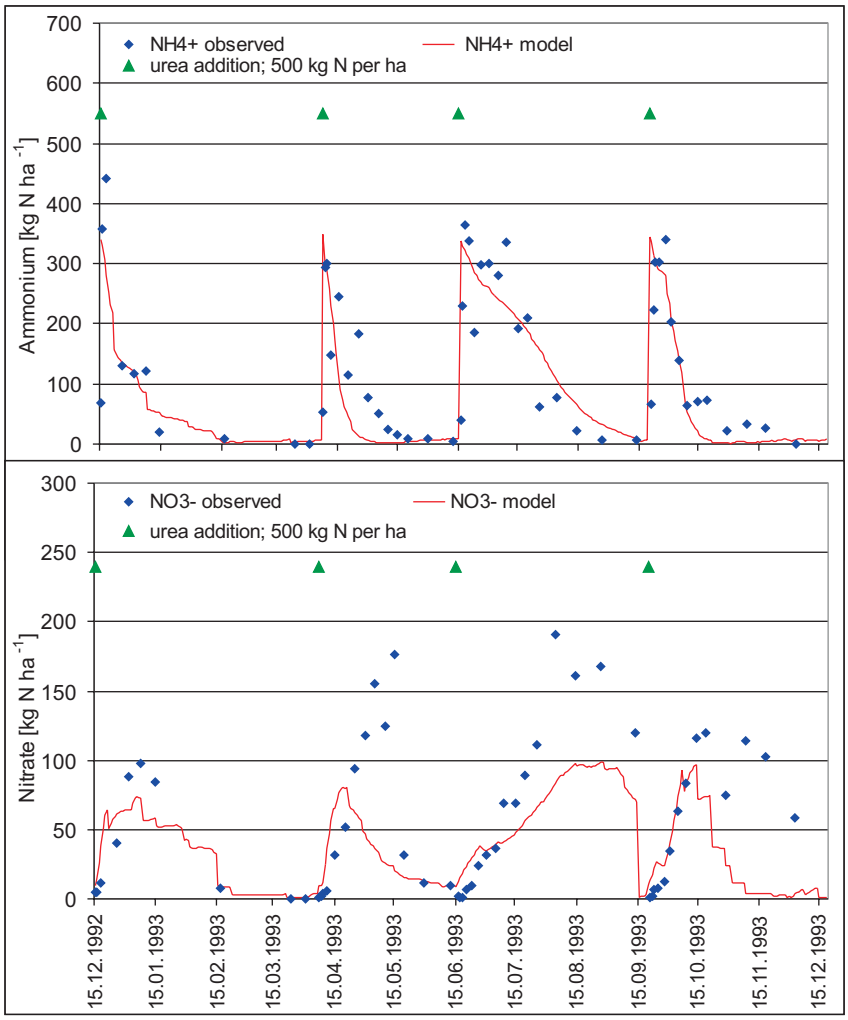

Figure 5-5. Fertilization and observed and simulated soil nitrate and ammonium content (0-15cm) under fertilized grassland near Christchurch, New Zealand. Field data from *Müller et al.* [1997].

For both the Flessa and the Ruser sites the increase of soil nitrate in January – April, which is caused by the freezing effect and/or later an increase in nitrification under increasing temperatures, is represented well by the model (Figure 5-6 and 5-7, exemplarily).

For the "Flessa C" site the observed winter/spring increase is much lower than at the "Flessa D" site. As will also be discussed later, the differences of soil characteristics between the two sites are only small (Table 5-6) and the Daycent simulation results for the two sites therefore are much more similar than the observed values. Thus, the winter/spring increase is overestimated for "Flessa C" (data not shown). After fertilizer application the increase in soil nitrate should be directly related to the amount of N added (50% ammonium; 50% nitrate). For the Flessa sites the observed increase in nitrate almost equals the theoretical increase from fertilizer application and is represented well by the model and the simulated decrease of soil nitrate content after fertilization is similar to the observation (Figure 5-6). The slightly underestimated nitrate content after the third fertilization event is caused by a coinciding rainfall event leaching more nitrate from the soil than observed. Therefore further model testing and development should address the calculation of nitrate leaching. This will not only improve the model performance for N_2O emissions but will also allow the model

application to assess the nitrogen export from agricultural systems to surface waters and groundwater.

At the Ruser sites, measurement uncertainties and spatially varying effective N application may partly lead to observed values differing from theoretical and simulated nitrate contents (Figure 5-7).

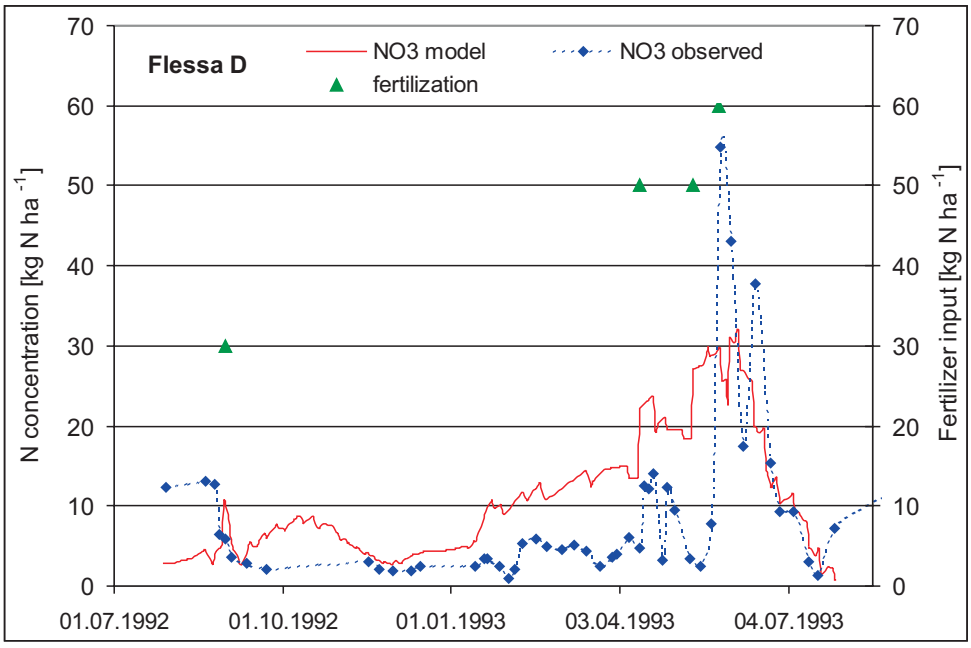

Figure 5-6. Fertilization and observed and simulated soil nitrate and ammonium content (0-25cm) under wheat cropping on a fine-loamy soil near Munich, Germany ("Flessa D"). Fertilizer is Ammonium Nitrate. Field data from *Flessa et al.*[1995].

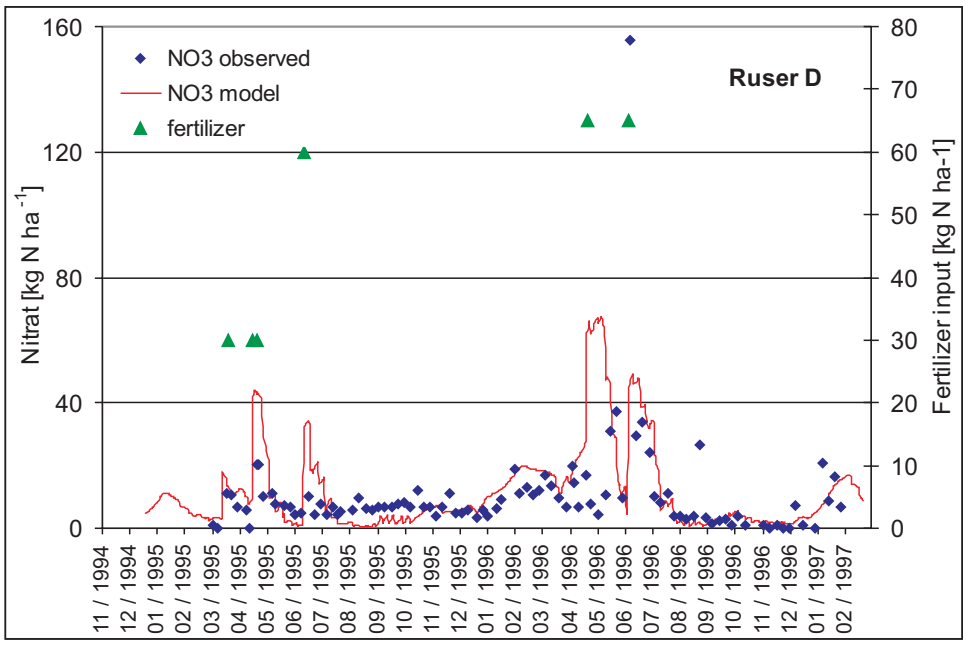

Figure 5-7. Fertilization and observed and simulated soil nitrate content (0-30cm) under a wheat - maize cropping near Munich, Germany ("Ruser D"). Fertilizer is Ammonium Nitrate. Field data from *Ruser et al.* [2001].

5.3.5 N_2O emissions

For all sites listed in Table 5-6 the observed and simulated N_2O emissions are presented and discussed in the following paragraph. Modelling efficiencies and annual emissions are presented in Table 5-6, both for the revised Daycent model and for the original Daycent version. At first, the four temperate case studies are presented, followed by the subtropical grassland site and the two tropical sites.

The measurements from the first German case study [*Flessa et al.*, 1995] represent a barley-wheat crop rotation with intercropped mustard as green manure on two slightly different soils (Table 5-5). The fine-silty soil ("Flessa C") has a slightly lower pH, organic carbon and organic nitrogen content, more clay and less sand content than the fine-loamy soil ("Flessa D") (Table 5-5). N_2O emissions are dominated by post-fertilization emissions and winter emissions (Figure 5-8). The emissions during spring, summer and autumn are represented rather well, while the winter emissions are underestimated by the revised Daycent model (Figure 5-8). Therefore the total annual emissions over the measurement period are underestimated for one site by 30% ("Flessa C") by 70% for the other site ("Flessa D") (Table 5-6). This is also reflected in the monthly modelling efficiencies, which amount to 0.21 for "Flessa C" while being negative for the other "Flessa D" (Table 5-6). Freeze-thaw emissions will be discussed in more detailed for all affected sites below.

The measurement data collected by *Ruser et al.* [2001] stem from different periods of a wheat – potato – wheat – maize crop-rotation conducted within the same research network as the data from *Flessa et al.* [1995] (Forschungsverbund Agrarökosysteme München, FAM). The monthly modelling efficiencies for three of the four experimental plots range from 0.13 to 0.7 for monthly averages (Table 5-6). Similarly as for the Flessa data the agreement between model results and observations is rather good for spring, summer, autumn and post-fertilization periods (Figure 5-9). For winter emission events, the model captures the period of freeze-thaw emissions well, and also the magnitude of peaks for the "Ruser D" site, while for the "Ruser C" site the high emissions during early spring are not simulated at all (Figure 5-9). This is also reflected by the fact that the modelling efficiencies excluding the freeze-thaw emissions are larger than the modelling efficiencies covering the entire period (data not shown). Beyond, the simulated emission sums over the winter period agree with observation, though the differences among sites cannot be reproduced completely. The emissions over the entire experimental period are underestimated by 31-58% (Table 5-6). On the one hand this can be attributed to the underestimation or omissions of some N_2O emission peaks after fertilization events, when the simulated and observed soil nitrate content is already low but when high emissions occur after strong rainfall events (e.g. Sept. 1995 and Sept 1996; "Ruser C"). On the other hand the calculation of accumulated emissions based on about weekly data that are assumed to represent the entire period until the next available measurement, may be debatable with respect to the short term dynamics of N_2O emissions but was regarded as the most reasonable approach, which has also been applied in the original paper [*Ruser et al.*, 2001].

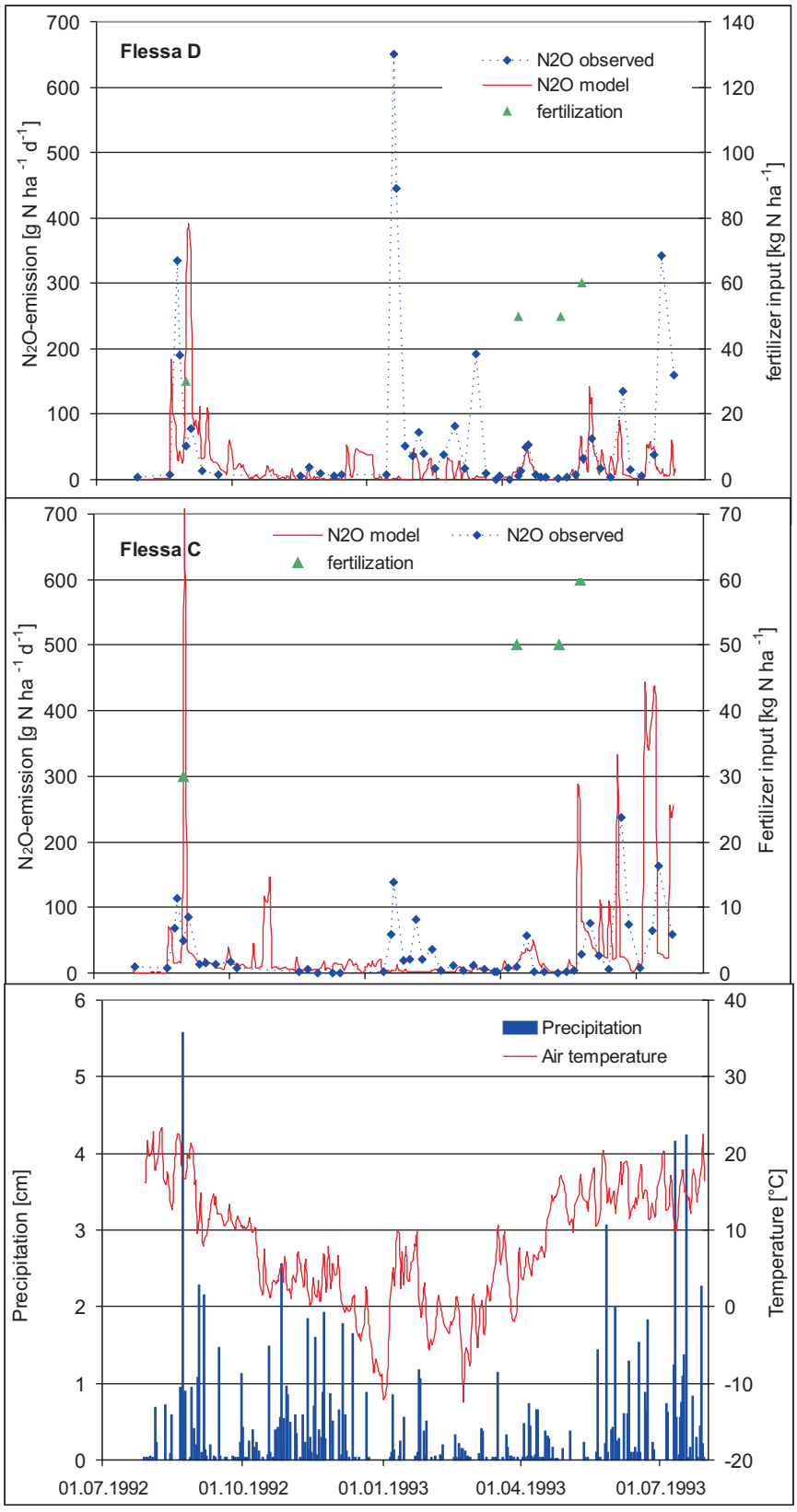

Figure 5-8. Precipitation, air temperature, fertilization and observed and simulated N_2O emission rates from wheat cropping on a fine-silty soil ("Flessa C") and a fine-loamy soil ("Flessa D") near Munich, Germany. Field data from *Flessa et al.* [1995].

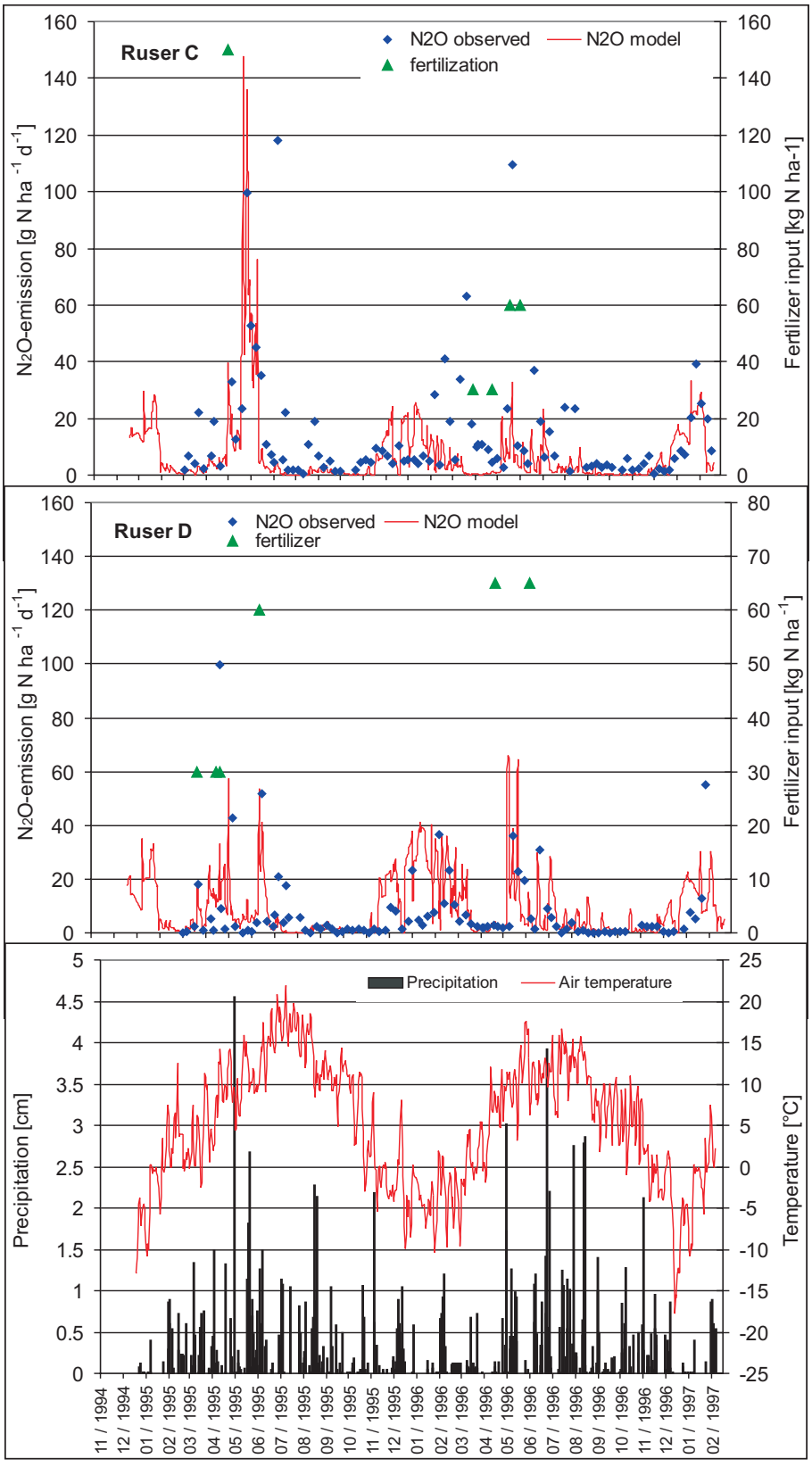

Figure 5-9. Precipitation, air temperature, fertilization and observed and simulated N_2O emission rates from potato - wheat ("Ruser C") and wheat - maize cropping ("Ruser D"). Field data from *Ruser et al.* [2001].

The formulation of mechanisms representing winter emissions in the Daycent model has been based on laboratory data (see Chapter 5.2.2.3), and has been only slightly modified based on field observations [*Flessa et al.*, 1995; *Ruser et al.*, 2001]. From laboratory data it is known that soil organic carbon content, duration of freezing period and freezing temperatures are key drivers for freeze-thaw emissions, which were accordingly implemented in the Daycent model. Based on these parameters, it is unclear why the winter emissions differ so much between the two sites "Flessa C" and "Flessa D", nor can the differences between the Ruser plots be explained thereby. Both the "Ruser C" and the "Ruser D" plot share elevated N_2O emissions during December – March. But while winter emissions at the "Ruser D" site mainly occur during this period of freeze-thaw cycles, highest winter emission peaks at the "Ruser C" site seem to be related to the thawing in March-April. In contrast to the emission dynamics observed on the Ruser sites, the Flessa sites show almost no increase of N_2O emissions during freezing periods, but are characterized by emission peaks during the following rather warm periods. The magnitude of these emission peaks with more than 600 g N_2O-N ha^{-1} largely exceeds the ones observed at the Ruser sites that reach 60 g N_2O-N ha^{-1} at most. One explanation for these fundamentally different dynamics may be the ploughed-under intercrop at the "Flessa C" site, which provided a pool of organic matter, easily degradable during freezing and subsequent decomposition during the following warm periods. To summarize, freeze-thaw processes are not yet well understood, therefore it is not possible to perfectly reproduce the dynamics in process models like Daycent. For the intended global application to estimating N_2O emissions, the objective was to include these processes in order to capture the main driving variables and the magnitude of these fluxes.

The other two experimental datasets for temperate agriculture analysed in the study do only cover non-winter periods and are located in Canada and the USA.

The maize cropping in Ottawa, Canada [*Grant and Pattey*, 2003], which covers only a rather short measurement period was selected as it has also been used to develop and test the original version of the Daycent model. The modelling efficiency for monthly averages of N_2O emissions is 0.8, and the total emissions over the measurement period agree well between model and observation (Table 5-6). Additionally, the maximum simulated emission rate agrees well with the maximum observed rate. The emission peak is related to an increase in precipitation and wfps about one month after the fertilizer addition. While the data show an immediate increase of emissions, a rather fast decrease and additional single peaks at later rainfall events, the observed emission rate increases and decreases slower (data not shown).

For emission measurements from a barley – wheat crop rotation in Colorado (*Mosier et al. 1986*) the modelling efficiency for monthly averages amounts to 0.3, and the simulated emission sum over the two measurement periods agrees well with the observation (Table 5-6). The modelling efficiency of the original model version, which had also been tested before for this site, was lower. Except one emission event where precipitation and fertilization about coincide, all observed N_2O emission peaks are strongly related to precipitation exceeding 20 mm (data not shown). However, as not all of these strong rainfall events really cause an increase in the observed emission rate N_2O emissions are overestimated by the Daycent model in these cases.

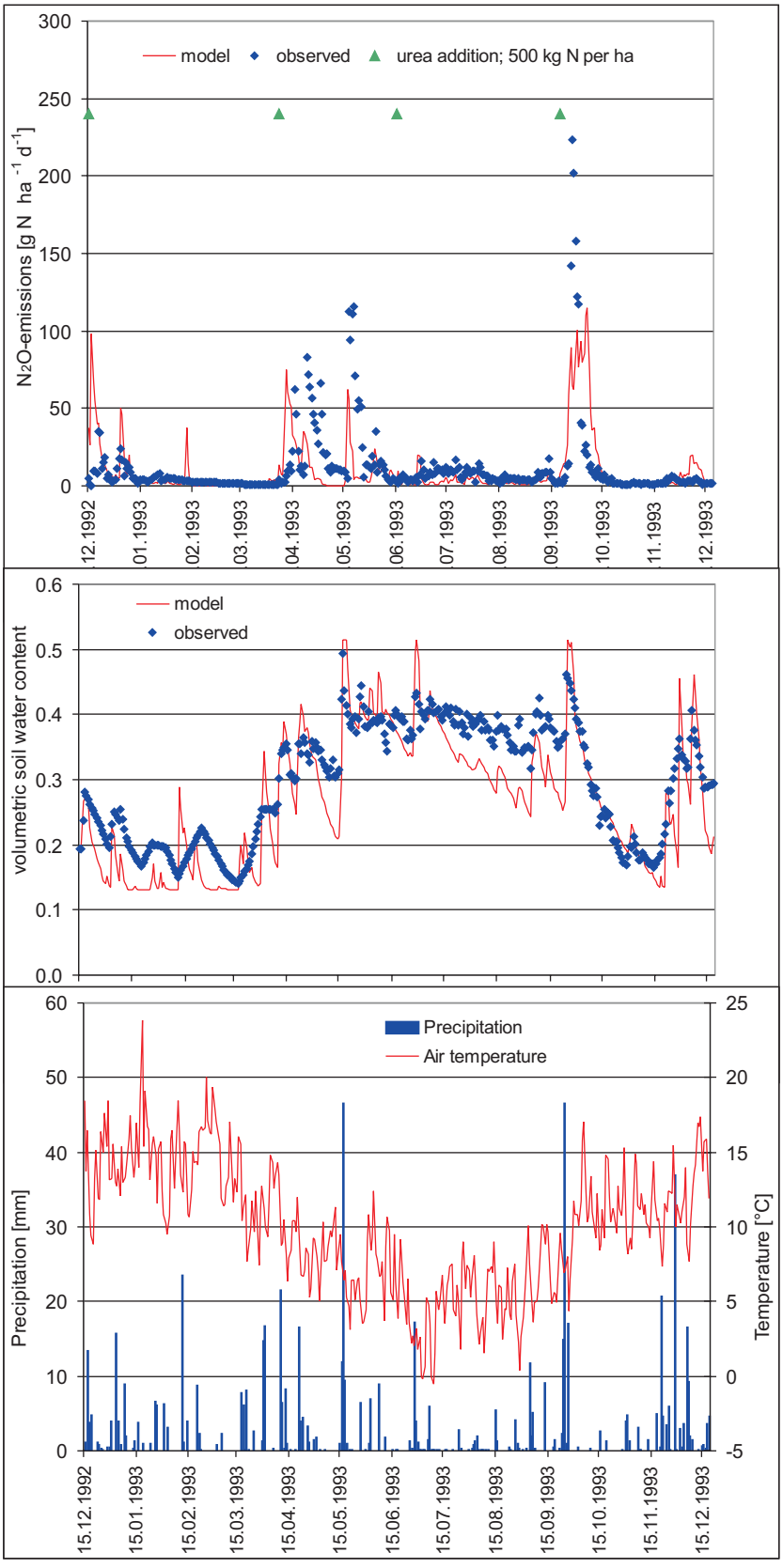

Figure 5-10. Precipitation, air temperature, observed and simulated volumetric soil water content (0-15cm), fertilization and observed and simulated N_2O emission rates from a fertilized grassland near Christchurch, New Zealand. Field data from *Müller et al.* [1998].

Figure 5-10 shows the application of the revised Daycent model to a fertilized grassland in New Zealand [*Müller et al.*, 1998]. In a previous study this dataset had already been used to validate the Daycent model and to identify model limitations (Chapter 3) that have then been dealt with during model improvement. The daily and monthly modelling efficiencies are 0.19 and 0.1, respectively, and the total emissions over the measurement period amount to 82% of the observed value (Table 5-6). Observed N_2O emission rates are highest after the rainfall events of > 40 mm in May and September. Under the resulting high volumetric water content the nitrification rate should strongly decrease, and emissions might be assumed to originate from denitrification. However, as nitrate concentration is still low, at the September rainfall event occurring 5 days after urea addition a main contribution had been attributed to nitrification [*Müller et al.*, 1998]. As Daycent simulates a strong decrease in nitrification rate with increasing soil water content, and as N_2O emissions from nitrification cannot exceed the 0.5% loss (Chapter 5.2), simulated emissions from nitrification are low and lead to the observed underestimation of emission peaks. For the strong rainfall event in May the underestimation of the nitrate content (Chapter 3.3.4) directly leads to an underestimation of this N_2O emission peak, which was assumed to originate mainly from denitrification [*Müller et al.*, 1998]. The magnitude of the third large N_2O emission peak is similar for observation and simulation results, but is simulated to occur too early. Low volumetric soil water content during summer and autumn leads to very low or no simulated N_2O emissions, which agrees well with the observations, while during winter despite low temperatures the simulated N_2O emissions amount to 25 g N_2O-N $ha^{-1}day^{-1}$, which again agrees well with observations (Figure 5-10).

A validation for subtropical climate was performed for a maize field in the Yaqui valley in Mexico [*Matson et al.*, 1998]. The modelling efficiency is 0.17 for monthly averages, and the simulated total sum meets the observed value (Table 5-6). One high emission peak with a maximum rate of > 1000 g N_2O-N ha^{-1} occurs after the pre-plant fertilization and irrigation (data not shown). This emission peak is also represented by the Daycent model but is markedly underestimated. Despite other rainfall and irrigation events and one other fertilizer application, subsequent observed and simulated N_2O emission rates remain low. This is not the case in the original Daycent version, consequently resulting in the large overestimation of total N_2O emissions (Table 5-6).

A further Daycent simulation for tropical climate was carried out for fertilized and unfertilized maize cropping in La Selva, Costa Rica [*Weitz et al.*, 2001]. For the fertilized field the modelling efficiency 0.66 for monthly averages, and total emissions amount to 95% of the observed value (Table 5-6). For the unfertilized field the total emissions also agree well, while the modelling efficiency is negative (Table 5-6). That is due to observed emission rates not being related to either management or rainfall events, and in the original publication also no correlation to any other parameter had been identified [*Weitz et al.*, 2001]. Simulated N_2O emission events for the fertilized field agree well with observations, both before fertilizer application and during the post-fertilization period, with only the second part of the second fertilization peak being slightly underestimated (Figure 5-11). Simulated N_2O emissions from the unfertilized field are negatively correlated to simulated water filled pore space. That applies for emissions from both nitrification and denitrification, as under almost water-saturated conditions N_2O emissions from denitrification are limited by the diffusivity of the soil and increase with increasing diffusivity. To some extent this phenomenon is supported by the observations, although during the extended period of soil drying in January the simulated emissions are highest during intermediate wfps, while observed emission rates peak at lowest wfps (Figure 5-11).

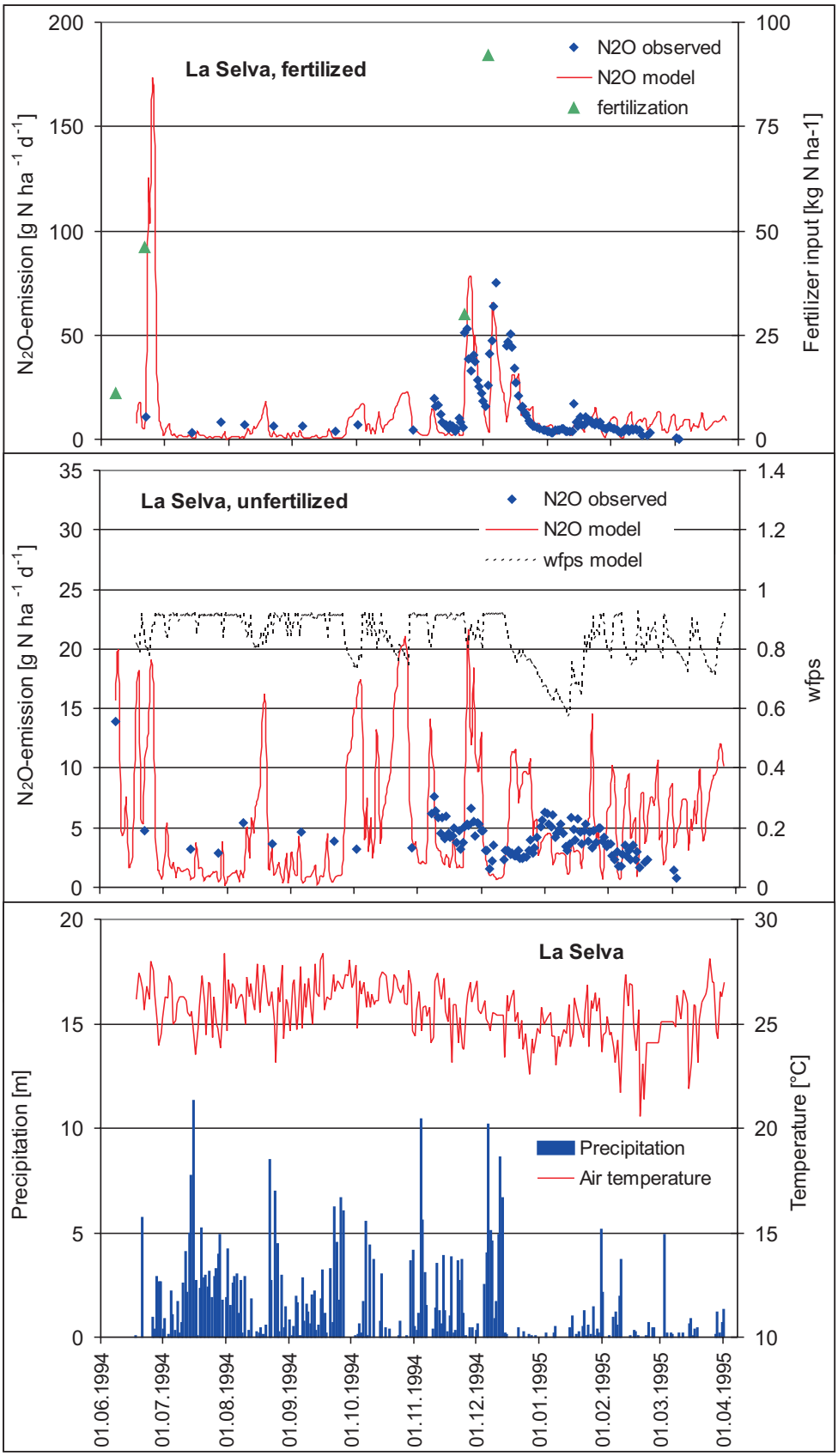

Figure 5-11. Fertilization and observed and simulated N_2O emission rates from fertilized and unfertilized maize cropping in La Selva, Costa Rica. Field data from Weitz et al. [2001].

5.3.6 Conclusions from site specific testing

The results from the Daycent test sites prove that the model reproduces the dynamics of soil water and soil ammonium content fairly well (ME = 0.15 – 0.76), and that also soil nitrate concentrations are simulated well (ME = 0.26 – 0.64) except for the Ruser sites, where nitrate concentrations even differ from what would be expected from fertilizer application.

For N_2O emissions both total emissions and the emission rates on a monthly basis are reproduced satisfactorily. Total N_2O emissions over the experimental periods for sites not including freeze-thaw emissions, amount to 82-111% of measured sum. For sites affected by freeze-thaw events, emissions sums tend to be underestimated, adding up to 29-70% of observed total N_2O emissions (Table 5-6). Likewise, the N_2O modelling efficiencies for sites not including winter emissions amount to 0.1-0.8 except for the unfertilized tropical site, while for the freeze-thaw affected sites they range from 0.13 to 0.7 and are negative in two cases.

These results suggest that the current approach to calculate freeze-thaw emissions needs to be improved in order to better reproduce the highly dynamic N_2O emission events during freezing and thawing periods. Because of their short-term dynamics it is strongly suggested that further model development with respect to winter emissions should rely on at least daily measurement data, and that laboratory results need to be included, as the understanding of processes is still rather incomplete.

When applying a former version of the Daycent model, the modelling efficiencies for monthly N_2O emissions are negative for all but two sites, and total simulated N_2O emissions strongly exceed the observed values in 7 of 12 cases (Table 5-6). Therefore it can be concluded that the revision of the trace gas module leads to an improvement of model performance, which is mainly due to the implementation of freeze-thaw emissions and a more detailed calculation of N_2O emissions from nitrification.

To conclude, the results obtained from the site-specific testing indicate that the Daycent model can be used to estimate N_2O emission from different agricultural systems throughout the world. This will allow assessing the interaction of climatic, soil and management parameters, to study the N_2O loss from fertilizer application in different regions of the world, and to calculate total emissions from agricultural soils.

5.4 Sensitivity analysis

In order to study the influence of environmental parameters on N_2O emissions simulated by the Daycent model, a sensitivity analysis was performed for maize cropping at a tropical and a temperate site. Using the input data from the global simulation setting, the following parameters were tested: fertilizer input, precipitation, field capacity, wilting point, maximum fraction of nitrate leached each day (all +/- 30%), sand content (+/- 50%, at the expense of the silt content), temperature (+/- 3°C throughout the entire year), saturated hydraulic conductivity (*10/ *0.1). The parameters were tested separately, varying one factor and keeping all others constant. Thereby known interdependencies between input parameters, like between sand content, field capacity and wilting point are ignored. The two selected sites correspond to the Costa Rican and the German site

from the case studies (10°n, 84°west and 48°n, 10°east; Chapter 3.4). For climate input data, both site-specific meteorological data and the daily weather database used for the global simulations (Chapter 5.5) were used. As the two different sources of weather data yielded very similar results except for one parameter at the temperate site, only the results for the global weather database are shown.

As expected, N_2O emissions strongly increase with increasing fertilizer input at both sites. By relating the additional N_2O emissions to the additional fertilizer input of the "+30% Fertilizer" sensitivity, the fertilizer induced emission calculated is 1.2% for the temperate and 2.9% for the tropical site. The first value is similar to the factor of 1.25% applied by *IPCC* [1997]. The finding that the fertilizer induced emissions under tropical climate are higher than for temperate sites can be explained by temperature dependency of decomposition, nitrification and denitrification and is in agreement with [*Bouwman et al.*, 2002b].

Simulated annual N_2O emissions increase with increasing precipitation at both sites. At the tropical site this effect is weak, as wfps is close to saturation throughout the year, while for the temperate site precipitation proves to be one of the most sensitive parameters (Figure 5-12).

As decomposition, nitrification and denitrification are positively correlated to temperature in the Daycent model, it can be assumed that emissions increase with increasing temperature though increased plant N uptake may partially compensate for this effect. N_2O emissions indeed increase with increasing temperature at the tropical site, even though the baseline temperature is rather high (25.8°C annual average). At the temperate site the additional effect of freeze-thaw emissions causes emissions to increase by both a temperature increase and a decrease of 3°C (Figure 5-12). This is not the case for the simulation based on weather data from a nearby weather station, where annual average temperatures are slightly lower, where the contribution of freeze-thaw emissions is therefore already higher in the baseline simulation, and where therefore the decrease in non-winter emissions is not entirely compensated by increased freeze-thaw emissions. This emphasizes the high sensitivity of the model results to freeze-thaw emissions as discussed before (Chapter 5.3), and indicates that future model development should pay special attention to these processes.

The sand content (a site specific parameter), and the maximum fraction of nitrate leached per day (a model parameter) directly and only affect the amount of nitrate lost through leaching, and therefore show a negative correlation to annual N_2O emissions at the temperate and the tropical site (Figure 5-12).

Additional effects of soil texture soil hydraulic properties and N_2O emissions operate through the derived parameters field capacity, wilting point and hydraulic conductivity. These parameters are a source of substantial uncertainty for the global scale simulations as they are not available from the global soil databases directly but need to be derived from texture by so called pedotransfer functions (PTFs). In general, an increase in field capacity and wilting point results in higher values of wfps, and therefore in higher simulated N_2O emissions, whereby the sensitivity to field capacity is higher (Figure 5-12). However, the 30% reduction of field capacity at the temperate site leads to a small increase in N_2O emissions. This is caused by plant growth being substantially impaired through the decrease in plant available water, thereby decreasing plant N uptake and increasing soil nitrogen content. For moderate reductions of field capacity and for the sensitivity based on data for a nearby weather station the direct effect of field capacity and wfps on emissions is not

compensated by reduced plant uptake but shows a continuous de- or increase for the topical site. The saturated conductivity of a soil can vary over several orders of magnitude [*Scheffer*, 2002], therefore a tenfold increase or decrease of this parameter was tested. As a higher hydraulic conductivity causes faster reduction of wfps it also reduces simulated N_2O emissions for both sites.

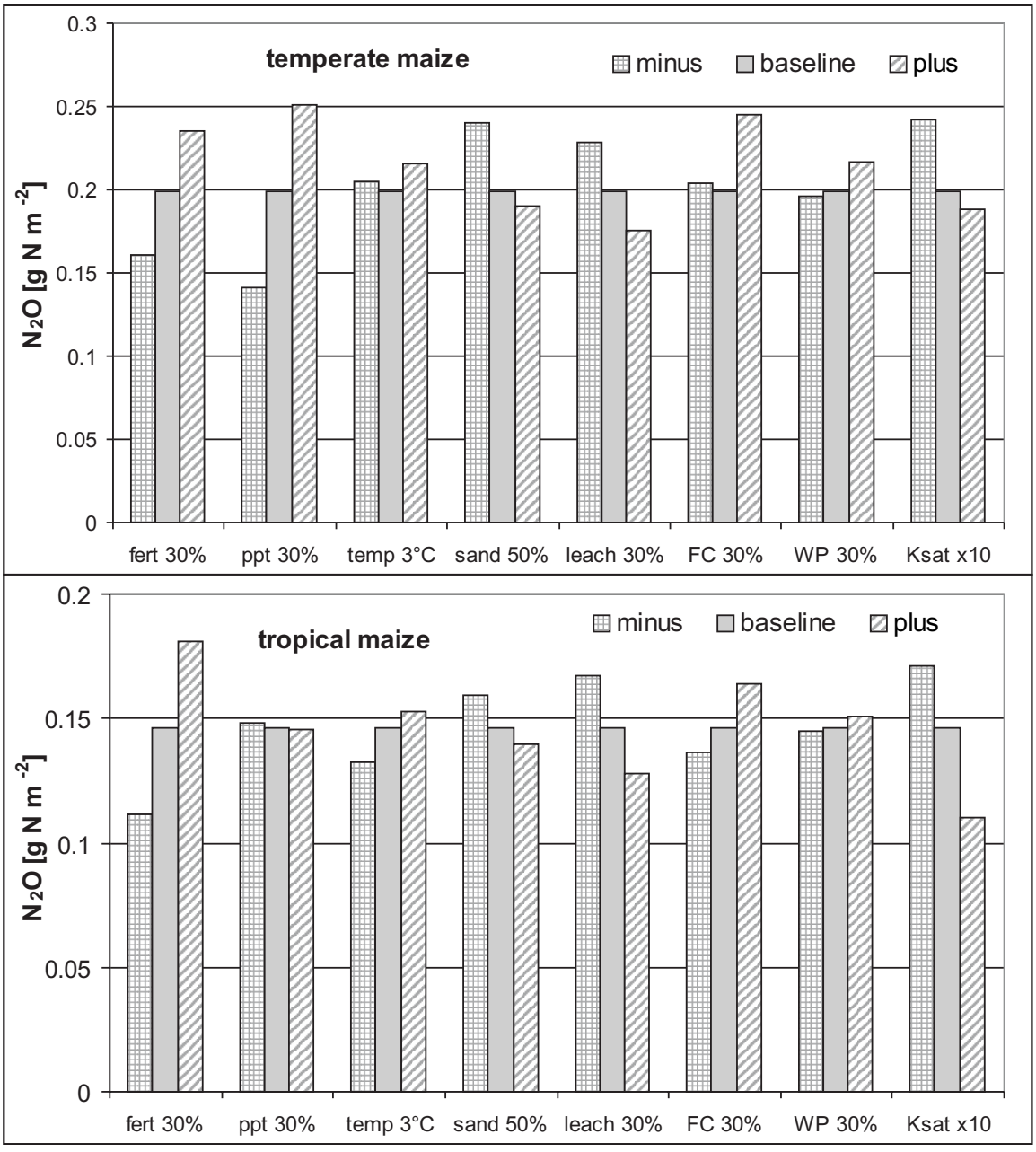

Figure 5-12. Sensitivity of annual N_2O emissions to changes in fertilizer input (fert), precipitation (prec), temperature (temp), sand content, maximum fraction of Nitrate that can be leached (leach), field capacity (FC), wilting point (WP) and saturated hydraulic conductivity (Ksat), for maize cropping at a temperate and a tropical site.

Soil water content has counteracting effects on N_2O emissions through its correlation to nitrification being positive below field capacity and being negative above field capacity, and through its positive correlation to nitrification but negative correlation to the fraction of N_2O lost

from denitrification. However, the overall effect for the two sites of the sensitivity study is that parameters that on average increase soil water content also increase the simulated N_2O emissions, except for one case where plant N uptake superposes this effect. This is consistent with other sensitivity studies, e.g. for the DNDC model [*Stange et al.*, 2000] or Expert-N [*Schulte-Bisping et al.*, 2003]. The simulated changes in annual N_2O emissions due to changes in climate variables demonstrate that the model is capable to react very sensitive to variations in climatic conditions.

As already mentioned above, the results from the sensitivity study were similar when using either data from a weather station, or the data derived from monthly averages for the respective 0.5° grid cell in the weather database (Chapter 5.5.3). This indicates that the applied approach to derive daily data from monthly averages does not introduce a large source of uncertainty for the Daycent simulation results.

5.5 Global datasets used

In the following section all inputs used for the global Daycent simulations are listed and discussed. Simulation of current N_2O emissions is based on datasets referring to the mid-1990ies (if available). All data sets used for the global simulation, their spatial resolution and the reference time period are listed in Table 5-7. In general, the global databases here are identical to the ones used in the study on global crop production (Chapter 2).

Table 5-7. Data sets used for the simulations at the global scale and simulation settings.

Data set	Spatial reference	Temporal reference	Reference
Weather data	0.5° lat x 0.5° lon	monthly averages 1961-1990	[*New et al.*, 2000]
Soil data – Bulk density, C, N	5 arc min x 5 arc min		[*Global_Soil_Data_Task_Group*, 2000]
Soil data – pH, texture	5 arc min x 5 arc min		[*FAO*, 1995]
Land use	Crop fraction on 5 arc min grid	early 1990ies	[*Leff et al.*, 2004]
Nitrogen deposition	3.75° lat x 3.75° lon interpolated to 1° lat x 1° lon	mid 1990ies	[*Dentener*, 2001]
Management – fertilizer nitrogen application	Country averages	mid 1990ies	[*IFA*, 2002]
Management – manure nitrogen application	Country averages	mid 1990ies	[*Siebert*, 2005]
Planting dates	0.5° lat x 0.5° lon	Based on climate 1961-1990	Chapter 3
Fertilizer application dates	Depending on planting & harvest dates; 0.5°lat x 0.5° lon, application in four events	Based on climate 1961-1990	Chapter 3
Manure application dates	Depending on planting and harvest dates; 0.5° lat x 0.5° lon, application in two events	Based on climate 1961-1990	Chapter 3
Irrigated area	Irrigated fraction on 5 arc min grid	mid 1990ies	[*Döll and Siebert*, 2000]
Global simulation	0.5° lat x 0.5° lon, using dominant soil type of 5 arc min soil map	60 years, last 30 year averages as results	

5.5.1 Land-use map

In order to calculate emission sums from agricultural soils a land-use map was needed to add up the simulated crop-specific N_2O emission rates over the area planted with the respective crops. The global map on the distribution of major crops by *Leff et al.* [2004] was used, which provides the fraction of crop-specific area within each five arc minute grid cell. As Daycent had been parameterised for nine major crops in a previous study (Chapter 2), these crop types were assigned to the classification used in the global land use map (Table 5-8).

5.5.2 Soil data

Data of soil properties at five arc minutes resolution were derived from the Data and Information System (DIS) framework activity of the International Geosphere–Biosphere Programme (IGBP) [*Global_Soil_Data_Task_Group*, 2000] (bulk density, organic carbon and nitrogen content) and from the FAO TERRASTAT database [*FAO*, 2002] (texture and pH). As texture is only resolved in three texture classes for dominant and associated soil type, typical texture was assigned to the three classes and calculated the weighted average over the dominant (80%) and subdominant (20%) soil type (Table 5-8), reflecting that the dominant soil type represents at least 80% of the grid cell [*FAO*, 2002].

Hydraulic properties of the soil (field capacity, wilting point and hydraulic conductivity) were calculated from texture and soil organic carbon by applying the formulas suggested by *Saxton et al.* [1986].

To save computing time calculations were not performed on the smallest spatial resolution of input datasets (5 arc minutes soil map), but on a 0.5 degree grid, using the dominant soil type from the finer 5 arc minutes grid.

Table 5-8. Assignment of soil texture to combinations of dominant and associated soil types of the global soil map [FAO, 2002].

Dominant soil type	Associated soil type	Sand [%]	Silt [%]	Clay [%]
organic soils	organic	not simulated		
organic soils	coarse	80	10	10
organic soils	medium	35	30	35
organic soils	fine	10	30	60
coarse textured soils	coarse	80	10	10
coarse textured soils	organic	80	10	10
coarse textured soils	medium	72	14	14
coarse textured soils	fine	66	14	20
medium textured soils	medium	40	30	30
medium textured soils	organic	40	30	30
medium textured soils	coarse	48	26	26
medium textured soils	fine	34	30	36
fine textured soils	fine	10	30	60
fine textured soils	organic	10	30	60
fine textured soils	coarse	24	26	50
fine textured soils	medium	16	30	54

5.5.3 Weather data

The Daycent model uses daily data on precipitation and maximum and minimum temperature, but on the global scale daily weather data are only available on a 2.5° x 2.5° grid, either as model results or as reanalysis data [*ECMWF*, 2004; *NOAA-CIRES*, 2004]. A finer 0.5° x 0.5° spatial resolution of weather data is only available as monthly averages, and can be obtained from the Climate Research Unit, East Anglia. These monthly averages of maximum and minimum temperature, precipitation and number of rain days for the period of 1961- 2000 [*New et al.*, 2000] were to produce daily weather data. By applying a cubic-spline, daily temperature data were calculated from monthly averages, and daily precipitation data were obtained by allocating rain days over a month using Markov chains and then distributing monthly precipitation evenly to the rain days [*Kaspar et al.*, 2004].

5.5.4 Nitrogen deposition

In order to account for nitrogen deposition that can amount to more than 100 kg N $ha^{-1}y^{-1}$ in industrialized regions, we apply global maps of annual nitrate and ammonium deposition in the mid-1990ies [*Dentener*, 2001]. Ammonium as assumed to occur as dry deposition, i.e. is equally distributed over the entire year, while daily nitrate deposition is function of daily precipitation.

5.5.5 Management

The term ”management” comprises all activities that are undertaken on a field during the year, like sowing, fertilizer application, ploughing, irrigation, and their timing. Though these parameters have an essential influence on crop production and N_2O emissions, they are often not directly available on the global scale. Therefore the next paragraph describes all management activities and underlying assumptions that were included in the Daycent simulations.

Fertilizer application

Only nitrogen was considered as a nutrient in Daycent and therefore fertilizer application only includes mineral nitrogen. Despite this simplification, ignoring possible limitations of plant growth by other nutrients, the strong correlation between nitrate and phosphor consumption (correlation coefficient of 0.987 for the year 1995 [*FAO*, 2004]) suggests that if farmers apply nitrogen fertilizer at a certain rate, they will apply other nutrients accordingly. For legumes, where sufficient nitrogen is provided by fixation, this argument does not hold.

The amount of nitrogen fertilizer applied per country and crop was derived from the international fertilizer industry association [*IFA*, 2002], which provides this information for important crop-producing countries and their main crops. The database contains the crop-specific fertilizer application rate and the fraction of area fertilized, which were multiplied to get average application rates. For country-crop combinations with no IFA data available (approximately 17% in cropland area) the amount of nitrogen that would be removed with yield levels according to FAO statistics were calculated as a proxy for nitrogen input and therefore assumed that the difference between the removed nitrogen and the reported manure application rate is applied as mineral fertilizer. To account for nitrogen losses via leaching and gaseous emissions these values were increased

uniformly by 60%. This is still a conservative assumption, as fertilizer efficiency is often as low as 50% [*Cassman et al.*, 2002; *Frink et al.*, 1999]. As a consequence, real fertilizer input and thus yield levels and N_2O emissions might be underestimated for these countries. In addition to the total amount of applied fertilizer, the model is sensitive to the type of mineral nitrogen (nitrate or ammonia). This is due to the processes of denitrification, nitrification and the fact that mainly nitrate is susceptible to leaching losses. The typical ratio between ammonia and nitrate as a global variable was derived from *USGS* [2003], resulting into 85% ammonia and 15% nitrate. This of course is a simplification, and future model development will apply country-specific information on fertilizer types as provided by *FAO* [2004].

Manure application

Nitrogen application from manure was derived from *Siebert* [2005]. Based on global livestock densities [*Gerber*, 2004] for 12 animal types and their specific nitrogen excretion, he calculated total nitrogen excretion per grid cell, applying a grid resolution of 5 arc minutes. However, it was decided to aggregate the nitrogen application via manure to the country level. This was done (i) to avoid artificial spatial yield patterns caused by nitrogen availability from manure and (ii) to be consistent with the application of mineral fertilizer, which is also available on country level. For aggregation, manure application rates were averaged over the entire agricultural area of a country, and this value was then reduced by 20% in order to account for application losses [*Bouwman et al.*, 1997; *ECETOC*, 2004; *FAO*, 2001a].

Fertilizer and manure application dates

Application dates of mineral fertilizer and manure are difficult to estimate at the global scale. As they are mainly linked to planting dates (Chapter 3.5.4.5) and crop growth, applied the following rules were used to define the application events: Manure is always applied in two identical applications 10 and 30 days after planting. Mineral fertilizer is equally distributed over four application events, taking place 45, 76, 107 and 138 days before the assumed harvest date. If the effective crop growth period is shorter than 140 days the fertilizer is applied in four, three or two equal intervals over this period, starting with the planting date, and never applying fertilizer more often than once a month. Though fertilizer application in four events does not reflect agricultural practice, this approach was necessary to achieve realistic fertilizer efficiencies. E.g., in reality farmers adjust fertilizer application to rainfall events in order to minimize losses, which is not implemented in the simulation model.

Irrigation

For all 0.5° grid cells that contain at least one 5 minutes cell irrigated by more than 1% according to a global map of irrigated areas [*Döll and Siebert*, 2000] irrigated crop production and resulting N_2O emissions were simulated. Irrigation is assumed to occur over the entire growth period, adding every week the amount of water required to meet the field capacity of the soil. Wetland rice is a special case of irrigation with water logging on top of the soil during most of the growing period. As we were not yet able to implement water logging in Daycent, the soil water content is filled to saturation, and for the trace gas simulation, wfps is set to 100% and gas diffusivity to 0.0 during the entire growth period of wetland rice, ignoring the drain period (about two weeks) before harvest.

Other management data

Global planting dates were calculated according to the procedure presented in chapter 2, which using a simplified crop growth routine to determine the planting month promising the highest possible yield. For other management events we made very simple global assumptions. It is assumed that 75% of the shoot is removed at harvest as straw, and that cultivation events are restricted to one single ploughing just before planting. Ploughing events in Daycent affect decomposition rates of organic matter and further homogenise the ploughing layer with respect to soil texture.

5.5.6 Initial conditions, simulation period

Matter fluxes between the organic soil pools and the mineralisation of organic matter release mineral nitrogen which directly affects N_2O emission rates. The rate at which mineral nitrogen is released by these processes depends on the pool sizes and the related transition rates, following first order dynamics. Thus, the initial conditions for the organic matter pools can be crucial with respect to the simulation of N_2O emissions. Although the carbon and nitrogen content of the soil is provided by IGBP-DIS, these values may not be in equilibrium under the conditions simulated by Daycent (with respect to climate, land cover and land use). Ideally one would first calculate equilibrium levels of soil organic matter under natural conditions and then retrace a site's development from that state, but as a complete spatially explicit history of global land use could not be constructed in this project, a simpler approach is applied. To avoid the initial effects of changing pool sizes a spin-up time of 30 years was used, followed by another 30 year over which the average N_2O emissions were calculated.

5.5.7 Crop parameters

Daycent has been parameterised, calibrated and tested in a previous study to simulate wheat, rice, maize, soybean tropical cereals, pulses, potato, cassava and cotton (Chapter 2). These crops cover together about 66% of the global agricultural area. In order to guarantee a complete coverage of the global agricultural area when calculating global N_2O emission sums, these crops were assigned to the crop types accounted for in the land use map (Table 5-9). For all crops except for wheat and cassava, two different varieties were used to cover the full climatic range under which these crops can be grown. These parameterisations differ in the effective temperature sum needed to reach maturity; all other characteristics are identical. Wheat is represented as spring wheat and winter wheat, and for cassava only a tropical variety is applied. For most crops, parameterisations were available in the Century model, only pulses, cotton and cassava had to be parameterised anew. However, the effective rooting depth and the effect of water stress on crop growth was adjusted for all crops. The calibration was performed by adjusting the energy biomass conversion factor, which defines the maximum possible amount of biomass production per incoming radiation.

Table 5-9. Assignment between crop types of the land use map [*Leff et al.,* 2004] and the crops parameterised in Daycent for the global simulations.

Crop type in Daycent	Crop type in Land use map
Wheat	Wheat, barley, rye
Rice	Rice
Maize	Maize, rapeseed, oil palm, sunflower, sugarcane, sugar beet, others
Tropical cereals	Sorghum, millet
Pulses	Pulses
Potato, sweet potato	Potato
Cassava	Cassava
Soybean	Soybean, groundnuts
Cotton	Cotton

5.6 Estimation of global N_2O emissions from agricultural soils

Based on the revised Daycent version (Chapter 5.2.2) and the compilation of global input datasets (Chapter 5.5) N_2O emission rates were calculated for the major agricultural crops that had been parameterised for global crop production in a previous study (Chapter 2). These crops are wheat, rice, maize, soybean, tropical cereals, potatoes, pulses, cassava and cotton, covering together about 60% of the agricultural area. Analogous to the previous study on crop production, the presentation here is confined to the four crops wheat, rice, maize and soybean, as all main observations can be discussed for this subset. N_2O emission rates calculated for the other crops are provided in Appendix B. However, for the calculation of the total N_2O emissions all crop types are accounted for (see below).

5.6.1 N_2O emission

N_2O emission calculated with the Daycent model for wheat, maize and wetland rice are presented in Figure 5-13. In general terms, simulated emissions are lowest for wetland rice, not exceeding 1.5 kg N $ha^{-1}y^{-1}$, except for China and a few other areas (Figure 5-13c). For wheat, the simulated emission rates are markedly higher, mainly ranging from 1 to 4.5 kg N $ha^{-1}y^{-1}$ (Figure 5-13a). Even larger fluxes are calculated for maize, exceeding 3 kg N $ha^{-1}y^{-1}$ in wide areas (Figure 5-13b). For all crops, N_2O emissions largely depend on nitrogen input to the soil via mineral fertilizer and manure, causing highest emissions mainly in China, Europe, the US and some other countries with high fertilizer inputs. For evaluation of N_2O emissions calculated by the Daycent model, the results are compared to emission measurements from experimental sites, to regional studies, and to the statistical model (Chapter 3). These comparisons provide valuable information about measured and simulated emission levels, regional differences and the effects of agricultural management, climate and soil parameters. However, it has to be noted that the amounts of fertilizers used in field experiments regional studies often differ from the fertilizer applications simulated in Daycent. The comparison to the statistical model often refers to crop specific results not presented in Chapter 3, and therefore crop specific emission maps are provided in Appendix C.

Wheat

Average simulated N_2O emissions for wheat amount to 1.55 kg N $ha^{-1}y^{-1}$ (Table 5-10), which is lower than the value of 2.2 calculated by the statistical model, but within its 95% confidence interval. For temperate regions, which mostly receive fertilizer input > 60 kg N $ha^{-1}y^{-1}$, the simulated emissions range from about 1.5 to 4 kg N $ha^{-1}y^{-1}$. This is in agreement with emission measurements from wheat and barley cropping on temperate soils included in the data compilation for the statistical model (Chapter 3), as 25 and 75% quantiles amount to 1.1 and 3.6 kg N $ha^{-1}y^{-1}$, respectively. For the US, simulated N_2O emissions are mostly below 2 kg N $ha^{-1}y^{-1}$, as nitrogen input applied in the Daycent simulations for the USA is 65 kg N $ha^{-1}y^{-1}$. This value is low compared to nitrogen inputs e.g. in Central Europe, and thus simulated N_2O emissions meet the expected range. Within Europe, highest emissions are simulated from agricultural soils in the UK. According to the data compilation mentioned above, emissions from experimental sites in UK are clearly above the average value for temperate regions [e.g. *Colbourn and Harper*, 1987; *Skiba et al.*, 1994] thereby supporting the Daycent simulation results. First, this effect is due to high fertilizer inputs in the UK and second, the warmer and wetter oceanic climate may additionally contribute to the elevated N_2O emission rates. However, the range in observed emissions is large, and other studies report emissions of 1-2 kg N $ha^{-1}y^{-1}$ even under high N input [*Dobbie and Smith*, 2003], therefore not allowing generalised conclusions. Beyond, simulated emissions are at least slightly overestimated due to an underestimation of wheat yields (about 10%), causing the effect of higher remaining soil nitrogen levels. However, the regional differences of simulated emissions within the UK agree with observations that emissions are lower in the east and south compared to the west and north due to soil properties and higher soil transpiration rates [*Dobbie and Smith*, 2003].

Simulated N_2O emissions for China exceed 3.5 kg N $ha^{-1}y^{-1}$ in large regions. This is due to the high nitrogen input of 120 kg N $ha^{-1}y^{-1}$ and additionally, due to the wide discrepancy between nitrogen input and plant N uptake (Chapter 2), leaving excess nitrogen in the soil. Consequently, simulated emissions are even higher than e.g. in Germany, where, on average, more fertilizer is applied. Simulated N_2O emissions from wheat cropping in South America and Africa are mostly below 2 kg N $ha^{-1}y^{-1}$ because of low nitrogen inputs (Figure 5-13a). However, in three South-African countries, nitrogen input is similar to the amounts applied in Europe and China, thereby producing emissions of up to 4 kg N $ha^{-1}y^{-1}$.

Table 5-10. Average of simulated N_2O emissions [kg N_2O-N $ha^{-1}y^{-1}$] and fertilizer induced emissions (FIE) as fraction of fertilizer lost [%] at the global scale.

	--- N_2O [kg N_2O-N $ha^{-1}y^{-1}$] ---		---- FIE [%]----
Crop type	rain fed	irrigated	
Wheat	1.55	1.96	1.74
Rice	2.46	1.09 [a]	0.77 [a]
Maize	1.97	2.88	2.55
Soybean	1.14	1.57	-

[a] Wetland rice, with saturated soil water conditions strongly reducing N_2O emissions during the cropping period.

Maize

Simulated average N_2O emissions for maize cropping are higher than for wheat and amount to 2.0 kg N $ha^{-1}y^{-1}$ (Table 5-10). This is lower than the value of 3.3 kg N $ha^{-1}y^{-1}$ calculated by the statistical model. This discrepancy can be explained by the high effect value attributed to the crop type "other" in the statistical model, which comprises maize and other crop types associated with high N_2O emissions like potato. As for all crop types, simulated N_2O emission rates are largely determined by nitrogen input (Figure 5-13c). Highest emissions are calculated for China due to both high fertilizer input and the discrepancy between N input and low plant N uptake, as described above for wheat. N_2O emissions simulated for maize cropping in Europe range between 1 and 4 kg N $ha^{-1}y^{-1}$. This result is in agreement with most other studies on N_2O emissions from maize cropping in temperate regions, included in the dataset for the statistical analysis. However, in some studies observed emissions even exceed 10 kg N $ha^{-1}y^{-1}$ [e.g.*Flessa et al.*, 1995]. These extreme emissions may be attributed to inter-annual climate variability, as N_2O emissions can differ by a factor of > 2.5 between years [*Kaiser et al.*, 1998]. As the Daycent simulation results presented here are average emissions based on the climate normal (1961-1990; see Chapter 5.5.3) such high values do not occur in the model results.

Simulated N_2O emissions for Southeast Asia, Africa and South America closely correlated to nitrogen input, with highest N inputs in Indonesia and the northern part of South America (>60 kg N $ha^{-1}y^{-1}$), intermediate input in Brazil and low nitrogen input in Argentina and most African countries <25 kg N $ha^{-1}y^{-1}$). Simulated N_2O emissions from these tropical regions are higher than from temperate soils receiving similar nitrogen input. This is also demonstrated by the fraction of fertilizer lost as N_2O, which is higher towards lower latitudes (Figure 5-15c) (see also Chapter 5.6.2). This is consistent with the positive correlation between N_2O emissions and both temperature and precipitation identified in the sensitivity analysis, and is in agreement with results from the statistical model, identifying higher emissions from tropical than from temperate climates [*Bouwman et al.*, 2002b].

The finding that simulated N_2O emissions from maize are higher than from wheat is confirmed by the statistical analysis of available N_2O emission measurements (Chapter 3). This crop-specific difference is most prominent in the US, where N_2O emissions from wheat amount to about 1.5 kg N $ha^{-1}y^{-1}$, while about 3 kg N $ha^{-1}y^{-1}$ are emitted from maize. Similar findings are reported by *Del Grosso et al.* [2005] on N_2O emission from agricultural soils in the US, who report N_2O emissions of about 1.2 kg N $ha^{-1}y^{-1}$ for wheat, and 2.5-6 kg N $ha^{-1}y^{-1}$ for maize, based on 5 case studies. Both for the experimental data and the Daycent simulation results the difference is largely caused by higher fertilizer application rates in maize cropping (150 kg N $ha^{-1}y^{-1}$ to maize and 65 kg N $ha^{-1}y^{-1}$ to wheat in the Daycent simulations). Beyond, N_2O emission from maize tend to be higher than emissions from wheat because of its higher biomass production and higher N content, resulting in higher N inputs to the soils via plant residues. However, this effect is small compared to the fertilizer effect, as the fraction of nitrogen lost from fertilizer application rates is only slightly higher for maize than for wheat (Figure 5-15c).

Rice

N_2O emission from wetland rice calculated by the Daycent model are lower than for wheat and maize (Figure 5-13b), which agrees well with field observations [*Cai et al.*, 1997; *Xu et al.*, 1997]. Water logging during most of the growing season causes anaerobic soil condition during that period, thereby reducing or even preventing N_2O emissions caused by nitrification and denitrification. After draining the rice fields, N_2O emissions increase [*Abao et al.*, 2000; *Cai et al.*, 1997]. This agricultural practise is also implemented in Daycent, by "preventing" drainage and keeping the wfps at saturation during the growing period, which is causing the observed dynamics. The average simulated emission rate amounts to 1.1 kg N $ha^{-1}y^{-1}$. In most regions except for China, the simulated N_2O emissions are below 1.0 kg $ha^{-1}y^{-1}$ (Figure 5-13c), which meets observed emission [e.g.*Pathak et al.*, 2002]. However, most studies only report N_2O emissions during the growth period, thereby complicating direct comparisons with simulated emissions. A recent compilation of > 100 N_2O emission measurements from rice fields reports average N_2O emissions of about 0.7 kg N ha^{-1} during the growing season [*Akiyama et al.*, 2005]. Taking into account that most emissions occur during the growing period [*Akiyama et al.*, 2005], the lower value of 0.7 kg N ha^{-1} over a shorter than simulated time period, corresponds well with the simulated global emission average of 1.1 kg N $ha^{-1}y^{-1}$. Simulated N_2O emissions from rice cropping in China are markedly higher than in all other regions (Figure 5-13c), which can be attributed to the large discrepancy between high nitrogen input (145 kg N $ha^{-1}y^{-1}$) and low nitrogen uptake by the rice plant, as has been observed before for wheat and maize (Chapter 2). Interestingly, even in the data compilation of N_2O field measurements from rice fields this effect is present: Both highest nitrogen input and highest emissions are reported from Chinese sites [*Akiyama et al.*, 2005].

N_2O emissions from wetland rice simulated for China are higher in the south (Figure 5-13c), a result that is mainly caused by higher temperatures and higher precipitation. This positive correlation of temperature and soil moisture to N_2O emissions is widely accepted [*Davidson et al.*, 2000; *Dawson and Murphy*, 1972] and has been discussed in chapter 5.2.2.and chapter 5.4. Regional studies that could be used to validate the spatial variability of simulated N_2O emissions from wetland rice are still rare. A recent upscaling of N_2O emissions from Indian rice fields by using the DNDC model also identified higher N_2O emissions from warmer regions [*Pathak et al.*, 2005], a finding which confirmed the Daycent simulation results. However, regional differences in management may often exceed the effects related to soil and climate. Therefore a more quantitative comparison to other regional studies, which mostly rely on subnational management data, can only be obtained via model inter-comparison projects, replacing the country-specific management currently applied in Daycent by subnational information. For a more detailed simulation of N_2O emissions from wetland rice, the Daycent model would need to simulate different water management systems with either continuous or intermitted flooding, which have a large effect on N_2O emissions [*Cai et al.*, 1997], and multiple cropping, which is currently not accounted for.

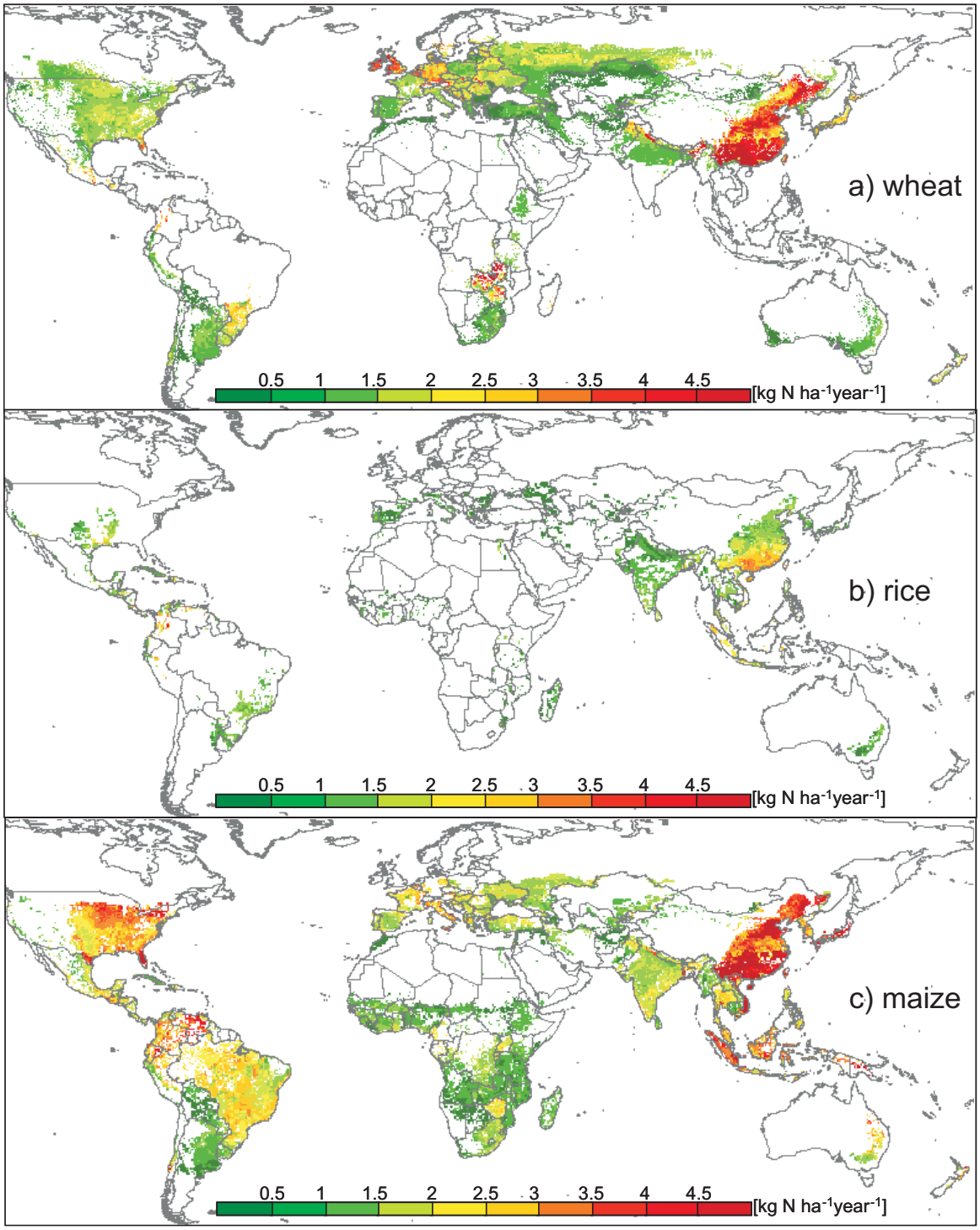

Figure 5-13. Simulated annual N_2O emissions [kg N $ha^{-1}y^{-1}$] for rain-fed wheat (a), wetland rice (b) and maize (c) cropping.

Soybean

Soybean, which belongs to the plant family of legumes, receives much lower nitrogen inputs than other crops, as its symbiosis with N fixing bacteria provides most of the nitrogen during plant growth. Simulated N_2O emissions from soybean cropping amount to 1.1 kg N $ha^{-1}y^{-1}$ on average (Table 5-10). Simulated values range from 0.3 to 2.1 kg N $ha^{-1}y^{-1}$ in North America and Europe,

while emissions of up to about 3 kg N $ha^{-1}y^{-1}$ are calculated for tropical regions and China (Figure 5-14). High simulated emissions in China can be attributed to the high nitrogen input (58 kg N $ha^{-1}y^{-1}$), which exceeds the nitrogen input in all other countries. For the global Daycent simulations identical manure application rates are assumed for all crops within one country, thereby probably overestimating the input for soybean and other legumes in countries with high manure application rates like China.

The emissions calculated for temperate regions are somewhat lower than observed emissions of e.g. 0.3 to 2 kg N $ha^{-1}y^{-1}$ [*Bremner*, 1980] or 0.46-3.08 kg N $ha^{-1}y^{-1}$ [*Rochette et al.*, 2004]. However, N_2O emissions from soybean cropping are highly uncertain [*Rochette et al.*, 2004]. To a greater extent than for other crops, they depend on the amount of residues left on the fields and to the N content in the straw. Even more, the amount of nitrogen fixed during the growing season, and the fraction of fixed nitrogen being added to the soil or taken up by the plant is highly uncertain. Therefore the simulation of the management of soybean crop residues and the process of nitrogen fixation should be improved in Daycent, because emissions seem to be underestimated in the present model version. This conclusion is also supported by results from the statistical model, which calculates average N_2O emissions of 2.5 kg N $ha^{-1}y^{-1}$ from soybean cropping.

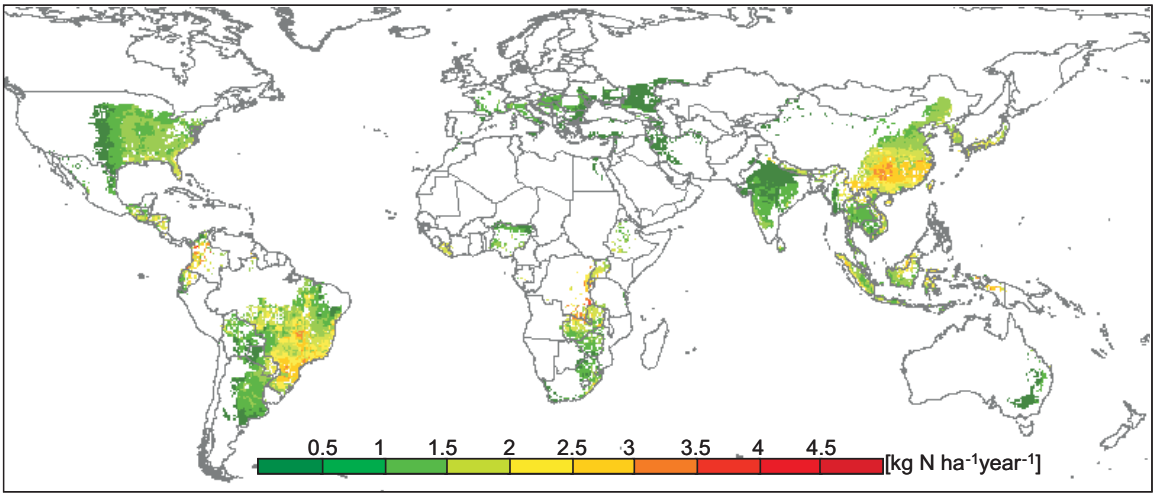

Figure 5-14. Simulated annual N_2O emissions [kg N $ha^{-1}y^{-1}$] for soybean cropping.

Irrigated agriculture

Simulated N_2O emissions from irrigated agriculture are higher than from rain fed agriculture for wheat, maize and soybeans (Table 5-10). This is in agreement with literature results [*Bronson and Mosier*, 1993; *Liebig et al.*, 2005], and is consistent with the results from the sensitivity analysis (Chapter 5.4). As N_2O emissions increase with increasing water input, the amount of irrigation water added is crucial to estimate emissions from irrigated agriculture. However, no information was available on irrigation water input at the global scale. For the irrigation scheme applied in the global simulations it is therefore assumed that as much water is added every week as needed to fill the soil pore volume to field capacity. This simplified approach assures that plant growth is not water limited during the entire cropping period, but probably overestimates irrigation water input in

many regions. Therefore a significant model improvement is expected by inferring crop-specific irrigation rates from water use efficiency for different crop types and global databases of agricultural water use [*Alcamo et al.*, 2003].

5.6.2 Fertilizer induced emissions

Fertilizer induced emissions are defined as the amount of N_2O emission that can be attributed to the fertilizer and manure applied to the field. In consequence, background emissions need to be defined, calculated and subtracted from the total emissions. Currently, the calculation of fertilizer induced emissions applied in the Kyoto IPCC guidelines are 1.25 +/- 1% of the applied fertilizer [*IPCC*, 1997]. Here a commonly used approach is followed [e.g. *Nevison et al.*, 1996] that was also used to develop the IPCC emission factor [*Bouwman et al.*, 1993]: Background emissions are calculated by assuming no fertilizer application, while keeping all other parameters and management events identical. The difference between the simulated total emissions and the background emissions is then divided by the fertilizer application rate to obtain the fraction of nitrogen input that is lost as N_2O. This fraction, as calculated by the Daycent model, is presented in Figures 5-15 for wheat, rice and maize. For soybeans, no such fertilizer induced emissions are calculated, as N_2O emissions from legumes do mainly arise from the nitrogen fixed by symbiotic bacteria.

The average fraction of fertilizer lost as N_2O from wheat cropping amounts to 1.55% (Table 5-10). This exceeds the IPCC factor of 1.25% and the values derived by *Bouwman* [2002b] and in Chapter 3. Highest values even exceeding 2.5% are calculated for regions where the nitrogen input exceeds the amount of N uptake by the plant (China, Zaire). Despite high fertilizer application rates in the UK, the Netherlands and Germany, the fertilizer induced emissions in these countries range between 1 and 1.5%, because plant uptake and crop yields are correspondingly high.

For maize cropping, the average fertilizer induced emissions are calculated to be 2.55%, which is higher than for wheat cropping and higher than the IPCC value. This large difference between wheat and maize is mainly due to the large tropical areas with high fertilizer induced emissions, influencing the global average. Site-specific comparisons between values for wheat and maize show much lower differences, e.g. in the US. The high fractions of fertilizer lost as N_2O calculated for tropical regions can be attributed both to higher temperature and precipitation, and to underestimated yields and plant N uptake in some tropical countries (Chapter 2).

The global average fraction of N_2O lost from nitrogen applied to wetland rice is significantly lower than that for wheat and maize, amounting to 0.77%. This agrees well with the statistical analysis of available N_2O emission measurements, in which fertilizer induced emissions from wetland rice were calculated as 0.7% of the N fertilizer applied [*Bouwman et al.*, 2002b]. According to the data compilation already cited above, the fertilizer induced emissions from experimental sites range from 0.003% to 1.16%, the average amounting to 0.31% of the fertilizer applied [*Akiyama et al.*, 2005]. Analogous to the discussion on N_2O emissions above, these values refer to the growing season, while the Daycent simulation results refer to an entire year.

From this analysis it becomes once more evident, that N_2O emissions from fertilizer applications largely depend on crop type, climatic conditions and the ratio between nitrogen input and nitrogen uptake by the crops. All these factors are not yet accounted for in the IPCC approach to estimate

fertilizer induced emissions [*Mosier et al.*, 1998], and are only partly accounted for by statistical approaches like the one in *Bouwman et al.* [2002b] or in Chapter 3. A detailed analysis of regional differences in fertilizer induced emissions that might have political implications with respect to the Kyoto protocol is beyond the scope of this study.

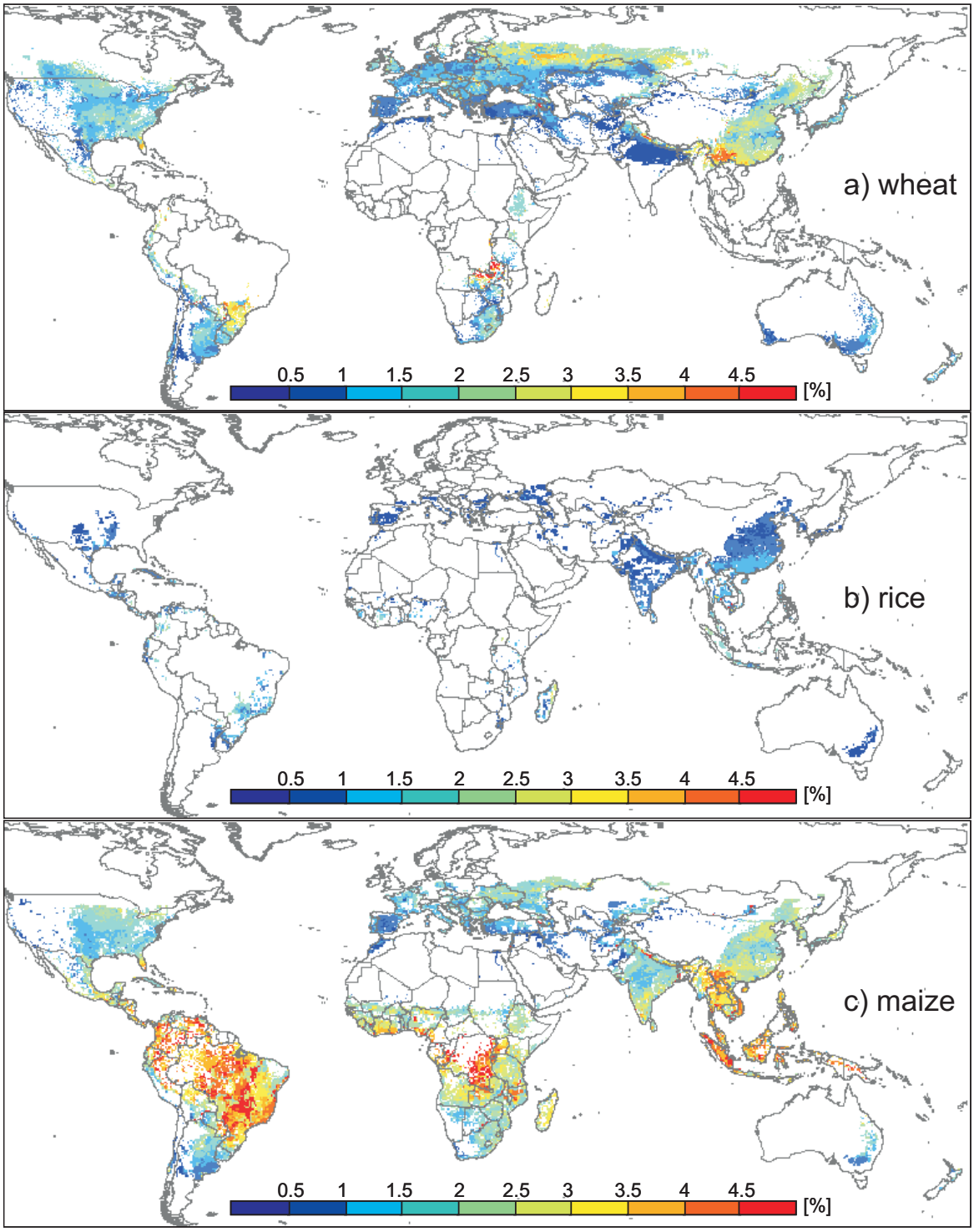

Figure 5-15. Fertilizer induced emission per nitrogen input [kg N_2O-N / kg N input] for rain-fed wheat (a), wetland rice (b) and maize (c) cropping.

5.6.3 Global N_2O emission sum

Global total N_2O emissions were calculated from the N_2O emission rates simulated for 9 crop types under irrigated and rain fed conditions, using the global land use map of [*Leff et al.*, 2004] and the global map of irrigated areas [*Döll and Siebert*, 2000]. In order to cover the entire agricultural area, the crop groups discriminated in the land use map are assigned to the crop types represented by the Daycent model according to Table 5-9. The land use map provides fractions of different crop types within a 5 arcmin grid cell (~ 10 km near the equator) without discriminating rain-fed and irrigated cropping, while the map of irrigated areas provides fractions of irrigated land without accounting for different crop types. Information on the crop-specific fractions of irrigated areas within one country is available for some counties and crops from FAO AQUASTAT [*FAO*, 2001b]. If no crop specific information was available, average values from FAO AQUASTAT [*FAO*, 2001b] were used instead. Thus, the following scheme was applied to calculate total N_2O emissions.

For all countries m and croptypes j:

$$\text{Sum rainfed } N2O_{mj} = (1 - \text{irrig}_{mj}) * \sum_{i=1}^{n} Cell\_area_i * N2O\_rf_{ji} * crop\_fraction_{ji}$$

$$\text{Sum irrigated } N2O_{mj} = C_{mj} * \sum_{i=1}^{n} Cell\_area_i * N2O\_irri_{ji} * irri\_fraction_i$$

$$C_{mj} = \frac{\text{irrigated area}_{mj}}{\text{total irrigated area}_m}$$

$$\text{irrigated area}_{mj} = \text{irrig}_m * \sum_{i=1}^{n} Cell\_area_i * crop\_fraction_{ji}$$

$$\text{total irrigated area}_m = * \sum_{i=1}^{n} Cell\_area_i * irri\_fraction_i$$

Cell_area = Land area within grid cell i
C_{mj} = Correction factor for irrigated areas for crop i in country m
$crop\_fraction_{ji}$ = fraction of crop type j in grid cell i
$irri\_fraction_i$ = irrigated fraction of a 5min grid cell according to [*Döll and Siebert*, 2000]
$irrig_m$ = fraction of irrigated area for crop j in country m
$N_2O\_rf_{ji}$ = N_2O emission rate [kg N $ha^{-1}y^{-1}$] in cell i for rain-fed crop j
$N_2O\_irri_{ji}$ = N_2O emission rate [kg N $ha^{-1}y^{-1}$] in cell i for irrigated crop j

i = grid cell index
j = crop type index (wheat, rice, maize, sorghum, pulses, potato, cassava, soybean, cotton)
n = number of 5 arcmin grid cells within one county
m = country index

Based on this calculation, total N_2O emissions amount to 2.1 Tg N y^{-1}. Comparisons of this value to other global estimates of N_2O emissions from agricultural soils are discussed in the following. Based on the IPCC approach, N_2O emissions from agricultural management amount to 4.2 Tg y^{-1} [*Mosier et al.*, 1998] (Table 5-1). This value includes both direct emissions from fertilizer input, manure input, crop residues and nitrogen fixation, and indirect emissions due to nitrogen leaching and volatilisation. The latter are not accounted for by Daycent calculations. The direct emissions of 2.1 Tg N y^{-1} (Table 5-11) account for the additional N_2O emissions due to agricultural management, therefore not including background emissions. Thus, total direct emissions comparable to the Daycent results need to be calculated from the direct emissions plus background

emissions. However, the uncertainty of background emissions is immense, therefore they were simply ignored by the IPCC [*Bouwman,* pers. communication]. For the comparison, the value of 1 kg N $ha^{-1}y^{-1}$ as calculated in the original study on the fertilizer induced emissions is used [*Bouwman et al.*, 1993]. Extrapolated to the global scale, this value adds up to 1.2 Tg N y^{-1} background emissions from global agricultural area, resulting 3.3 Tg y^{-1} total direct emissions from agricultural soils. Compared to the latter value, the Daycent estimate of 2.1 Tg y^{-1} is somewhat lower. This can be partly attributed to the fact that the 2.1 Tg y^{-1} calculated by *Mosier et al.*. [1998] does also include grasslands, which is not accounted for in the Daycent calculations. As the fraction of fertilizer and manure applied to grassland amounts to about 8% globally [*Bouwman et al.*, 2005], the value of 2.1 Tg y^{-1} would be reduced to 1.9 Tg y^{-1} for emissions from agricultural fields. Beyond, the emissions estimated by the Daycent model may be slightly too low, due to an underestimation of emissions from legumes.

Table 5-11. Global source estimates for N_2O emissions [Tg N_2O-N $year^{-1}$] from agricultural soils.

Reference	This study	*Mosier et al.* (1998) *Kroeze et al.* (1999)	*Olivier et al.* (1998)	*Nevison et al.* (1996)	*Potter et al.* (1996)	*Bouwman et al.* (2002b)	Chapter 3
Base year	1990ies	1994	1990	1990	1990	1995	1998
Emissions from agricultural soils	2.1	2.1 [a b]	1.9 [b]	2.1 [a]		2.7	3.2
Range		0.6 – 14.8	0.7 – 4.3	0.1 – 3.5	1.2 – 4.0	1.6 – 4.6 [c]	1.6 – 6.6 [c]
Method	Daycent model	IPCC factors	IPCC factors	NBM model	CASA model	Statistical model	Statistical model

[a] only fertilizer induced emissions
[b] including grasslands
[c] 95% confidence interval

The total global emissions from agricultural soils estimated by an earlier statistical approach [*Bouwman et al.*, 2002b] and in Chapter 3 amount to 2.7 and 3.2 Tg y^{-1}, respectively (Table 5-11), with uncertainty ranges of 1.6 to 4.6 and 1.6 to 6.6, respectively. These estimates slightly exceed the value calculated with the Daycent model, which may partly be attributed to rather high background emissions calculated in the statistical approach: N_2O emission measurements often stem from soils receiving high fertilizer input, and therefore the database used for the statistical analysis also includes a large share of measurements from high input systems. Combined with the exponential nature of the statistical function this favours overestimated background emission rates, which amount to 1.7 kg N $ha^{-1}y^{-1}$ on average. Altogether, the total N_2O emissions from agricultural soils calculated with the Daycent model fall within the confidence range of all statistical approaches listed in Table 5-11, and are similar to the proposed estimates.

Besides the Daycent approach presented in this study, there are two other process-based models estimating global N_2O emissions as a function of mineralisation rates (NBM model [*Nevison et al.*, 1996], CASA model; [*Potter et al.*, 1996]). According to the NBM model, the global N_2O emissions that are attributed to fertilizer applications amount to 2.1 Tg y^{-1} [*Nevison et al.*, 1996], not including background emissions. This value agrees with the 2.1 Tg y^{-1} calculated by [*Mosier et al.*, 1998], though not accounting for nitrogen input via crop residues. Simulation results with the

CASA model range between 1.2 and 4 Tg y^{-1} from global agricultural soils (Table 5-11), and are in a similar range as all other studies.

To conclude, the Daycent simulation results are in agreement to other global N_2O emission estimates from the cited studies. However, the wide uncertainty range inherent in all N_2O emission estimates indicates that further confirmation of model results needs to be based on extended model validation based on field measurements and improved global input datasets.

5.7 Conclusions and Outlook

As we have seen, estimates of total N_2O emissions from agricultural soils are highly uncertain. Statistical approaches operating on average site characteristics are valuable to derive best estimates and uncertainty ranges based on the plenty of measurements available. However, the 95% confidence interval in these estimates of at -50% and +100% will probably remain large even when including more measurements, as N_2O emissions are governed by processes at spatial and temporal scales beyond the resolution of any statistical model. Additionally, the application of statistical approaches is confined to the conditions they are developed on. Therefore process-based models that include short-term dynamics of soil processes are required to assess future N_2O emissions under changed environmental and management conditions. Furthermore, the application of process-based models is expected to reduce the uncertainty of N_2O emission estimates.

The Daycent model with its refined calculation of nitrification and denitrification, and a scheme to account for winter emissions, accurately simulating soil water content, soil ammonium content and soil nitrate content, the main driving forces for N_2O emission, and is capable to represent emissions from different crop types under both temperate an tropical climate (ME = 0.1 to 0.6 for most sites and monthly averages).

The model evaluation has shown that further model improvement can be expected by refining the calculation of nitrate leaching, by refining soil gas diffusion processes, and by including dynamics of bacterial populations. Freeze-thaw emissions, which were ignored in the original version, are now accounted for in the Daycent model and meet observed winter emissions at some of the study sites, while underestimating others. As the understanding of the highly dynamic freeze-thaw emission events is still limited, an improved implementation of these emission events will need to rely on additional detailed laboratory data.

Additional to these model uncertainties that should be addressed in future work, the global scale application of the Daycent model is also is affected by uncertainties in input datasets. The sensitivity analysis has shown that N_2O emissions are sensitive to changes in temperate and precipitation. On the one hand site this proves that the model can be applied to represent regional differences in emissions, and to study the effect of climate change on N_2O emission rates. On the other hand, the dependency of N_2O emissions on precipitation indicates that an uncertainty in simulated emissions might arise from the climate data used. However, the results from the sensitivity analysis were similar when using either data from weather stations or data derived from monthly averages on a 0.5 ° grid. Therefore it can be concluded that the method applied does not introduce a major source of uncertainty in simulated N_2O emissions. Additionally, it can be

concluded from the sensitivity analysis that the effect of different pedotransfer functions for field capacity and soil hydraulic conductivity should be assessed, as these variables have been shown to have a significant influence on simulated N_2O emissions.

The application of the Daycent model to estimate N_2O emissions from agricultural soils at the global scale has proven that simulated emissions are in agreement with observed values for rice, wheat and maize, while emissions from soybean seem to be underestimated. Therefore future work should address the representation of soils N dynamics under leguminous crops. Beyond, several important agricultural practices like double cropping, water management in wetland rice and crop rotations should be accounted for in future applications, and calculations of N_2O emissions from irrigated agriculture will be improved by including information on agricultural water use.

Total simulated N_2O emissions from agricultural soils agree with estimates from other studies. This indicates, together with the site specific model testing and the agreement of emission rates to observed values in different world regions, that the application of the Daycent model at the global scale adequately represents soil nitrogen dynamics and the effect of environmental and management parameters.

However, as the uncertainty range of total N_2O emission estimates is large, further validation of the Daycent model needs to be based on site-specific evaluation. So far, it is not possible to give an uncertainty range of the total N_2O emissions estimated by the Daycent model that could be compared to the uncertainty of the other estimates. In contrast to statistical approaches, the uncertainty of process-based models is difficult to calculate, as both model uncertainties and the uncertainty of input parameters, which are often not known, need to be included. As a first approach to estimate the uncertainty of the Daycent simulation results, further site-specific validations should be performed to derive a confidence interval for annual emissions.

At the global scale, the modelling framework for N_2O emissions from agricultural soils, consisting of a revised version of the Daycent model and a consistent global database of environmental and management data can be used for a number of further applications: It is now possible to study the effect of climate change and agricultural intensification like increased fertilizer input and expansion of irrigated agriculture on N_2O emissions at the global scale. Thereby both total N_2O emissions for global change scenarios can be calculated, and regional differences in the effects of climate change and fertilizer application on N_2O emissions can be assessed. Furthermore, this modelling framework can be applied to assess the effect of agriculture on nitrogen leaching, and, by a possible combination with a global water model, the input of nitrogen to surface waters and coastal zones.

6 Concluding remarks

The overall objective of this thesis was to provide a consistent modelling framework for plant growth, water, carbon and nutrient cycles in agricultural systems at the global scale, focussing as a start on the simulation of crop production and resulting N_2O emissions.

From a conceptual perspective, it is evident that soil organic matter dynamics, trace gas emissions, nutrient cycling, nutrient leaching and plant growth are mutually interdependent and therefore need to be addressed in a consistent and comprehensive modelling approach. However, missing or uncertain input datasets, limited knowledge about the processes involved, or problems of upscaling may hamper the development of such a model at the global scale. On the other hand, there is an urgent need for global agricultural models to assess present day and potential future large-scale changes in land use, to study the impacts of climatic change on crop yields in different world regions, to examine the environmental consequences of agricultural practises, and to analyse potential feedback effects between the terrestrial, the aquatic and the climate system.

The global modelling approach for agricultural systems presented in this thesis overcomes some of the limitations inherent in current global crop models, and provides the first process-based simulation of global agricultural N_2O emissions. It is based on the existing agroecosystem model Daycent, which was refined and adapted to simulate crop production and N_2O emissions at the global scale: In a preparatory step, required input datasets were compiled, and a simulation system was implemented to allow grid-base calculations of the Daycent model. For its application as global crop model (chapter 2) the Daycent model was adapted and parameterised for the simulation of 9 major crop types and tested against national and subnational census data. In order to quantify the effect of important driving forces on N_2O and NO emissions a compilation of available emissions measurements has been analysed (chapter 3). For the simulation of N_2O emission with Daycent, a case study (chapter 4) and literature review were used to identify model limitations and possible improvements. Based on that, the simulation of N_2O emissions in the Daycent model was refined and tested against experimental data (chapter 5). The revised model version was then used to estimate current N_2O emissions from agricultural soils at the global scale (chapter 5). In this final chapter, most relevant conclusions resulting from these previous chapters are reflected, main achievements and limitations are highlighted, and an outlook on future research is given.

6.1 Modelling global crop production

Comparison between simulated crop yields and census data proved that the Daycent model is capable of reproducing major effects of agricultural management. National averages of yields were represented well, the modelling efficiency amounting to 0.66 for wheat, rice and maize, and to 0.32 for soybean. Beyond, spatial patterns of simulated yields mostly correspond to observed crop distributions and subnational census data.

A quantitative validation of model performance based on subnational data is often hampered by missing subnational management information. Fertilizer input and management can largely differ within one country and thereby influence regional differences in crop yields. Therefore

homogenous fertilizer application rates within one country as applied in Daycent will cause deviations to observed crop yields. For further model validation, it is suggested to use field scale data of crop growth from different environmental and management conditions in agricultural systems around the world.

However, the model evaluation presented here marks a substantial improvement compared to the other available global crop modelling studies. All other global crop models have not been validated against census data except for one recent publication of the EPIC model [*Tan and Shibasaki*, 2003], which provides a visual comparison of average crop yields to FAO data, but without reporting modelling efficiencies.

From evaluation of the Daycent model it must be concluded that large scale crop modelling is subject to a wide range of uncertainties, with respect to both input data (particularly management), and the representation of processes influencing crop growth (e.g. formulation of water stress, phenological stages, impact of slope, etc.). Further model improvement will be achieved by refining the implementation of water stress on crop growth, by including phosphorous limitation for legumes, and by accounting for the effect of slope on surface runoff, water and nutrient availability. With respect to input data it became evident that the diversity of agricultural management at the global scale should be accounted for by implementing regional differences in crop varieties and sub-national variability of management practices. Beyond, sequential cropping and crop rotations, which are relevant for soil nutrient dynamics and realistic planting dates, should be included in future model improvement.

6.2 Estimating N_2O and NO emissions with statistical models

A comprehensive compilation of N_2O and NO emission measurements has been analysed in order to derive quantitative effects of environmental and management factors on N_2O and NO emissions. The limited number of significant correlations and their large uncertainty hindered their intended application to improve the Daycent trace gas sub-model. However, the results of the statistical analysis yielded some interesting conclusions. For N_2O emissions from agricultural soils eight factors with a significant influence on N_2O emissions were identified, with the resulting statistical model having a 95% confidence interval of about -50% and +100%. In contrast, the 95% confidence interval of the statistical models developed for NO emissions from agriculture and N_2O and NO emissions from soils under natural vegetation was at least -70% and +250%. As these three subsets of emission data were represented by 5 times less measurement data than available for agricultural N_2O, it can be concluded that the number of emissions measurements needs be largely increased to reduce the uncertainty of these statistical models.

Though represented by a similar number of emission measurements, twice as much significant factor were identified for N_2O emissions from soils under natural vegetation compared to NO emissions from agricultural or natural soil. This indicates, that N_2O emissions stronger depend on average site characteristics as included in the dataset than NO emissions do.

It needs to be stated that all factors identified to have a significant effect on NO or N_2O emissions in the statistical analysis were already known as important factors from either laboratory or field

scale studies, and that the correlations are less significant compared to laboratory studies on the driving forces of N_2O emissions. Therefore it needs to be concluded that statistical analysis of N_2O and NO emissions and site-specific environmental and management factors cannot be used to improve process-based models. Even more, the compelling result from this analysis is that other, perhaps process-based approaches seem to be inevitably needed to improve N_2O and NO emission estimates.

Nevertheless, the statistical models developed here are valuable to delimit possible emission ranges and to serve as a benchmark to the highly dynamic process models. Beyond, there are several areas of application where statistical models of N_2O emissions are needed. The national greenhouse gas inventories as required by the Kyoto protocol will certainly be based on statistical approaches during the next years, and also the calculation of greenhouse gas emissions in life cycle assessments will dominantly apply emissions factors, though process-based approaches are gaining importance.

6.3 Process-based modelling of N_2O emissions

The revised Daycent version, including a scheme for freeze-thaw emissions and a more detailed representation of nitrification and denitrification has been proven to correctly simulate soil water content, soil ammonium content and soil nitrate content, and to represent monthly averages of N_2O emissions from different crop types under both temperate an tropical climate with a modelling efficiency of ME = 0.1 to 0.6 for most sites.

Further model improvements can be expected from a more detailed calculation of soil gas diffusion, nitrate leaching and by addressing dynamics of bacterial populations. For freeze-thaw emissions, the scheme applied in the Daycent model is a first approach to capture the temporal dynamics and the contribution to total annual emissions from these processes. However, these processes are still poorly understood, and substantial model improvement will only be possible if additional insight in the mechanisms is gained in plot-scale or laboratory studies.

From the sensitivity analysis it can be concluded, that the Daycent model is able to react sensitive to changes in climate parameters, allowing its application to study the effect of regional climatic differences and the impact of climate change on N_2O emissions. The parameters field capacity and hydraulic conductivity were identified to have a significant impact on simulated N_2O emissions, and as they can only be derived from pedotransfer functions at the global scale, further model simulations should be carried out to assess the effect of different available pedotransfer functions on global N_2O emissions.

Results from the application of the Daycent model to estimate N_2O emissions from agricultural soils at the global scale agree with observed emission rates for wheat, rice and maize. For the simulation of N_2O emissions from soybean, which tend to be underestimated at the moment, a refined representation of both the process of nitrogen fixation and the agricultural management, especially handling of crop residues, is expected to increase the model performance.

In agreement to the initial assumption that crop production and N_2O emissions are strongly interdependent and need to be addressed in a common modelling approach, it has been shown that

the difference between nitrogen application and plant N uptake has a strong effect on simulated N_2O emissions and on the fraction of fertilizer lost as N_2O. This effect is not accounted for by IPCC approach but has a strong influence on the fertilizer induced emissions in some regions.

Total simulated N_2O emissions from agricultural soils are in agreement with estimates from other studies. This indicates, together with the results from the site specific model testing, that the Daycent model correctly represents soil nitrogen dynamics and the effect of environmental and management parameters on N_2O emissions. As the comparison between estimates of total N_2O emissions strongly depends on assumptions on background emissions, which are highly uncertain, and for which a large discrepancy between the Daycent simulation results and the statistical model exists, we suggest that the concept of background emissions from agricultural soils and their calculation should be addressed in future work.

6.4 Outlook and future research

The adaptation of the Daycent model presented here has been proven to represent crop yields and agricultural N_2O emissions at the global scale, applying a consistent approach to plant growth, water, carbon and nutrient cycles. With such a tool it is now possible to study the effects of climate change and inter-annual climate variability on crop yields and N_2O emissions in different world regions, to assess the impact of agricultural management on soil nitrogen dynamics and N_2O emissions, and to calculate agricultural water demand and the impact of irrigation on crop yields. Beyond, this model provides a basis to analyse the effect of agricultural management on nutrient leaching, soil degradation or the emission of other trace gases. Beyond, its integration in the global land use model currently developed at the Center for Environmental Systems Research (CESR) in Kassel will allow to study feedbacks between land use change and crop productivity.

7 Bibliography

Abao, E. B., jr, K. F. Bronson, R. Wassmann, and U. Singh (2000), Simultaneous records of methane and nitrous oxide emissions in rice-based cropping systems under rainfed conditions, *Nutrient Cycling in Agroecosystems*, *58*, 131-139.

ABS (2000), A spatially consistent sub-set of AgStats data 1982/83 to 1996/1997, Australian Bureau of Statistics.

Acevedo, E., P. Silva, and H. Silva (2002), Wheat growth and physiology, in *Bread wheat - Improvement and Production*, edited by B. C. Curtis, Rajaram, S., Macpherson, H.G., FAO, Rome.

Akiyama, H., K. Yagi, and X. Y. Yan (2005), Direct N_2O emissions from rice paddy fields: Summary of available data, *Global Biogeochemical Cycles*, *19*, art. no.-GB1005.

Alcamo, J. (Ed.) (1994), *Image 2.0: Integrated Modelling of Global Climate Change*, Kluwer Academic Publishers, Dodrecht, Boston, London.

Alcamo, J., R. Leemans, and E. Kreileman (Eds.) (1998), *Global Change Scenarios of the 21st Century*, 296 pp., Elsevier, Oxford, UK.

Alcamo, J., P. Doll, T. Henrichs, F. Kaspar, B. Lehner, T. Rosch, and S. Siebert (2003), Global estimates of water withdrawals and availability under current and future "business-as-usual" conditions, *Hydrological Sciences Journal - Journal Des Sciences Hydrologiques*, *48*, 339-348.

Alexander, M. (1977), *Introduction to soil microbiology (2nd edition)*, 467 pp., Wiley and Sons, New York.

Allen, R. G., L. S. Pereira, D. Raes, and M. Smith (1998), *Crop evapotranspiration - guidelines for computing crop water requirements*, FAO, Rome.

Ambus, P., and G. P. Robertson (1998), Automated near-continuous measurement of carbon dioxide and nitrous oxide fluxes from soil, *Soil Science Society of America Journal*, *62*, 394-400.

Anderson, I. C., and J. S. Levine (1986), Relative rates of nitric oxide and nitrous oxide production by nitrifiers, denitrifiers, and nitrate respirers, *Applied and Environmental Microbiology*, *51*, 938-945.

Aulakh, M. S., T. S. Khera, and J. W. Doran (2000), Mineralization and denitrification in upland, nearly saturated and flooded subtropical soils. II. Effect of organic manures varying in N content and C:N ratio, *Biology and Fertility of Soils*, *31*, 168-174.

Avalakki, U. K., W. M. Stron, and P. G. Saffigna (1995), Measurement of gaseous emissions from denitrification of applied nitrogen-15 II. Effects of temperture and added straw, *Australian Journal of Soil Research*, *33*, 89-99.

Bailey, L. D., and E. G. Beauchamp (1973), Effects of temperature on NO_3 and NO_2 reduction, nitrogeneous gas production, and redox potential in a saturated soil, *Canadian Journal of Soil Science*, *53*, 213-218.

Batjes, N. H. (2002), Revised soil parameter estimates for the soil types of the world, *Soil Use and Management.*, *18*, 232-235.

Baumgärtner, M., and R. Conrad (1992), Effects of soil variables and season on the production and consumption of nitric oxide in oxid soils, *Biology and Fertility of Soils*, *14*, 166-174.

Bobbink, R., M. Hornung, and J. G. M. Roelofs (1998), The effects of air-borne nitrogen pollutants on species diversity in natural and semi-natural European vegetation, *Journal of Ecology*, *86*, 717-738.

Bollmann, A., and R. Conrad (1998), Influence of O_2 availability on NO and N_2O release by nitrification and denitrification in soils, *Global Change Biology*, *4*, 387-396.

Boogaard, H. L., H. Eerens, I. Supit, C. A. van Diepen, I. Piccard, and P. Kempeneers (2002), Description of the MARS Crop Yield Forecasting System, European Commision Joint Research Centre, Brussels.

Bouwman, A. F., I. Fung, E. Matthews, and J. John (1993), Global analysis of the potential for N_2O production in natural soils, *Global Biogeochemical Cycles*, *7*, 557-597.

Bouwman, A. F. (1996), Direct emission of nitrous oxide from agricultural soils, *Nutrient Cycling in Agroecosystems*, *46*, 53-70.

Bouwman, A. F., D. S. Lee, W. A. H. Asman, F. J. Dentener, K. W. Van der Hoek, and J. G. J. Olivier (1997), A global high-resolution emission inventory for ammonia, *Global Biogeochemical Cycles*, *11*, 561-587.

Bouwman, A. F., L. J. M. Boumans, and N. H. Batjes (2002a), Emissions of N2O and NO from fertilized fields: Summary of available measurement data, *Global Biogeochemical Cycles, 16(4)*, art. no. 2001GB001811.

Bouwman, A. F., L. J. M. Boumans, and N. H. Batjes (2002b), Modeling global annual N2O and NO emissions from fertilized fields, *Global Biogeochemical Cycles, 16(4),* art. no. 2001GB001812.

Bouwman, A. F., L. J. M. Boumans, and N. H. Batjes (2002c), Estimation of global NH3 volatilization loss from synthetic fertilizers and animal manure applied to arable lands and grasslands, *Global Biogeochemical Cycles, 16(2),* art. no. 2000GB001389.

Bouwman, A. F., G. Van Drecht, and K. W. Van der Hoek (2005), Global and regional surface nitrogen balances in intensive agricultural production systems for the period 1970-2030, *Pedosphere*, *15*, 137-155.

Brady, N. C. (1990), *The nature and properties of soils*, Macmillan Publishing Company, New York.

Brady, N. C., and R. R. Weil (2002), *The nature and properties of soils*, 13. ed., 960 pp., Mcmillan Publishing Company, New York.

Bramley, R. G. V., and R. E. White (1990), The variability of nitrifying activity in field soils, *Plant and Soil*, *126*, 203 - 208.

Bremner, J. M., and K. Shaw (1958), Denitrification in soil. II. Factors affecting denetrification., *Journal of Agricultural Science*, *51*, 40-52.

Bremner, J. M., Robbins, S.G. and Blackmer, A.M. (1980), Seasonal variability in emission of nitrous oxide from soil, *Geophysical Research Letters*, *7*, 641-644.

Bronson, K. F., and A. R. Mosier (1993), Effect of nitrogen fertilizer and nitrification inhibitors on methane and nitrous oxide fluxes in irrigated corn, in *Biogeochemistry of global change*, edited by R. S. Oremland, pp. 278-289, Chapman & Hall.

Brovkin, V., M. Claussen, V. Petoukhov, and A. Ganopolski (1998), On the stability of the atmosphere-vegetation system in the Sahara/Sahel region, *Journal Of Geophysical Research-Atmospheres*, *103*, 31613-31624.

Bruinsma, J. E. (2003), *World agriculture: towards 2015/2030. An FAO perspective*, 432 pp., Earthscan, London.

Butterbach-Bahl, K., M. Kesik, P. Miehle, H. Papen, and C. Li (2004), Quantifying the regional source strength of N-trace gases across agricultural and forest ecosystems with process based models, *Plant And Soil*, *260*, 311-329.

Cai, Z. C., G. X. Xing, X. Y. Yan, H. Xu, H. Tsuruta, K. Yagi, and K. Minami (1997), Methane and nitrous oxide emissions from rice paddy fields as affected by nitrogen fertilisers and water management, *Plant And Soil*, *196*, 7-14.

Cao, M., J. B. Dent, and O. W. Heal (1995), Modelling methane emissions from rice paddies, *Global Biogeochemical Cycles*, *9*, 183–195.

Cassman, K. G., A. Dobermann, and D. T. Walters (2002), Agroecosystems, nitrogen-use efficiency, and nitrogen management, *AMBIO*, *31*, 132-140.

Century-Manual (2005), *Century Reference and User's Guide*, URL: http://www.nrel.colostate.edu/projects/century5/reference/index.htm.

Century-Parameterisation-Workbook (2005), vailable at www.nrel.colostate.edu/projects/century5.

Challinor, A. J., W. T.R., C. P.Q., S. J.M., and G. D.I.F. (2004), Design and optimisation of a large-area process-based model for annual crops, *Agricultural and forest meteorology*, *124*, 99-120.

Colbourn, P., and I. W. Harper (1987), Denitrification in drained and undrained arable clay soil, *Journal of Soil Science*, *38*, 531-539.

Coleman, K., D. S. Jenkinson, G. J. Crocker, P. R. Grace, J. Klír, M. Körschens, P. R. Poulton, and D. D. Richter (1997), Simulating trends in soil organic carbon in long-term experiments using RothC-26.3, *Geoderma*, *81*, 29-44.

Collins, W. J., D. S. Stevenson, C. E. Johnson, and R. G. Derwent (1997), Tropospheric ozone in a global-scale three-dimensional Lagrangian model and its response to NO_x emission controls, *Journal of Atmospheric Chemistry*, *26*, 223-274.

Crutzen, P. J. (1981), Atmospheric chemical processes of the oxides of nitrogen, including nitrous oxide, in *Denitrification, nitrification and atmospheric nitrous oxide*, edited by C. C. Delwiche, pp. 17-44, John Wiley & Sons, New York.

Davidson, E. A. (1991), Fluxes of nitrous oxide and nitric oxide from terrestrial ecosystems, in *Microbial production and consumption of greenhouse gases: methane, nitrogen oxides and halomethanes.*, edited by J. E. Rogers and W. B. Whitman, pp. 219-235, American Society of Microbiology, Washington, D.C.

Davidson, E. A., and W. Kingerlee (1997), A global inventory of nitric oxide emissions from soils, *Nutrient Cycling in Agroecosystems*, *48*, 37.

Davidson, E. A., S. E. Trumbore, and R. Amundson (2000), Biogeochemistry - Soil warming and organic carbon content, *Nature*, *408*, 789-790.

Dawson, R. N., and K. L. Murphy (1972), The temperature dependency of biological denitrification, *Water Research*, *6*, 71-83.

de Klein, C. A. M., and R. S. P. van Logtestijn (1996), Denitrification in grassland soils in The Netherlands in relation to irrigation, nitrogen application rate, soil water content and soil temprerature, *Soil Biology & Biochemistry*, *28*, 231-237.

de Pauw, E., F. O. Nachtergaele, J. Antoine, G. Fisher, and H. T. V. Velthuizen (1996), A provisional world climatic resource inventory based on the length-of-growing-period concept, in *National soil reference collections and databases (NASREC)*, edited by N. H. Batjes, et al., pp. 30-43, International Soil Reference and Information Centre (ISRIC), Wageningen.

Del Grosso, S., D. Ojima, W. Parton, A. Mosier, G. Peterson, and D. Schimel (2002), Simulated effects of dryland cropping intensification on soil organic matter and greenhouse gas exchanges using the DAYCENT ecosystem model, *Environmental Pollution*, *116*, S75.

Del Grosso, S. J., W. J. Parton, A. R. Mosier, D. S. Ojima, A. E. Kulmala, and S. Phongpan (2000), General model for N_2O and N_2 gas emissions from soils due to dentrification, *Global Biogeochemical Cycles*, *14*, 1045.

Del Grosso, S. J., A. R. Mosier, W. J. Parton, and D. S. Ojima (2005), DAYCENT model analysis of past and contemporary soil N_2O and net greenhouse gas flux for major crops in the USA, *Soil Tillage Res.*, *83*, 9-24.

DeLuca, T. H., D. R. Keeney, and G. W. McCarty (1992), Effect of freeze-thaw events on mineralization of soil nitrogen, *Biology and Fertility of Soils*, *14*, 116-120.

Dentener, F. (2001), Global maps of Nitrogen Depostion at a 1° resolution, personal communication.

Dixon, J., A. Gulliver, and D. Gibbon (2001), *Farming Systems and Poverty*, 406 pp., FAO and Worldbank, Rome and Washington D.C.

Dobbie, K. E., and K. A. Smith (2003), Nitrous oxide emission factors for agricultural soils in Great Britain: the impact of soil water-filled pore space and other controlling variables, *Global Change Biology*, *9*, 204-218.

Döll, P., and S. Siebert (2000), A digital global map of irrigated areas, *ICID Journal*, *49*, 55-66.

Donner, S. D., and C. J. Kucharik (2003), Evaluating the impacts of land management and climate variability on crop production and nitrate export across the Upper Mississippi Basin, *Global Biogeochemical Cycles*, *17*, art. no.-1085.

Doran, J., M. LN, and Stramatiadis (1988), Microbial activity and N cycling as regulated by water-filled pore space, *paper presented at 11th International Conference, Int. Soil Tillage Research Org. (ISTRO)*.

Dorland, S., and E. G. Beauchamp (1991), Denitrification and ammonification at low soil temperatures, *Canadian Journal of Soil Science*, *71*, 293-303.

Duxbury, J. M., L. A. Harper, and A. R. Mosier (1993), Contributions of agroecosystems to global climate change, in *Agricultural ecosystem effects on trace gases and global climate change*, edited by D. E. Rolston, et al., pp. 1-18, American Society of Agronomy Inc., Crop Science Society of America Inc., Soil Science Society of America Inc., Madison, Wisconsin, USA.

ECETOC (2004), Ammonia emissions to air in Western Europe, *ECETOC Technical Report No. 62, 196 pp.,* European Centre for Ecotoxicology and Toxicology of Chemicals, Brussels

ECMWF (2004), ECMWF Re-Analysis ERA-40, *URL: http://www.ecmwf.int/products/data/archive/descriptions/e4/index.html [Accessed in March 2004]*.

Edwards, A. C., and K. Killham (1986), The effect of freeze/thaw on gaseous nitrogen loss from upland soils, *Soil Use and Management*, *2*, 86-91.

Eitzinger, J., M. Trnka, J. Hosch, Z. Zalud, and M. Dubrovsky (2004), Comparison of CERES, WOFOST and SWAP models in simulating soil water content during growing season under different soil conditions, *Ecological Modelling*, *171*, 223-246.

Ellis, S., M. T. Howe, K. W. T. Goulding, M. A. Mugglestone, and L. Dendooven (1998), Carbon and nitrogen dynamics in a grassland soil with varying pH: Effect of pH on the denitrification potential and dynamics of the reduction enzymes, *Soil Biology and Biochemistry*, *30*, 359-367.

Engel, T., and E. Priesack (1993), Expert-N, a building block system nitrogen models as a resource for advice, research, water management and policy, in *Integrated Soil and Sediment Research: A Basis for Proper Protection*, edited by H.J.P.Eijsackers and T. Hamers, pp. 503-507, Kluwer Academic Publishers, Dordrecht, The Netherlands.

Eurostat (2004), General and Regional Statistics Database, edited, URL: http://epp.eurostat.cec.eu.int. [Accessed: March 2005].

FAO-Geoweb (2004), Global Information and Early Warning System - GeoWeb, *URL: http://geoweb.fao.org. [Accessed in March 2005]*.

FAO (1978), Report on the Agro-Ecological-Zones Project, Vol. 1: Methodology and results for Africa, FAO, Rome.

FAO (1995), FAO Digital Soil Map of the World, FAO, Rome.

FAO (2001a), *Global estimates of gaseous emissions of NH_3, NO and N_2O from agricultural land*, FAO, Rome.

FAO (2001b), Review of agricultural water use per country, *URL: http://www.fao.org/ag/agl/aglw/aquastat/water_use/index.stm. [Accessed in March 2005]*.

FAO (2002), TERRASTAT. Global land resources GIS models and databases for poverty and food insecurity mapping, FAO, Rome.

FAO (2003), Securing Food for a Growing World Population, in *The UN World Water Development Report: Water for People, Water for Life.*, UNESCO, p. 35 pp., UNESCO, Paris.

FAO (2004), FAOSTAT database collections, Food and Agriculture Organization of the United Nations, Rome; URL: http://faostat.fao.org. [Acccessed: March 2005].

Federer, C. A., and L. Klemedtsson (1988), Some factors limiting denitrification in slurries of acid forest soils, *Scand. J. For. Res.*, *3*, 425-435.

Firestone, M. K., and E. A. Davidson (1989), Microbiological basis for NO and N_2O production and consumption in soils, in *Exchange of trace gases between terrestrial ecosystems and the atmosphere*, edited by M. O. Andreae and D. S. Schimel, pp. 7-21, Wiley and Sons, Chichester.

Fischer, G., H. van Velthuizen, M. Shah, and F. Nachtergaele (2002), Global Agro-ecological Assessment for Agriculture in the 21st Century: Methodology and Results., 154 pp, International Institute for Applied Systems Analysis, Laxenburg, Austria.

Flessa, H., P. Dorsch, and F. Beese (1995), Seasonal-Variation of N_2O and CH_4 fluxes in differently managed arable soils in southern Germany, *Journal Of Geophysical Research-Atmospheres*, *100*, 23115-23124.

Freibauer, A., and M. Kaltschmitt (2003), Controls and models for estimating direct nitrous oxide emissions from temperate and sub-boreal agricultural mineral soils in Europe, *Biogeochemistry*, *63*, 93-115.

Frink, C., P. Waggoner, and J. Ausubel (1999), Nitrogen fertilizer: Retrospect and prospect, *P NATL ACAD SCI USA*, *96*, 1175-1180.

Frolking, S. E., A. R. Mosier, D. S. Ojima, C. Li, W. J. Parton, C. S. Potter, E. Priesack, R. Stenger, C. Haberbosch, P. Dorsch, H. Flessa, and K. A. Smith (1998), Comparison of N_2O emissions from soils at three temperate agricultural sites: simulations of year-round measurements by four models, *Nutrient Cycling in Agroecosystems*, *52*, 77-105.

Galloway, J. N., F. J. Dentener, D. G. Capone, E. W. Boyer, R. W. Howarth, S. P. Seitzinger, G. P. Asner, C. C. Cleveland, P. A. Green, E. A. Holland, D. M. Karl, A. F. Michaels, J. H. Porter, A. R. Townsend, and C. J. Vorosmarty (2004), Nitrogen cycles: past, present, and future, *Biogeochemistry*, *70*, 153-226.

Ganzeveld, L. N., J. Lelieveld, F. J. Dentener, M. C. Krol, A. F. Bouwman, and G. J. Roelofs (2002), Global soil biogenic NO_x emissions and the role of canopy processes, *Journal of Geophysical Research*, *107 (D16)*, 4289, doi 4210.1029/2001JD001289.

Gerber, P. (2004), Estimated livestock densities. Several digital data sets for different regions and livestock types available from the FAO-GeoNetwork (http://www.fao.org/geonetwork/srv/en/main.search), FAO, Rome.

Global_Soil_Data_Task_Group (2000), Global Gridded Surfaces of Selected Soil Characteristics (International Geosphere-Biosphere Programme - Data and Information System).

Goodroad, L. L., and D. R. Keeney (1984), Nitrous oxide emission from forest, marsh, and prairie ecosystems, *Journal of Environmental Quality*, *13*, 448-452.

Goodroad, L. L., and D. R. Keeney (1984), Nitrous oxide emissions from soils during thawing, *Canadian Journal of Soil Science*, *64*, 187-194.

Granli, T., and O. C. Bøckman (1994), Nitrous oxide from agriculture, *Norwegian Journal of Agricultural Sciences*, *Supplement No. 12*, 1-128.

Grant, R. F., and E. Pattey (2003), Modelling variability in N_2O emissions from fertilized agricultural fields, *Soil Biology & Biochemistry*, *35*, 225-243.

Heistermann, M., and J. A. Priess (2005), The Landshift Model, in *The earth's changing land: An encyclopedia of land use and land cover change*, edited by H. Geist, Greenwood Publishing Group, Westport, CT.

Herrmann, A., and E. Witter (2002), Sources of C and N contributing to the flush in mineralization upon freeze-thaw cycles in soils, *Soil Biology & Biochemistry*, *34*, 1495-1505.

Hofstra, N., and A. F. Bouwman (2005), Denitrification in agricultural soils: Summarizing published data and estimating global annual rates, *Nutrient Cycling in Agroecosystems*, Accepted.

Hoogenboom, G., J. W. Jones, and K. J. Boote (1992), Modeling the growth, development and yield of grain legumes using SOYGRO, PNUTGRO and BEANGRO: A review, *Transactions of the ASAE. 35(6),* 2043-2056.

Hooper, A. B., and K. R. Terry (1979), Hydroxylamine oxidoreductase of Nitrosomonas: Production of nitric oxide from hydroxylamine, *Biochim. Biophys. Acta*, *571*, 12-20.

Howarth, R. W., G. Billen, D. Swaney, A. Townsend, N. Jaworski, K. Lajtha, J. A. Downing, R. Elmgren, N. Caraco, T. Jordan, F. Berendse, J. Freney, V. Kudeyarov, P. Murdoch, and Z. L. Zhu (1996), Regional nitrogen budgets and riverine N&P fluxes for the drainages to the North Atlantic Ocean: Natural and human influences, *Biogeochemistry*, *35*, 75-139.

IFA (2002), Fertilizer use by crop. 5th edition; URL: http://www.fertilizer.org/ifa/statistics.asp. [Accessed in March 2005]. International Fertilizer Industry Association, Rome.

IFA/IFDC/FAO (2003), Fertilizer use by crop. 5th edition, Food and Agriculture Organization of the United Nations, Rome.

Iglesias, A., and M. I. Minguez (1997), Modelling crop climate interactions in Spain: Vulnerability and Adaptation of Different Agricultural Systems to Climate Change, *Mitigation and Adaptation Strategies for Global Change*, *1*, 273-288.

IMAGE-team (2001), The IMAGE 2.2 implementation of the SRES scenarios. A comprehensive analysis of emissions, climate change and impacts in the 21st century, National Institute for Public Health and the Environment, Bilthoven.

IPCC (1997), Revised 1996 guidelines for national greenhouse gas inventories, Intergovernmental panel on Climate Change / Organization for Economic Cooperation and Development, Paris.

IPCC (2001), *Third assessment report. Working Group I*, Cambridge University Press, Cambridge.

IPCC (1996), *IPCC Guidelines for National Greenhouse Gas Inventories*, 950 pp., IPCC, Bracknell, UK.

Janssen, P. H. M., and P. S. C. Heuberger (1995), Calibration of Process-Oriented Models, *Ecological Modelling*, *83*, 55-66.

Jenkinson, D. S., A. D. E, and W. A (1991), Model estimates of CO_2 emissions from soil in response to global warming, *Nature*, *351*, 304-306.

Jiang, P., and K. D. Thelen (2004), Effect of soil and topographic properties on crop yield in a north-central corn-soybean cropping system, *Agronomy Journal*, *96*, 252-258.

Jones, C. A., and J. R. Kiniry (1986), CERES-Maize: A simulation model of maize growth and development, Texas A&M University Press, College Station, Texas.

Jordan, C. F. (1985), *Nutrient cycling in tropical forest ecosystems: principles and their application in management and conservation*, 179 pp., Wiley, Chichester.

Kaiser, E. A., K. Kohrs, M. Kucke, E. Schnug, O. Heinemeyer, and J. C. Munch (1998), Nitrous oxide release from arable soil: Importance of N-fertilization, crops and temporal variation, *Soil Biology & Biochemistry*, *30*, 1553-1563.

Kaiser, E. A., and R. Ruser (2000), Nitrous oxide emissions from arable soils in Germany. An evaluation of six long-term field experiments, *Journal of Plant Nutrition and Soil Science (Zeitschrift für Planzenernährung and Bodenkunde)*, *163*, 249-259.

Kapetanaki, G., and C. Rosenzweig (1997), Impact of Climate Change on Maize Yield in Central and Northern Greece: A Simulation Study with CERES-Maize, *Mitigation and Adaptation Strategies for Global Change*, *1*, 251-271.

Kaplan, W. A., S. C. Wofsy, M. Keller, and J. M. d. Costa (1988), Emission of NO and deposition of O_3 in a tropical forest system, *Journal of Geophysical Research*, *93*, 1389-1395.

Kaspar, T. C., D. J. Pulido, T. E. Fenton, T. S. Colvin, D. L. Karlen, D. B. Jaynes, and D. W. Meek (2004), Relationship of corn and soybean yield to soil and terrain properties, *Agronomy Journal*, *96*, 700-709.

Keeney, D. R., I.R. Fillery, and G. P. Marx (1979), Effect of temperature on gaseous nitrogen products of denitrification in a silt loam soil, *Soil Science Society of America Journal*, *43*, 1124-1128.

Kelly, R. H., W. J. Parton, G. J. Crocker, P. R. Grace, J. Klír, P. R. Poulton, and D. D. Richter (1997), Simulating trends in soil organic carbon in long-term experiments using the Century model, *Geoderma*, *81*, 75-90.

Kenny, G. J., R. A. Warrick, B. D. Campbell, G. C. Sims, M. Camilleri, P. D. Jamieson, N. D. Mitchell, H. G. McPherson, and M. J. Salinger (2000), Investigating climate change impacts and thresholds: An application of the CLIMPACTS integrated assessment model for New Zealand agriculture, *Climatic Change*, *46*, 91-113.

Kester, R. A., M. E. Meijer, J. A. Libochant, W. de Boer, and H. J. Laanbroek (1997), Contribution of nitrification and denitrification to the NO and N_2O emissions of an acid forest soil, a river sediment and a fertilized grassland soil, *Soil Biology & Biochemistry*, *29*, 1655-1664.

Kiese, R., and K. Butterbach-Bahl (2002), N_2O and CO2 emissions from three different tropical forest sites in the wet tropics of Queensland, Australia, *Soil Biology & Biochemistry*, *34*, 975-987.

Kiese, R., H. Papen, E. Zumbusch, and K. Butterbach-Bahl (2002), Nitrification activity in tropical rain forest soils of the coastal lowlands and Atherton Tableands, Queensland Australia, *Zeitschrift für Pflanzenernährung und Bodenkunde*, *165*, 682-685.

Kreileman, G. J. J., and A. F. Bouwman (1994), Computing land use emissions of greenhouse gases, *Water, Air and Soil Pollution*, *76*, 231-258.

Kroeze, C., A. Mosier, and L. Bouwman (1999), Closing the global N_2O budget: A retrospective analysis 1500- 1994, *Global Biogeochemical Cycles*, *13*, 1-8.

Kucharik, C. J. (2003), Evaluation of a process-based agro-ecosystem model (Agro-IBIS) across the U.S. Cornbelt: Simulations of the interannual variability in maize yield, *Earth Interactions*, *7*, 1-33.

Leff, B., N. Ramankutty, and J. A. Foley (2004), Geographic distribution of major crops across the world, *Global Biogeochemical Cycles*, *18*, GB1009, doi:1010.1029/2003GB002108.

Li, C., S. Frolking, and T. A. Frolking (1992), A model of nitrous oxide evolution from soil driven by rainfall events: 1. Model structure and sensitivity, *Journal of Geophysical Research*, *97*, 9759-9776.

Li, C., J. D. Aber, F. Stange, K. Butterbach-Bahl, and H. Papen (2000), A process-oriented model of N_2O and NO emissions from forest soils: 1. Model development, *Journal of Geophysical Research*, *105*, 4369-4384.

Liebig, M. A., J. A. Morgan, J. D. Reeder, B. H. Ellert, H. T. Gollany, and G. E. Schuman (2005), Greenhouse gas contributions and mitigation potential of agricultural practices in northwestern USA and western Canada, *Soil Tillage Res.*, *83*, 25-52.

Lipiec, J., J. Arvidsson, and E. Murer (2003), Review of modelling crop growth, movement of water and chemicals in relation to topsoil and subsoil compaction, *Soil Tillage Res.*, *73*, 15-29.

Malhi, S. S., and W. B. McGill (1982), Nitrification in three Alberta soils: effect of temperature, moisture and substrate concentration, *Soil Biology & Biochemistry*, *14*, 393-399.

Martikainen, P. J., and W. d. Boer (1993), Nitrous oxide production and nitrification in acidic soil from a Dutch coniferous forest, *Soil Biology and Biochemistry*, *25*, 343-347.

Martin, R. E., M. C. Scholes, A. R. Mosier, D. S. Ojima, E. A. Holland, and W. J. Parton (1998), Controls on annual emissions of nitric oxide from soils of the Colorado shortgrass steppe, *Global Biogeochemical Cycles*, *12*, 81-91.

Matson, P. A., R. Naylor, and I. Ortiz-Monasterio (1998), Integration of environmental, agronomic, and economic aspects of fertilizer management, *Science*, *280*, 112-115.

Matsuoka, Y., T. Morita, and M. Kainuma (2001), Integrated Assessment Model of Climate Change: The AIM Approach, paper presented at 14th Toyota Conference, Terrapub, Shizuoka, Japan.

McGill, W. B., H. W. Hunt, R. G. Woodmansee, and J. O. Reuss (1981), PHOENIX, a model of the dynamics of carbon and nitrogen in grassland soils, in *Terrestrial nitrogen cycles processes, ecosystem strategies and management impacts*, edited by F. E. Clark and T. Rosswall, pp. 49-115, Royal Swedish Academy of Sciences, Stockholm.

Meixner, F. (1994), Surface exchange of odd nitrogen oxides, *Nova Acta Leopoldina*, *288*, 299-348.

Meixner, F. X., T. Fickinger, L. Marufu, D. Serca, F. J. Nathaus, E. Makina, L. Mukurumbira, and M. O. Andreae (1997), Preliminary results on nitric oxide emission from a southern African savanna ecosystem, *Nutrient Cycling in AgroEcosystems*, *48*, 123-138.

Mitchell, T. D., and P. D. Jones (2005), An improved method of constructing a database of monthly climate observations and associated high-resolution grids, *Int. J. Climatol.*, *25*, 693-712.

Mosier, A., C. Kroeze, C. Nevison, O. Oenema, S. Seitzinger, and O. van Cleemput (1998), Closing the global N_2O budget: nitrous oxide emissions through the agricultural nitrogen cycle - OECD/IPCC/IEA phase II development of IPCC guidelines for national greenhouse gas inventory methodology, *Nutrient Cycling in Agroecosystems*, *52*, 225-248.

Motavalli, P. P., C. A. Palm, W. J. Parton, E. T. Elliott, and S. D. Frey (1994), Comparison of laboratory and modeling simulation methods for estimating soil carbon pools in tropical forest soils, *Soil Biology & Biochemistry*, *26*, 935-944.

Müller, C., R. R. Sherlock, and P. H. Williams (1997), Mechanistic model for nitrous oxide emission via nitrification and denitrification, *Biology and Fertility of Soils*, *24*, 231-238.

Müller, C., R. R. Sherlock, and P. H. Williams (1998), Field method to determine N_2O emission from nitrification and denitrification, *Biology and Fertility of Soils*, *28*, 51-55.

Müller, C., and R. R. Sherlock (2004), Nitrous oxide emissions from temperate grassland ecosystems in the Northern and Southern Hemispheres, *Global Biogeochemical Cycles*, *18*, art. no.-GB1045.

Myneni, R. B., C. D. Keeling, C. J. Tucker, G. Asrar, and R. R., and Nemani (1997), Increased plant growth in the northern high latitudes from 1981–1991, *Nature*, *386*, 698–702.

Nevison, C. D., G. Esser, and E. A. Holland (1996), A global model of changing N_2O emissions from natural and perturbed soils, *Climatic Change*, *32*, 327-378.

New, M., M. Hulme, and P. Jones (1999), Representing twentieth-century space-time climate variability. Part I: Development of a 1961-90 mean monthly terrestrial climatology, *Journal of Climate*, *12*, 829-856.

New, M. G., M. Hulme, and P. D. Jones (2000), Representing twentieth-century space-time climate variability. Part II: Development of 1901-1996 monthly grids of terrestrial surface climate, *Journal of Climate*, *13*, 2217-2238.

NOAA-CIRES (2004), NCEP Reanalysis data, provided by the NOAA-CIRES Climate Diagnostics Center, Boulder, Colorado, USA, from their Web site at http://www.cdc.noaa.gov/.

Ojima, D., A. Mosier, S. Del Grosso, and W. J. Parton (2000), TRAGNET analysis and synthesis of trace gas fluxes, *Global Biogeochemical Cycles*, *14*, 995-997.

Ojima, D. A., W.J.Parton, and C.Keough (2004), Discussions on the simulation of crop growth, soil nutrient dynamics and N_2O emission with the Daycent model.

Oldeman, L. R., R. T. A. Hakkeling, and W. G. Sombroek (1990), World map of the status of human induced soil degradation. An explanatory note, International Soil Reference and Information Centre, Wageningen.

Olivier, J. G. J., A. F. Bouwman, K. W. Van der Hoek, and J. J. M. Berdowski (1998), Global air emission inventories for anthropogenic sources of NO_x, NH_3 and N_2O in 1990, *Environmental Pollution*, *102*, 135-148.

Otter-Nacke, S., D. C. Godwin, and J. T. Ritchie (1986), Testing and validating the CERES-Wheat Model in diverse environments, 146 pp.

Papen, H., and K. Butterbach-Bahl (1999), A 3-year continuous record of nitrogen trace gas fluxes from untreated and limed soil of a N-saturated spruce and beech forest ecosystem in Germany 1. N_2O emissions, *Journal of Geophysical Research*, *104*, 18487-18503.

Parton, W. J., J. W. B. Stewart, and C. V. Cole (1988), Dynamics of C, N, P, and S in grassland soils: A model, *Biochemistry*, *5*, 109-131.

Parton, W. J., A. R. Mosier, D. S. Ojima, D. W. Valentine, D. S. Schimel, K. Weier, and A. E. Kulmala (1996), Generalized model for N_2 and N_2O production from nitification and denitrification, *Global Biogeochemical Cycles*, *10*, 401-412.

Parton, W. J., M. Hartman, D. Ojima, and D. Schimel (1998), DAYCENT and its land surface submodel: description and testing, *Global and Planetary Change*, *19*, 35-48.

Parton, W. J., E. A. Holland, S. J. Del Grosso, M. D. Hartman, R. E. Martin, A. R. Mosier, D. S. Ojima, and D. S. Schimel (2001), Generalized model for NO_x and N_2O emissions from soils, *Journal of Geophysical Research-Atmospheres*, *106*, 17403-17420.

Parton, W. J., and D. S. Ojima (2003), The Daycent model as obtained from Bill Parton in November 2003.

Parton, W. J., 1978 (1978), The Abiotic Section of ELM, in *Grassland Simulation Model*, edited by G. S. Innis, Springer, New York, Berlin, Heidelberg.

Pathak, H., A. Bhatia, S. Prasad, S. Singh, S. Kumar, M. C. Jain, and U. Kumar (2002), Emission of nitrous oxide from rice-wheat systems of Indo- Gangetic plains of India, *Environmental Monitoring And Assessment*, *77*, 163-178.

Pathak, H., C. Li, and R. Wassmann (2005), Greenhouse gas emissions from Indian rice fields: calibration and upscaling using the DNDC model, *Biogeosciences*, *2*, 113–123.

Payne, R. W., D. B. Baird, A. R. Gilmore, S. A. Harding, P. W. Lane, D. A. Murray, D. M. Soutar, R. Thompson, A. D. Todd, G. T. Wilson, R. Webster, and S. J. Welham (2000), *Genstat release 4.2. Reference manual*, Lawes Agricultural Trust (Rothamsted Experimental Station), Harpenden, Hertfordshire, U.K.

Pielke, R. A., G. Marland, R. A. Betts, T. N. Chase, J. L. Eastman, J. O. Niles, D. D. S. Niyogi, and S. W. Running (2002), The influence of land-use change and landscape dynamics on the climate system: relevance to climate-change policy beyond the radiative effect of greenhouse gases, *Philosophical Transactions Of The Royal Society Of London Series A-Mathematical Physical And Engineering Sciences*, *360*, 1705-1719.

Ping, J. L., C. J. Green, K. F. Bronson, R. E. Zartman, and A. Dobermann (2004), Identification of relationships between cotton yield, quality, and soil properties, *Agronomy Journal*, *96*, 1588-1597.

Poth, M., and D. D. Focht (1985), ^{15}N kinetic analysis of N_2O production by *Nitrosomonas europaea*: an examination of nitrifier-denitrification, *Applied and Environmental Microbiology*, *49*, 1134-1141.

Potter, C. S., J. T. Randerson, C. B. Field, P. A. Matson, P. M. Vitousek, H. A. Mooney, and S. A. Klooster (1993), Terrestrial ecosystem production: a process model based on global satellite and surface data, *Global Biogeochemical Cycles*, *7*, 811-841.

Potter, C. S., P. A. Matson, P. M. Vitousek, and E. A. Davidson (1996), Process modeling of controls on nitrogen trace gas emissions from soils worldwide, *Journal of Geophysical Research-Atmospheres*, *101*, 1361-1377.

Priemé, A., and S. Christensen (2001), Natural pertubations, drying-wetting and freezing-thawing cycles, and the emission of nitrous oxide, carbon dioxide and methane from farmed organic soils, *Soil Biology & Biochemistry*, *33*, 2083-2091.

Remde, A., and R. Conrad (1991), Role of nitrification and denitrification for NO metabolism in soil, *Biogeochemistry*, *12*, 189-205.

Ritchie, G. A. F., and D. J. D. Nicholas (1972), Identification of the sources of nitrous oxide produced by oxidative and reductive processes in *Nitrosomonas europaea*, *Biochemical Journal*, *126*, 1181-1191.

Ritchie, J. T., U. Singh, D. C. Godwin, and L. Hunt (1991), A users guide to CERES-Maize - version 2.10, International Fertilizer Development Center, Muscle Shoals, AL.

Robertson, G. P., and J. M. Tiedje (1984), Denitrification and nitrous oxide production in successional and old-growth Michigan forests, *Soil Science Society of America Journal*, *48*, 383-389.

Rochette, P., D. A. Angers, G. Belanger, M. H. Chantigny, D. Prevost, and G. Levesque (2004), Emissions of N_2O from alfalfa and soybean crops in eastern Canada, *Soil Science Society Of America Journal*, *68*, 493-506.

Rohde, H. (1990), A comparsion of the contribution of various greenhouse gases to the Greenhouse Effect, *Science*, *248*, 1217-1219.

Ruser, R., H. Flessa, R. Schilling, F. Beese, and J. C. Munch (2001), Effect of crop-specific field management and N fertilization on N_2O emissions from a fine-loamy soil, *Nutrient Cycling in Agroecosystems*, *59*, 177-191.

Ryden, J. C. (1981), N_2O exchange between a grassland soil and the atmosphere, *Nature*, *292*, 235-237.

Saad, A. L. O., and R. Conrad (1993), Temperature dependence of nitrification, denitrification and turnover of nitric oxide in different soils, *Biology and Fertility of Soils*, *15*, 21-27.

Saarikko, R. A. (2000), Applying a site based crop model to estimate regional yields under current and changed climates, *Ecological Modelling*, *131*, 191-206.

Saiko, T. A., and I. S. Zonn (2000), Irrigation expansion and dynamics of desertification in the Circum-Aral region of Central Asia, *Applied Geography*, *20*, 349-367.

Saxton, K. E., W. J. Rawls, J. S. Romberger, and R. I. Papendick (1986), Estimating generalized soil-water characteristics from texture, *Soil Sci Soc Am J*, *50*, 1031-1036.

Scheffer, F. (2002), *Lehrbuch der Bodenkunde*, Spektrum Akademischer Verlag, Berlin.

Schimel, J. P., and J. S. Clein (1996), Microbial response to freeze-thaw cycles in tundra and taiga soils, *Soil Biology & Biochemistry*, *28*, 1061-1066.

Scholze, M., A. Bondeau, F. Ewert, C. Kucharik, J. A. Priess, and P. Smith (2005), Advances in large-scale crop modelling, *EOS 86(26), 245-246*.

Schulte-Bisping, H., R. Brumme, and E. Priesack (2003), Nitrous oxide emission inventory of German forest soils, *Journal Of Geophysical Research-Atmospheres*, *108*, art. no.-4132.

Sharpley, A. N., and J. R. Williams (1990), EPIC-Erosion/Productivity Impact Calculator: I Model documentation, Technical Bulletin No. 1768, 235 pp, US Department of Agriculture.

Shelton, D. R., A. M. Sadeghi, and G. W. McCarty (2000), Effect of soil water content on denitrification during cover crop, *Soil Science*, *165*, 365-371.

Siebert, S. (2005), Global-Scale Modeling of Nitrogen Balances at the Soil Surface, *Frankfurt Hydrology Paper*, *2*.

Silver, W. L., J. Neff, M. McGroddy, E. Veldkamp, M. Keller, and R. Cosme (2000), Effects of soil texture on belowground carbon and nutrient storage in a lowland Amazonian forest ecosystem, *Ecosystems*, *3*, 193-209.

Simek, M., J. E. Cooper, T. Picek, and H. Santruckova (2000), Denitrification in arable soils in relation to their physico-chemical properties and fertilization practice, *Soil Biology and Biochemistry*, *32*, 101-110.

Simek, M., and J. E. Cooper (2002), The influence of soil pH on denitrification: progress towards the understanding of this interaction over the last 50 years, *European Journal of Soil Science*, *53*, 345-354.

Skiba, U., D. Fowler, and K. Smith (1994), Emissions of NO and N_2O from soils, *Environmental Monitoring And Assessment*, *31*, 153-158.

Skiba, U., D. Fowler, and K. A. Smith (1997), Nitric oxide emissions from agricultural soils in temperate and tropical climates: sources, controls and mitigation options, *Nutrient Cycling in Agroecosystems*, *48*, 139-153.

Skiba, U., L. Sheppard, C. E. R. Pitcairn, I. Leith, A. Crossley, S. v. Dijk, V. H. Kennedy, and D. Fowler (1998), Soil nitrous and nitric oxide emissions as indicators of elevated atmospheric deposition rates in seminatural ecosystems, *Environmental Pollution*, *102 S1*, 457-461.

Smith, P., J. U. Smith, D. S. Powlson, W. B. McGill, J. R. M. Arah, O. G. Chertov, K. Coleman, U. Franko, S. Frolking, D. S. Jenkinson, L. S. Jensen, R. H. Kelly, H. Klein-Gunnewiek, A. S. Komarov, C. Li, J. A. E. Molina, T. Mueller, W. J. Parton, J. H. M. Thornley, and A. P. Whitmore (1997), A comparison of the performance of nine soil organic matter models using datasets from seven long-term experiments, *Geoderma*, *81*, 153-225.

Snedecor, G. W., and W. G. Cochran (1980), *Statistical methods (7th edition)*, 507 pp., the Iowa State University Press, Ames, Iowa.

Stanford, G., S. Dzienia, and R. A. vander Pol (1975), Effect of temperature on denitrification rate in soils, *Soil Science Society of America Proceedings*, *39*, 867-887.

Stange, F., K. Butterbach-Bahl, H. Papen, S. Zechmeister-Boltenstern, C. S. Li, and J. Aber (2000), A process-oriented model of N_2O and NO emissions from forest soils 2. Sensitivity analysis and validation, *Journal of Geophysical Research-Atmospheres*, *105*, 4385-4398.

Stark, J. M., and M. K. Firestone (1996), Kinetic chracteristics of ammonium-oxidizer communities in a California oak woodland-annual grassland, *Soil Biology & Biochemistry*, *28*, 1307-1317.

Stauffer, B. R., and A. Neftel (1988), What we have learnt from the ice cores about the atmospheric Changes in the Concentrations of Nitrous Oxide, Hydrogen Peroxide and Other Trace Species., in *The changing atmosphere*, edited by R. F.S. and I. I.S.A., John Wiley & Sons Ltd., Chichester.

Stoate, C., N. D. Boatman, R. J. Borralho, C. R. Carvalho, G. R. de Snoo, and P. Eden (2001), Ecological impacts of arable intensification in Europe, *Journal Of Environmental Management*, *63*, 337-365.

Strauss, P., and E. Klaghofer (2001), Effects of soil erosion on soil characteristics and productivity, *Bodenkultur*, *52*, 147-153.

Supit, I., A. A. Hooijer, and C. A. van Diepen (1994), System description of the WOFOST 6.0 crop simulation model implemented in CGMS, vol. 1: Theory and Algorithms, Joint Research Centre, Commission of the European Communities, Luxembourg.

Tan, G. X., and R. Shibasaki (2003), Global estimation of crop productivity and the impacts of global warming by GIS and EPIC integration, *Ecological Modelling*, *168*, 357-370.

Tiedje, J. M. (1988), Ecology of denitrification and dissimilatory nitrate reduction to ammonium, in *Biology of Anaerobic microorganisms*, edited by A. J. B. Zehnder, pp. 179-244, Wiley and Sons, New York.

Trenkel, M. E. (1997), Improving fertilizer use efficiency. Controlled-release and stabilized fertilizers in agriculture, International Fertilizer Industry Association, Paris.

Tubiello, F. N., and F. Ewert (2002), Simulating the effects of elevated CO_2 on crops: approaches and applications for climate change, *European Journal of Agronomy*, *18*, 57-74.

USDA (2004a), Crops County and District Data, *URL: http://www.nass.usda.gov:81/ipedbcnty/c_groupcrops.htm. [Accessed in March 2005]*.

USDA (2004b), Major World Crop Areas and Climatic Profiles Online Version, *URL: http://www.usda.gov/oce/waob/jawf/profiles/updates.htm. [Accessed in March 2005]*.

USGCRP (2001), Agriculture, in *Climate Change Impacts on the United States: The Potential Consequences of Climate Variability and Change. Foundation Report. URL: http://www.usgcrp.gov/usgcrp/Library/nationalassessment/foundation.htm. [Accessed: March 2005]*, National Assessment Synthesis Team, US Research Programme on Global Change.

USGS (2003), Nitrogen Statistics and Information, URL: http://minerals.usgs.gov/minerals/pubs/commodity/nitrogen. [Accessed: March 2005].

Van Drecht, G., A. F. Bouwman, E. W. Boyer, P. Green, and S. Siebert (2005), A comparison of global spatial distributions of nitrogen inputs for nonpoint sources and effects on river nitrogen export, *Global Biogeochemical Cycles 19(4),* GB4S06.

Veldkamp, E., and M. Keller (1997), Fertilizer-induced nitric oxide emissions from agricultural soils, *Nutrient Cycling in Agroecosystems*, *48*, 69-77.

Venterea, R. T., and D. E. Rolston (2000), Mechanistic modeling of nitrite accumulation and nitrogen oxide gas emissions during nitrification, *Journal of Environmental Quality*, *29*, 1741-1751.

Verchot, L. V., E. A. Davidson, J. H. Cattanio, I. L. Ackerman, H. E. Erikson, and M. Keller (1999), Land use change and biogeochemical controls of nitrogen oxide emissions from soils in eastern Amazonia, *Global Biogeochemical Cycles*, *13*, 31-46.

Vitousek, P. M. (1984), Litterfall, nutrient cycling and nutrient limitation in tropical forests, *Ecology*, *65*, 285-298.

Vitousek, P. M., and R. L. Sanford (1986), Nutrient Cycling in moist tropical forest, *Annual Review of Ecology and Systematics, 17*, 137-167.

Vos, G. J. M., I. M. J. Bergevoet, J. C. Vedy, and J. A. Neyroud (1994), The fate of spring applied fertilizer N during the autumn-winter period: comparison between winter-fallow and green manure cropped soil, *Plant and Soil*, *160*, 201-213.

Wagner-Riddle, C., G. W. Thurtell, G. K. Kidd, E. G. Beauchamp, and R. Sweetman (1997), Estimates of nitrous oxide emissions from agricultural fields over 28 months, *Canadian Journal of Soil Science*, *77*, 135-144.

Wang, J. Y. (1960), A critique of the heat unit approach to plant response studies, *Ecology*, *4*, 785-790.

Ward, K. J., B. Klepper, R. W. Rickman, and R. R. Allmaras (1978), Quantitative estimation of living wheat-root lengths in soil cores, *Agronomy Journal*, *70*, 675-677.

Weitz, A. M., E. Linder, S. Frolking, P. M. Crill, and M. Keller (2001), N_2O emissions from humid tropical agricultural soils: effects of soil moisture, texture and nitrogen availability, *Soil Biology & Biochemistry*, *33*, 1077-1093.

White, J. W., and M. P. Reynolds (2001), A Physiological Perspective on Modeling Temperature Response in Wheat and Maize Crops, in *Modeling Temperature Response in Wheat and Maize. Natural Resources Group. Geographic Information Systems Series 03-01*, edited by J. W. White, and Reynolds, M.P., Natural Resources Group.

Wijler, J., and C. C. Delwiche (1954), Investigations on the denitrifying processes in soil, *Plant and Soil*, *5*, 155-169.

Wilhelm, E. P., R. E. Mullen, P. L. Keeling, and G. W. Singletary (1999), Heat stress during grain filling in maize: Effects on kernel growth and metabolism, *Crop Science*, *39*, 1733-1741.

Williams, E. J., and F. C. Fehsenfeld (1991), Measurement of soil nitrogen oxide emissions at three North American ecosystems, *Journal of Geophysical Research*, *96*, 1033-1042.

Williams, J. R., C. A. Jones, and P. T. Dyke (1984), A modelling approach to determining the relationship between erosion and soil productivity, *Transactions of the ASAE*, *27*, 129-144.

Wrage, N., G. L. Velthof, M. L. van Beusichem, and O. Oenema (2001), Role of nitrifier denitrification in the production of nitrous oxide, *Soil Biology & Biochemistry*, *33*, 1723-1732.

Xu, H., G. Xiing, Z. Cai, and H. Tsuruta (1997), Nitrous oxide emissions from three rice paddy fields in China, *Nutrient Cycling in Agroecosystems*, *49*, 23-28.

Ye, R. W., B. A. Averill, and J. M. Tiedje (1994), Denitrification - production and consumption of nitric oxide, *Applied And Environmental Microbiology*, *60*, 1053-1058.

Yienger, J. J., and H. Levy (1995), Empirical model of global soil-biogenic NO_x emissions, *Global Biogeochemical Cycles*, *100*, 11447-11464.

Zaitchik, B., R. Smith, and F. Hole (2002), Spatial analysis of agricultural land use changes in the Khabour river basin of northeaster Syria, paper presented at ISPRS Commission I Symposium.

Zhang, Y., C. S. Li, X. J. Zhou, and B. Moore (2002), A simulation model linking crop growth and soil biogeochemistry for sustainable agriculture, *Ecological Modelling*, *151*, 75-108.

Zumft, W. G. (1993), The biological role of nitric oxide in bacteria, *Archives of Microbiology*, *160*, 253-264.

Appendix A: Simulated yields for tropical cereals, cassava, potato, pulses and cotton, masked with the crop area according to *Leff et al.* [2004].

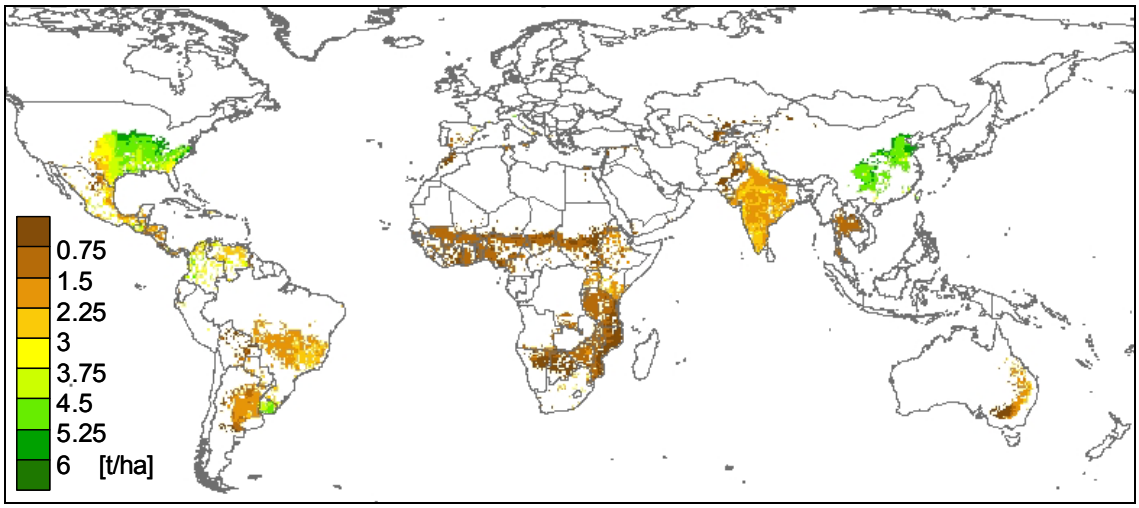

Sorghum and Millet: Yields simulated by the Daycent model for rain fed cropping [t ha^{-1}]

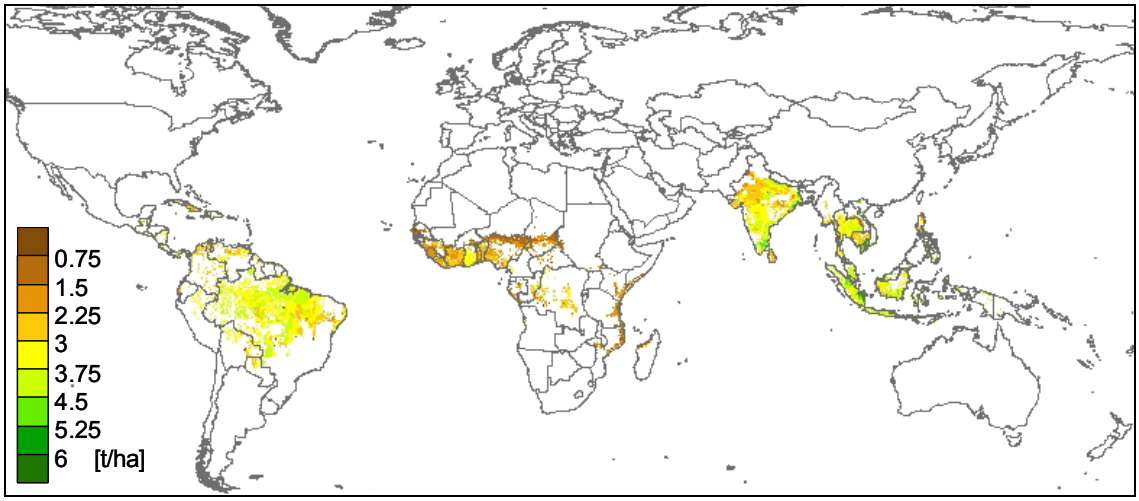

Cassava: Yields simulated by the Daycent model for rain fed cropping [t ha^{-1}]

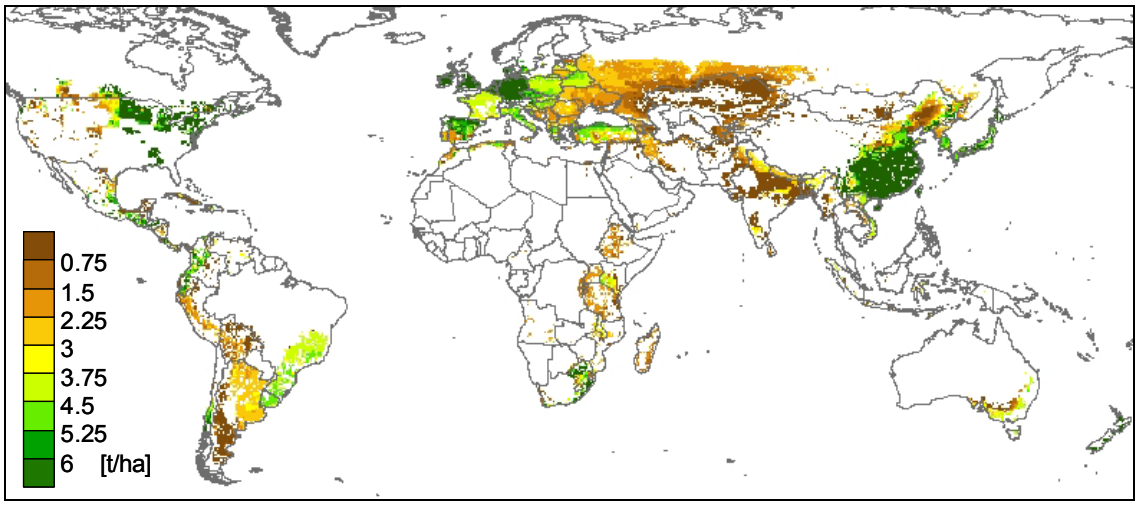

Potato: Yields simulated by the Daycent model for rain fed cropping [t ha^{-1}]

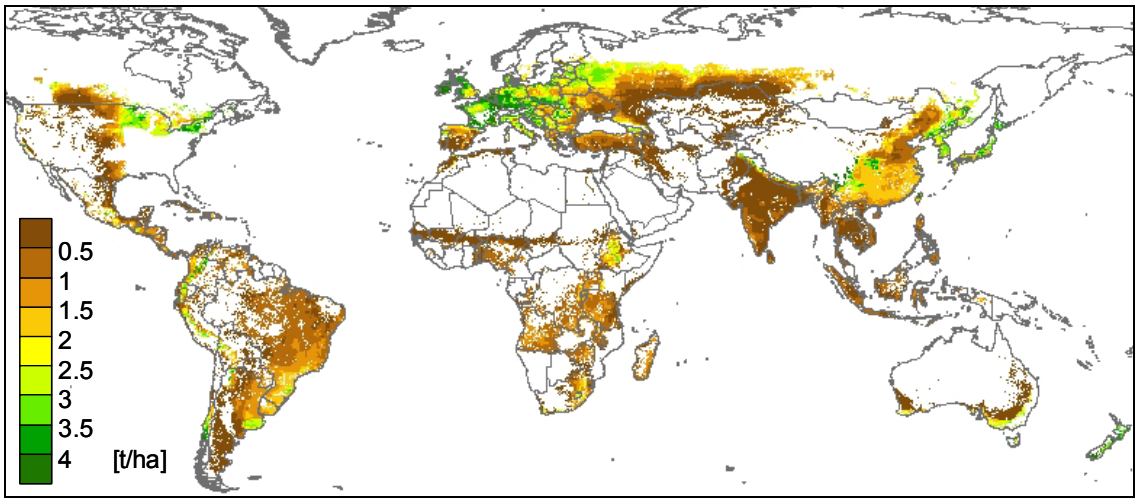

Pulses: Yields simulated by the Daycent model for rain fed cropping [t ha^{-1}]

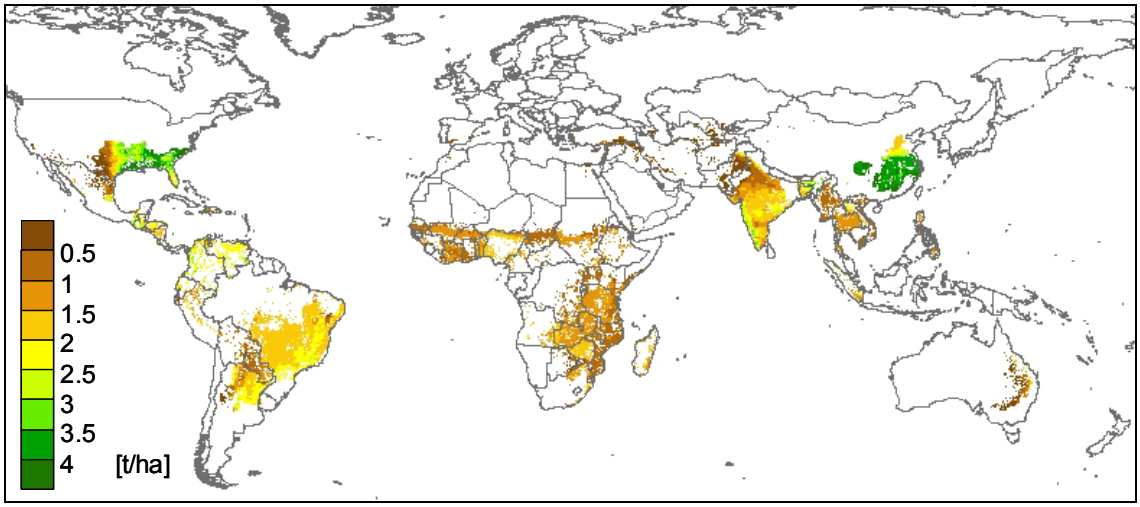

Cotton: Yields simulated by the Daycent model for rain fed cropping [t ha^{-1}]

Appendix B: Simulated N_2O emissions for tropical cereals, cassava, potato, pulses and cotton, masked with the crop area according to *Leff et al.* [2004].

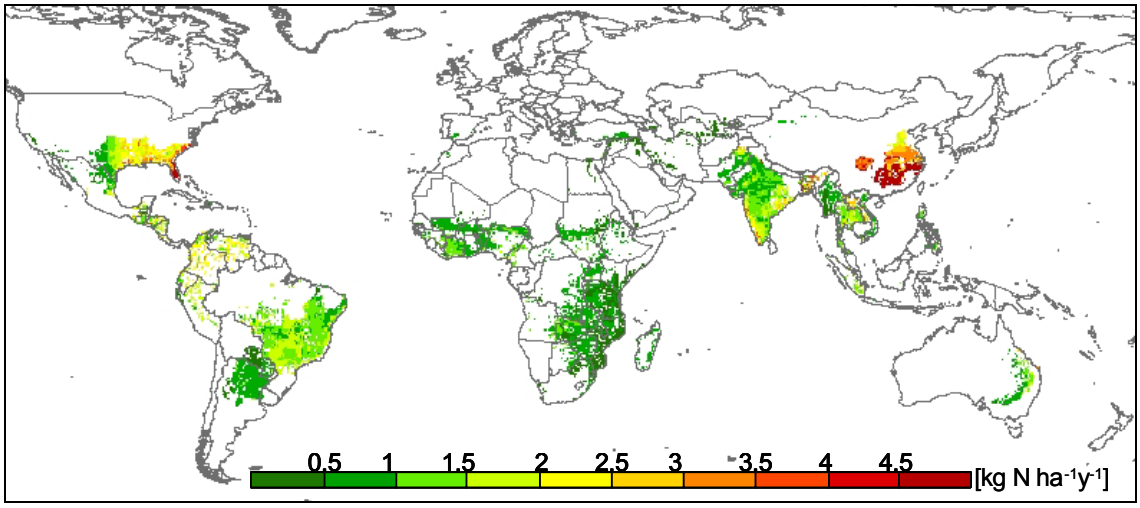

Sorghum and Millet: N_2O emissions simulated by the Daycent model for rain fed cropping [kg N ha^{-1} y^{-1}]

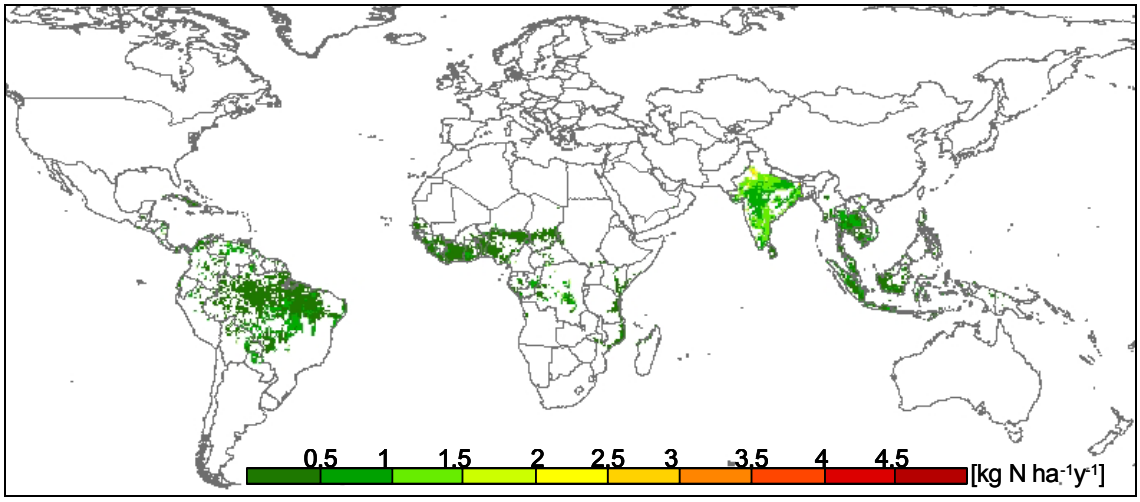

Cassava: N_2O emissions simulated by the Daycent model for rain fed cropping [kg N $ha^{-1}y^{-1}$]

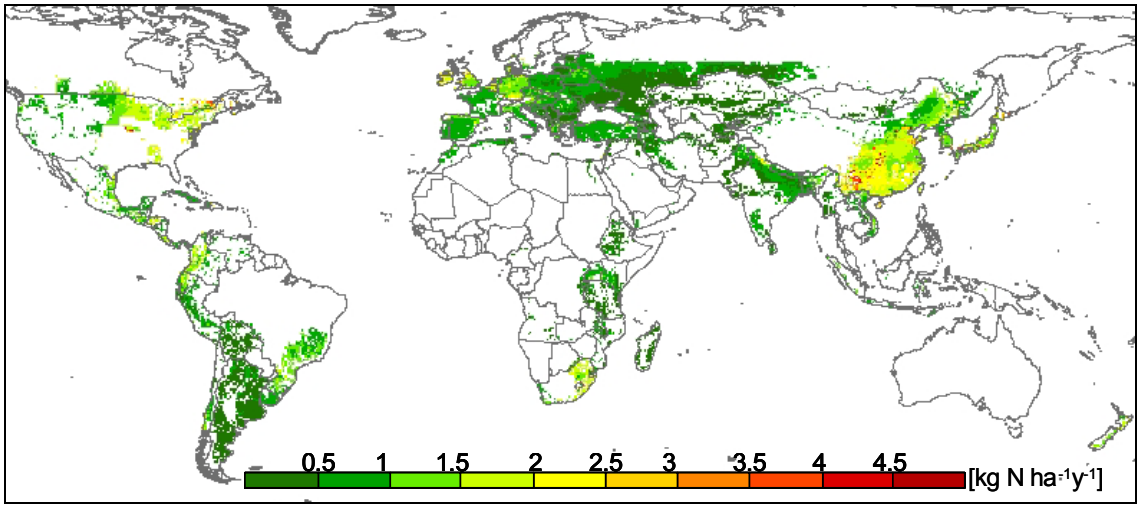

Potato: N_2O emissions simulated by the Daycent model for rain fed cropping [kg N ha^{-1} y^{-1}]

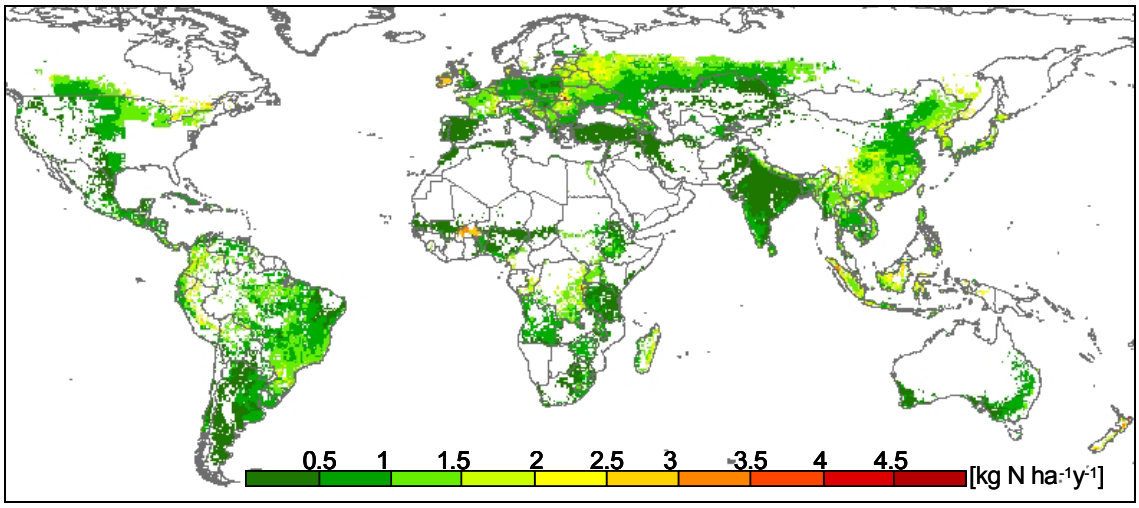

Pulses: N_2O emissions simulated by the Daycent model for rain fed cropping [kg N ha^{-1} y^{-1}]

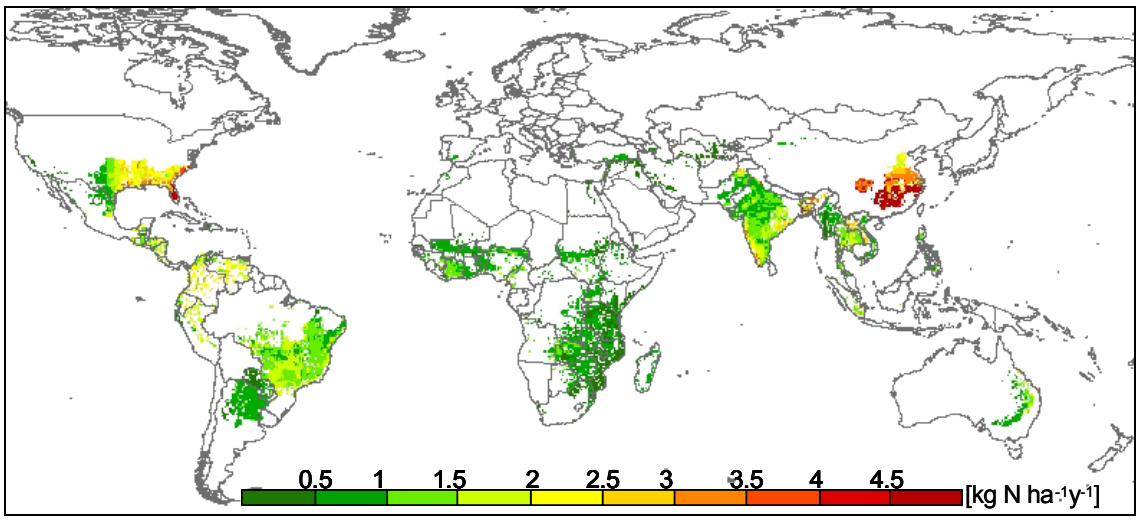

Cotton: N_2O emissions simulated by the Daycent model for rain fed cropping [kg N ha^{-1} y^{-1}]

Appendix C: N_2O emissions for wheat (a), wetland rice (b), maize (c) and soybean (d) as calculated by the statistical model (Chapter 3), using the same input data as applied for the Daycent simulations (Chapter 4).